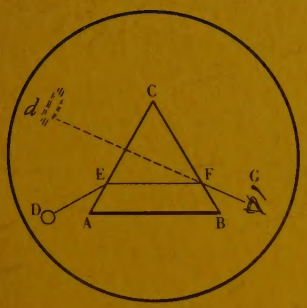

UNIVERSITY OF ILLINOIS
JAN 22 1962
CHICAGO

optics and spectroscopy

volume xi
number 3
september 1961

OPTICAL SOCIETY OF AMERICA
USSR ACADEMY OF SCIENCES

RUSSIAN EDITORIAL STAFF FOR
OPTIKA I SPEKTROSKOPIYA sponsored by
USSR ACADEMY OF SCIENCES

Editor: S. E. FRISH

Assistant Editor: P. P. FEOFILOV
Corresponding Secretary: L. S. SAZONOV

Associate Editors:

M. V. VOLKENSTEIN	V. P. LINNIK	N. N. SOBOLEV
M. M. GUREVICH	S. L. MANDEL'SHTAM	A. N. TERENIN
M. A. EL'IASHEVICH	I. V. OBREIMOV	A. I. TUDOROVSKII
A. A. LEBEDEV	V. K. PROKOF'EV	V. M. CHULANOVSKII

Translated from *OPTIKA I SPEKTROSKOPIYA* on the initiative of THE OPTICAL SOCIETY OF AMERICA, INC. with a grant-in-aid from THE NATIONAL SCIENCE FOUNDATION. *Optics and Spectroscopy* is a cover-to-cover translation of *Optika i Spektroskopiya* and no attempt is made to edit the material other than to correct obvious misprints. The views are those of the original authors and do not represent the Optical Society of America.

TRANSLATION EDITORIAL STAFF

Scientific Editors

CYRUS FELDMAN, *Oak Ridge National Laboratory*

CARL W. GARLAND, *Massachusetts Institute of Technology*

MATHEW G. GIBBONS, *Oakland, California*

Administrative Editor: PATRICIA R. WAKELING, *OSA*

Published monthly by the Optical Society of America, Inc. Executive office: 1155 Sixteenth Street, N.W., Washington, D.C. Subscriptions for one year to members of the Society: Associates $13.00; Regular members and Fellows $17.00. Subscriptions for non-members of the Society: One year U. S. and Possessions, $25.00; Foreign $28.00. Back numbers: $3.00 per copy. Subscriptions, changes of address and undeliverable copies should be referred to the Executive offices in Washington, D.C. The office of publication is 2500 South State Street, Ann Arbor, Michigan. Second class postage paid at Ann Arbor, Michigan.

Printed in the U.S.A. by Edwards Brothers, Inc., Ann Arbor, Michigan.

HE EXTENDED FOK METHOD IN A MULTICONFIGURATION APPROXIMATION FOR THE HELIUM ATOM

K. K. Eringis, P. Sh. Fridberg, and V. K. Shugurov (pp. 297-300)

Received 3 October 1960

A method which takes account of electrostatic electron repulsion in the construction of the wave function of an atom was used to compute the energy of the ground state of helium in the two- and three-configuration approximations $1s^2$-$2s^2$, $1s^2$-$2p^2$, and $1s^2$-$2s^2$-$2p^2$. The energies of the terms of the configuration $2p^2$ for helium and helium-like ions were also found. The results were compared with those obtained by the usual approximation.

ODUCTION

One widely used method of gaining accuracy in quan- mechanical calculations is the multiconfiguration oximation. It produces the desired results more ly and more rapidly in proportion to the skill with the wave functions of the initial (one-configura- approximation are selected. For example, the lation of the energy of the ground state of the m atom in a multiconfiguration approximation with id of Fock's numerical functions[1] requires con- ably fewer corrections than does the same calculation analytic functions.[2]

The functions customarily taken as initial functions hose which describe the state of the atom in a given guration. However, in deriving the concept of con- ation itself we assume the Coulomb interaction be- electrons to be small in comparison with the inter- n of the electron with the nucleus. Thus we disre- electron repulsion in constructing the wave func- of an atom. We take it into consideration indirectly in solving the Hartree-Fock equation for the radial common to all electrons with quantum numbers nl. natural, therefore, to try to improve the initial func- by constructing them in this way which, at least to extent, has taken account of the mutual repulsion ectrons.

Reference 3 attempts a solution of this question on asis of the two-electron functions of the helium lem, and also introduces a new concept of the term figuration." However, such a method cannot be used actice because there is no simple solution of the lem for helium, and the existing classification of gurations and terms on the basis of the solution of ydrogen problem, the theory of rotation groups, and Pauli principle clearly reflects the experimental It also is easy to visualize—which cannot be said e new concept of configuration introduced in ref. 3. The results obtained in ref. 4 show that the elec- in an atom are grouped in a shell corresponding to uantum number nl. Since, on the average, electrons ging to the same shell interact more strongly than rons from different layers, it is possible to im- e the wave function of each shell separately.

In the present paper the energy of the ground state e helium atom is calculated in the two- and three- guration approximations $1s^2$-$2s^2$, $1s^2$-$2p^2$, and $2s^2$-$2p^2$, using wave functions which take electron lsion into account.[5]

The fact that electron interaction is taken into ac- t in constructing the wave function $\psi(l^k)$ is evident the fact that the shell nl is described not by one radial function P(nl), but by several. In ref. 6 this system was given the name of the extended method. For one shell it is sufficient to introduce two different radial functions, because the energy of the terms of configuration l^k with any number of electrons k is expressed by integrals depending chiefly on two P's. However, it is impossible on this basis to prove that the radial part depends on the projection of the spin m.[7,8] As a matter of fact, if in any system of coordinates we assign to P_i the quantum number m, then, transforming to another system, we lose the relationship between the radial functions and the new numbers m. In addition, the wave functions proposed in ref. 8 are not eigenfunctions of the spin-momentum operator, that is, one-electron functions are not spinors, as they should be in describing the electron. When we work with such functions our conclusions cannot be accurate, and we are denied the full use of the powerful apparatus of irreducible tensor operators and coefficients of parentage.

WAVE FUNCTIONS

The principle of our method of taking account of mutual electron repulsion in constructing a function[5] consists in the following: Wave function $\psi(l^k)$ of configuration l^k may be expressed by one-electron functions, using the Clebsch-Gordan coefficients and coefficients of parentage,[9] in the form

$$\psi(l^k) = RY, \tag{1}$$

where the radial part is expressed by the usual approximation

$$R = \prod_{i=1}^{k} \frac{1}{r_i} P(nl\,|\,r_i), \tag{2}$$

and Y refers to the angular spin parts. From Eq. (1) we obtain the expression for energy (in atomic units):

$$E = kI + \frac{1}{2} k\cdot(k-1)\left(F_0 + \sum_{p>0} a_p F_p\right), \tag{3}$$

$$I = \int_0^\infty P(nl\,|\,r)\left[-\frac{1}{2}\frac{d^2}{dr^2} + \frac{l(l+1)}{2r^2} - \frac{N}{r}\right] P(nl\,|\,r)\,dr$$

$$= \frac{1}{2}\int_0^\infty\int_0^\infty \rho\left[-\frac{1}{2}\frac{d^2}{dr_>^2} - \frac{1}{2}\frac{d^2}{dr_<^2} + \frac{l(l+1)}{2r_>^2} + \frac{l(l+1)}{2r_<^2} - \frac{N}{r_>} - \frac{N}{r_<}\right]\rho\cdot dr_1 dr_2, \tag{4}$$

$$\rho = P(nl\,|\,r_1)\,P(nl\,|\,r_2), \tag{5}$$

$$F_p = \int_0^\infty\int_0^\infty \rho^2 \frac{r_<^p}{r_>^{p+1}}\,dr_1 dr_2, \tag{6}$$

where $r_<$ and $r_>$ are the smaller and larger, respectively, of r_1 and r_2 and N is the charge on the nucleus.

The multipliers a_p in formula (3) are considerably smaller than unity and may be disregarded initially. Then variation of (3) with respect to ρ leads to a differential equation with separable variables, the solution of which is the product of the hydrogen functions

$$\rho = P(Z|r_<)\,P(Z'|r_>)$$

with the parameters

$$Z = N, \quad Z' = N - k + 1.$$

The difference in the values of the parameters allows for the electron interaction expressed by the integral F_0 in Eq. (3). The calculations performed by varying the two parameters Z and Z′ in the case of configuration s^2 (ref. 10) and p^2 (ref. 6) in the Hartree approximation showed that, as must be the case, the difference between the values of the two parameters is equal to unity, within the limits of error.

The terms forming the sum of Eq. (3) do not permit of strict separation of the variables when $l > 0$, but they can be taken into account roughly by assuming that $Z' \to Z' - b$. To find the value of b, we must solve the equation

$$\frac{b}{k-1} F_0 = \sum_{p>0} a_p F_p. \qquad (7)$$

Now shell 1 is described by two radial functions, P(Z) and P(Z′), with $Z' = Z - k + 1 - b$. Consequently, R in Eq. (1) will be expressed by a symmetrized sum of products similar to Eq. (2). There should be no antisymmetrization, since if there were, Eq. (1) would not satisfy the Pauli principle.

By way of example, let us write $R(l^k)$ for k = 2 and 3. For brevity, setting

$$P(Z|r_1)\,P(Z'|r_2)\,P(Z''|r_3)\ldots = (ZZ'Z''\ldots),$$

we have

$$R(l^2) = A\,[(ZZ') + (Z'Z)], \qquad (8)$$
$$R(l^3) = B\,[(ZZZ') + (ZZ'Z) + (Z'ZZ) + (ZZ'Z') + (Z'ZZ') + (Z'Z'Z)],$$

where A and B result from the conditions of normalization.

The $\psi(l^k)$ evolved in this way are of course eigenfunctions of the operators L^2 (square of the orbital momentum), its projection L_z, the spin squared S^2, and its projection S_z. In calculating the matrix elements we may, as before, use tensor operators. Integration over angles and summing over spins lead to the same result as before, and the radial integrals are generalized in conformity with Eq. (8). The adaptation of the method to more complex configurations presents no special difficulties if orthogonality of the functions belonging to different layers is ensured by their angular parts.

Wave functions in a multiconfiguration approximation are written in the usual way.[11]

NUMERICAL RESULTS

The wave functions obtained as above were applied to the investigation of the ground state of the helium atom in the two- and three-configuration approximations $1s^2$-$2s^2$.

To clarify the part played by the addendum b, the energy of the terms of configuration $2p^2$ was found. The value of b in Eq. (7) was determined by the method of successive approximations: the integrals entering into Eq. (7) were calculated with the difference $Z - Z' = k$ and the value of b_1 was found; then the calculation was repeated with $Z - Z' = k - 1 + b$, etc. In practice the calculations could be limited to the first approximation. For example, for helium in state $(2p^2)^1S$, when b has the maximum value, the second approximation does not alter the first four significant figures in the value of the energy. Thus in Table 1, for helium and other ions with the configuration $2p^2$, we derive values for the term energies by using the value b resulting from the first approximation. For purposes of comparison, Table 1 also gives the results of the calculations with the usual analytic functions.[12] It is obvious that in all cases the new functions give lower values for the energy. The experimental values are taken from ref. 13.

Table 1. The Energy of the Terms of the Helium Atom and Helium-Like Ions in Configuration $2p^2$ (in atomic units)

	^3P			^1D			^1S		
	Z	b	E	Z	b	E	Z	b	E
I	2.123	−0.086	−0.7042	2.131	0.018	−0.6747	2.142	0.173	−0.4
II	—	—	−0.6988	—	—	−0.6640	—	—	−0.6
III	—	—	−0.711	—	—	—	—	—	—
I	3.126	−0.093	−1.7896	3.141	0.018	−1.7378	3.164	0.187	−1.6
II	—	—	−1.7847	—	—	−1.7289	—	—	−1.6
I	4.130	−0.095	−3.3776	4.141	0.019	−3.3011	4.166	0.189	−3.1
II	—	—	−3.3707	—	—	−3.2937	—	—	−3.1

We must emphasize that the values of the parameters are close to the atomic number N of the element in the periodic table. For helium, the value Z = 2 leads to $E(^1S) = -0.6315$, $E(^3P) = -0.7004$, and $E(^1D) = -0.66$ which coincides with the results in Table 1 within one-half percent and agrees better with experiment than do the result of the usual analytic functions with a variational parameter. This is a definite indication of the accuracy of the proposed method and leads us to hope that calculations performed with appropriate functions and values of parameters Z = N will give satisfactory results.

Table 2 shows the values of the energy of state $(1s^2)^1S$ of the helium atom in two- and three-configuration approximations. Value Z(1s) is taken from ref. 5, Z(2s) = 3.50, Z(2p) = 5.50, and Z′(2p) = 4.34. The data in Table 2 show that our results are better not only in comparison with the values for the energy obtained using the customary analytic functions[2] but also in comparison with values obtained using Fock's numerical functions[1] in the same approximation.

We should mention that the usual analytic functions even in five-configuration approximations[2] (that is, with nine independent parameters), give poorer values for the

Table 2. The Energy of the Ground State of the Helium Atom in a Multiconfiguration Approximation (in atomic units)

	$1s^2 - 2s^2$	$1s^2 - 2p^2$	$1s^2 - 2s^2 - 2p^2$
I	−2.8797	−2.8963	−2.8995
II	−2.861	−2.870	−2.882
III	−2.8776	−2.8814	−2.8968

Notes: I – Calculation using the new functions: II – calculation using analytic functions;[12] III – experimental value.[13]

y than the new ones with three configurations. Only
-configuration approximations do Fock's numerical
ons lead to the value E = −2.9000,[1] practically
ing with the results we obtained with three configura-
pproximations.

ERENCES

a. I. Vizbaraite, V. I. Shironas, V. I. Kavetskis, and
. P. Yutsis, Opt. i Spektr. 1, 277 (1956).
. I. Kavetskis and A. P. Yutsis, Zhur. Eksptl. i
eoret. Fiz. 25, 257 (1953).
. Kröner, Z. Naturforsch. 15a, 260 (1960).
. P. Yutsis, Ya. I. Vizbaraite, I. V. Batarunas, and
. I. Kavetskis, Trudy Akad. Nauk Litovsk. SSR B2,
(1958).
5. G. S. Skvortsova, V. K. Shugurov, and K. K. Eringis, Trudy Akad. Nauk Litovsk. SSR B4, 27 (1959).
6. K. K. Eringis, Ya. I. Vizbaraite, and A. P. Yutsis, Trudy Akad. Nauk Litovsk. SSR B3, 67 (1961).
7. P. O. Löwdin, Phys. Rev. 97, 1509 (1955).
8. G. W. Pratt, Phys. Rev. 102, 1303 (1956).
9. G. Racah, Phys. Rev. 63, 367 (1943).
10. C. Eckart, Phys. Rev. 36, 878 (1930).
11. A. P. Yutsis, Zhur. Eksptl. i Teoret. Fiz. 23, 129 (1952).
12. A. P. Yutsis, Zhur. Eksptl. i Teoret. Fiz. 23, 357 (1952).
13. C. E. Moore, Atomic energy levels as derived from the analysis of optical spectra. U. S. Natl. Bur. Standards Circ. 467, At. Energy Levels 1, 309 pp. (1949).

THE EXCITATION OF ATOMS AND IONS BY ELECTRON IMPACT
I. Calculation Ignoring Exchange

L. A. Vainshtein (pp. 301-307)

Received 7 October 1960

The Born method and the distorted wave method (without exchange) are used to calculate the effective excitation cross sections for a large number of transitions in different atoms and ions. The results obtained by these two methods are evaluated, along with the importance of partial waves with large momenta.

nterest in the elementary excitation and ionization
sses is growing rapidly at the present time. This
gely due to the fact that a knowledge of the effec-
ross section of these processes is necessary in the
of gas discharge plasmas. Experimental data are
nadequate, despite many recept papers on experi-
al studies of the excitation and ionization functions
rticular by Frish's group in the USSR and by that
e and others in the USA). The excitation and ioni-
n of multiply charged ions is a particularly urgent
em. Systematic calculation of the cross sections of
cular processes by existing methods is very perti-
although new methods must also be developed.
The present paper gives the results of a calculation
ective cross sections in the Born approximation and
distorted wave approximation, ignoring exchange.
onsider this first step a necessary preliminary to
ore exact, but extremely involved, methods which
for exchange and electron correlation. Prelimi-
results of this type of calculation for the 1^1S-n^1P
ition in the He atom were published in ref. 1.
The derivation of the radial equations of collision
y was discussed in ref. 2 for hydrogen and in ref.
the general case. In the present paper, we will use
ymbols and definitions used in ref. 3. In the two-
approximation (ignoring transitions through inter-
ate levels) the problem reduces to the solution of a
m of two equations of the type:

$$\left\{\frac{d^2}{dr^2}-\frac{l(l+1)}{r^2}-2U_\Gamma(r)+k^2\right\}F_\Gamma(r)=2U_{\Gamma\Gamma'}(r)\,F_{\Gamma'}(r), \quad (1)$$

$$\left\{\frac{d^2}{dr^2}-\frac{l'(l'+1)}{r^2}-2U_{\Gamma'}(r)+k'^2\right\}F_{\Gamma'}(r)=2U_{\Gamma\Gamma'}(r)\,F_\Gamma(r), \quad (1')$$

e $\Gamma = \gamma LS\tilde{l}_{1/2}L_TS_T$ is the set of quantum numbers for the system, L_TS_T are the total momenta of the system, $\tilde{l}_{1/2}$ are the momenta of the partial wave of the outer electron, and γLS are the quantum numbers of the atom. If we ignore exchange interaction:

$$U_{\Gamma\Gamma'}=\sum_x a^x_{\Gamma\Gamma'}\frac{1}{r}\,y^x_{ll'}(r), \quad U_\Gamma=U^c_\Gamma+U_{\Gamma\Gamma'}, \quad (2)$$

$$y^x_{ll'}(r)=\int_0^r\left(\frac{r_1}{r}\right)^x P_l(r_1)\,P_{l'}(r_1)\,dr_1+\int_r^\infty\left(\frac{r}{r_1}\right)^{x+1}P_l(r_1)\,P_{l'}(r_1)\,dr_1, \quad (3)$$

where $P_l(r)$ and $P_{l'}(r)$ are the radial functions of the optical electron and U^c_Γ is the potential of the atomic residue.

An exact solution of system (1)-(1') is usually called the strong coupling approximation. The distorted wave approximation is obtained by dropping the right-hand side of Eq. (1). Then the equations of the system may be solved independently and the cross section of the transition γLS-$\gamma' L'S'$ can be expressed by

$$\sigma=\sum_{ll'}\sigma_{ll'}, \quad \sigma_{ll'}=\frac{16\pi a_0^2}{k^3k'}\sum_{L_T}\left|\int_0^\infty \bar{F}_\Gamma U_{\Gamma\Gamma'}\bar{F}_{\Gamma'}dr\right|^2. \quad (4)$$

Here $\bar{F}_\Gamma$ and $\bar{F}_{\Gamma'}$ are solutions of the homogeneous equation with asymptote:

$$F_\Gamma\sim\sin\left(kr-\frac{l\pi}{2}+\frac{z}{k}\ln 2kr+\delta_\Gamma\right), \quad (5)$$

where z is the charge of the excited ion.

The preliminary results given in ref. 1 showed that allowing for strong coupling affects the magnitude of the cross section relatively little. At the same time, the distorted wave approximation requires approximately one third the time and greatly simplifies the programming.

We can calculate the total Born cross section without recourse to a breakdown into partial waves:

$$\sigma^B = \frac{8\pi a_0^2}{gk^2} \sum_{MM'} \int_{k-k'}^{k+k'} |\langle \gamma LS | \sum_i e^{i\mathbf{sr}_i} | \gamma' L' S' \rangle|^2 \frac{ds}{s^3}. \quad (6)$$

Using the well-known expansion of a plane wave in spherical harmonics, and carrying out the summation over the magnetic quantum numbers, we obtain:

$$\sigma^B = \sum_{\varkappa=|l-l'|}^{l+l'} \sigma_\varkappa^B, \quad \sigma_\varkappa^B = \frac{8\pi a_0^2}{gk^2} \cdot \frac{(2\varkappa+1)\,Q_\varkappa}{[(2\varkappa+1)!!]^2} \int_{k-k'}^{k+k'} \rho_\varkappa^2(s) \frac{ds}{s^3}. \quad (7)$$

$$\rho_\varkappa(s) = (2\varkappa+1)!! \int_0^\infty P_0(r)\, P_1(r)\, j_\varkappa(sr)\, dr \to s^\varkappa \rho_{\varkappa'}, \quad (8)$$

$$s \to 0.$$

where j_κ is the spherical Bessel function, ρ_κ is the radial integral of the 2κ-pole radiative transition. Q_κ includes the part of the matrix elements which depend on the momenta, and has the same form as in the theory of electric multipole interactions. With a genealogical characterization of terms:

$$Q_\varkappa = (2S+1)(2L+1)(2L'+1) \begin{Bmatrix} l\ L\ L_1 \\ L'\ l'\ \varkappa \end{Bmatrix}^2 (2l+1)(2l'+1) \begin{pmatrix} l\ l'\ \varkappa \\ 0\ 0\ 0 \end{pmatrix}^2, \quad (9)$$

where L is the orbital momentum of the initial ion.

Equation (7) may be written in the form:

$$\sigma_\varkappa^B = q_\varkappa \Phi_\varkappa(x), \quad (10)$$

$$q_\varkappa = \frac{2f'_\varkappa}{\varepsilon_{01}^2} \pi a_0^2, \quad \Phi_\varkappa(x) = \frac{2^{\varkappa+2}(\varkappa+36\delta_{\varkappa 0})}{(\varkappa+1)\,x^2} \int_{x-x'}^{x+x'} \frac{[\rho_\varkappa(\varepsilon_{01}s_1)]^2}{\varepsilon_{01}^{\varkappa'}\rho_{\varkappa'}^2} \cdot \frac{ds_1}{s_1^3}. \quad (10')$$

$$\varkappa' = \varkappa + 2\delta_{\varkappa 0}.$$

The quantity f'_κ is simply related to the oscillator strength f_κ by:

$$f'_\varkappa = \left(\frac{mc^2}{E_{01}}\right)^{\varkappa-1} f_\varkappa = \frac{(\varkappa+1)(2\varkappa+1)\,Q_\varkappa \varepsilon_{01}^{\varkappa'}}{g2^\varkappa(\varkappa+36\delta_{\varkappa 0})[(2\varkappa+1)!!]^2} \rho_{\varkappa'}^2. \quad (10'')$$

Hereinafter, we will replace k and k' by the electron momenta x and x' in "threshold" units:

$$x = \sqrt{\frac{E}{E_{01}}} = \frac{k}{\varepsilon_{01}^{1/2}}, \qquad x' = \sqrt{x^2 - 1} = \frac{k'}{\varepsilon_{01}^{1/2}}, \quad (11)$$

where E_{01} is the excitation energy, and $\varepsilon_{01} = E_{01}/\mathrm{Ry}$ is the excitation energy expressed in Rydberg units. The functions $\sigma(x')$ have identical abscissa scales for very varied transitions.

Equation (7) corresponds to the expansion of σ in terms of multipole interactions. For approximate estimates it is usually sufficient to limit this to the first nonzero term for $\kappa = |l - l'|$. The quantity $q_{\kappa=|l-l'|}$ will hereinafter be designated simply by q. Calculations show that in most cases, σ is close to q for $x' \sim 1$ (see Table 2 below).

Calculations were carried out for a large number of transitions from the ground state and excited states in the following atoms and ions: H, He, Na, C^+, C^{2+}, C^{3+}, C^{4+}, C^{5+}. All the calculations were performed on an electronic computer using the same program. The program was universal and suitable for any atom or ion (thanks to the use of "threshold" units).

Owing to space limitations, we will give detailed results for the hydrogen atom only. For each transition, Table 1 gives the cross sections obtained in the Born approximation (B) and in the distorted wave approximation (DW). The bottom row gives the values of q calculated by using the same wave functions of the optical electron.

We now turn to the qualitative nature of the results obtained.

1. In most of the above calculations, we assumed that at energies of a few electron volts it was adequate to confine our attention to partial waves with minimum $\tilde{l}$ and $\tilde{l}'$. In fact, this is completely unjustified (see refs. 1, 5, 6). Figure 1 shows excitation cross sections of different transitions in the hydrogen atom (partial cross sections are identified by the values of $\tilde{l} - \tilde{l}'$, the total cross sections by σ). In addition, the sum of the partial cross sections with $l, l' \leq 6$ and the total Born cross section σ^B are given. It is easily seen that for the S-P transition, the partial cross sections (0-1) and (1-0) make a negligible contribution to σ. The (1-0) curve cannot be plotted on the scale of the diagram. At low velocities transition (2-1) is most important. For high velocities the number of partial waves increases rapidly, and at $x' >$ it apparently reaches some tens. Their further calculation raises great difficulties in all cases. However, since the wave with $\tilde{l} > 6$ is fairly accurately described by the Born approximation, we can calculate the total σ from the equation:

$$\sigma = \sigma^B + \sum_{ll'}^{6} (\sigma_{ll'} - \sigma_{ll'}^B).$$

It must be noted that this relationship of the partial cross sections is typical of distorted wave methods. In the Born approximation with $x' < 0.6$, the (1-0) transition predominates (Fig. 1b). However, in both approximations the transitions with $\Delta\tilde{l} = -1$ are considerably more important than those with $\Delta\tilde{l} = +1$.

A similar increase in the importance of the partial waves with high $\tilde{l}$ in the distorted wave approximation occurs for other transitions, although for S-S transitions (Fig. 1c) the sum of the partial cross section converges

Table 1. Excitation Cross Sections of the Hydrogen Atom (in units of πa_0^2)*

Transition x'	1^1S-2^1S		1^1S-3^1S		1^1S-2^1P		1^1S-3^1P		1^1S-3^1D		2^1S-3^1P		2^1P-3^1S		1^1S-4^1P		1^1S-4^1S	
	B	DW	B	DW	B	DW	B	DW	B	DW	B	DW	B	DW	B	DW	B	DW
0.2	129°	695°	237^{-1}	129°	412°	215°	757^{-1}	320°	814^{-2}	144^{-1}	488^{0}	276°	100^{1}	488^{0}	275^{-1}	142^{0}	862^{-2}	415^{-1}
0.4	214°	709°	388^{-1}	104°	779°	137^{1}	141°	344°	151^{-1}	257^{-1}	282^{1}	444^{1}	152^{1}	213^{1}	507^{-1}	130^{0}	140^{-1}	360^{-1}
0.6	245°	520°	439^{-1}	864^{-1}	106^{1}	147^{1}	187°	319°	197^{-1}	247^{-1}	675^{1}	206^{2}	155^{1}	218^{1}	669^{-1}	120^{0}	158^{-1}	303^{-1}
0.8	240°	415°	424^{-1}	702^{-1}	123^{1}	139^{1}	212°	292°	216^{-1}	225^{-1}	110^{2}	169^{2}	134^{1}	123^{1}	755^{-1}	108^{0}	152^{-1}	246^{-1}
1.2	189°	268°	328^{-1}	454^{-1}	131^{1}	129^{1}	218°	228°	200^{-1}	172^{-1}	170^{2}	193^{2}	104^{1}	102^{1}	765^{-1}	800^{-1}	117^{-1}	159^{-1}
1.6	140°	182°	240^{-1}	297^{-1}	121^{1}	114^{1}	196°	176°	161^{-1}	148^{-1}	191^{2}	189^{2}	857^{0}	791^{0}	681^{-1}	598^{-1}	854^{-2}	105^{-1}
2.0	104°	127°	177^{-1}	217^{-1}	106^{1}	990^{0}	168°	149°	126^{-1}	125^{-1}	188^{2}	177^{2}	733^{0}	671^{0}	581^{-1}	493^{-1}	628^{-2}	730^{-2}
2.4	785^{-1}	795^{-1}	134^{-1}	159^{-1}	919^{0}	850^{0}	143°	125°	980^{-2}	104^{-1}	—	—	—	—	492^{-1}	438^{-1}	473^{-2}	566^{-2}
q	259°		394^{-1}		144^{+1}		194°		487^{-1}		424^{2}		130^{1}		638^{-1}		135^{-1}	

*The mantissa and decimal multiplier are given. For example, 237^{-1} means 0.237×10^{-1}.

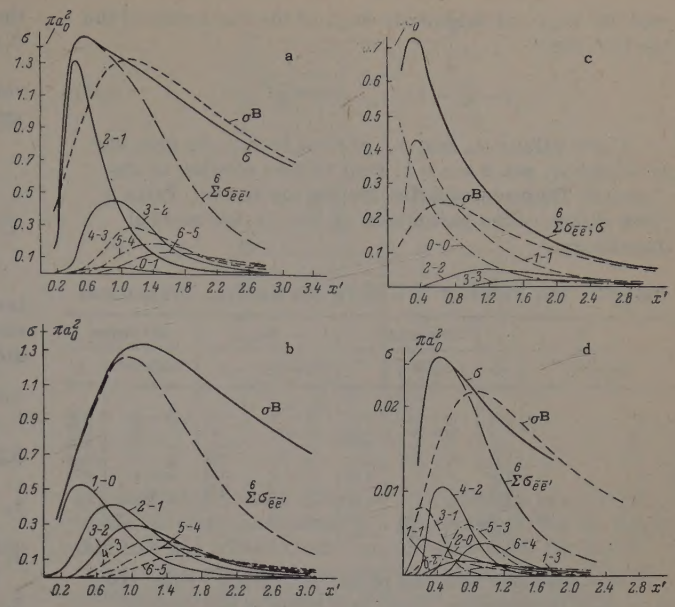

Fig. 1. Partial and total excitation cross sections for transitions; a, 1S-2P; c, 1S-2S; d, 1S-3D; and b, the Born excitation cross section for the transition 1S-2P in the hydrogen atom.

e rapidly owing to exponential damping of the potential $U_{\Gamma\Gamma'}$.

2. Calculation of the distortion of the incident and ered waves by the atomic potential leads to a shift e total scattering maximum towards the threshold . 1a, c, d). In almost all cases the maximum is at- d at $E < 0.1E_{01}$. For ions with $z > 1$, and also for sitions between excited levels, the increase of $\sigma(x')$ mes more rapid as $x' \to 0$ (Fig. 2). The distorted method (without exchange) therefore gives higher s sections than the Born method at low energies. At 1 the two methods give closely similar results for otal cross section, although the partial cross sec- may differ greatly.

The monotonic trend of the excitation function, ob- d almost from the very threshold, contradicts ex- mental data, at least for optically resolved transitions. The absolute values of the cross section in the range $x' < 2$ are apparently too high.

We should also note the anomaly in the $\sigma(x')$ curve for Na and several alkali-like ions—the excitation function has several maxima (Fig. 3).

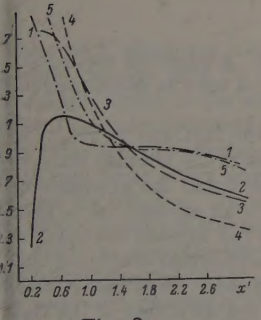

Fig. 2

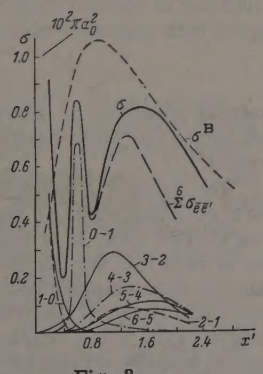

Fig. 3

Fig. 2. The excitation function plotted for various transitions in the distorted wave approximation. Atom (ion) and transition: curve 1—C^{4+}, 2S-3P; curve 2—He, 1S-2P; curve 3—He, 1S-6P; curve 4—He, 2S-2P; curve 5—C^{5+}, 2S-3P.

Fig. 3. Partial and total excitation cross sections for the transition 3S-3P in the sodium atom.

3. The field of the atomic residue U_Γ^c was calculated by using simple Slater-type analytical functions. The wave functions of the optical electron P_l and $P_{l'}$ were obtained by numerical integration of the semiempirical radial equation with a deformed atomic residue.[4] For transitions between states with $l = l'$ it is necessary to insure the most accurate possible orthogonality of the functions P_l and $P_{l'}$. Otherwise superfluous terms of the type $1/r$ appear in the nondiagonal potential $U_{\Gamma\Gamma'}$ which leads to excitation cross sections which are much too high (sometimes by 1-2 orders). To secure orthogonality, we must use identical scale multipliers for the field in the initial and final states of the atom. Here, only an insignificant deviation of the energy parameter of the final state from the experimental value is permitted.

In all cases except hydrogen, approximate atomic wave functions must be used. Calculations show that the sensitivity of σ to the type of wave functions is about the same as for the oscillator strength, so that σ/q, as a rule, hardly varies at all. For transitions with $\Delta l = 0$ this is true only when the functions are orthogonalized.

The diagonal potentials $U_{\Gamma\Gamma}$ and $U_{\Gamma'\Gamma'}$ contain terms corresponding to a multipole interaction [$\kappa \geq 2$ in Eq. (2)]. Calculations show that these terms are important only in the region $x' < 0.4$. If they are dropped, calculation for transitions of the type P-P, P-D, etc., are considerably simplified since then the function $\overline{F}_\Gamma$ is independent of L_T and the summation over L_T in (4) can be made analytically.

4. In some cases it is sufficient to use the Born approximation for estimates. Then a simple analytical equation can be used:

$$\sigma = q\Phi(x), \quad \Phi(x) = \frac{4c(x^2-1)}{x^2(x^2-1+a)}. \qquad (13)$$

Here q is given by Eq. (10') with $\kappa = \kappa_{min} = |l - l'|$ and the parameters a and c are determined from the

position (x_m) and magnitude (σ_m) of the maximum of the function $\sigma(x)$:

$$a = x_m^2 - 1 = x_m'^2, \quad c = \frac{\sigma_m x_m^4}{4q}. \qquad (13')$$

If the values x_m and σ_m are not known, we can, approximately, put a = c = 1. $\Phi(x)$ is then similar to the classical Thomson equation for the ionization. Table 2 gives values of the parameter $c_1 = \sigma_m^B/q$ for several transitions.

Table 2. The Value of $c_1 = \sigma_m^B/q$ for Several Transitions

H		He singlet		Na		C^{2+} singlet	
Transition	c_1	Transition	c_1	Transition	c_1	Transition	c_1
$1s-2p$	0.91	$1s-2p$	0.82	$3s-3p$	1.33	$2s-2p$	2.35
$1s-3p$	1.12	$1s-3p$	0.89	$4s-4p$	1.44	$2s-3p$	0.37
$2s-3p$	0.45	$2s-2p$	2.35	$3s-4p$	10.8	$2s-3s$	0.38
$2p-3s$	1.19	$2s-3p$	0.39	$3p-4s$	0.85	$2s-4s$	0.58
$1s-4p$	1.20	$1s-2s$	1.59	$3s-4s$	0.34	$2s-3d$	0.76
$1s-2s$	0.95	$1s-3s$	1.72	$3s-3d$	0.70	—	—
$1s-3s$	1.11	$2s-3s$	0.43	$3s-4d$	1.10	—	—
$1s-4s$	1.17	$1s-3d$	0.38	$4s-3d$	3.0	—	—
$1s-3d$	0.44	$2s-3d$	0.80	—	—	—	—

We must now note one point. According to Eq. (10'), $\sigma_m \sim \varepsilon_{01}^{-2}$. On the other hand, according to the general theorem on the maximum of the cross section, $\sigma_1(x) \leq (2l+1)k^{-2} = (2l+1)x^{-2}\varepsilon_{01}^{-1}$. Since in the region $x \sim x_m \sim \sqrt{2}$, only 2-3 waves contribute to the cross section, we must expect the value of the total cross section also to be proportional to ε_{01}^{-1} and not to ε_{01}^{-2}. Therefore the Born method introduces a particularly large error for $\varepsilon_{01} \leq 1$ (at $f' \approx 1$). Apparently, this is the reason for the success of Seaton's modification of Bethe's method in the case of the 3s-3p transition in the sodium atom (ε_{01} 0.155).

Equation (13) can easily be averaged over a Maxwe velocity distribution. The resulting excitation frequenc is:

$$\langle v\sigma \rangle = 4.3cq \cdot \left(\frac{\varepsilon_{01}}{a}\right)^{1/2} e^{-\beta} u(\beta a), \quad \beta = \frac{E_{01}}{kT}, \qquad (1$$

$$u(z) = 2z^{1/2}[1 + ze^z E_1(-z)] < 0.8,$$

$$u(z) \approx 2z^{1/2} \text{ for } z \ll 1, \quad u(z) = 2z^{-1/2} \text{ for } z \gg 1. \qquad (1$$

Finally, I wish to thank N. A. Yavlinskii for his interest in the work and his cooperation in the machine computation, and also G. G. Dolgov for frequent discussion of the results.

REFERENCES

1. L. A. Vainshtein and G. G. Dolgov, Opt. i Spektr. 7, 3 (1959), Optics and Spectroscopy 6, 80 (1959).
2. I. Percival and M. Seaton, Proc. Cambridge Phil. Soc. 53, 654 (1957).
3. L. A. Vainshtein and I. I. Sobel'man, Zhur. Eksptl. i Teoret. Fiz. 39, 767 (1960), Soviet Phys.-JETP 12, 536 (1961).
4. L. A. Vainshtein, Opt. i Spektr. 3, 313 (1957).
5. H. S. W. Massey, Handbuch der Physik vol. 36, p. 38 (1956).
6. M. Blaha, Bull. Astron. Inst. Czechoslov. 9, 160 (1958).
7. M. J. Seaton, Proc. Phys. Soc. A68, 457 (1955).

A DIRECT METHOD OF MEASURING THE MEAN LIFETIME OF EXCITED IONIC LEVEL

Yu. M. Kagan and Ya. P. Koritskii (pp. 308-311)

Received 19 October 1960

A method is suggested for measuring the mean lifetime of excited ionic levels. Measurements of the n = 4 level of He II give values which agree with quantum-mechanical values in order of magnitude.

1. In order to solve many physical problems it is necessary to know the values of such atomic constants as the mean lifetime of excited levels. The only direct methods which we know of for determining the mean lifetime of excited atoms and ions are based on the well-known idea of Wien, which makes use of observation of the attenuation of emission from excited atoms or ions as a function of either the distance from the point of excitation[1,2] or the time elapsed since the start of the emission.[3] The main difficulty with the first type of experiment is the impossibility of precisely localizing the point of excitation. In the second type of experiment, it is difficult to precisely determine the amount of error introduced by the apparatus (the method of delayed coincidence). Moreover, in both types of experiment important secondary processes may occur in the medium in which the excitation takes place (collisions of the second kind, diffusion of radiation, etc.). Because of these drawbacks, and also because the number of papers devoted to the determination of the mean lifetime of atoms and ions by direct methods is very small, a consideration of other methods should be of interest. A possible method of measuring the mean lifetime of ions is discussed in thi article.

The method is based on the fact that an electron beam colliding with gas atoms in the normal state creates excited ions. It is assumed that the pressure of th gas is such that the lifetime of an excited ion is less than the time elapsing before the excited ion collides with a gas atom. If there is a constant electric field present, then in the course of their lives the ions have time to acquire a velocity in the direction of the field. Measurement of this velocity makes it possible to determine the mean lifetime of an excited ion.

If the atoms from which the ions are formed are in random motion, the mean drift velocity of the ions $\bar{v}_2$ i connected with the mean lifetime of ions in the excited state by the relationship[4]

$$\bar{v}_2 = \tau \frac{eE}{M},$$

where e and M are the ionic charge and mass, re-

tively, and E is the electric field strength. The
n drift velocity $\bar{v}_2$ can be measured by the Doppler
of the ionic line

$$\delta\lambda = \lambda \frac{\bar{v}_2}{c} = \lambda\tau \frac{eE}{Me}. \qquad (2)$$

2. The electron gun used in our work is shown in
1. The electron source was an elongated tungsten
ode in the form of a helix, 1.4 cm long and 0.5 cm in
eter. The diameter of the wire was 0.25 mm, and
eating current amounted to about 5 amp. The ac-
rating anode A_1 was placed at a distance of 2 mm
the cathode. A second anode A_2 was placed at a
nce of 2 mm from A_1. The apertures in the anodes
nd A_2 were rectangles measuring 0.4 × 1 cm. The
ron collector A_3 and the anode A_2 were at the same
ntial. Ions formed as a result of collisions between
rons and atoms of the gas moved under the action
e field between grids C_1 and C_2 (openings in the
were 0.5 × 0.5 mm). The voltages on the elec-
s were obtained from an electronically regulated
ly. The electron energy, determined by the potential
ode A_2 relative to cathode K, in our case was 250
. The electron gun current was 4-5 ma; the field
gth in the space between grids C_1 and C_2 was 120
/cm. An investigation of the field distribution be-
n the grids, which was performed by an electrolytic
method, showed that in the center of the region
which radiation was observed the deviation of the
ric field from homogeneity did not exceed 20%. The
was filled with spectrally pure helium at a pres-
of 3×10^{-2} mm Hg. Under these conditions the time
een collisions of an excited ion with atoms is $\sim 10^{-6}$
which is several orders of magnitude greater than
fetime of an excited ion.

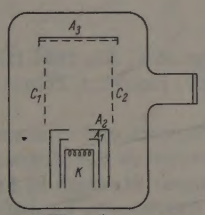

Fig. 1

The line studied was He II 4686 A. Observations
made through grid C_2 using a glass double-prism
trograph, made in the shops of Physico-Technical
ntific Research Institute, Leningrad University, and
ort focal length camera. A Fabry-Perot etalon with
d 10 mm Invar rings was placed between the colli-
or and the prisms. The plates were made of fused
tz with multiple dielectric coatings.

In order to measure the small shifts δλ we used
nethod discussed in ref. 5. Using a slit whose jaws
movable independently of one another, we obtained
successive photographs of the interference rings of
given line, looking along the direction of the field and
e opposite direction, respectively. The quantity 2δλ
calculated from the displacement of neighboring rings.
ause of the very low intensity of the line under study
exposures were as long as 12 hr.

3. The 4686 A line of He II is emitted during a trans-
from the fourth quantum level to the third. The
n scheme corresponding to this line is presented in
2. The wavelengths of the more intense components

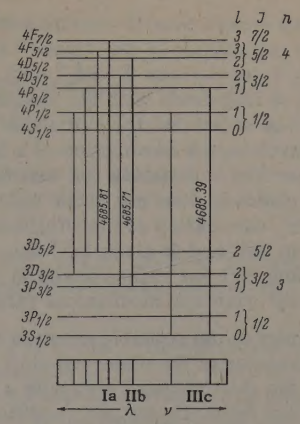

Fig. 2

are indicated on this diagram. The relative intensities of the various components are presented in Fig. 3. Since this line has a broad and complex structure, the use of our etalons resulted in an overlapping of components of different orders. Pictures obtained using etalons of thicknesses t = 10 and 5 mm are shown in Figs. 4a and 4b, respectively. For the line investigated, the etalon constant Δλ was 0.22 A for the 5-mm etalon and 0.11 A for the 10-mm etalon. Because of the fact that in helium the Doppler width of lines is large ($\sim 3 \times 10^{-2}$ A for our line), all of the components in Fig. 4a and two of the components in Fig. 4b are unresolved. Under our conditions the Doppler width was several times greater than the instrumental width. The constancy of temperature and pressure during the exposure were demonstrated by the absence of any shift of atomic lines.

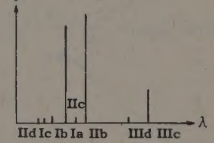

Fig. 3

δλ was calculated by means of the formula

$$\delta\lambda = \left(1 + \frac{\Delta x_{k,\,k+1}}{\theta_k}\right) \frac{\delta x_k}{\Delta x_{k,\,k+1}} \Delta\lambda, \qquad (3)$$

where $\Delta x_{k,k+1}$ is the distance between rings k and k + 1; θ_k is the diameter of the k-th ring; δx_k is the shift in the k-th ring; $\Delta\lambda = \lambda^2/2t$ is the etalon constant. Measurements were made on the second ring. Values of τ calculated by Eq. (2) from four different films gave results ranging from 0.7×10^{-9} to 1.1×10^{-9} sec.

Comparison with quantum-mechanical data for the 4686 A line[6] is complicated by the fact that our results refer not to the lifetime of a separate component of this

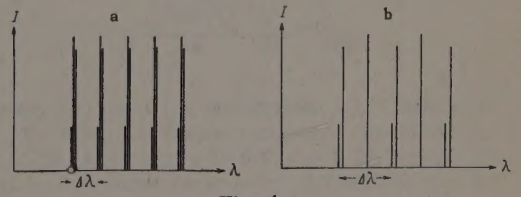

Fig. 4

line but to some average over the components. A quantum-mechanical calculation of the "mean" lifetime of an ion in the n = 4 level gives 2×10^{-9} sec, which agrees in order of magnitude with the results we obtained. It should be noted that the calculation of "mean" lifetime itself involves the assumption of a Boltzmann distribution of excited ions among the various sublevels of n = 4, which probably does not occur under our conditions. However, calculation of the lifetimes of the individual levels 4p, 4d, and 4f gives 10^{-9} sec. We can therefore conclude that our values agree in order of magnitude with the quantum-mechanical values.

4. Let us analyze the possible sources of error. The Doppler character of the observed shift was shown by the fact that the shift changed sign with a change in the direction of the field. Under our conditions the Stark effect had no significance because of the lowness of the electron concentration in the beam (in our case it was about 10^8). For this same reason the beam causes practically no distortion of the external field between the grids. It is easy to show that the shift caused by the transfer of the components of the momentum of the electron in the direction of the field from electron to ion or atom in the excitation process is several times less than the shift of ionic lines which we observed. This was confirmed by the absence of any measurable shift of the atomic lines. Stepwise excitation of an ion, i.e., excitation by collision of an electron with the ion, leads to an increased shift because the ion acquires a certain velocity in the field before excitation. In this case Eq. (2) is not applicable. The absence of this effect was proven by the linear dependence of the intensity of the 4648 A line on the current density in the beam (Fig. 5). The maximum current density that we used did not exceed that used in ref. 1, in which a linear dependence was also observed.

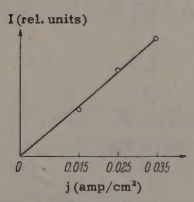

Fig. 5

Cascade transitions can lead to an increase in the observed mean lifetime. The role of these transitions may be evaluated in the following way: The decrease of the number of excited particles in the state i is given by an equation of the form

$$-\frac{dn_i}{dt} = \frac{n_i}{\tau_i} - \sum_{i+1}^{\infty} n_k A_{ki},$$

where n_k is the concentration of particles in the higher excited level. Let us set $n_k = n_1$, which in every case augments the role of cascade transitions. Then

$$-\frac{dn_i}{dt} = \frac{n_i}{\tau_i}\left[1 - \tau_i \sum_{i+1}^{\infty} A_{ki}\right].$$

The quantity $\tau_i \sum_{i+1}^{\infty} A_{ki}$ for our level has the same value as the summation for the same level in hydrogen. According to ref. 6, this summation for n = 4 is equal to about 15%. Thus, the role of cascade transitions is insignificant under our conditions.

The contour of ionic lines in a field is asymmetric. Generally speaking, this can cause difficulties in measuring the shifts. Obviously, the degree of asymmetry must depend on the parameter $\bar{v}_2/\bar{v} = \tau eE/M\bar{v}$, where $\bar{v}$ is the thermal velocity of the ions. Under our condition this parameter amounts to ~0.7. More precise calculat of the contour shows that the asymmetry in this case is negligible. This has been confirmed experimentally.

The measurement process itself involved certain errors. The observed shift was very small (of the orde of hundredths of a millimeter). The highly sensitive film that was used had coarse grain and was subject to fogging. In addition, the two halves of the line were not always equally intense. However, these errors do not alter the order of magnitude of the measured value.

REFERENCES

1. L. Maxwell, Phys. Rev. **38**, 1664 (1931).
2. M. Ardenne, Zhur. Eksptl. i Teoret. Fiz. **26**, 362 (1954).
3. A. Osherovich, Reports and Communications from a Conference Devoted to the Measurement and Calculation of Oscillator Strength in Atomic Spectra. Leningrad State University, Leningrad, 1959.
4. Yu. Kagan and V. Perel', Vestnik Leningrad. Univ. No. 16, 49 (1959).
5. S. Frish and Yu. Kagan, Zhur. Eksptl. i Teoret. Fiz. **17**, 577 (1947).
6. H. A. Bethe and E. E. Salpeter, Quantum mechanics of one- and two-electron systems, Handbuch der Physik, Chapter 3. Springer, Berlin, 1933.

TIME RESOLVED EMISSION SPECTRA OF A SPARK DISCHARGE IN INERT GASES IN THE REGION 5000-10,000 A

M. P. Vanyukov, V. R. Muratov, and I. A. Mukhitdinova (pp. 312-318)

Received 8 October 1960

The instantaneous spectra of spark discharges in helium, neon, argon, krypton, and xenon were investigated by the accumulation method, using highly sensitive 3-channel equipment.

The time-resolved emission spectra of spark dis-ges in argon, krypton, and xenon between 2500 and A were studied in ref. 1. A photoelectric method used in these investigations. The time-resolved tra were recorded from the screen of an oscillo-e using a "mask" method.[2,3] The disadvantage of this procedure is the fact that its threshold sensitivity, which is determined by photocurrent fluctuations, cannot be improved beyond certain limits which depend on the parameters of the equipment and the light source investigated.[3] In the light of this, much can be expected from equipment based on the accumulation principle.[4,5]

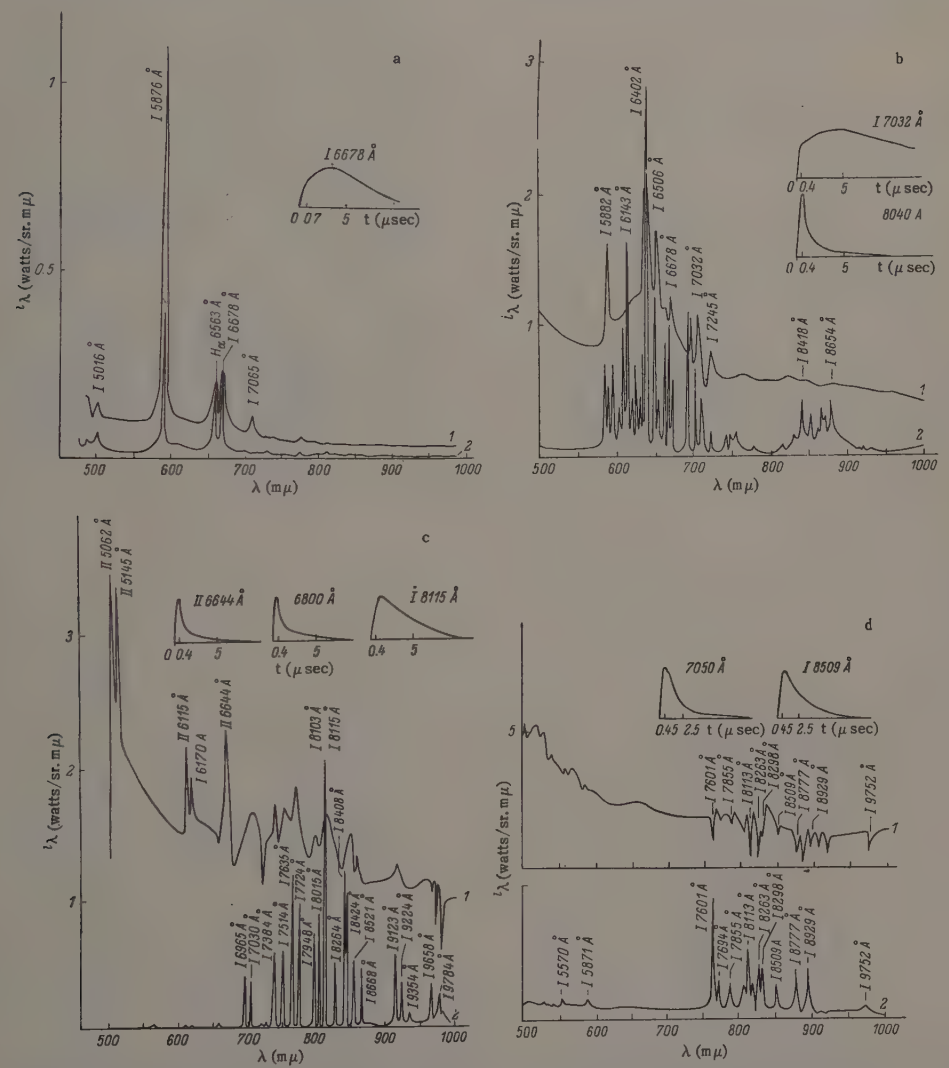

Fig. 1. Spectral density i_λ of the discharges in helium (a), neon (b), argon (c), and krypton (d). Conditions and parameters of the discharge: a—P = 10 atm, C = 0.05μf, U = 6 kv, L = 0.2 μh, t in μsec: curve 1—0.7, curve 2—5; b—P = 14 atm, C = 0.05 μf, U = 6 kv, L = 0.2 μh, t (in μsec): curve 1—0.4, curve 2—5; c—P = 2 atm, C = 0.05 μf, U = 6 kv, L = 0.2 μh, t (in μsec): curve 1—0.4, curve 2—5; d—P = 3.5 atm, C = 0.05 μf, U = 6 kv, L = 0.2 μh, t (in μsec): curve 1—0.45, curve 2—2.5.

In this case, it is possible to work at practically any sensitivity because of the increased observation time resulting from the increase in the number of discharges measured.

In this work, a new and highly sensitive method was used to obtain the time-resolved emission spectra of spark discharges in inert gases in order to widen the scope and improve the accuracy of previously[1] obtained data on these spectra.

EXPERIMENTAL RESULTS

The time-resolved spectra were obtained with equipment having a time resolution of ~5 × 10^{-8} sec and a spectral resolution of ~0.2 A.[5] The width of the spectral interval isolated by the monochromator was varied from 2 to 10 A during the exposure. The absolute spectral density values were determined with the aid of a special light source which was calibrated in energy units (the calibration of the source was performed at the Actinometric Laboratory of the All-Union Scientific Research Institute of Metrology). The spark discharges occurred in demountable pulse discharge tubes filled with helium, neon, or argon, and in sealed lamps filled with krypton and xenon.

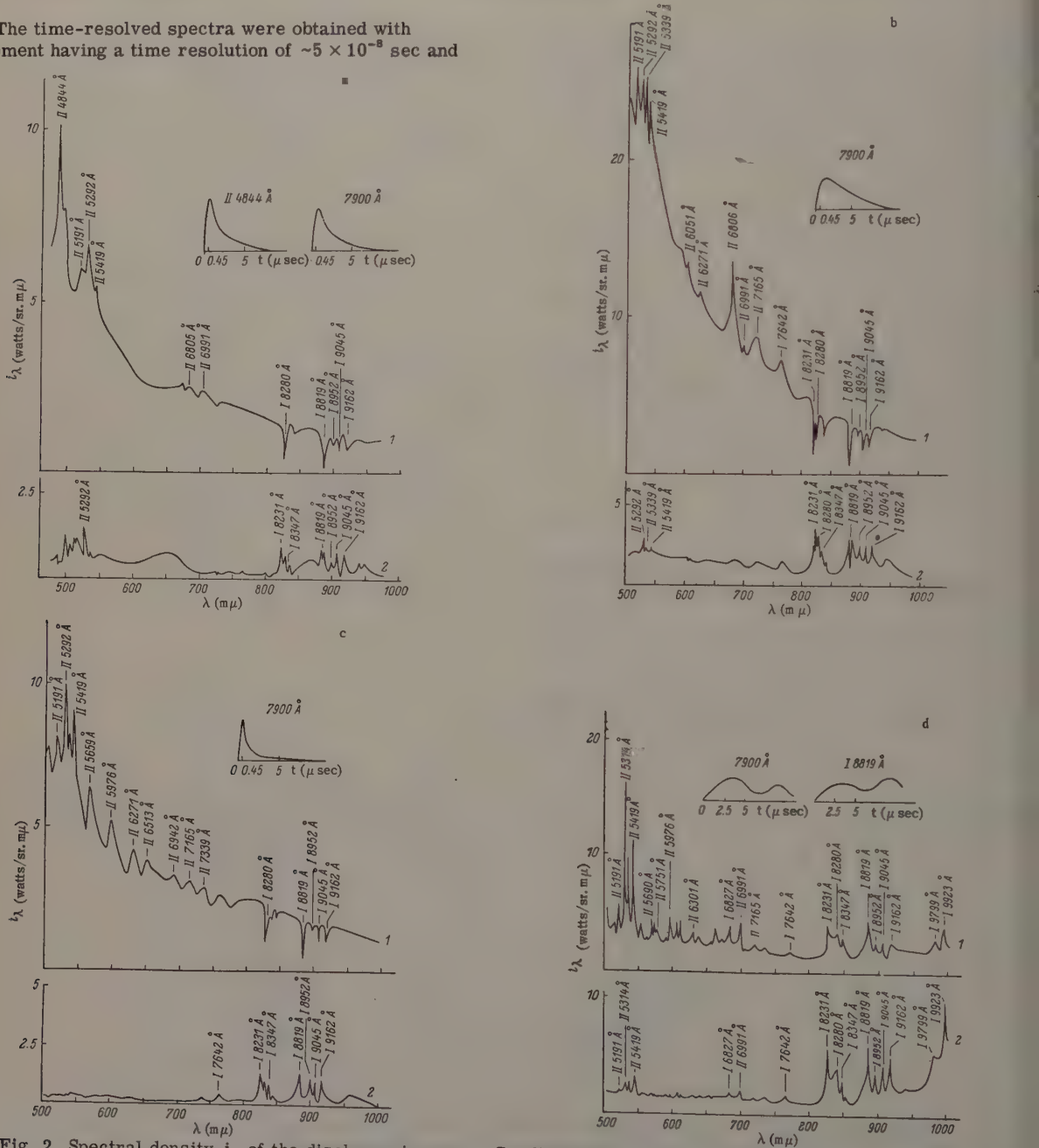

Fig. 2. Spectral density i_λ of the discharge in xenon. Conditions and parameters of discharge: a—P = 5 atm, C = 0.05 μf, U = 6 kv, L = 0.2 μh, t (in μsec): curve 1—0.45, curve 2—5; b—P = 5 atm, C = 0.05 μf, U = 12 kv, L = 0.2 μh, t (in μsec): curve 1—0.45, curve 2—5; c—P = 5 atm, C = 0.01 μf, U = 12 kv, L = 0.2 μh, t (in μsec): curve 1—0.45, curve 2—5; d—P = 5 atm, C = 0.05 μf, U = 12 kv, L = 54 μh, t (in μsec): curve 1—2.5, curve 2—5.

The instantaneous values of the spectral density e measured at different intervals after the beginning ne discharge. The results of the measurements of ctral density i_λ in helium, neon, argon, krypton, and on at the same discharge energy (~1 joule) are shown igs. 1 and 2a. Oscillograms of the intensity of the k discharge in narrow spectral intervals (~10 A) are given on these figures.

Investigation of the spectra shows that as the atomic ber of the gas increases, there is an increase in the nsity of the discharge, accompanied by the appearance bsorption lines in the long wavelength region of the ctra. At first an intense continuous background is ob- ed, on which very highly broadened (and therefore in y cases unresolved) spectral lines are superimposed. eavy gases ionic lines are observed during the first ments. Subsequently, the continuous background and spark lines rapidly fade out, but the arc lines are tted for a long time. The light intensity decreases h faster in the visible region than in the infrared.

Emission spectra of spark discharges in xenon, re- ded at various values of the discharge parameters, presented in Fig. 2. Investigation of the spectra ws that as the working voltage and capacitance in- ase, there is a general increase in the instantaneous es of the light intensity, especially in the visible re- of the spectrum. Increasing the inductance con- erably reduces the intensity of the continuous back- und in the visible region, but has almost no effect in infrared.

The dependence of the spectral density on various charge parameters was investigated for the wave- gths of some arc and spark lines, and also for the tinuous background. It was established that as the tage and capacitance increase and the inductance de- ases, there is an increase in the growth of the light ensity. The growth rate decreases with increasing atomic number and decreasing excitation energy of atoms which emit light of the given wavelength. Thus, for example, in the discharge in xenon, the light intensity in the infrared region does not change when the inductance is reduced from 3.6 to 0.2 μh.

The dependence of intensity on pressure was investigated for the discharge in argon. It was established that the intensity of AI 8115 A is practically independent of pressure, whereas the intensities of AII 6643 A and the background at 6800 A increase with increasing pressure.

The results obtained show that absorption of the emitted light plays an important part in the discharge. Since the coefficient of absorption of the continuous spectrum increases with increasing atomic number, and since the wavelength dependence of the coefficient of absorption[6] is determined by fhe factor $(e^{h\nu/kT} - 1)/\nu^3$, the strongest absorption is observed in the long wavelength region of the spectra of spark discharges in heavy inert gases. This was confirmed by experiment.

REFERENCES

1. M. P. Vanyukov, A. A. Mak, and V. R. Muratov, Opt. i Spektr. **6**, 17 (1959), Optics and Spectroscopy **6**, 8 (1959).
2. M. P. Vanyukov and L. D. Khazov, Doklady Akad. Nauk SSSR **92**, 523 (1953).
3. M. P. Vanyukov, A. A. Mak, and V. R. Muratov, Opt.-Mekh. Promyshl. No. 12, 36 (1958).
4. B. A. Ermakov and A. A. Mak, Pribory i Tekh. Ekspt. No. 3, 94 (1959).
5. M. P. Vanyukov, B. A. Ermakov, A. A. Mak, and V. R. Muratov, Vestnik Leningrad. Gosudarst. Univ. No. 16, Ser. Fiz. i Khim. No. 3, 25 (1959).
6. H. Maecker and T. Peters, Z. Physik **139**, 448 (1954).

RESTRICTED MOTIONS IN TRANSITION METAL COMPLEXES

I. B. Bersuker (pp. 319-324)

Received 12 September 1960

It is shown that restricted motions which lead to a splitting of the energy levels of the system are possible in certain free octahedral complexes of transition metals. These motions arise by virtue of the presence of three equivalent equilibrium configurations of the ligands, corresponding to the three possible directions of distortion of the octahedron in connection with its internal asymmetry. The height of the potential barrier between these configurations is determined in the crystal-field theory approximation, and the magnitudes of the splittings of the levels are computed on the assumption that the potential surface consists of parabolic hollows. Examples of the numerical calculations are presented for certain aquo complexes, from which it follows that these splittings may be detected by microwave methods.

INTRODUCTION

It is known that the equilibrium configuration of the ligands around the central ion in the 6-coordinated complexes of certain transition metals (and rare-earth elements) does not correspond to the highest possible symmetry, i.e., to a regular octahedron, even when these complexes are free and all the ligands are identical. The deviations of the positions of the ligands from the positions of maximum symmetry—the "internal asymmetry"—find an explanation, in principle, on the basis of the Jahn-Teller theorem. In the previous work[1] we carried out an investigation of the internal asymmetry for high-spin ionic complexes (the weak-field case) with the electronic configuration of the central ion being d^n (above the closed shells), where n = 1, 2,...10; and formulas for the quantitative characterization of this asymmetry were obtained in the crystal-field theory approximation. It was shown that the equilibrium configuration of six identical ligands in the cases d^1, d^2, d^4, d^6, d^7, and d^9 corresponds to a tetragonally distorted octahedron, in which one diagonal is shorter or longer than the other two. It is essential that, in the case of internal asymmetry, three directions of distortion of the octahedron are possible, and consequently there exist three equilibrium configurations which are equivalent to each other. In this connection, there arises the question of the possibility of transitions among these configurations, which, when potential barriers are present, should have the character of restricted motions and should lead to a splitting of the corresponding energy levels. In the present communication, the results of an examination of this question are set forth.

THE EQUIVALENT CONFIGURATIONS

The possibility of the appearance of restricted motions is connected with the presence of several equivalent equilibrium configurations of the system, which are determined by the minima of the potential energy surface. For an ionic complex of the type AB_6, in the crystal-field theory approximation (for the case of a weak field), one can obtain an approximate expression for this surface as a function of the interatomic distances.[1] For the central-ion electronic configurations d^n (n = 1, 2, 4, 6, 7, and 9), it has three equivalent hollows, each of which contains a minimum of the surface. In the three equivalent equilibrium configurations of the complex which correspond to these minima (we shall designate them by I, II, and III), the ligands are located in pairs on three mutually perpendicular axes, and the equilibrium distances from the central ion satisfy the following relations:

$$\left.\begin{array}{lllll} \text{I} & R_{01}=R_{04}, & R_{02}=R_{05}=R_{03}=R_{06}, & R_{01}\gtrless R_{02}, \\ \text{II} & R_{02}=R_{05}, & R_{01}=R_{04}=R_{03}=R_{06}, & R_{02}\gtrless R_{01}, \\ \text{III} & R_{03}=R_{06}, & R_{01}=R_{04}=R_{02}=R_{05}, & R_{03}\gtrless R_{01} \end{array}\right\} \quad (1)$$

(the numbering of the ligands is chosen so that the opposite pairs are formed by ligands 1-4, 2-5, and 3-6 respectively.)

Each of the three equilibrium configurations (1) corresponds to a tetragonally distorted octahedron, in which one diagonal is either shorter or longer than the other two (a shortened or a lengthened octahedron). For configuration I, diagonal 1-4 is different from the others; for configurations II and III, diagonals 2-5 and 3-6 respectively. The difference in the lengths of the two diagonals $\xi = 2|R_{01} - R_{02}|$ is the same in all three cases; if ξ is assumed to be small we can obtain

$$\xi = \frac{a}{K}, \quad (2)$$

where

$$a = \left(\frac{2\mu_{\text{eff.}}}{21}\right)\left[9F_2''(R_0) - 5F_4''(R_0)\right] \quad (3)$$

for the central-ion electronic configurations d^1 or d^6 and for ligands which are point dipoles with the effective dipole moment $\mu_{\text{eff.}}$ (for ligands which are point ions the formula is analogous), and

$$a = \left(\frac{\mu_{\text{eff.}}}{14}\right)\left[12F_2''(R_0) + 5F_4''(R_0)\right] \quad (4)$$

in the case of the electronic configurations d^4 and d^9;

$$F_n(R) = \left(\frac{1}{R^{n+1}}\right)\int_0^R r^n f^2(r)\, r^2 dr + R^n \int_R^\infty \left(\frac{1}{r^{n+1}}\right) f^2(r)\, r^2 dr, \quad (5)$$

f(r) is the radial part of the wave function of the corresponding d-electron and $K = k_{11} - 2k_{12} + k_{14}$, where the k_{ij}'s are the force constants of the complex. The value of K corresponds to the restoring force coefficient in a type e_g normal vibration of the complex.

In the cases of the central-ion electronic configurations d^1 and d^6, the equilibrium octahedra are shortened; for d^9 and d^4 they may be either shortened or lengthened; and for d^2 and d^7 they are lengthened. In the latter cases (d^2 and d^7), the magnitude of the internal asymmetry ξ

ry small, so that this case (like d^3, d^5, d^8, and d^{10} is insignificant from the standpoint of restricted ons.

Since the energy values and the symmetry of the ronic wave functions are identical for the equilibrium gurations I, II, and III, and the positions of the min- (and the shape of the potential surface) are sym- ic, these configurations are equivalent.

GHT AND SHAPE OF THE POTENTIAL BARRIER

Between the different equilibrium configurations of omplex there exists a potential barrier, the transi- probability through which determines the possibility e establishment of restricted motions. Determina- of the shape of the barrier, which requires a com- investigation of the potential energy surface as a tion of many variables, encounters great difficulties. efore, we limit ourselves to the assumptions usual ch cases about the shape of the barrier, reinforced ertain indirect considerations. Here we take into unt that the splitting of the levels which we seek de- s not so much on the shape of the barrier as on the enclosed by it; i.e., it depends in large measure on eight and on the distance between the minimum ts, which are open to an approximate estimate. On asis of symmetry considerations, we assume that most energetically favorable transitions (i.e., those acterized by minimum barrier height) are those be- n configurations with different directions of distor- of the octahedron, in which the ligands do not depart their locations on three mutually perpendicular . For such a transition, evidently, one pair of ligands most distant ones) approaches the central ion and her pair moves away from it, which corresponds to e e_g doubly degenerate normal vibration of the com- (the double degeneracy arises on account of the two pendent possibilities of such a motion). Such a transi- mechanism by means of type e_g vibrations seems t probable to us.

By substituting into the expression for the many-di- sional potential energy surface the values of the an- which correspond to the location of the ligands on e mutually perpendicular axes, we obtain a certain s section of it; i.e., a potential surface which de- ls only on the absolute distances of the ligands from central ion. The unsymmetrical part of this surface, ch is most significant for us, has the form—for the figurations d^0 and d^4, for example—:

$$A_{1g}) = \mu_{\vartheta\phi\phi}\left\{\sum_{i=1}^{6}\psi(R_i) + \frac{2}{7}\left[\sum_{i=1}^{6}\varphi^2(R_i) - \frac{1}{2}\sum_{i\neq k}^{6}\varphi(R_i)\varphi(R_k) + 3\left(\varphi(k_1)\varphi(R_4) + \varphi(R_2)\varphi(R_5) + \varphi(R_3)\varphi(R_6)\right)\right]^{1/2}\right\}, \quad (6)$$

re

$$\psi(R) = F_0'(R) + \left(\frac{1}{3}\right)F_4'(R), \qquad \varphi(R) = F_2'(R) + \left(\frac{5}{12}\right)F_4'(R).$$

This expression attains its greatest limiting value n $R_1 = R_2 = R_3 = R_4 = R_5 = R_6$, which corresponds to regular octahedral configuration. At this point, con- iently, the maximum of the potential barrier is ched. However, no single derivative of the potential face exists at that point, which allows us to assume the parabolic shape of the potential surface near the minima remains so up to the point where the value of the barrier is greatest. The assumed shape of the potential barrier is shown schematically in the figure. Some conventional parameter which characterizes the deviation of the equilibrium configuration of the complex from the regular octahedral configuration (for example, the normal coordinate for the e_g vibration) is laid off along the 0_x axis.

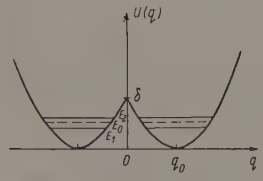

An analogous situation exists for the electronic configurations d^1 and d^6.

For the height of the barrier, we have

$$\delta = E'' - E', \quad (7)$$

where E″ is the energy of the complex for the regular octahedral configuration and E′ is the energy of the complex at the minimum points. In ref. 1 we determined the magnitude of the additional term splitting ΔE which arises on transition of the system from the regular octahedral configuration into the equilibrium configuration. Knowing ΔE, one can easily determine δ as well, if one uses the theorem of the conservation of the center of gravity of a multiplet. For the configurations d^9 and d^4, the ground energy level A_{1g} is obtained as a result of the splitting of the doubly degenerate (for the regular octahedral configuration) term E_g into the nondegenerate ones A_{1g} and B_{1g}. Consequently,* $\delta = (1/2)\Delta E$. For the term

*Here we do not take into account any change in the energy of the skeleton.

splitting, we found[1] $\Delta E = (2/3)K\xi^2$, in consequence of which

$$\delta = \left(\frac{1}{3}\right)K\xi^2. \quad (8)$$

The height of the potential barrier for the electronic configurations d^1 and d^6 is also computed according to the same formula.

THE SPLITTING OF THE ENERGY LEVELS

Let us assume that the vibrations of the complexes near the three equivalent equilibrium positions I, II, and III may be described by the wave functions ψ_I, ψ_{II}, and ψ_{III} respectively. Since the energy E_0 of these three states is the same, we have to consider here a case of triple degeneracy. However, if we take account of the possibility of transitions of the system from one equilibrium state to another (i.e., the nonstationary character of each of these states), then the degeneracy, generally speaking, is removed and the energy level is split. It is easy to show that the proper zero-order functions in the case under consideration will be the following linear combinations of the starting functions:

$$\left.\begin{aligned}\Psi_1 &= \left(\frac{1}{\sqrt{3}}\right)(\psi_I + \psi_{II} + \psi_{III}),\\ \Psi_2 &= \left(\frac{1}{\sqrt{6}}\right)(2\psi_I - \psi_{II} - \psi_{III}),\\ \Psi_3 &= \left(\frac{1}{\sqrt{2}}\right)(\psi_{II} - \psi_{III}).\end{aligned}\right\} \quad (9)$$

For the state Ψ_1, the energy E_1 lies below E_0, while for Ψ_2 and Ψ_3 the energies coincide and are equal to E_2, which lies above E_0. Consequently, the vibrational level E_0 is split into two.

The magnitude of the splitting, $E_2 - E_1$, may be approximately found in the following way. Let us write down the Schrödinger equations (one-dimensional) for ψ_I and Ψ_1, multiplying the first by Ψ_1 and the second by ψ_I; let us subtract one from the other, term by term, and integrate from 0 to ∞. Taking into account that at the point zero (the barrier maximum) the three functions ψ_I, ψ_{II}, and ψ_{III} are equal to each other and the sum of their derivatives equals zero, and assuming that these functions overlap each other only slightly, we may obtain[2]

$$E_1 - E_0 = \left(-\frac{3\hbar^2}{2M}\right)\psi_I(0)\,\psi_I'(0),$$

where M is the mass of the oscillator.

Analogously,

$$E_2 - E_0 = \left(\frac{3\hbar^2}{4M}\right)\psi_I(0)\,\psi_I'(0),$$

and, consequently,

$$E_2 - E_1 = \left(\frac{9\hbar^2}{4M}\right)\psi_I(0)\,\psi_I'(0). \qquad (10)$$

Since we have assumed that the potential surface has a parabolic shape with a fairly high barrier, we may take the usual oscillator functions for the function ψ_I. For the ground state

$$\psi_I = \left(\frac{M\omega}{\pi\hbar}\right)^{1/4}\exp\left[-\frac{M\omega\,(q-q_0)^2}{2\hbar}\right]. \qquad (11)$$

We find the position of the minimum, q_0, from the condition $U(0) = \delta$, while in accordance with the assumption about the shape of the barrier (see figure),

$$U(q) = \frac{M\omega^2(q-q_0)^2}{2}; \quad q > 0, \qquad (12)$$

Substituting the values of $\psi_I(0)$ and $\psi_I'(0)$ into formula (10), we obtain

$$E_2 - E_1 = \left(\frac{9}{4\sqrt{\pi}}\right)\hbar\omega p^{3/2}\exp(-p), \qquad (13)$$

where $p = 2\delta/\hbar\omega$, and ω is the angular frequency of the type e_g vibration under consideration, which leads to transitions between the equivalent configurations.

For the first excited vibrational state, one can analogously obtain

$$E_2 - E_1 = \left(\frac{9}{2\sqrt{\pi}}\right)\hbar\omega p^{3/2}(p-1)\exp(-p). \qquad (14)$$

We can give up the oscillator-function approximation for determining the splitting and, taking account of the considerable height of the barrier and the large mass of the oscillator, we can substitute quasiclassical functions into formula (10). Then we obtain

$$E_2 - E_1 = \left(\frac{9}{8\pi}\right)\hbar\omega\exp\left[-\left(\frac{2}{\hbar}\right)\int_0^{q_1}\sqrt{2M\,(U(q)-E_0)}\,dq\right] \qquad (15)$$

$$= \left(\frac{9}{8\pi}\right)\hbar\omega\left[\frac{p^{1/2}+(p-2n-1)^{1/2}}{(2n+1)^{1/2}}\right]^{2n+1}\exp\left[-p^{1/2}(p-2n-1)^{1/2}\right],$$

where n is the quantum number of the oscillator energy state being considered.

It is striking that formulas (13) and (14), on the one hand, and formula (15) on the other give almost identical results (see table).

The formulas which have been obtained may lead to a form more convenient for calculation. Setting $K = M\omega^2$ and taking account of formulas (2) and (8), we obtain, for the ground state (in atomic units):

$$E_2 - E_1 = \left(\frac{9a}{2\sqrt{6\pi}}\right)(M\omega)^{-1/2}\exp\left(-\frac{2a^2}{3M\omega^3}\right) \qquad (16)$$

and for the first excited state

$$E_2 - E_1 = \left(\frac{9a}{\sqrt{6\pi}}\right)(M\omega)^{-1/2}\left[\left(\frac{2a^2}{3M\omega^3}\right) - 1\right]\exp\left(-\frac{2a^2}{3M\omega^3}\right). \qquad (17)$$

It can be seen from these formulas that the splitting of the levels increases very rapidly with an increase in the vibration frequency ω (of the type e_g vibration).

It is evident that the quantity $E_2 - E_1$ determines the frequency of the transitions of the system between the equivalent configurations, as restricted by the presence of the potential barrier. When allowance is made for interaction with rotations of the complex, the energy levels undergo further splitting, and in place of one transition frequency one obtains a series of frequencies which make up a restricted-motion spectrum (somewhat like the inversion spectrum of ammonia).

THE POSSIBILITY OF EXPERIMENTAL DETECTION

Direct detection of the restricted motions reduces to the determination of the above-described splitting of the levels. The latter may manifest itself in the rotation vibration spectra, we suppose, and also in the form of absorption in the microwave region (analogous to the inversion absorption of ammonia).

It should be emphasized that our calculations have been carried out for the free complexes. Therefore, the results obtained pertain principally to complexes in the gaseous and liquid states (in the latter case, collisions may also exert an influence). However, they may be used as an estimate for the crystalline state as well, provided only that the influence of the following coordination spheres is sufficiently symmetrical and not strong enough to stabilize one direction of distortion of the internal asymmetry octahedron.

In order to determine the order of magnitude of the splitting of the levels on account of restricted motions, we have performed an approximate numerical calculation for certain aquo complexes of transition metals, for which the internal asymmetry was previously computed. The constant a was determined to the same approxima

Magnitudes of the Splittings of the Ground and First Excited Vibrational Levels of Certain Aquo Complexes as a Result of Restricted Motions

Complex	Electronic configuration of the central ion	a (atomic units)	ω (cm^{-1})	Splitting $E_2 - E_1$ (cm^{-1})			
				Ground state		First excited st	
				Oscillator function approximation	Quasi-classical approximation	Oscillator function approximation	Quasi-clas-sical ap-
$Ti(H_2O)_6^{3+}$	d^1	0.0288	300	1.4	1.3	15	1
$Co(H_2O)_6^{3+}$	d^6	0.0294	300	1.1	1.0	13	1
$Fe(H_2O)_6^{2+}$	d^6	0.0174	250	10	9.4	65	5
$Mn(H_2O)_6^{3+}$	d^4	0.0714	300	$7.8 \cdot 10^{-15}$	$7.3 \cdot 10^{-15}$	$6.2 \cdot 10^{-13}$	6.0 ·
			500	0.31	0.29	4.8	4
$Cr(H_2O)_6^{2+}$	d^4	0.0525	250	$9.6 \cdot 10^{-14}$	$8.8 \cdot 10^{-14}$	$7.0 \cdot 10^{-12}$	6.8 ·
			500	12	11	93	8
$Cu(H_2O)_6^{2+}$	d^9	0.0571	250	$1.1 \cdot 10^{-16}$	$1.0 \cdot 10^{-16}$	$9.5 \cdot 10^{-15}$	9.2 ·
			500	5.8	5.3	53	4

and under the same simplifying assumptions as in 1.

The numberical results of the calculations of the ttings of the ground and first excited vibrational ls according to formulas (16) and (17) are presented e table for values of the frequencies ω which are e to the real ones. For comparison, the results of ulations in the quasiclassical approximation accord- o formula (15) are also presented.

It can be seen from the table that, for aquo com- es of transition metal ions with the electronic con- rations d^9 and d^4 at the vibration frequency values nd 250-300 cm^{-1} which are usual for these com- es[3,4] (the exact data for $\omega(e_g)$ are unknown to us), splitting is too small to be detected, and it becomes tantial (~1 cm^{-1}) only for frequencies $\omega \sim 500$ cm^{-1} ch are correct for other complexes of these metals). For aquo complexes of metals with the configurations d^1 and d^6, this splitting falls squarely in the microwave region. This estimate permits one to hope that restricted motions in transition metal complexes may be detected by microwave methods.

REFERENCES

1. I. B. Bersuker, Doklady Akad. Nauk SSSR **132**, 587 (1960); Strukturn. Khim. **2**, 350 (1961).
2. L. Landau and E. Lifshits, "Quantum Mechanics: Nonrelativistic Theory," p. 208. Gosudarst. Tekh. Izd., Moscow, 1948. Addison-Wesley, Reading, Mass., 1958.
3. L. Schultz, J. Chem. Phys. **10**, 194 (1942).
4. J. Damaschun, Z. physik. Chem. **B16**, 81 (1932).

INFRARED SPECTRA OF PHTHALOCYANINES
Interaction of Sublimed Layers of Phthalocyanines With Gaseous CH_3COOH, HCl, and HBr

A. N. Sidorov and A. N. Terenin (pp. 325-331)

Received 29 August 1960

The interaction of sublimed layers of phthalocyanines agnesium, zinc, iron (II), copper, and of the phthalo- ine without metal with gaseous CH_3COOH, HCl (DCl), HBr (DBr) has been investigated by means of the ab- tion spectra in the infrared (670-3800 cm^{-1}) and ble regions. It is shown that it is a completely re- ible interaction which takes place in accordance the acid-base mechanism: during the formation of complexes of phthalocyanine with the molecules of bove-mentioned compounds there is a transfer of a on from the molecule of the acid to the nitrogen s of the phthalocyanine, and at the same time the plex so formed acquires ionic structure. The mole- s HCl and HBr attach themselves to the nitrogen s of the pyrrolic groups as well as to the peripheral ogen atoms of the phthalocyanine molecule. The COOH molecules attach themselves only to the periph- nitrogen atoms. The influence of the central metallic n on the ability of the phthalocyanine molecule to n complexes with the adduct molecule is discussed. ng the phthalocyanines of magnesium, zinc, iron, er, and without metal only the first three interact HCl and a series of other adducts. On the other all the investigated phthalocyanines interact with more active HBr molecules. During the interaction e phthalocyanine without metal with DBr the iso- exchange H → D in the imino groups takes place.

In a previous article[1] we described our investiga- of the infrared spectra of sublimed layers of phthalo- ines with various central atoms and in different talline modifications. Making use of the observed lts we now propose to investigate a problem of some- greater complexity, i.e., that of the interaction of imed layers of phthalocyanines with gaseous adducts. ng the latter we shall at first consider the molecules e acids HCl, HBr, and CH_3COOH. The choice of e molecules was determined by the relative sim- ty of their structures and by the availability of their ared spectra.

The method of preparing the phthalocyanine layers* and of obtaining their spectra was previously described.[1] The gaseous HCl and DCl were obtained from the reaction of concentrated H_2SO_4 and D_2SO_4 on NaCl; the gaseous HBr and DBr were obtained by the reaction of water (ordinary or heavy) with PBr_3. The preparation of these gases and their subsequent purification from water vapor were carried out under vacuum conditions. The amount of H atom impurity in DCl and DBr was about 10-15 percent of the total number of the atoms H and D. The cell with the phthalocyanine samples was filled with gaseous HCl, DCl, HBr, and DBr to 200 mm, and with CH_3COOH vapor to 10 mm Hg pressure (the vapor pressure at room temperature).

*The authors are very grateful to Mr. V. F. Borodkin for making available to us the phthalocyanines used in this investigation.

1. During the introduction of gaseous HCl, HBr, their deuterated derivatives, or the CH_3COOH vapor into the cell containing the phthalocyanine layer, the color of the latter rapidly changes from blue to green. The changes taking place at the same time in the electronic and infrared spectra of the phthalocyanines are illustrated in Figs. 1 and 2. The penetration of the adduct molecules during their interaction with the phthalocyanines takes place throughout the whole depth of the layer, as can be deduced from the fact that several absorption lines characterizing the layer of the phthalocyanine in vacuum conditions disappear completely.

We must note first of all that among the phthalocyanines Mg-, Zn-, Fe-, Cu-, and H_2Phc (Phc is the abbreviation for the phthalocyanine skeleton $C_{32}H_{16}N_8$) the last two do not interact with HCl. This could be seen from the absence of any changes in the spectrum of the layer during its contact with the adduct molecules. All the phthalocyanines investigated by us, i.e., Mg-, Zn-, Cu-, and H_2Phc interact with HBr. MgPhc interacts with

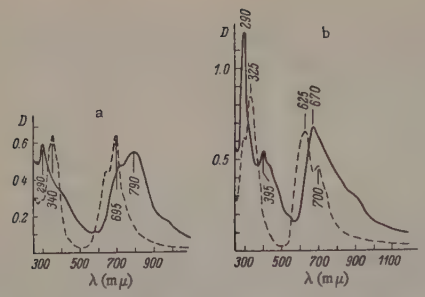

Fig. 1. The absorption spectra of sublimed layers of Mg-phthalocyanine (a) and phthalocyanine without metal (b). Broken curve—α-modification in air; solid curve—the same layer in the atmosphere of DBr.

the vapors of acetic acid. Other phthalocyanines were not investigated in CH_3COOH vapor. The interaction of the phthalocyanine without metal with the HBr molecules, which we have discovered, points to the fact that the central metallic atom is not indispensable for the formation of the complex phthalocyanine + molecule of acid. The latter is most probably attached to the nitrogen atoms of the phthalocyanine molecules with the unshared electron pairs. At the same time the central metallic atom has a significant effect on the phthalocyanine molecule. In the phthalocyanines Mg-, Zn-, and FePhc, in contrast to Cu- and H_2Phc, this effect is observed in the activation of the pigment molecule with respect to the attachment of the HCl molecules. The HBr molecules are more active by themselves than HCl and interact with all the phthalocyanines.

2. After exposure of the layer MgPhc to the vapors of CH_3COOH (in vacuum conditions or in the air) a series of changes take place in the infrared spectrum of the layer (Fig. 2c), which may serve to characterize the molecular complex MgPhc + CH_3COOH. To these changes correspond the splitting of the absorption line at 890 cm^{-1} into two components, shifts and intensity changes of the absorption lines of MgPhc, and the appearance of completely new lines: a weak line at 3200 cm^{-1}, a strong and broad line with two maxima about 2860 and 2950 cm^{-1}, a weak line at 1715 cm^{-1}, a very strong one at 1575 cm^{-1}, a very weak one at 1440 cm^{-1}, and others (Fig. 2c). The evacuation of the CH_3COOH vapor from the cell containing the MgPhc layer does not result in any significant changes in the spectral characteristics of the formed complex. The absorption lines at 1575 and 1440 cm^{-1} in the spectrum of this complex may be unambiguously assigned to the asymmetric and symmetric vibrations of the CH_3COO^- ion.[2] Thus it may be concluded that the molecule of acetic acid dissociates on contact with MgPhc and gives up its proton to the pigment molecule. The forces of the ionic bond tend to retain the CH_3COO^- ion in the vicinity of the protonated phthalocyanine molecule. The complex of the phthalocyanine of magnesium with the acetic acid may thus be represented by the formula

$$MgPhcH_n^+(CH_3COO^-)_n.$$

Besides the dissociated molecules of CH_3COOH in the MgPhc layer there evidently exists a small fraction of the undissociated molecules bonded to the pigment by the relatively weak forces of physical adsorption. To these molecules the weak line at 1715 cm^{-1} may be as-

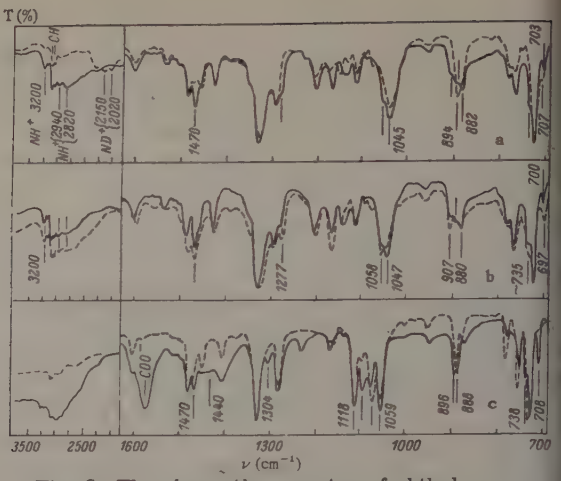

Fig. 2. The absorption spectra of phthalocyanines with metal under different conditions. a—The same layer of Mg-phthalocyanine in HCl (solid curve) and in DCl (broken curve); b—the same layer of Zn-phthalocyanine in HCl (solid curve) and in HBr (broken curve); c—layers of Mg-phthalocyanine (β-modification) in vacuum (broken curve) and in air after exposure to acetic acid vapors (solid curve).

signed, corresponding to the valence vibrations of the C=O bond.[2]

As was indicated above, the nitrogen atoms in the phthalocyanine molecule may serve as the bonding sites for the proton. Therefore, the absorption lines in the 2500-3300 cm^{-1} region, characterizing the complex MgPhc + CH_3COOH, may be assigned to the valence vibrations of the NH^+ bonds formed as a result of the protonization of the molecule MgPhc.[2] In order to solve the problem as to which of the nitrogen atoms of the MgPhc molecule the CH_3COOH molecule is added we must consider the electronic absorption spectra. The "red" absorption line of the sublimed MgPhc layer which in the α-modification of this pigment contains two maxima at 695 and 635 mμ (Fig. 1) is shifted towards the longer wavelength region (bathochromic effect) during the formation of the complex MgPhc + acid. The position of the maxima of the "red" line in the spectra of the MgPhc complexes is as follows: for the complex with HCl it is 745 and 680 mμ, for the complex with CH_3COOH it is 77[illegible] and 690 mμ, and for the complex with HBr it is 790 and 715 mμ (Fig. 1).

The bathochromic effect in the spectra of phthalocyanines which follows their interaction with acids cannot be explained exclusively by the change of the crystalline modification of the layer resulting from the formation of the complex, since this effect is observed not only in the spectrum of the sublimed layer but also in the spectrum of the acetone solution of MgPhc after the addition of HCl.[3] Evstigneev and Krasnovskii, who observed the bathochromic effect when phthalocyanines were dissolved in concentrated sulfuric acid, assumed that, as in the case of a series of other pigments containing chromophore systems involving nitrogen atoms and conjugated bonds, the bathochromic effect caused by the interaction of phthalocyanines with acids may be explained by the addition of the proton to the nitrogen atom of the chromo-

e system. At the same time, inasmuch as chlorophyll dissolution in H_2SO_4 does not show any bathochromic t, it must follow that the proton attaches itself not to central but to the peripheral nitrogen atoms which together the pyrrolic groups of the phthalocyanine ecule.[4] Apparently, the bathochromic effect which ows the interaction of sublimed phthalocyanine films gaseous acid molecules may be also explained by the ling of protons to the peripheral nitrogen atoms.

The bathochromic effect in the spectra of sublimed rs of MgPhc was also previously observed after exre of these layers to the water vapor or after their nersion in ether, acetone, and ethanol. The appearof this effect was associated with the formation of complexes of MgPhc with adducts.[5] The problem of lization of the adduct molecule in the complex had been investigated at that time. Apparently, this must nvestigated separately for each individual complex.

3. The comparison of the infrared spectra of the plex MgPhc + CH_3COOH, of the complex MgPhc + , and of the layer of MgPhc in vacuum (Fig. 2) shows , while the spectrum of the complex MgPhc + COOH retains the basic characteristics of the spec- of the original layer MgPhc, the spectrum of the plex MgPhc + HCl shows little similarity with the trum of the original sample. Apparently, HCl causes nger perturbations on the MgPhc molecule than does COOH. We assume that these perturbations are re- d to the fact that the HCl molecules attach themselves only to the peripheral nitrogen atoms, as is the case the CH_3COOH molecules, but also to the nitrogen ms of the pyrrolic groups in the phthalocyanine mole- . This assumption is based on the following facts. le the evacuation of CH_3COOH from the cell with the ple does not lead to significant changes in the spec- of the complex MgPhc + CH_3COOH, the spectrum of complex MgPhc + HCl undergoes the following signif- t changes after the evacuation of the gaseous HCl: e of the absorption lines characterizing the complex ppear while others remain. In particular, the in- sity of the lines at 882, 907, 1045, 1277, 1470 cm^{-1} of several others is decreased, and the intensity of absorption lines characteristic of the spectrum of original MgPhc layer is increased. Evidently, the ve-mentioned changes are associated with the re- val of a fraction of HCl molecules from the pigment er. However, there is no complete regeneration of phthalocyanine from the complex with HCl even when sample is heated under vacuum up to 250° C. After there still remain in the spectrum of the sample absorption lines at 705, 1304, 1470 cm^{-1} and several ers corresponding to the spectrum of the original Phc layer. The line at about 890 cm^{-1} persists in g split into two components. In general the spectrum he complex MgPhc + HCl after the evacuation of the strongly resembles the spectrum of the complex Phc + CH_3COOH (Fig. 2c), if from the latter one exdes the absorption lines corresponding to the vibra- s of the CH_3COO^- ion. It follows that the molecules HCl which remain in the phthalocyanine layer after the uum treatment are attached to the peripheral nitro- atoms in the same way as the CH_3COOH molecules, le the complex which is formed also possesses ionic ucture (in the spectrum of the complex the absorption s corresponding to the NH^+ bonds are observed), ch may be represented by the formula $MgPhcH_n^+Cl_n^-$ The HCl molecules which leave the pigment layer during the vacuum treatment after interaction with phthalocyanine also possess ionic structure but they are attached to the nitrogen atoms of the pyrrolic groups. The conclusion about the ionic structure of these molecules is made on the basis of a very great resemblance in the infrared spectra of the phthalocyanine complexes with HCl and with HBr (in the presence of gas in the cell, see Fig. 2b). This resemblance, especially in the region of valence vibrations of the NH^+ bonds (2500-3300 cm^{-1}), would not exist if the adduct molecule had not been dissociated.

The absorption lines in the 2500-3300 cm^{-1} region are apparently common both to the peripheral as well as to the pyrrolic NH^+ bonds. This follows from the fact that as the HCl is being evacuated from the cell with the sample, the intensity of all the lines in this region (with the exception of the lines corresponding to the CH bonds) decreases uniformly and at the same rate. The presence in the spectra of the phthalocyanine complexes with HCl and HBr of the absorption lines which may be assigned to the valence vibrations of the NH^+ bonds, as well as the possibility of the isotope exchange $H \rightarrow D$ in the imino groups of H_2Phc in the presence of DBr (see below), shows that the nitrogen atoms of the pyrrolic groups as well as the peripheral nitrogen atoms may constitute the centers to which the HCl and HBr molecules are attached during their interaction with the phthalocyanine. The attachment of the HCl molecules to the nitrogen atoms of the pyrrolic groups results in significant changes in the spectrum of the pigment which may be explained by a strong perturbation of the system of conjugated bonds in the pigment molecule with the resulting change in its symmetry.

4. As can be seen from the comparison of the spectra shown in Fig. 2a, when DCl is substituted for HCl a series of changes take place in the spectrum of the complex. These changes are either related to the vibrations of the bonds NH^+ (ND^+) or to those vibrations of the complex in which the protons (deuterons) that have become attached during the formation of the complex participate to some extent. Let us point out some of the most characteristic changes which take place on substituting DCl for HCl. The lines corresponding to the valence vibrational frequencies of the NH^+ bonds are being shifted into the region of the characteristic frequencies of the ND^+ bonds (2000-2400 cm^{-1}, Fig. 2a). Instead of the line around 1058 cm^{-1} a line at 894 cm^{-1} appears. Apparently, this line is related to one of the deformational vibrations of the NH^+ bonds. The basis for the assignment of the lines at 1058 and 894 cm^{-1} to one and the same type of vibration of the complex lies in the fact that in the spectra of the complexes FePhc with HCl and DCl the corresponding lines are shifted in the same direction—to 1067 and 912 cm^{-1}, respectively. Inasmuch as the position of the above-mentioned lines depends on the type of the central metallic atom they must be assigned to the vibrations of the pyrrolic bonds NH^+ (ND^+). The interpretation of the remaining changes which may be easily recognized from Fig. 2 is made difficult by the existence of two different types of bonds NH^+ (and ND^+)—peripheral and pyrrolic—each of which may participate in several types of deformational frequencies.

It must be noted that the appearance of the spectrum of the complex does not depend at all on the crystalline modification of the original layer MgPhc. Depending on the type of the central metallic atom the appearance of the spectrum of the complex MetPhc +

HCl changes only in some insignificant details (variation in the position of the individual absorption lines).

A significant difference is observed between the complex H_2Phc + HBr and the complexes MetPhc + HBr, as should have been expected, since in the first place the spectra of the original layers H_2Phc and MetPhc significantly differ from one another[1] and in the second there must take place in the complex H_2Phc + HBr some interaction between the attached HBr molecules and the imino groups NH of the H_2Phc molecule. The existence of such interaction is confirmed by the shift of the absorption lines corresponding to the valence vibrations of the NH^+ bonds in the spectrum of the complex H_2Phc + HBr in the direction of lower frequencies, in comparison with the corresponding lines in the spectra of MetPhc + HBr.

5. Judging by the spectral data there exists no difference in principle in the interaction of the HCl and HBr molecules with the phthalocyanines. This is confirmed by the resemblance which we have already noted above between the spectra of the complexes ZnPhc + Hcl and ZnPhc + HBr which differ from each other only in the intensity of individual absorption lines (Fig. 2b). A resemblance is observable between the spectra of the complexes MgPhc with HCl and HBr. The difference between HCl and HBr in comparison with CuPhc and H_2Phc lies in the fact that HBr interacts with this phthalocyanine while HCl does not. This poses the problem of elucidating the role of the activating effect of the atoms of zinc, iron, and especially magnesium on the phthalocyanine molecule which makes possible the formation of the complex phthalocyanine + adduct. Other compounds besides HCl, such as pyridine and water, may also become adducts.[6]

If one assumes that all four peripheral N atoms and the two pyrrolic N atoms which are not coordinated with the central metallic atom or hydrogen are capable of attaching the adduct molecules, then the number of the latter per phthalocyanine molecule must be as follows: in the complex with HCl and HBr—6, in the complex with CH_3COOH—4. Barrett, Frye, and Linstead[7] discovered that the phthalocyanine of bivalent iron upon its distillation from aniline or o-toluidine may form complexes with six molecules of these compounds. This confirms the ability of the phthalocyanine molecule to form a complex with six molecules of HCl and HBr and at the same time gives basis for the assumption that the molecules of aniline and o-toluidine are attached to the nitrogen atoms (4 peripheral and 2 pyrrolic) during the formation of the complex with FePhc.

6. All the changes in the infrared spectrum of the sublimed film of the phthalocyanine taking place during the formation of its complex with HCl, HBr, and CH_3COOH from the gaseous phase are completely reversible. There was no tranformation of MgPhc into a pigment without metal under the conditions of our experiment, such as had taken place in a solution of MgPhc upon the addition of HCl,[3] even though we exposed the MgPhc layer to gaseous HCl for a prolonged period of time (3 days). The regeneration of the original phthalocyanine from its complex with the acid molecules may be achieved in two different ways: either by vacuum treatment of the sample by heating it up to 280-300° C for one to two hours, or by exposing the sample to the vapors of organic base (pyridine) for several hours with the subsequent vacuum treatment at 100° C. The vacuum treatment in this case is necessary for the elimination of pyridine.

The spectrum of complex CuPhc + HBr after exposure to the pyridine vapors loses all features which are characteristic for this complex. It represents a simple superposition of the spectrum of the mixture of α- and β-modifications of the original CuPhc[1] with a series of additional absorption lines about 682* (v.s.), 754 (v.s.), 920 (w.), 995 (w.), 1030 (w.), 1055 (m.), 1191 (m.), 1245 (w.), 1481 (s.), 1528 (s.), 1604 (s.), 1632 cm^{-1} (m.), and a wide band of medium intensity in the region 2500-3300 cm^{-1} with the absorption maximum around 2870 cm^{-1}. The intense absorption lines at 1481 and 1632 cm^{-1} apparently correspond to the characteristic vibrational frequencies of the pyridinium ion $C_5H_5NH^+$.[8] The broad band in the 2500-3300 cm^{-1} region may be assigned to the valence vibrations of the NH^+ bonds of this ion. The above-mentioned data lead us to the conclusion that the pyridine molecule on contact with the complex CuPhc + HBr captures the HBr molecule with the formation of $C_5H_5NH^+Br^-$ salt, thereby regenerating the CuPhc molecule. Apparently, all the remaining additional absorption lines in the spectrum of the complex correspond to the vibrations of the hydrogen bromide salt of the pyridine whose molecules, judging by the spectral data, do not interact with CuPhc.

*The abbreviated descriptions of the line intensities: v.s.—very strong; s.—strong; m.—medium; w.—weak.

7. It is known that the hydrogens on the imino groups of pheophytine in organic solvents do not exchange with deuterium of the heavy water.[9] We did not observe such exchange in the imino groups even on triturating H_2Phc powder with the heavy water (the exchange was checked by the absorption spectra in the region of valence vibrations of the imino group). The reversibility of the interaction of H_2Phc with HBr which we have investigated suggested the possibility that such an exchange could take place with the help of DBr. Indeed it was found that when the H_2Phc powder was exposed to gaseous DBr under vacuum conditions and subsequently treated in vacuum at 280-300°C, with the purpose of regeneration of phthalocyanine, the spectrum of the sample obtained by this means exhibited an absorption line corresponding to the valence vibrations of the ND bond.[1] The presence of this line in the spectrum proves unambiguously that the isotopic exchange in the imino groups had taken place.

The mechanism of isotopic exchange in the imino groups of phthalocyanine without metal may be described in the following way. Two atoms of the pyrrolic kernels which are not bonded to the central H atoms attach to themselves two DBr molecules thereby forming ionic ND^+ bonds. The positive charge of these bonds is uniformly distributed among the two D atoms and two H atoms of the imino groups, thereby resulting in the equal probability of their separation during the regeneration of the phthalocyanine molecule from its complex with DBr. Repeated treatment of phthalocyanine with gaseous DBr and subsequent regeneration of it by heating in vacuum may lead to complete exchange of the H atoms of the imino groups by the D atoms. Thus, if the HBr impurity in DBr is negligibly small it is possible to obtain practically completely N-deuterated phthalocyanine without metal.

REFERENCES

1. A. N. Sidorov and I. P. Kotlyar, Opt. i Spektr. 11, 175 (1961), Optics and Spectroscopy 11, 92 (1961).

L. J. Bellamy, "Infrared Spectra of Complex Molecules." Izd. Inostrannaya Lit., Moscow, 1957. Wiley, London, 1954.
I. A. Akimov and G. A. Korsunovskii, Opt. i Spektr. 8, 427 (1960).*

e cannot trace this reference—Translation Editor.

V. B. Evstigneev and A. A. Krasnovskii, Doklady Akad. Nauk SSSR 58, 1399 (1947).
E. K. Putseiko and A. N. Terenin, Zhur. Fiz. Khim. 30, 1019 (1956);
A. Terenin and E. Putseiko, J. Chim. Phys. 681 (1958);
E. Putseiko, Doklady Akad. Nauk SSSR 124, 796 (1959), Soviet Phys-Doklady 4, 136 (1959);
E. K. Putseiko, "The Problems of Photosynthesis," p. 77. Izd. Akad. Nauk SSSR, Moscow, 1959.
6. A. N. Sidorov and A. N. Terenin, Doklady Akad. Nauk SSSR 104, 575 (1955);
A. N. Terenin and A. N. Sidorov, Proc. Colloq. Spectrosc. Intern. VI, p. 573. (Suppl. to Spectrochim. Acta), 1957.
7. P. A. Barrett, D. A. Frye, and R. P. Linstead, J. Chem. Soc. 1157 (1938).
8. G. M. Barrow, J. Am. Chem. Soc. 78, 5802 (1956).
9. J. Weigl and R. T. Livingston, J. Am. Chem. Soc. 74, 4160 (1952).

FFECT OF TEMPERATURE ON THE ABSORPTION OF MONOSUBSTITUTED BENZENES IN THE REGION OF THE C—H STRETCHING VIBRATIONS

M. P. Lisitsa and I. N. Khalimonova (pp. 332-341)

Received 26 September 1960

The changes in the frequencies, intensities, and structure of the vibrational absorption bands of toluene, aniline, bromobenzene, chlorobenzene, and nitrobenzene (region of the C—H stretching vibrations) which are brought about by a change in the state of aggregation and in the temperature have been studied.

RODUCTION

The studies whose results are presented below were ried out with the purpose of establishing the role of shape and specificity of a vibration in the tempera- - e dependence of the intensities of the corresponding orption bands. Principal attention is paid to the bands nging to the stretching vibrations of the C—$H_{arom.}$ ds of monosubstituted benzenes. It was shown in a vious communication[1] that the introduction of various stituents into the benzene ring destroys the specificity he vibrations just cited—their frequencies and inten- es change. It is therefore to be expected that such a akdown will also affect the course of the temperature endence, confirming our view concerning the pre- inant influence of external factors governed by inter- ecular interactions.

Since all the test materials were studied in two es of aggregation—solid and liquid—the effect of a se transition on the fundamental parameters of the rational bands was also analyzed.

OCEDURE

We shall point out only a few details of the pro- ure, those connected with the specifics of the tem- ature experiments (the remaining data, including the ors in the measurements, are presented in ref. 1). e investigations were carried out using the hermetic l and cryostat described in refs. 2 and 3. A correc- n for the temperature variation of density was made he values obtained for the absorption coefficients of liquids. In the case of crystals, this change is less an order of magnitude[4] and, within the temperature ge which we used, it amounts to not more than 1-1.5% aromatic hydrocarbons;[5] accordingly, the corre- nding correction may be neglected for the solid phase. alculating the integrated absorption values, a correction for the wings was likewise not introduced, since it did not exceed the errors of the measurements.

DISCUSSION OF THE RESULTS

Effect of the phase transition. The portions of the spectra which we investigated are represented in Figs. 1a-1f. In each of these figures, one of the curves corresponds to the liquid phase (it was obtained for a tem-

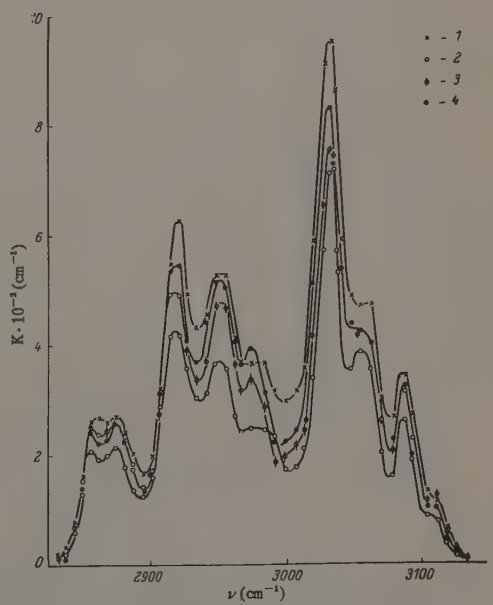

Fig. 1a. Absorption spectra of toluene. State of aggregation and temperature (°C): 1—liquid, −90; 2—crystal, −100; 3—crystal, −130; 4—crystal, −160.

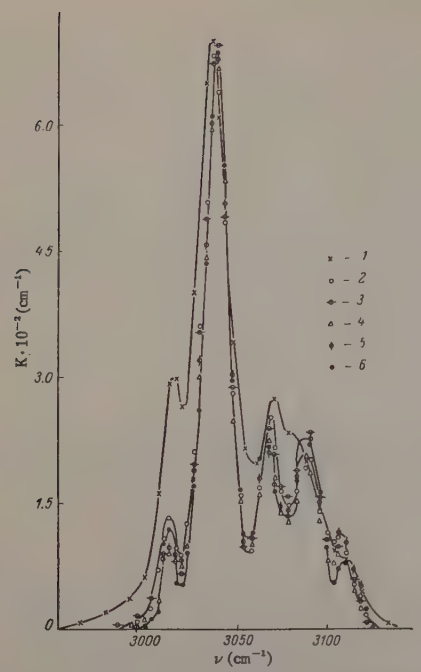

Fig. 1b. Absorption spectra of aniline. State of aggregation and temperature (°C): 1—liquid, −5; 2—crystal, −10; 3—crystal, −60; 4—crystal, −100; 5—crystal, −130; 6—crystal, −165.

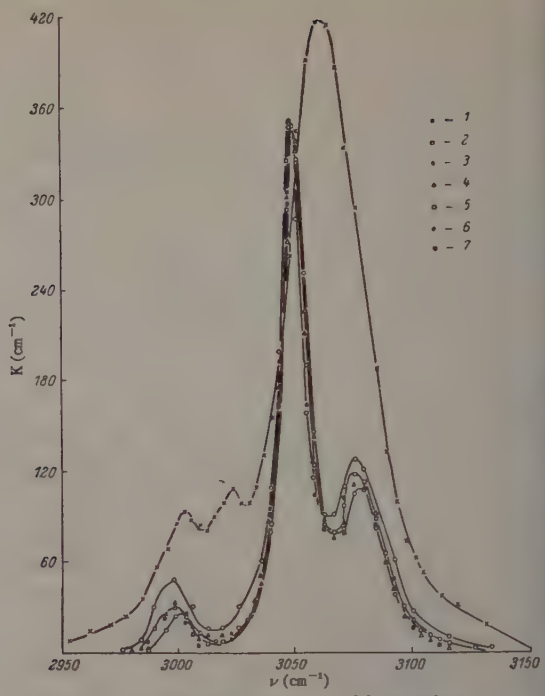

Fig. 1c. Absorption spectra of bromobenzene. State of aggregation and temperature (°C): 1—liquid, −25; 2—crystal, −35; 3—crystal, −60; 4—crystal, −90; 5—crystal, −120; 6—crystal, −160; 7—crystal, −175.

perature close to the melting point). The remaining curves refer to the crystals and will be used hereafter for evaluation of the temperature dependence. Let us examine that particular curve which corresponds to the highest temperature. All the differences between this curve and the curve corresponding to the liquid phase can evidently be associated with the change in the state of aggregation, since the maximum temperature difference for which they were obtained does not exceed 20°C.

It follows from the data presented that, for the stretching vibrations of the C—$H_{arom.}$ bonds (to which, in Figs. 1a-1e, the most intense maxima* correspond),

*The frequencies and an interpretation of all the maxima are given in ref. 1.

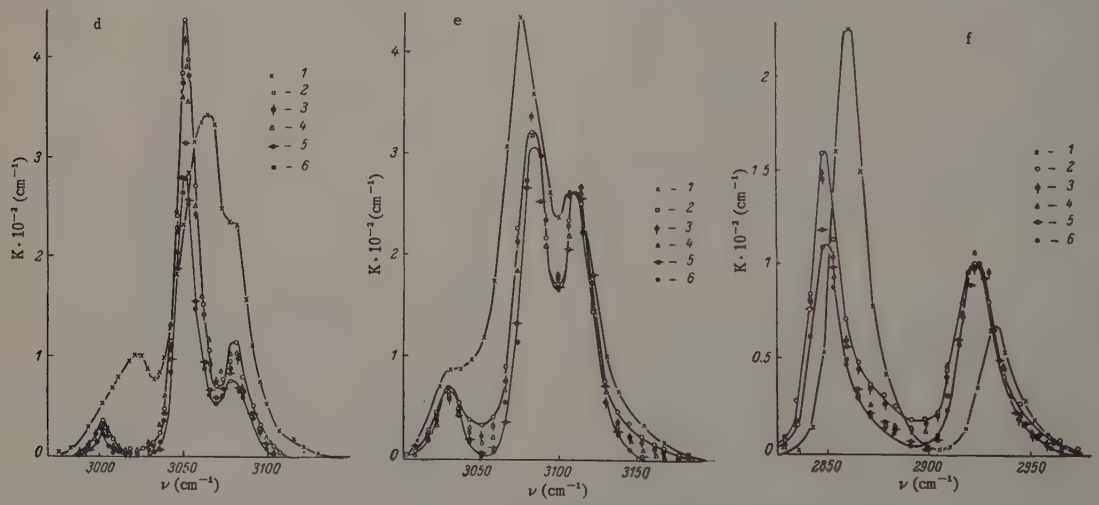

Fig. 1d. Absorption spectra of chlorobenzene. State of aggregation and temperature (°C): 1—liquid, −30; 2—crystal, −50; 3—crystal, −80; 4—crystal, −140; 5—crystal, −165.
Fig. 1e. Absorption spectra of nitrobenzene in the region of the stretching vibrations of the C—$H_{arom.}$ bonds.
Fig. 1f. Absorption spectra of nitrobenzene in the region of the combination frequencies $(\nu_s + \nu_{as})NO_2$ and $(\nu_3 + \nu_4)C-C$. State of aggregation and temperature (°C) for 1e and 1f. 1—liquid, 15; 2—crystal, −5; 3—crystal, −50; 4—crystal, −90; 5—crystal, −130; 6—crystal, −170.

the magnitude of the integrated absorption, S, under-
s substantial variations. Thus, in the cases of bro-
enzene, chlorobenzene, and nitrobenzene, the value
diminishes by approximately a factor of two during
liquid-to-crystal phase transition. For toluene and
ine, this diminution has a somewhat smaller value.
note that, in all the cases examined, the change in S
t be greater than follows from the figures, since in
culating the absorption coefficients of the crystals we
ld not take account of the correction for the increase
ensity produced by the crystallization of the substance.
In two cases (toluene, aniline), the frequencies of the
d maxima remain practically unchanged; in two (bro-
enzene and chlorobenzene), they diminish somewhat
roughly 10 cm^{-1}); and in one (nitrobenzene) the fre-
ncy increases (~10 cm^{-1}).
The intensities of the bands of the remaining vibra-
s shown in Figs. 1 also decrease during the phase
sition. The band of the $\nu_3 + \nu_4$ vibration of the C—C
ds of nitrobenzene (Fig. 1f) constitutes an exception;
absorption in this band increases almost twofold.
positions of all the maxima remain unchanged for
ene and aniline only. In the remaining cases, roughly
of the total number of bands are shifted toward
er wavelengths.
Thus toluene and aniline behave in exactly the same
, which is apparently connected with the presence of
tron-donating groups in their molecules. On the other
d, there is also much in common in the behavior of
mobenzene, chlorobenzene, and nitrobenzene, the spec-
of which in the solid phase are quite closely alike in
pe. In this case, the presence of electrophilic sub-
uents is the factor unifying these molecules. It is ap-
priate to single out bromobenzene and chlorobenzene
m the latter group of compounds: the identify of their
tra may indicate isomorphism of their crystals. Un-
unately, data on the crystal structure of the com-
nds studied are unknown to us; however, the over-
lming majority of di- and trisubstituted benzenes with
same substituents crystallize in the monoclinic sys-
with two layers of more or less close-packed mole-
es.[6] The same crystal system probably exists in our
e also; however, the similarity of the unit cells will
reater within the limits of each of the two groups
ntioned above.
The causes of the reduction in band intensity as a
ult of crystallization have been discussed previously.[7]
far rarer case of an increase in the absorption, as
erved for the band of the $(\nu_3 + \nu_4)$ vibration of the C—C
d in nitrobenzene, does not lend itself to interpreta-
. As was established in the work of ref. 1, there is
nance interaction between the vibrations $\nu_s CH_3$
2919 cm^{-1}) and $2\delta_{as}CH_3$ (ν = 2968 cm^{-1}) of toluene,
between νC—$H_{arom.}$ and $(\nu_1 + \nu_3)$C—C of aniline (ν =
8 cm^{-1}), bromobenzene (ν = 3077 cm^{-1}), chloroben-
e (ν = 3077 cm^{-1}), and nitrobenzene (ν = 3110 cm^{-1});
a result of this, the intensities of the overtone $2\delta_{as}$
of the combination frequencies $\nu_1 + \nu_3$ are com-
able with the intensities of the fundamental frequen-
s ν_s and νC—$H_{arom.}$. As a result of crystallization of
substance, the resolution of the bands of the reso-
ng vibrations was improved, which allowed us to de-
mine more exactly the value of the integrated absorp-
for each of them and to satisfy ourselves of the cor-
tness of the conclusion reached in ref. 1 concerning
presence of resonance.

Temperature effect for the solid phase. Analysis of curves (Fig. 1a-1f) relating to different tempera-

tures leads to the conclusion that there are no structural changes in the spectra on cooling. It is also impossible to discern substantial changes in the shape of the bands, with the exception, perhaps, of weakened absorption in the wings. The magnitude of the integrated absorption in the bands of the νC—$H_{arom.}$ vibrations also changes little: for toluene it decreases, for bromobenzene it remains unchanged, in the other cases it increases. It is more convenient to establish these changes with the help of the dependences represented in Fig. 2, in which are also presented data on the integrated absorption in the bands of the other vibrations. It is easy to see that the influence of temperature proves to be relatively slight for all the substances, while the change in the absorption in the bands of the different vibrations has the same character, qualitatively, as for the vibration of the C—$H_{arom.}$ bond. Another pecularity attracts one's attention: namely, the linearity of the temperature depend-

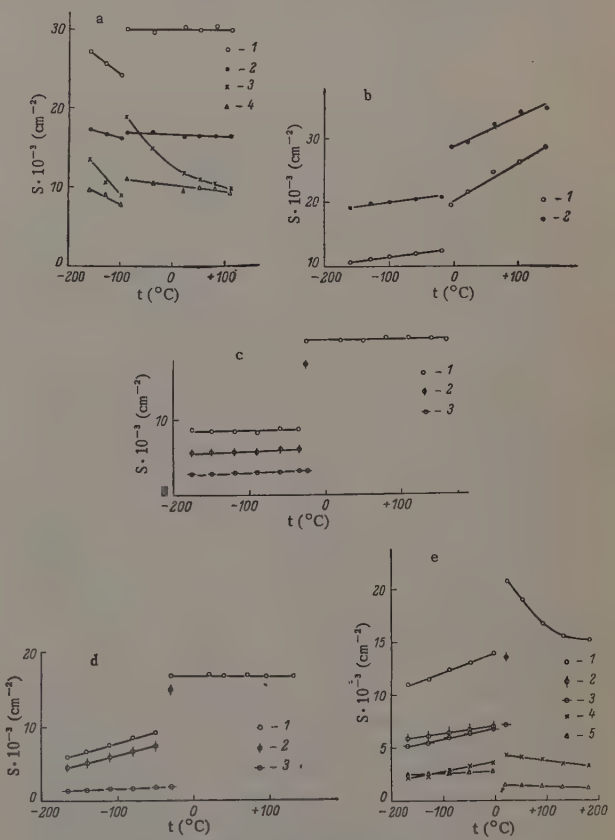

Fig. 2. Temperature dependences of the magnitude of the integrated absorption S in the bands of various vibrations of crystalline and liquid toluene (a), aniline (b), bromobenzene (c), chlorobenzene (d), and nitrobenzene (e). Phase transition temperature (°C): a—(−95), b—(−6), c—(−30), d—(−45), 4—(6). Vibration: a: 1—$\nu CH_{arom.}$, 2—$\nu_s CH_3$, 3—$\nu_{s'} CH_3$, 4—$2\delta_{as}$. b: 1—$\nu CH_{arom.}$, 2—group of bands in the ν = 2950-3150 cm^{-1} region. c, d: 1—S[$\nu CH_{arom.}$] + S[$\nu_1 + \nu_3$)CC], 2—$\nu CH_{arom.}$, 3—$(\nu_1 + \nu_3)$CC. e: 1—S[$\nu CH_{arom.}$] + S[$(\nu_1 + \nu_3)$CC], 2—$\nu CH_{arom.}$, 3—$(\nu_1 + \nu_3)$CC, 4—$(\nu_s + \nu_{as})NO_2$, 5—$(\nu_3 + \nu_4)$CC.

ences. Such a result has previously been obtained for various vibrations of other molecular compounds.[2,3,8-10]

No sufficiently complete theory of the temperature dependence for molecular crystals has yet been worked out. The first outline of one, pertaining to the case of free excitons with simultaneous formation of phonons, was given by Davydov.[11] As has already been noted in ref. 3, an increase in the integrated absorption with temperature—i.e., the result obtained by us for aniline, chlorobenzene, and nitrobenzene—is to be expected on the basis of the conclusions of the author of ref. 11. However, in line with its incompleteness, the theory does not touch on other possibilities at all (constancy of the absorption, or its decrease with temperature). The case of the formation of localized excitations also remained unexamined. The study of this problem was continued by Strizhevskii, who recently developed a theory for the case of weak exciton-phonon coupling (crystals of the cubic system with a van der Waals type of bond).[12] After certain simplifications, the fundamental relationship of this theory may be represented in the form

$$\varkappa_\nu = \frac{\frac{a}{\nu} T}{(\nu_0 - \nu)^2 + bT^2}. \qquad (1)$$

Here κ_ν is the absorption coefficient; a and b are parameters, of which only the first depends on the temperature, but substantially less strongly than κ; ν_0 is the frequency corresponding to κ_{max}. We assume that the maximum of the absorption curve and the point of inflection of the dispersion curve correspond to one and the same frequency. If this condition is violated, the value ν_0 will not be associated with the maximum.

It follows from (1) that, as the temperature increases, the absorption at the maximum must diminish and that in the wings must increase. In consequence of the overlapping of the bands, it is difficult to state anything definite about the changes in the wings; however, the change in the absorption coefficients at the maximum can easily be established on the basis of the curves represented in Fig. 1. For example, for all the bands of toluene without exception (Fig. 1a), a decrease in the absorption coefficient takes place as proposed by the theory. In the remaining cases, the coefficient either increases or remains unchanged, indicating a different character—intermediate or strong—for the exciton-phonon coupling.

The theory employed here gives no direct indications of the character of the temperature variations of the integrated absorption. However, with the help of (1) it is not difficult to come to the conclusion that it may be anything (rise, fall, constancy). Thus, integrated-absorption data cannot as yet be used as a criterion enabling us to establish the limits of applicability of the theory. Such a possibility could appear only after determination of the parameters entering into (1).

We note one more circumstance. If in (1) we set $\nu = \nu_0$, then

$$\varkappa_{max} = \frac{A}{T}, \qquad (2)$$

i.e., the temperature decrease in the absorption coefficient at the band maximum does not depend on the frequency of the vibrational transition. This conclusion is confirmed by experiment.

The cause of the lack of correspondence between the conclusions of the theory and the majority of the experimental curves is to be found both in the original premises of the theory and in the question of how close the exciton-phonon coupling is to weak coupling. Actually, it is difficult to assume in advance that, even in those cases for which the decrease in κ_{max} required by the theory takes place, the strength of the coupling will be identical.

Temperature effect for the liquid phase. In view of the considerable overlapping of the bands, we did not always succeed in unequivocally resolving them into their component parts. In the cases of bromobenzene, chlorobenzene, and nitrobenzene, such resolution proved possible only for a temperature close to the melting point. Therefore, the magnitude of the integrated absorption of the separate components is shown in Fig. 2 only for one temperature (isolated points). This enables us to judge the change in absorption brought about by the phase transition, at least. For higher temperatures, the total absorption of the adjoining bands was determined.

The measurements have shown that, for the bands corresponding to the vibrations of the C—$H_{arom.}$ bonds, the different monosubstituted benzenes are characterized by qualitatively different temperature dependences: there is none in the cases of toluene, bromobenzene, and chlorobenzene, there is an increase of the integrated absorption with temperature for aniline, and a decrease for nitrobenzene. We have here encountered for the first time the fact of an increase in the intensity of a vibrational band when a liquid is heated. As will be shown below, this anomaly has an entirely satisfactory explanation.

The most interesting conclusion emerging from the results which we have obtained consists of the small part played by such intramolecular factors as the shape and specificity of the vibration. In the case of the materials which we have investigated, these factors do not even ensure the expected parallelism in the temperature behavior of the intensities of the vibrations of the C—H_{ar} bonds for substituted benzenes with a given type of substituent (electron-donating or electrophilic). This shows once again that a change in the structure of the intermolecular force field plays the decisive role in the temperature dependence. It is therefore no wonder that for bromobenzene and chlorobenzene, the molecules of which are under the influence of fields of identical structure, the dependences prove to be identical also.

Before passing to the elucidation of the causes of the different characters of the temperature dependences, let us pause briefly at the behavior of the other absorption bands. The changes in the intensities of the bands of the ν_s and ν_{as}' fundamental frequencies of the methyl group of the toluene molecule prove to be different (Fig. 2a): as the temperature rises, the intensity of the symmetric vibration remains practically unchanged, but that of the antisymmetric one falls quite rapidly. Thus in this case the form of the vibration plays a definite role. One must not think that this result contradicts the conclusion formulated above, since the intermolecular field is here entirely identical for both vibrations, and this allows each of them to show its individuality to a greater or lesser degree.

It is striking that, in the case of the ν_{as}' vibration of the CH_3 group, the previously-established[9] rule of a linear decrease with temperature of the intensities of the vibrational absorption bands of molecular liquids is violated. Possibly this violation is only apparent, since the pronounced overlapping of the bands does not allow us to establish the magnitude of the integrated absorption with the necessary accuracy at each temperature, all the more since the band of the $\nu_{as}''CH_3$ vibration, the temperature

iation of which may be different, is located close to band under consideration (it cannot be separated phically). If the error were completely eliminated, established character of the dependence would have to associated with a structural change in the toluene ecule. The rotation of the CH_3 group becomes more e as the temperature increases, and the deviations of shape from a regular pyramid (see ref. 1) diminish. a result, the splitting of the doubly degenerate vibra- ν_{as} gradually disappears (this is confirmed by the pe of the absorption curves) and the temperature de- ase in the intensity of the $\nu_{a'}$ vibration is moderated, le the absorption in the band of the $\nu_{a''}$ vibration is ed to the absorption in the fundamental band.

An analogous violation of the linear regularity is ob- ved for the total absorption in the bands of the vibra- of the C—$H_{arom.}$ bonds and the $\nu_1 + \nu_3$ vibration of C—C bonds of nitrobenzene (Fig. 2e). In this case can no longer use the line of argument presented ve, but another argument may be put forward in justi- tion of the relationship mentioned. In the work of 1, the existence of resonance was established between C—$H_{arom.}$ and $(\nu_1 + \nu_3)$C—C vibrations of the sub- nces under study. If for the isolated molecule the in- rated absorption of the doublet does not depend, in the t approximation, on the natural separation, then for liquid, in consequence of the perturbing action of the roundings, the absorbing power of the two-oscillator tem will be a function of the distance between the un- turbed levels. Insofar as a change in temperature ds, in a number of cases, to a shift (even though all) in the vibrational levels, just so far will a reso- ce effect be superimposed on the usual course of the perature dependence, as a result of which the line- ty breaks down.

The explanation just presented is very general and y be employed in the examination of any resonance blet. In the case which we have encountered in the sent work, this explanation assumes the following en- ly specific form. Analysis of Fig. 3 shows that, in nparison with the fundamental frequency, the intensity he $\nu_1 + \nu_3$ vibration of the C—C bonds falls off more idly with temperature, so that at t = 180°C its con- bution to the total absorption is small, while the con- bution of the fundamental frequency remains consid- ble. Therefore, the pronounced fall in the total ab- ption at low temperatures is brought about in con- erable measure by the change in the weak component. higher temperatures, the change in the total absorp- n curve (Fig. 2e) represents essentially the tempera- e dependence of the fundamental frequency alone, in ordance with which the rate of fall diminishes.

Let us now turn to the vibrations of the C—$H_{arom.}$ ds. As has already been noted above, the investiga- ns which we have carried out have shown the differ- character of the temperature dependence of their in- sities for different substances. The case of aniline, which a fairly marked increase in absorption with nperature is observed (Fig. 2b), arouses especial in- est. This fact may indicate that, together with pure n der Waals interaction, there exists an intermolecular eraction of a different kind. Actually, for all five nosubstituted benzenes the effect of the Boltzmann tor must be the same, since we are speaking of the ne vibration (the difference in the frequency does not ceed 60 cm^{-1}, and at $\nu = 3000$ cm^{-1} it has practically effect on the value of the Boltzmann factor, which, in- entally, hardly differs from zero). In view of the

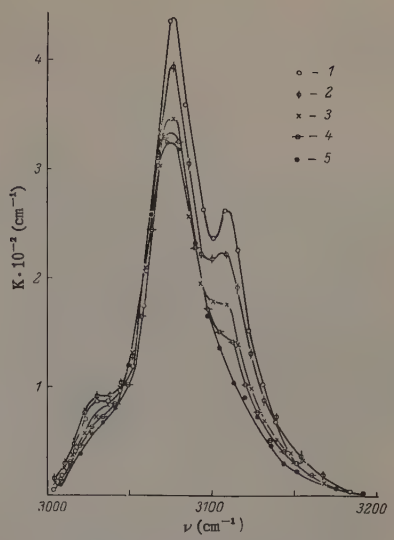

Fig. 3. Absorption spectra of liquid nitrobenzene in the region of the combination frequencies $(\nu_s + \nu_{as})NO_2$ and $(\nu_3 + \nu_4)CC$. Temperature (°C): curve 1—15, curve 2—50, curve 3—90, curve 4—130, curve 5—180.

sameness of the vibrations, one would hardly expect a substantial difference in the effect of anharmonicity either. One will be best justified in assuming the formation of intermolecular bonds of the type H...N—H in aniline. The large halfwidth of the absorption bands of the N—H bonds and the low value of the halfwidth for the absorption band corresponding to vibrations of the C—H bonds indicates that only the atoms of the substituent group take part in the formation of complexes. On elevation of the temperature, breakdown of the H...N—H bonds takes place and there is an increase in the nondirectional interaction between the surroundings and the molecule, which favors an increase in the intensity of the absorption band under consideration.

The interpretation presented in ref. 9 for the temperature dependence is too general and has not, as yet, achieved any serious theoretical substantiation. Considering also the enormous difficulties which arise on theoretical examination of any problem associated with the study of the properties of a liquid, we find it expedient to make use of that repeatedly verified parallelism in the properties of condensed systems which depends on the existence of short-range order in a liquid. With certain limitations, this parallelism permits us to carry over into the physics of the liquid state the exciton concepts which have been confirmed in recent years in solid-state physics. Since, in the overwhelming majority of the cases known to us, including some of those described above, the temperature changes in the vibrational absorption bands of molecular liquids agree in general with the requirements of the theory,[12] it may be supposed that weak exciton-phonon coupling is possibly the most characteristic coupling for liquids. In our case, the band of the $(\nu_s + \nu_{as})NO_2$ vibration is a typical example of the manifestation of such coupling: the absorption coefficient at the maximum of this band falls off with an increase in temperature, but at a distance from the maximum it increases. Therefore, regardless of the fairly marked lowering of the intensity at the maximum, the magnitude of the integrated absorption diminishes slightly with an

increase in temperature, which is brought about by the compensating increase in the absorption beyond the half-width limits.

REFERENCES

1. M. P. Lisitsa and I. N. Khalimonova, Opt. i Spektr. 11, 185 (1961), Optics and Spectroscopy 11, 97 (1961).
2. M. P. Lisitsa and Yu. P. Tsyashchenko, Opt. i Spektr. 9, 188 (1960), Optics and Spectroscopy 9, 99 (1960).
3. M. P. Lisitsa and Yu. P. Tsyashchenko, Opt. i Spektr. 9, 438 (1960), Optics and Spectroscopy 9, 229 (1960).
4. "Physical Methods of Organic Chemistry," vol. 1, p. 82, Izd. Inostrannaya Lit., Moscow, 1950.
5. V. M. Kozhin and A. I. Kitaigorodskii, Zhur. Fiz. Khim. 27, 534, 1676 (1953); ibid. 29, 2074 (1955).
6. A. I. Kitaigorodskii. "Organic Crystal Chemistry," Izd. Akad. Nauk SSSR, Moscow, 1955.
7. O. V. Vakulenko, G. G. Kirei, and M. P. Lisitsa, Opt i Spektr. 11, 196 (1961), Optics and Spectroscopy 11, 103 (1961).
8. M. P. Lisitsa and V. N. Malinko, Izvest. Akad. Nauk SSSR, Ser. Fiz. 22, 1117 (1958).
9. M. P. Lisitsa, V. N. Malinko, and I. N. Khalimonova, Opt. i Spektr. 7, 638 (1959), Optics and Spectroscopy 7, 386 (1959).
10. M. P. Lisitsa and Yu. P. Tsyashchenko, Opt. i Spekt 9, 742 (1960), Optics and Spectroscopy 9, 389 (1960).
11. A. S. Davydov. "Theory of Light Absorption in Molecular Crystals," Izd. Akad. Nauk Ukrain. SSR, Kiev, 1951.
12. V. L. Strizhevskii, Opt. i Spektr. 8, 623 (1960), Optics and Spectroscopy 8, 329 (1960).

SECOND-ORDER RAMAN SPECTRA IN SOME LIQUIDS

Ya. S. Bobovich (pp. 342-348)

Received 24 September 1960

The first- and second-order Raman spectra of CCl_4, $SiCl_4$, $GeCl_4$, $SnCl_4$, and $TiCl_4$ are investigated. Based on analysis of the data obtained, conclusions are drawn regarding the magnitude and the sign of the ratio of the second and first polarizability derivatives with respect to the normal coordinate. The question of the influence of the character of the chemical bond in the molecules investigated on the intensity of their spectra is discussed. An interpretation of the anomalous behavior of carbon tetrachloride is given.

I. INTRODUCTION

In a preceding paper[1] it was shown in a large number of examples that there exists a parallel between the magnitude of the first polarizability derivative with respect to the natural coordinate and the character of the chemical bond formed by the vibrating atoms. Further information on this question permitting one to refine the presentations and also the light scattering phenomenon itself can be obtained by a comparative measurement of the intensity of the overtones and fundamental vibrations.

As is known, generally speaking, both mechanical and electro-optical anharmonicity acting simultaneously are required for the appearance of higher order scattering spectra. While the development of the general theory of the phenomenon is connected with great difficulties, still, in the simplest case where one examines a single vibrational transition $0 \rightarrow 2$ for a diatomic molecule the intensity of the first overtone can be described in the form of the comparatively simple expression

$$T_{\text{overtone}} \sim (\nu_{\text{exc.}} - 2\nu_{\text{vib.}})^4 \left[\frac{\partial\alpha}{\partial Q} \cdot Q_{0\rightarrow 2} + \frac{1}{2}\frac{\partial^2\alpha}{\partial Q^2}(Q^2)_{0\rightarrow 2}\right]^2 \frac{1+\rho}{6-7\rho}, \quad (1)$$

in which ν_{exc} and ν_{vib} are the frequencies of the exciting line and the vibrational band, respectively, $\partial\alpha/\partial Q$ and $\partial^2\alpha/\partial Q^2$ are the first and second polarizability derivatives with respect to the normal coordinate Q (coinciding in the given case with the natural coordinate q), $Q_{0\rightarrow 2}$ and $(Q^2)_{0\rightarrow 2}$ are respectively the matrix elements of the first and second degree coordinates calculated in the anharmonic approximation, and ρ is the degree of depolarization of the vibrational band.

Thus, the electro-optical problem of finding the first overtone intensity in the approximation chosen demands an investigation of the second derivative $\partial^2\alpha/\partial Q^2$. As Vol'kenshtein[2] has shown for the case where one electronic transition is predominant this quantity is developed into the algebraic sum of two terms

$$\left(\frac{\partial^2\alpha}{\partial Q^2}\right)_0 \sim \frac{2\nu_e^3 + 3\nu_e\nu_{\text{exc}}^2}{(\nu_e^2 - \nu_{\text{exc}}^2)^3}\left(\frac{\partial\nu_e}{\partial Q}\right)_0^2 - \frac{\nu_e^2 + \nu_{\text{exc.}}^2}{(\nu_e^2 - \nu_{\text{exc.}}^2)^2}\left(\frac{\partial^2\nu_e}{\partial Q^2}\right)_0, \quad (2)$$

where ν_e is the frequency of the predominant electronic vibrational transition.

Applying a Morse function* to approximate the upp

* Such an approximation, generally speaking, is admissible if the molecules examined dissociate from the upper state into neutral atoms (refer also to ref. 1).

potential curve we have

$$\left(\frac{\partial\nu_e}{\partial Q}\right)_0^2 \cong \frac{4a'^4 D'^2 Q'^2}{h^2}, \quad (3)$$

$$\left(\frac{\partial^2\nu_e}{\partial Q^2}\right)_0 \cong \frac{2}{h}\{(1 + 3a'Q')\,D'a'^2 - Da^2\}. \quad (4)$$

Here D' and a' are Morse function parameters for the excited state, Q' is the change of the equilibrium distance for the electronic excitation, and h is Planck's co

stant (the nonprimed quantities refer to the normal electronic state).

A rough evaluation of each of the terms in (2) shows that they are of the same order of magnitude; however, for some values of the parameters the second of them can be significantly larger or smaller than the first in absolute magnitude. In particular, it can go to zero. Then also the sign of the expression will vary. In the same way, the ratio of the intensities of the overtone and corresponding fundamental vibrations is also determined.

The examination carried out above is susceptible to generalization to the case of completely symmetric vibrations of some complex molecules, for example, with symmetric tetrahedra. Then, however, for the transition from normal to natural coordinates it is necessary to multiply the right-hand side of expression (1) by (2) as was also done in ref. 1. In the general case, the solution of the mechanical problem is required, and this definitely hinders the interpretation of quantitative data. The difficulties of studying the overtones also arise due to the fact that as a rule they have a low intensity. In complex molecules of not high symmetry, characterized by rich spectra, one must take account of the possibility of superposition of the overtones and fundamental vibrations. All of these circumstances limit the group of compounds amenable to quantitative measurements. In the present work only the tetrachlorides of a series of Group IV elements of the periodic system (CCl_4, $SiCl_4$, $GeCl_4$, $SnCl_4$, and $TiCl_4$) were studied. However, investigation of these compounds is of great interest for another reason: one of them, carbon tetrachloride, exhibits a deviation from the general rule which consists of a correlation between the magnitude of the polarizability derivative α with respect to the natural coordinate q and the type of chemical bond.[1]

The spectra were investigated using a DFS-12 photoelectric apparatus. Weakening of the fundamental vibrations was carried out using a NS-10 light filter having a transmission in the region of the mercury blue line equal to 0.45%. In all cases the integrated intensity of the bands was compared.

II. DESCRIPTION AND DISCUSSION OF THE RESULTS

The experimental material obtained in the study is given in Table 1. Carbon tetrachloride is not included in this table because the data referring to it almost completely coincide with the literature data.[3] In the following we will use only information on the intensity of the fundamental completely symmetric vibrations ν_1 of carbon tetrachloride (I = 1000) and of its first overtone $2\nu_1$ (I = 0.1).

Table 1. First- and Second-Order Raman Spectra of Tetrachloride Molecules*

Molecule	First-order scattering*	Second-order scattering**
$SiCl_4$	424 (ν_1, 1130), 150 (ν_2, 1130), 221 (ν_3, 920), 608 (ν_4, 190)	840 ($2\nu_1$, 0.2), 820 ($\nu_3+\nu_4$, 0.4)
$GeCl_4$	396 (ν_1, 3000), 120 (ν_2, 1560), 160 (ν_3, 1460), 453 (ν_4, 1200)	845 ($\nu_1+\nu_4$, 1.80), 785 ($2\nu_1$, 1.38), 620 ($\nu_3+\nu_4$, 3.0), 575 ($\nu_2+\nu_4$, 2.19), 340 ($\nu_1-\nu_2$, ?, 30), 285 ($\nu_2+\nu_3$, ?, 18)
$SnCl_4$	366 (ν_1, 5600), 104 + 134 ($\nu_2+\nu_3$, 8600), 403 (ν_4, 2000)	770 ($\nu_1+\nu_4$, 5.6), 730 ($2\nu_1$, 3.36), 525 ($\nu_3+\nu_4$, $\nu_3+\nu_4$, 16.8), 310 ($\nu_4-\nu_2$, 67.2)**, 265 ($\nu_1-\nu_3$, 33.6)**, 230 ($\nu_1-\nu_3$, $\nu_3+\nu_3$, 8.4)
$TiCl_4$	386 (ν_1, 9300), 120 + 141 (ν_2 and ν_3, 16800), 495 (ν_4, 2000)	995 ($2\nu_4$, 5.6), 875 ($\nu_1+\nu_4$, 33.5), 770 ($2\nu_1$, 25.1), 620 ($\nu_2+\nu_4$, $\nu_3+\nu_4$, 102.3), 270 ($\nu_1-\nu_2$, $\nu_2+\nu_3$, ?), 235 ($2\nu_2$, ?)

*The first number is the band frequency (in cm^{-1}), the second (in brackets) is the band intensity on a single scale. For brevity we denote by ν_1, ν_2, ν_3, and ν_4 respectively, the completely symmetric, twofold degenerate and threefold degenerate vibrations.

**The values of these frequencies are very close to those for the fundamental vibrations of the $HSnCl_3$ molecule. Therefore the possibility of error in their assignment to overtones is not excluded. In ref. 3 overtones with such frequencies were not observed.

As is seen from the data presented, the overtone bands grow in intensity in the given series much faster than the fundamental vibration bands. This appears quite clearly for the vibrations ν_1 and $2\nu_1$. Comparison, for example, of the data for $GeCl_4$ and $TiCl_4$ shows that the fundamental vibration ν_1 is intensified approximately three times while at the same time its overtone $2\nu_1$ is intensified approximately eighteen times. The connection between this behavior of the vibrations and the properties of the second derivative $\partial^2\alpha/\partial q^2$ is completely obvious: in comparison with the first derivative $\partial\alpha/\partial q$, generally speaking, it depends more sharply on the different parameters of the excited states.

We will investigate this question in more detail. Taking the ratio of the intensity of the overtone to the intensity of the fundamental vibration and using the known expressions for the matrix elements of the coordinate calculated in the anharmonic approximation[3,4] we obtain the equation

$$\frac{I_{\text{overtone}}}{I_{\text{fund}}} = \left(\frac{\nu_{\text{exc.}} - 2\nu_{\text{vib}}}{\nu_{\text{exc.}} - \nu_{\text{vib}}}\right)^4 \left\{\left(\frac{X_e}{2}\right)^{1/3} + \frac{1}{2}\, b\, \frac{\alpha''}{\alpha'}\right\}^2, \qquad (5)$$

in which X_e is the anharmonic constant, b is the zero point amplitude equal to $\sqrt{h/8\pi^2 \mu \nu_{\text{vib}}}$, and α' and α'' are, for brevity, the mentioned first and second polarizability derivatives with respect to the normal (or natural) coordinate (the remaining symbols are as before). Like the authors of ref. 3, for the evaluation of the anharmonic constant we make use of the approximate relationship $X_e = h\nu_{\text{vib}}/4D$, substituting in place of D the quadruple value of the mean bond energy in accord with the data of ref. 5. Solving Eq. (5) for α''/α' we obtain for each of the molecules two values of this quantity. The final results of this calculation are shown in Table 2.

Table 2. Values of the Quantity α''/α' Calculated Using Eq. (5)

Molecule	α''/α' (in A)
CCl_4*	−0.865 or −2.175
$SiCl_4$	−0.42 or −2.03
$GeCl_4$	0.02 or −2.44
$SnCl_4$	0.26 or −2.6
$TiCl_4$	2.03 or −4.13

*Other values of the quantity α''/α' are deduced in ref. 3, but these are evidently connected with a calculational error.

It is seen from the table that for carbon tetrachloride and silicon tetrachloride both values of α''/α' are negative, while for the other substances they are positive as well as negative. The particular position of carbon tetrachloride and silicon tetrachloride becomes understandable if we evaluate the contribution of the mechanical anharmonicity to the relative overtone intensity. Indeed, evaluation of this quantity by the formula $I_{\text{overtone}}/I_{\text{fund.}} = \alpha' q_{0\to 2}/\alpha' q_{0\to 1} = x_e/2$ shows that, for example, for CCl_4 it is 0.6×10^{-3}, exceeding by six times the observed value of $I_{\text{overtone}}/I_{\text{fund.}}$. Accordingly, the second derivative, α'', must be negative and this is in accordance with the calculation. In the case of the $GeCl_4$, $SnCl_4$, and $TiCl_4$

molecules the terms determining the contribution of the mechanical anharmonicity do not exceed the magnitude of the measured intensity, and in connection with this the second derivative α'' does not necessarily have to be negative.

In principle, one can assume that the negative sign of the ratio α''/α' is determined not by the numerator, but by the denominator, i.e., by the first derivative α'. This assumption, however, is doubtful since it corresponds to a strengthening of the bond on the electronic excitation of the molecule, i.e., a decrease of the quantity q', a case which is seldom observed in practice.

For a unique choice between the alternative values of the ratio α''/α' we will evaluate the parameters of the potential curve of the predominant electronic state. This can be done successfully and quite reliably in the case of the CCl_4, $SiCl_4$, and $TiCl_4$ molecules.

Initially, we will examine the CCl_4 molecule making use of the Morse approximation. Taking the experimental values of D from ref. 5 and the vibrational force constant k from ref. 6, with the assistance of the relation $2Da^2 = k$ we find the constant a. The inequality $(1 + 3a'q')D'a'^2 > Da^2$ [refer to expressions (2) and (4)] emerges directly from the negative sign of the second derivative, α''. The approximate relationship $D'a'^2 = 0.75Da^2$ satisfies this inequality if only q' is sufficiently large. As ν_e we will take the experimental value of the absorption limit lying at 44,000 cm^{-1}.[7]

For the $SiCl_4$ and $TiCl_4$ molecules we will use those conditions emerging from comparison of the quantities $I_{overtone}/I_{fund.}$ measured and obtained by a calculation method taking account only of the mechanical anharmonicity. They lead to the relations $\alpha'' < 0$ and $(\partial^2\nu_e/\partial q^2) \cong 0$ respectively. As before, the value of the constants D and a and of the frequency ν_e are found from the experimental data[5,7] where the equality $Da''^2 = 0.75Da$ is taken to be valid. Then the quantity q' turns out to be less than in the preceding case, particularly for the $TiCl_4$ molecule.

A summary of the starting data and of the final results of the calculation is contained in Table 3. While the calculation is, admittedly, only of an approximate character, still it permits one to draw a series of conclusions. First of all, it appears that the predominant electronic state does not correspond in any of the cases to the lowest potential curve intersecting the potential curve of the normal state: the predominant state lies rather high. Moreover, as is seen from Table 3, the ratio of the derivatives α''/α' for carbon tetrachloride and silicon tetrachloride coincide very closely with one of the negative values found earlier, and for titanium tetrachloride with the positive of the two values. This provides a basis for the conclusion that with the help of the calculation carried out one can sufficiently reliably determine which of the two values of α''/α' has a true physical meaning even in the two other investigated cases. Obviously this ratio is positive.

On the basis of the calculation carried out the assumption was made that one electronic transition is preferentially predominant for the Raman spectra of the tetrachlorides. The probability of the assumed model is proven by the close coincidence of the quantities α''/α' found by the different methods. As still one more argument in favor of this assumption one can introduce the data on the ratio of the intensities of the fundamental bands of the completely symmetric vibrations of the CC $SiCl_4$, and $TiCl_4$ molecules. The calculation shows that these quantities in written order are relatively 1:1.29:9. The corresponding experimental values are equal to 1, 1.13, and 9.3.

Table 3. Calculated Values of the Quantity α''/α'

Molecule	$\nu_e \times 10^{-13}$ (sec^{-1})	$D \times 10^{12}$ (ergs)	$a \times 10^{-8}$ (cm^{-1})	$D' \times 10^{12}$ (ergs)	$a' \times 10^{-8}$ (cm^{-1})	$q' \times 10^{8}$ (cm)	α''/α' (A)
CCl_4	1.3	5	1.35	4.7	1.2	4	− 0.79
$SiCl_4$	1.15	6	1.5	5	1.4	1.75	− 0.46
$TiCl_4$	0.90	7	1.3	6.2	1.2	1	2.00

In order to judge as to whether the data on the Ram spectral intensities of the tetrachlorides investigated may serve as a measure of the covalent nature of the corresponding bonds one must verify that the predominant state is the lowest ionic state. In this case the London criterion[1] is applied to the interpretation of the data. The calculation of the Morse function, applied earlier for the purpose of simplification, by no means excludes the ionic character of the curve.

We will assume that the essential state is in reality the lowest ionic. We will approximate the ionic curve b a Born potential $E = -(c\epsilon^2/q) + (d\epsilon^2/q^n)$ where ϵ is the charge of the ion, n is a constant which one can take equal to 9, and c and d are unknown constants. In orde to determine the values of these constants it is sufficien to form expressions for $(\partial\nu_e/\partial q)_{q_0}$ and $(\partial^2\nu_e/\partial q^2)_{q_0}$, to equate them to the quantities found earlier from formul (3) and (4), and to solve the system of two equations wit two unknowns. It is completely evident that such ionic curves will equally well satisfy the experimental facts a the atomic ones introduced earlier if only they are normalized to the initial values of ν_e.

For the purpose of descriptiveness we depict all of the potential curves for the CCl_4 (a) and $TiCl_4$ (b) molecules in the figure. One's attention is drawn to the fact that the upper ionic curve of the CCl_4 molecule is distinguished by a low stability: its right hyperbolic branc corresponds to an extraordinarily low value of c (0.04). On the other hand the curve of the $TiCl_4$ molecule is nor mal and has a constant c which is very close to 1. This circumstance demands great caution in evaluating the character of the corresponding bands.

Up until the present time it was assumed that the distance between the asymptotes of the curves of the normal and closest lying ionic states could serve as a measure of the covalent nature of the bonds. In this formulation the London criterion is valid only with respect to those curves for which the hyperbolic branches satisfy the single simple equation $E = -\epsilon^2/q$ ($c = 1$). In the general case it is more correct to compare the posi tion of the minimum of the ionic curve with respect to the atomic asymptote.

As seen from the figure, this minimum for the CCl molecule lies higher and for the $TiCl_4$ molecule lower than the corresponding asymptotes. Accordingly, one must assign a higher covalent nature to CCl than to the TiCl bond. In this it is very important that the distance considered be essentially determined by the position of the asymptote of the lowest curve not influencing the intensity of the Raman bands. This means that the partic lar position of carbon tetrachloride is explained by the inadequacy of the spectroscopic criterion of bond type. Understandably, the question itself of the nature of this inadequacy remains open. Judging by the same indications the CCl_4 bonds are also markedly more covalent than the $SiCl_4$ bonds which is in complete accord with generally assumed ideas.

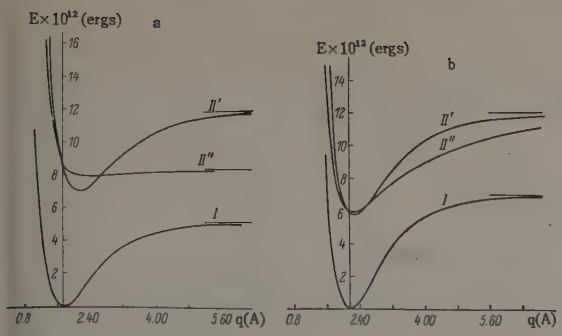

Potential curves for the CCl_4 (a) and $TiCl_4$ (b) molecules. Curves II′ and II″ refer respectively to the atomic and ionic upper states. At the point of intersection of the atomic and ionic curves with the vertical line (the ordinate axis), denoting the optical transition, the derivatives $\partial\nu_e/\partial q$ and $\partial^2\nu_e/\partial q^2$ for each curve are equal.

The trend of the band intensities in the spectra of e other tetrachlorides evidently correctly reflects the emical bond bypes. This is seen from the data of able 4 in which a comparison of some properties of ese molecules is presented. It is considered that with n increase in the covalent nature of the bond, the sum the covalent radii of the atoms more closely approxiates the length of the bond formed by them.[8] On the her hand, it follows from analysis of the experimental ta that at the same time there is a decrease in the magtude of the vibrational force constant. It is seen from able 4 that for the $SiCl_4$, $GeCl_4$, and $SnCl_4$ molecules sitioned in a series according to increasing Raman nd intensities (or the derivatives $\partial\alpha/\partial q$) the degree of ortening of the bond and the magnitude of the force conant indeed decrease. It is logical to assume a growth the covalent nature of the bonds in the same series. his is supported by the trend of the atomic electrogativity differences (the last column of Table 4). Acrding to the evidence of the magnitude of the bond

Table 4. Comparison of Some Bond Parameters in a Series of Tetrachlorides

Molecule	Bond length R (A)	Sum of the covalent radii R_A+R_B (A)	Shortening of the bond R_A+R_B-R (A)	Force constant $k\times10^{-5}$ (dyne/cm)	Electronegativity difference E_A-E_B
$SiCl_4$	2.02	2.16	0.14	2.68	1.25
$GeCl_4$	2.08	2.21	0.13	2.42	1.13
$SnCl_4$	2.30	2.39	0.09	2.30	0.83
CCl_4	1.76	1.78	0.02	1.82	0.58

shortening and the value of the force constant, CCl_4 should be placed after $SnCl_4$.

Finally, we note that the stability of the upper potential curves for the $TiCl_4$ molecule excludes the possibility of the continuous absorption by these molecules which is observed in practice. Evidently this contradiction is only apparent and is explained by the predissociation nature of the continuous spectrum. In the case of complex molecules this phenomenon is extraordinarily widespread.

REFERENCES

1. Ya. S. Bobovich, Opt. i Spektr. 11, 161 (1961), Optics and Spectroscopy 11, 85, (1961).
2. M. V. Vol'kenshtein, M. A. El'yashevich, and B. I. Stepanov, "Molecular Vibrations," Vol. 2, Gosudarst. Izd. Tekh.-Teoret. Lit., Moscow-Leningrad, 1949.
3. H. L. Welsh, M. F. Crawford, and G. D. Scott, J. Chem. Phys. 16, 97 (1948).
4. Ya. S. Bobovich and V. M. Pivovarov, Opt. i Spektr. 3, 227 (1957).
5. T. Cottrell, "Strength of Chemical Bonds," p. 258. Izd. Inostrannaya Lit., Moscow, 1950.
6. K. Kohlrausch, "Raman Spectra," p. 138, Izd. Inostrannaya Lit., Moscow, 1952.
7. H. Sponer, "Molekulspektren und Ihre Anwendung auf ghelishe Problene," p. 106. Springer, Berlin, 1936.
8. L. Pauling, "Nature of the Chemical Bond." Gosudarst. Izd. Khim. Lit., Moscow, 1947.

DETERMINATION OF MACRORADICAL CONFORMATIONS BY THEIR ELECTRON PARAMAGNETIC RESONANCE (EPR) SPECTRA

I. S. Milevskaya and M. V. Vol'kenshtein (pp. 349-352)

Received 24 October 1960

The EPR spectra of several macroradicals have been found to depend on the internal rotation angles, i.e., on the conformation of the radicals. The nature of this dependence is explained, making possible in a number of cases the determination of macroradical conformation from the appearance of its EPR spectrum. The internal rotation angles φ_1 are determined for a series of radicals.

1. There have been a large number of investigations[1-7] in which the EPR spectra of polymeric radicals obtained by various means have been studied.

In the spectra of a complete series of macroradicals (polymethylmethacrylate, polyethylmethacrylate, polymethacrylic acid, etc.) anomalies have been observed, consisting of violations of the fundamental hyperfine structure relation[8]

$$m = 2nI + 1, \qquad (1)$$

where m is the number of absorption lines, and n is the number of equivalent nuclei with spin I (in our case protons with I = 1/2) with which the unpaired electron interacts. The most probable structural formulas of the radicals referred to are:

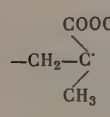
polymethylmethacrylate (PMMA),

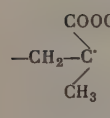
polyethylmethacrylate (PEMA),

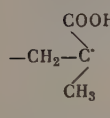
polymethacrylic acid (PMAA).

Each of these radicals has five equivalent protons which can interact with the unpaired electron and should give, according to Eq. (1), six absorption lines, Experimentally, however, all of these radicals show similar spectra consisting of a quintet and superimposed quartet of lines. A qualitative explanation of this phenomenon has been given by Symone,[3] who supposed that, as a consequence of the lack of free rotation of the methylene group in the macroradical, conformations were possible in which either one or both protons lay in the nodal plane of the unpaired electron and did not participate in the interaction.

This assertion required quantitative verification, inasmuch as cases are known (aromatic radicals) in which the protons lying in the nodal plane still interact strongly with the unpaired electron. Besides, it was of interest to ascertain which conformations pertained to the observed spectrum and to what extent it was generally possible to form conclusions about the radical conformations on the basis of the EPR spectra. This question is the subject of the present paper.

2. We consider the interaction of the unpaired elec tron with the protons of the methylene group attached t the trigonal C atom (Fig. 1). Isotropic hyperfine splitti of EPR spectra is caused by the presence of a nonzero spin density on the σ-orbits of the C—H bonds. McCon nell[9] has defined an operator ρ_χ giving the spin density on an atomic orbital χ by the following equation:

$$\rho_\chi \sum_\mu s_{\mu\sigma} = \sum_\mu \Delta_{\chi(\mu)} s_{\mu\sigma},$$

where $\Delta_{\chi(\mu)}$ is a three-dimensional δ-function, i.e.,

$$\langle \chi'(\mu) | \Delta_{\chi(\mu)} | \chi''(\mu) \rangle = \delta_{\chi\chi'} \delta_{\chi\chi''}.$$

A nonzero spin density in the methyl and methylen groups is possible only through the admixture of excite triplet states. Using the results of McLachlan,[10] who calculated the spin density at the protons of a methyl group attached to a trigonal atom by the method of valence schemes with hyperconjugation, we obtain

$$\rho_{H_i} = \frac{I(t_i, \psi_{p_z})}{2I(t_i, h_i)} \rho_p.$$

Here ρ_p is the unpaired electron density on the trigona atom ($\rho_p = 1$) and I(a,b) are the exchange integrals for the corresponding atomic orbitals. In calculating the exchange integral appearing in the numerator of Eq. (4 it is necessary to take into account its dependence on the relative orientation of the p_z orbital and the direction of the i-th C—H bond. In order to fix the direction of the C—H bonds, we shall introduce into the hybridize carbon functions t_i a parameter φ_1, which defines the angle of rotation of the three bonds formed by the tetra hedral atom relative to the bond joining it to the trigon atom. In other words, φ_1 is the angle of internal rotation in the radical about the C—C bond we have indicat The tetrahedral hybridized functions that depend on the internal rotation angle as parameter have the form

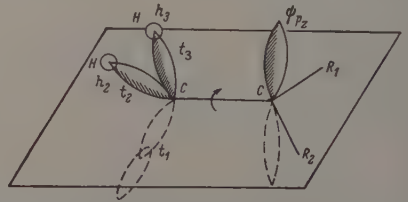

Fig. 1. Relative disposition of methylene group and unpaired electron orbitals. R_1—CH_3 group; R_2—$COOCH_3$, $COOC_2H_5$, COOH groups respectively in PMMA, PEMA, and PMAA.

$$t_0=\frac{1}{2}\psi_s+\frac{\sqrt{3}}{2}\psi_{p_x},$$

$$t_1=\frac{1}{2}\psi_s-\frac{1}{2\sqrt{3}}\psi_{p_x}+\sqrt{\frac{2}{3}}\sin\varphi_1\psi_{p_y}+\sqrt{\frac{2}{3}}\cos\varphi_1\psi_{p_z},$$

$$t_2=\frac{1}{2}\psi_s-\frac{1}{2\sqrt{3}}\psi_{p_x}+\sqrt{\frac{2}{3}}\sin(\varphi_1+120°)\psi_{p_y}+\sqrt{\frac{2}{3}}\cos(\varphi_1+120°)\psi_{p_z},\quad(5)$$

$$t_3=\frac{1}{2}\psi_s-\frac{1}{2\sqrt{3}}\psi_{p_x}+\sqrt{\frac{2}{3}}\sin(\varphi_1+240°)\psi_{p_y}+\sqrt{\frac{2}{3}}\cos(\varphi_1+240°)\psi_{p_z}.$$

The exchange integral $I(t_i, \psi_{p_z})$, when the mutually thogonality of the atomic orbitals $\psi_s, \psi_{p_x}, \psi_{p_y}$, and $_z$ is taken into account, transforms to

$$I(t_i, \psi_{p_z})=\frac{2}{3}\cos^2\varphi_i I(\psi_{p_z}, \psi_{p_z'}),\quad i=1, 2, 3,\quad(6)$$

ere $\varphi_2=\varphi_1+120°$, $\varphi_3=\varphi_1+240°$.

Since the internal rotation of the methyl group rela- e to the C—C bond occurs at a relatively fast rate, it permissible to average over the angle φ_1 in Eq. (6) en the calculation of the spin density on the methyl oup orbitals is carried out. In this case the exchange egral (6) is the same for all three C—H bonds and als

$$I(t_i, \psi_{p_z})_{\text{methyl.}}=-\frac{1}{3}I(\psi_{p_z}, \psi_{p_z'}),\quad(7)$$

ich agrees with McLachlan's result.[10] In the case of methylene group, it is impossible to carry out this eraging, since the spatial orientation of the C—H bonds this case is determined by the angle of internal rota- n, which has a completely definite value for each lymeric radical. Thus the exchange integral (6) has same value for both C—H bonds of the methylene oup only for the following values of the internal rota- n angle: φ_1 = 90, 180, and 270° (−90). For all other lues of φ_1 the methylene group protons will interact ferently with the unpaired electron, and the splitting nstants for these protons will differ.

3. The magnitude of hyperfine splitting in an EPR ectrum is calculated from the formula[8]

$$\Delta H=Q\rho,\quad(8)$$

ere ρ is the unpaired electron density at the trigonal om, and Q is a semiempirical constant which can be termined from the relation

$$Q=a_H\rho_H.\quad(9)$$

Here a_H = 500 gauss is the magnitude of the splitting rresponding to ρ_H = 1, i.e., to the case when the un- ired electron is located on an atomic 1s orbital.[8] Cal- lating ρ_H, we have for the methyl group

$$\rho_H=\frac{I(\psi_{p_z}, \psi_{p_z'})}{6I(t_i, h_i)}\rho_p\quad(10)$$

d for the methylene group

$$\rho_{H_i}=\frac{1}{3}\cos^2\varphi_i\frac{I(\psi_{p_z}, \psi_{p_z'})}{I(t_i, h_i)}\rho_p,\quad i=2, 3.\quad(11)$$

Altmann[11] has made a theoretical evaluation of the change integral $I(\psi_{p_z}, \psi_{p_z'})$ and obtains a value of 1.24 for an interatomic spacing of 1.54 A. The integral

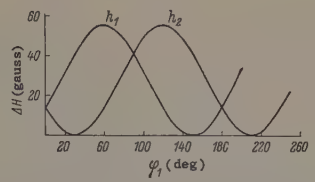

Fig. 2. Dependence of splitting of the EPR spectrum on the internal rotation angle φ_1 for the methylene group protons.

$I(t_i, h_i)$ can be evaluated empirically from the C—H bond energy;[10,12] it equals 3.75 ev. Upon substituting these values into Eqs. (8)-(11) we find that the splitting for each methyl group proton equals 28 gauss. The amount of splitting given by the proton pair on the methylene group is shown in Fig. 2 as a function of the internal rotation angle. At φ_1 = 16° one of the protons on the CH_2 group will give a splitting of 28 gauss (same as a CH_3 proton), whereas the other gives 4 gauss. Such a conformation yields a spectrum consisting of the regular quintet with binomial intensity distribution from four equivalent protons, with the fifth proton causing each quintet component to split into two lines, 4 gauss apart. These doublets are not resolved on account of the unusually wide lines obtained experimentally. It should be possible to observe the quintet within the range $10° < \varphi_1 < 20°$. A conformation corresponding to a quartet of lines in the spectrum cannot be found. Apparently this spectrum belongs to a different radical, as previously suggested.[6,7]

Isotactic PMMA crystallizes in the form of a 5_2 spiral.[13] T. M. Birshtein has made a theoretical determination of the internal rotation angle corresponding to such a spiral. If one assumes that all the angles in the main chain are tetrahedral, the internal rotation angles are equal to $\varphi_1 = 10°$ and $\varphi_2 = 140°$, whereas under the presumption that the main chain angle for the CH_2 group equals 122°, $\varphi_1 = -20°$, $\varphi_2 = 150°$ (here φ_2 is the angle of internal rotation relative to the other C—C bond of the main chain). These results show that the value of internal rotation angle φ_1 that we have obtained is completely reasonable.

The authors thank E. M. Saminskii and T. M. Birshtein for valuable discussions.

REFERENCES

1. E. E. Schneider, M. J. Day, and G. Stein, Nature 168, (1951).
2. E. E. Schneider, Discussions Faraday Soc. 19, 157 (1955).
3. D. J. E. Ingram, M. C. R. Symone, and M. G. Townsend, Trans. Faraday Soc. 54, 409 (1958).
4. R. J. Abraham, H. W. Melville, D. W. Ovenall, and D. H. Whiffen, Trans. Faraday Soc. 54, 1133 (1958).
5. R. J. Abraham and D. H. Whiffen, Trans. Faraday Soc. 54, 1291 (1958).
6. S. E. Bresler, E. N. Kazbekov, and E. M. Saminskii, High Molecular Weight Compounds 1, 132 (1959). (sic)
7. S. E. Bresler, E. N. Kazbekov, and E. M. Saminskii, High Molecular Weight Compounds 1, 1374 (1959). (sic)
8. D. J. E. Ingram, "Free Radicals as Studied by Electron Spin Resonance." London, 1958.
9. H. M. McConnell, J. Mol. Spectroscopy 1, 11 (1957).

10. A. D. McLachlan, Mol. Phys. 1 (3), 233 (1958).
11. S. L. Altmann, Proc. Roy. Soc. (London) A210, 327, 343 (1951).
12. T. L. Cottrell, "The Strength of Chemical Bonds." Butterworth, London 1954. Izd. Innostrannaya Lit., Moscow, 1956.
13. J. D. Stroupe and R. E. Hughes, J. Am. Chem. Soc. 80, 2341 (1958).

LIGHT SCATTERING IN CRYSTALLINE POLYMERS
II. Investigation of the Temperature Dependence of the Index of Refraction of the Crystalline and Amorphous Phases of Polychloroprene and the Determination of the Degree of Crystallization

O. N. Trapeznikova, G. E. Novikova, and S. V. Minakova (pp. 353-358)

Received 11 October 1960

The temperature dependence of the index of refraction was measured in 11% and 7% crystalline polychloroprene and also in amorphous polychloroprene. The mole refraction and the temperature dependence of the index of refraction of the crystalline phase were calculated. The intensity of the depolarized component of scattered light was shown to have a temperature dependence caused by changes of the relative index of refraction of the crystalline and amorphous phases with temperature. A method was proposed for quantitatively determining the relative amounts of the amorphous and crystalline phases in polychloroprene.

INTRODUCTION

In an earlier paper[1] we investigated the fusion process in polychloroprene by measuring the temperature dependence of the light scattering function. Since the form of this curve remains constant up to the temperature of fusion, we conclude that there is no decrease in the size or number of crystals, but that there is a decrease in the anisotropy of the crystals due to an increase in thermal motions and to the approach of the index of refraction of the crystalline phase to that of the amorphous phase. Stein[2] also has concluded that during fusion the dimensions of the scattering particles are constant. We used a polarizing microscope to investigate the fusion of polymers (polyethylene, gutta percha), and as the temperature increased we observed the gradual extinction of the crystallites as a whole with no change in their size or number. If the sample is rapidly cooled after the field of view is completely dark, the former pattern reappears.

In our opinion, all these investigations indicate that the observed decrease in intensity of the scattered and transmitted light is caused by a change of the index of refraction of the crystalline and amorphous phases. Therefore, it is of interest to determine by direct measurement the temperature dependence of the index of refraction of the separate crystalline and amorphous phases. These data can then be compared with the results of our investigation of fusion processes.

At present we have data on the values of the index of refraction of the amorphous phase for few crystalline polymers. Determination of these quantities for the crystalline phase is usually accomplished by measuring the index of refraction of a strongly oriented amorphous sample. Since the literature contains little information on this subject,[3-5] an investigation of the temperature dependence of the index of refraction of polymers also has intrinsic significance. As is shown below, a knowledge of these quantities makes it possible to determine the percentage content of the crystalline phase in the sample.

EXPERIMENTAL METHOD AND INTERPRETATION OF RESULTS

For our measurements we used polychloroprene, a substance we had investigated earlier.[1] Polychloropren is not highly crystallized at room temperature, it has a easily attained fusion temperature (40-50°C), and it cr tallizes slowly at room temperature (several weeks).

Using a method described previously[1] the samples were prepared as films from which were cut pieces of the desired size. Since the samples were measured both on a refractometer and on a light scattering apparatus and were taken from the same film, the film had to be thin enough to avoid chromatic dispersion and at the same time thick enough to allow measurements wit a refractometer. The optimum thickness was 0.10-0.1 mm.

We measured directly the index of refraction of th sample n_s and the index of refraction of the amorphou phase n_a. The measurements were made on an IRF-22 Abbe refractometer in reflected light. The polychloroprene film was attached to the prism without using an intermediate liquid (contact with the prism was achiev by pressure on the sample). The portion of the sample facing the light source had to be cut evenly and be perpendicular to the plane of the prism. The temperature was regulated with a thermostat and was measured wit a copper-constantan thermocouple. As a preliminary t measurement the surface of the prism was checked fo the absence of temperature gradients. The part of the refractometer containing the film and thermocouple w enclosed in asbestos for better thermal stability.

The measurements were taken in the following order: first we measured n_s by heating the sample from room temperature up to 60-70°C during which process readings on the refractometer were made at a series fixed temperatures (n_s remained constant for approximately twenty minutes). The temperature dependence n_a could be measured either while gradually lowering the temperature or, after quickly cooling the sample,

ile heating the still melted amorphous sample (the re-
lts of these two methods were identical).*

his was possible because of the slow crystallization of
lychloroprene which for t = 25°C was practically un-
servable.

Figure 1 gives the results of our measurements of
samples with different degrees of crystallization.
is easy to see that the larger the amount of crystalline
ase the higher the index of refraction. Since both sam-
es were crystallized at the same temperature (18°C),
ey had the same temperature of fusion (42°C). Obviously,
mples crystallized at different temperatures would
ve indices of refraction with some other temperature
pendence. The index of refraction of the amorphous
ase is the same for all samples in the given tempera-
re interval and depends linearly on the temperature.
turned out to be possible to measure n_a of polychlo-
prene at even lower temperatures because there was
noticeable crystallization during the measurement.

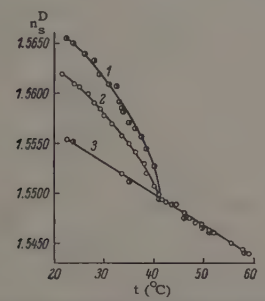

Fig. 1. The temperature dependence of the index of refraction of polychloroprene samples with different degrees of crystallization φ. φ: curve 1—11%; curve 2—7%; curve 3—0%.

Figure 2 gives the temperature dependence of the
lex of refraction of the sample n_s and of the amorphous
ase n_a in the interval above 3°C. The temperature de-
ndence of n_a exhibits an insignificant deviation from
earity at temperatures below room temperature. In
is region measurements give n_a the following temper-
ure dependence:

$$n = 1.5629 - 0.000476t + 0.000003t^2.$$

It is assumed that the magnitude of the index of re-

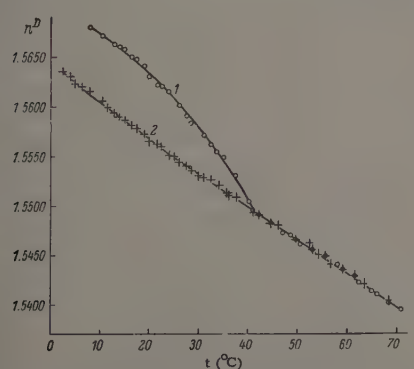

Fig. 2. The change of the index of refraction of polychloroprene samples upon heating (curve 1) and upon cooling (curve 2).

fraction of a partially crystallized sample is the sum of the fractional contributions of the crystalline and amorphous phases, thus

$$n_s = n_c \varphi + (1 - \varphi) n_a, \quad (1)$$

where n_s, n_c, and n_a are the indices of refraction of the sample under investigation, the crystalline phase, and the amorphous phase respectively (n_c is the average of the values corresponding to different crystallographic axes), and φ is the fraction of the sample in the crystalline phase.

To calculate n_c from this formula one must know the fractional content φ of crystalline phase. As was mentioned above it follows from our previous observations that φ remains constant with temperature almost up to the temperature of fusion. From experiments on the direct determination of the crystal cell size at various temperatures Swan[6] has drawn conclusions in complete agreement with ours.

If V_s, V_a, and V_c are the specific volumes of the sample, of the amorphous phase, and of the crystalline phase, respectively, then we find from an equation analogous to (1) that

$$\varphi = \frac{V_a - V_s}{V_a - V_c}. \quad (2)$$

V_c was calculated from x-ray data on the size of the crystal cell and the number of monomer components in a cell.[7] At room temperature V_c was found to be 0.7371 cm^3. To determine the temperature dependence of V_s and V_a dilatometric measurements were made on the films from which were taken the samples measured on the refractometer. We used a quartz pycnometer, 0.699 mm^3 (sic) in volume, into the neck of which was inserted a capillary 12 cm high and 0.6 mm internal diameter (the uniformity of the capillary was checked with a microscope). The expansion of the pycnometer with temperature was determined experimentally so that correction for the expansion could be made in our calculations. As soon as the weighed material was placed in the pycnometer, the system was subjected to high vacuum for 12 hr and then (also under vacuum) was sealed with distilled mercury. First we determined the specific volume and density of the samples at room temperature. The calculated density was 1.2503 and 1.2431 gm/cm^3 for the samples with greater and lesser degrees of crystallization respectively. Next, the pynconometer, containing the substance and the mercury, was placed in a special furnace which had a window for observing movements of the mercury meniscus. The height of the meniscus was measured to an accuracy of 0.01 mm by means of a cathetometer. When determining the change of specific volume, corrections were made for expansion of the mercury and of the pyncnometer.

Just as for the refractometer measurements, the change in sample volume was measured at increasing temperatures up to complete fusion and even higher up to 60°C. Next the temperature dependence of V_a was measured while cooling the melted (amorphous) sample. In most cases it is difficult to measure V_a at room temperature and it is not always correct to use a linear extrapolation of the specific volume of the melted sample to room temperature.[6] As mentioned earlier, polychloroprene crystallizes very slowly at room temperature so it is possible to measure V_a directly right down to room temperature. To determine the degree of crystallization it is sufficient to know V_a and V_s at a temperature for

which V_c is calculated. Using formula (2) the values of φ for our samples were 11% and 7%.

Figure 3 gives the results of these measurements. Naturally V_s is lower for the more crystallized sample than for the less crystallized sample. Fusion occurs at exactly the same temperature (45°C) for both samples which implies that they crystallized at the same temperature (room temperature). It was noted that the temperatures of fusion obtained from measurements with the refractometer and the dilatometer differ by 3°. In the specified temperature interval V_s is linear with temperature to a first approximation and is the same for both samples.

Figure 4 is the temperature dependence of n_c of both samples as calculated from formula (1). As the graph shows, n_c goes from 1.6475 at room temperature down to the value of n_a at 42°C. The data for both samples agree to an accuracy of better than 0.3%. It is to be emphasized that our deductions are quantitatively valid only in the temperature interval where φ is constant. Consequently, in the immediate neighborhood of 42° n_c is not correct. A criterion for applying our calculations is considered below.

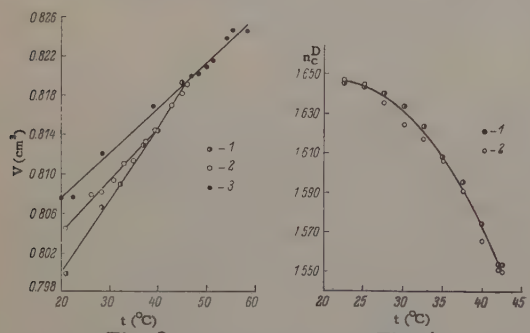

Fig. 3

Fig. 4

Fig. 3. The temperature dependence of the specific volume of the polychloroprene samples with different amounts of crystallization φ. φ: curve 1—11%; curve 2—7%; curve 3—0%.

Fig. 4. The temperature dependence of the index of refraction of the crystalline phase of samples with 11% crystallization (1) and with 7% crystallization (2).

Using the measurements taken with the refractometer and the dilatometer we calculated the mole refraction

$$R = \frac{n^2 - 1}{n^2 + 2} V$$

of the amorphous substance and of the two samples with different degrees of crystallization from room temperature up to 58°C. The results are given in the table. The table shows that there is a change in refraction that depends on the degree of crystallization. Although these changes are small (less than 0.7%), they all exceed errors of measurement and have a systematic trend. For the amorphous sample (φ = 0) the refraction is practically independent of temperature. For partially crystallized samples R decreases, with an increase in temperature, to the value corresponding to the amorphous state.

As mentioned above we have proposed that the temperature dependence of the intensity of scattered light is a result of the change of the relative index of refraction

The Dependence of Mole Refraction on Temperature and on the Degree of Crystallization

t (°C)	$\varphi = 0$	$\varphi = 7\%$	$\varphi = 11\%$
22	0.2597	0.2609	0.2614
25	0.2597	0.2610	0.2616
30	0.2599	0.2609	0.2616
35	0.2599	0.2602	0.2613
37	0.2600	0.2603	0.2611
39	0.2600	0.2600	0.2608
44	0.2601	0.2600	0.2600
46	0.2602	0.2602	0.2602
50	0.2603	0.2603	0.2603
55	0.2603	0.2603	0.2603
58	0.2603	0.2603	0.2603

of the crystalline and amorphous phases as a function of temperature. Therefore, it is of great interest to apply our data on the temperature dependence of n_c and n_a to our investigation of the fusion process in polychloroprene using scattered light.

As was shown in a preceding paper,[1] the most characteristic feature in scattering from anisotropic particles is the significant depolarization of the scattered light (chiefly in the forward direction). Therefore, we investigated the temperature dependence of the intensity of the depolarized component of the scattered light I_+ in the sample with 11% crystallization by means of the apparatus previously described.[1] This temperature dependence is shown in Fig. 5. Since the scattering function retains its shape on undergoing changes with temperature, the temperature dependence of I_+ can be investigated at any scattering angle, and we chose 8°.

In the formulas defining the scattering function for scattering from coarse inhomogeneities and from particles which are little different from the surrounding media,[3] there appears the quantity α^2 related to the index of refraction by the expression

$$\alpha = \frac{m^2 - 1}{m^2 + 2},$$

where m is the relative index of refraction of the particles and the surrounding media. If the number and size of particles remains unchanged during fusion, then the change in intensity is related only to the temperature dependence of α^2. Thus the temperature dependence of I_+ is equivalent experimentally to the temperature dependence of the coefficient of extinction. Consequently, this quantity α^2, which characterizes the scattering qualities of the medium, must be considered in the expression for I_+.

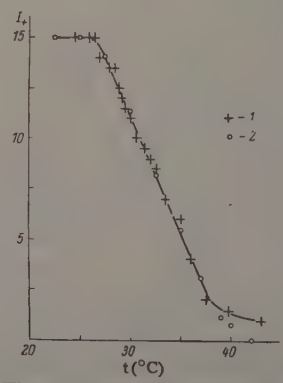

Fig. 5. The temperature dependences of I_+ (1) and α^2 (2) for a sample with φ = 11%.

Using a suitable scale we plotted values of α^2, calculated for different temperatures, and obtained the curve of Fig. 5. The graph shows that the points are in good agreement with the curve up to 38°C, i.e., up near the final melting temperature. Such good agreement further confirms the validity of our supposition that the vision process of polymers is a second order phase transition which is connected with the gradual disordering of the crystalline phase and the approach of its properties to those of the amorphous phase. Above 38°C φ changes with temperature which fact explains the divergence of the curves of $I_+(t)$ and $\alpha^2(t)$ above 38°C. This result serves as a criterion for the application of formula (1) in our calculations.

If the numerical values of n_c and n_a are known, the relative amounts of amorphous and crystalline phases may be determined by means of Eq. (1). For this purpose it is necessary only to measure the index of refraction of the investigated sample. If the sample is too disordered and no sharp boundary can be seen in the refractometer at room temperature, the sample must be heated to a temperature at which the boundary becomes distinct in order to make use of the data on the temperature dependence of n_c and n_a. It is also necessary that the temperature not be too close to the temperature of complete melting.

We have determined values of n_c for polychloroprene which crystallized at room temperature. Therefore, these data can be used only for similar samples. Obviously n_a does not depend on the temperature of crystallization of the sample and is valid for polychloroprene in general. The method we have described is reliable and simple to use.

REFERENCES

1. O. N. Trapeznikova and G. E. Smirnova, Opt. i Spektr. 3, 631 (1957).
2. J. J. Keane and R. S. Stein, J. Polymer Sci. 20, 327 (1956).
3. J. P. Bianchi, W. G. Leutzel, and F. P. Price, J. Polymer Sci. 27, 561 (1958).
4. A. Arnold, I. Madorsky, and L. A. Wood, Anal. Chem. 23, 1656 (1951).
5. C. D. West, Ind. and Eng. Chem. 10, 627 (1938).
6. P. R. Swan, J. Polymer Sci. 42, 525 (1960).
7. E. O. Kraemer, F. E. Bartell, and S. S. Kistler, Advances in Colloid Science, 2 (1946).
8. K. S. Shifrin, "Scattering of Light in Disordered Media." Gosudarst. Izd. Tekh.-Teoret. Lit. Moscow-Leningrad, 1951.

ON THE INFLUENCE OF CRYSTAL STRUCTURE ON THE VIBRATIONAL SPECTRUM OF THE HYDROGEN BOND

A. I. Stekhanov and Z. A. Gabrichidze (pp. 359-361)

Received 30 August 1960

Raman spectra have been obtained for hexa- and hepta-hydrated magnesium, nickel, and zinc sulfates. It has been established that the structure of the crystal lattice influences the vibrational spectrum of the hydrogen bond.

Investigations of the vibrational spectra of the hydrogen bond in crystals offer a possibility of obtaining important information on the nature and properties of this bond of intermolecular interaction, and also make it possible to elucidate a number of questions about the structure and dynamics of the crystal lattice. In the present work, investigations have been undertaken on the Raman spectra of the crystal hydrates $MgSO_4 \cdot 7H_2O$, $ZnSO_4 \cdot 7H_2O$, $NiSO_4 \cdot 7H_2O$, and $NiSO_4 \cdot 6H_2O$, with the aim of clarifying the peculiarities in the manifestation of the hydrogen bond in these crystals, and of studying the influence of the structure of the crystal lattice on the vibrational spectrum of the hydrogen bond.

In order to study the Raman spectra, we grew large (dimensions 40 × 15 × 15 mm) and homogeneous monocrystals of the above-mentioned crystal hydrates from aqueous solutions of magnesium, nickel, and zinc sulfates. Raman scattering was excited in the crystals by the light of the 2537 A resonance line of mercury, emitted by a low-pressure quartz mercury lamp, and was analyzed by means of a quartz spectrograph with a dispersion of 10 A/mm in the region of the OH vibrations.

Microphotometer tracings of the Raman spectra obtained at room temperature for $MgSO_4 \cdot 7H_2O$, $NiSO_4 \cdot 7H_2O$, and $ZnSO_4 \cdot 7H_2O$ crystals in the OH vibration region are presented in Fig. 1. As can be seen from the figure, the

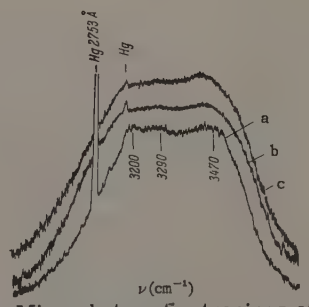

Fig. 1. Microphotometer tracings of the Raman spectra of $MgSO_4 \cdot 7H_2O$ (a), $NiSO_4 \cdot 7H_2O$ (b), and $ZnSO_4 \cdot 7H_2O$ (c) crystals at room temperature.

vibrations of the OH groups manifest themselves in the spectra of these crystals in the form of a smooth intense band extending from 2800 to 3700 cm^{-1}. Against the background of this band, one can note three broad maxima in each case. In the spectrum of $MgSO_4 \cdot 7H_2O$, the maxima are located around 3200, 3290, and 3470 cm^{-1}; in the spectrum of $NiSO_4 \cdot 7H_2O$, at 3170, 3280, and 3440 cm^{-1}; and in the spectrum of $ZnSO_4 \cdot 7H_2O$, at 3160, 3270, and 3430 cm^{-1}.

Lowering of the temperature to 77°K leads to splitting of the OH vibration band into a series of narrow bands. This is well illustrated in the microphotometer tracings represented in Fig. 2. (The frequencies of the narrow maxima are given in the table, and the frequencies of the deformation vibrations found by us for the OH group are also presented here.)

Crystals	Vibration frequencies of the OH group (cm^{-1})									
	νstretch									νdef.
$MgSO_4 \cdot 7H_2O$ . .	3068	3130	3190	3264	3297	3336	3361	3401	3454	1670
$NiSO_4 \cdot 7H_2O$ . .	3063	3127	3174	3246	3280	3322	3361	3399	3438	1665
$ZnSO_4 \cdot 7H_2O$ . .	3050	3127	3170	3240	3270	3313	3354	3392	3425	1663

The spectrum of nickel sulfate hexahydrate is shown in Fig. 3. At room temperature, the spectrum of this crystal in the OH vibration region is represented by a broad band with maxima at 3100 (superimposed on a mercury line), 3290, and 3430 cm^{-1} (Fig. 3, a). At low temperature, as in the case of the heptahydrated sulfates, a discontinuous spectrum (Fig. 3, b) is found in place of the band; the frequencies of the lines equal 3110, 3137, 3216, 3283, 3315, 3351, 3392, 3429, and 3456 cm^{-1}.

As can be seen from Figs. 1 and 2, the spectra of the heptahydrate crystals are very similar to one another both in the number of lines in the spectrum and in the distribution of intensities. Actually, to each maximum in the spectrum of one of the crystal hydrates, one can match the maximum corresponding to it in the spectrum of another. However, on more detailed examination one can note that the frequencies of corresponding maxima in the spectra of these crystals are regularly displaced relative to one another. Specifically, the values of the frequencies in the $MgSO_4 \cdot 7H_2O$ spectrum are greater than the corresponding frequencies for $NiSO_4 \cdot 7H_2O$, and the latter in their turn are somewhat greater than for $ZnSO_4 \cdot 7H_2O$.

Comparison of the spectra of the heptahydrate crystals and of the $NiSO_4 \cdot 6H_2O$ crystal at room temperature

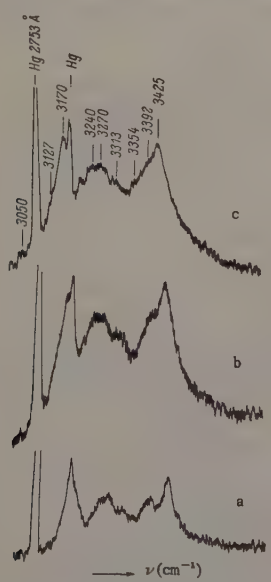

Fig. 2. Microphotometer tracings of the Raman spectra of $MgSO_4 \cdot 7H_2O$ (a), $NiSO_4 \cdot 7H_2O$ (b), and $ZnSO_4 \cdot 7H_2O$ (c) crystals at a temperature of 77°K.

(Fig. 1 and Fig. 3, a) shows that the OH vibration band the $NiSO_4 \cdot 6H_2O$ spectrum is markedly broadened on th long-wavelength side, and the structure of the bands ob served at low temperature differs greatly in the two cases, as can be plainly seen on comparison of the microphotometer tracings presented in Fig. 2.and Fig. 3,

Let us turn to an examination of the results obtain The similarity of the spectra of the heptahydrate crystals which have been examined finds its explanation in the fact that these crystals are isomorphous; their cry tal lattices belong to the single space group D_2^4 and the dimensions of their unit cells correspond closely.[1] It is therefore natural to expect that both the number and lengths of the hydrogen bonds will be approximately th same in all three crystals. Accordingly, the isomorph crystals must have similar spectra, which is observed in the case of the heptahydrate crystals (Figs. 1 and 2) A second confirmation of the effect of crystal structur on the vibrational spectrum of the OH group is the large difference between the spectrum of nickel sulfate hexahydrate and the spectrum of the heptahydrate (des their closely-similar chemical compositions). In actu fact, the crystal structure of $NiSO_4 \cdot 6H_2O$ belongs to th space group D_4^4.[2] Correspondingly, this crystal posses in the region of the stretching vibrations of the OH gro a spectrum of its own which is not like the spectrum o $NiSO_4$ heptahydrate.

Thus, the results obtained in the investigation of t hexa- and heptahydrates enable us to draw a conclusio concerning the important role of the structure of the crystal lattice in the formation of the OH vibration ban in crystal spectra. It appears possible to explain the difference noted above in the spectra of the crystalline heptahydrates of $MgSO_4$, $NiSO_4$, and $ZnSO_4$ by the non-identical effect of the cations Mg^{++}, Ni^{++}, and Zn^{++} o the hydrogen bond. The difference in the crystal radii the cations leads to a somewhat different additional po ization of the water molecules surrounding them, whic brings about a small difference in the energies of the h drogen bonds formed in the crystals. According to the conclusions of Sokolov's theory,[3] this must lead to a n identical displacement of the OH vibration band of the water molecule, as observed in our experiments.

A detailed interpretation of the complicated struct of the OH vibration band which is found in the Raman spectra of the crystal hydrates studied does not appea possible at the present time, since we do not have ade quate data available on the structure of these crystals,

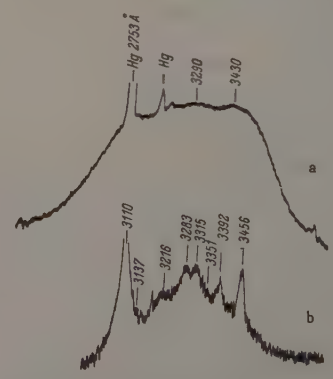

Fig. 3. Microphotometer tracings of the Raman spectra of a $NiSO_4 \cdot 6H_2O$ crystal at room temperature (a) and at a temperature of 77°K (b).

rticularly on the position of the hydrogen atom. One n only express the hypothesis that the most intense nes in the observed structure of the OH vibration band, in the case of other crystals,[4,5] are associated with e presence of two equilibrium positions for the proton the complex $R_1OH---OR_2$. In the region of the OH vi- ation band, overtones of the deformation vibrations of e water molecule should also appear. However, the mbination frequencies formed from the deformation equencies presented in the table do not coincide with y of the observed band maxima. It is more probable at the weak lines of the OH vibration band may be oduced by interaction of the stretching vibrations with anslational intermolecular vibrations of the water olecules in the crystals.[6]

REFERENCES

1. H. G. Westenbrink, Proc. Amsterdam 29, 1223, 1374 (1926).
2. C. A. Beevers and H. Lipson, Z. Kristallogr. 83, 123 (1932).
3. N. D. Sokolov, Zhur. Eksptl. i Teoret. Fiz. 23, 404 (1952).
4. A. I. Stekhanov, Doklady Akad. Nauk SSSR 106, 433 (1956).
5. A. I. Stekhanov, Izvest. Akad. Nauk SSSR, Ser. Fiz. 21, 311 (1957).
6. A. I. Stekhanov, Doklady Akad. Nauk SSSR 92, 281 (1953).

NOTES ON THE CONCEPTS OF "YIELD," "MEAN LIFETIME," AND "DECAY LAW" AND THEIR USE IN LUMINESCENCE

V. L. Levshin

Received 19 October 1960

The concepts of "yield," "lifetime," and "decay law" of luminescence are analyzed; the difficulties which arise during their use in complex cases of luminescence are pointed out. Attention is given to the difference of the physical meaning of the yield concept for short- and long-duration luminescence. A definition of luminescent yield suitable for stationary luminescent processes of both short and long duration is proposed. The use of the yield concept for nonstationary processes is considered. Formulas corresponding to various cases are presented for calculating the yield of nonstationary processes. The need of studying the characteristics of partial processes is pointed out.

TRODUCTION

Usually luminescence is characterized by a spec- um, polarization, yield, build-up and decay laws, and rations. Use of the concepts of spectrum and polariza- on does not present any difficulties; if necessary, it can asily be made precise since the connection of these haracteristics of the luminescence with definite elec- onic-vibrational transitions and with the interaction the emitter and its surroundings is obvious. The situ- ion is different with respect to the yield and lifetime of minescence. Examination of the literature shows that equently these terms are not used critically, and in fact orrespond to essentially different quantities. On the her hand, the complexity of the kinetics of many types luminescence makes it necessary to exercise great are in using them.

The purpose of the present work is to analyze the oncepts of yield and lifetime and to propose precise def- itions for their use in various cases of luminescence.

UMINESCENT YIELD

Definition of the yield concept for continuous luminescence and for nonstationary luminescence.

(a) Continuous stationary luminescence. The definition of fluorescent yield proposed by S. I. Vavilov by analogy with the definition of the yield of photochemical reactions has the following formulation: "The fluorescent yield means the part of the total absorbed radiation which is transformed into the energy of secondary fluorescent radiation."[1] In the quantum version of the definition of yield, energy is replaced by the corresponding number of quanta.

From the given definition of yield it follows that this quantity is intended to characterize the transformation of energy or quanta after their absorption by matter. Thus, for a measurement of the yield it is necessary to record a certain number of absorbed quanta and then the number of quanta produced at the expense of those absorbed.

In practice, the number of quanta absorbed is determined by calculation, and the number of quanta emitted is measured. For fluorescence lasting $\sim n \times 10^{-9}$ sec, these operations produce no uncertainty because: (1) the absorption spectrum, as Vavilov[2] showed, shows essentially no change during excitation, and the number of absorbed quanta can be determined precisely; (2) in the case of fluorescence, the stationary state corresponding to a given excitation is established practically instantaneously in comparison with the inertia of the recording instrument; consequently, one can disregard processes of build-up and decay. All groups of molecules excited at different times during the excitation period and emitting at different times effect a transformation of excitation energy under identical conditions; (3) during fluorescence the measuring device records the emitted quanta which are formed at the expense of light absorbed by the material immediately at the time of measurement of the emission.

An expression for the yield in this case can be written in the form

$$Y = \frac{I_L \Delta_1 t}{I_A \Delta_2 t} = \frac{I_L}{I_A}, \quad (1)$$

where I_L is the number of luminescent quanta and I_A is the number of quanta absorbed per unit time. Since build-up and decay are vanishingly short in comparison with the period of the apparatus, I_L and I_A are constant and the duration of excitation and of luminescence $\Delta_1 t$ and $\Delta_2 t$ are equal.

An entirely different physical meaning is implied in the quantities I_L' and I_A' in the case of continuous luminescence if we define the yield, as is usually done, by the formula

$$Y' = \frac{I_L'}{I_A'}. \quad (1')$$

For a continuous luminescence process, the identity of form of formulas (1) and (1') conceals an essential difference in their contents. For instantaneous processes, it is the luminescence arising immediately at the expense of energy absorbed at the instant of measurement which is recorded, but when the luminescent intensity of continuous processes is measured with low-inertia recording devices, the luminescence measured is produced at the expense of energy supplied to the luminescent material not at the time of observation, but much earlier. Thus the observed luminescence is not the result of excitation at a given instant (the energy of which is not utilized) but a consequence of a definite state of excitation attained by the material at the expense of energy absorbed earlier. Since a stationary process exists, and in any given time interval the material emits and absorbs a certain amount of energy, we can speak about the yield as the coefficient of utilization of the energy fed into the material. However, the energy directed into the material is not immediately transformed into emission, but only maintains the state of excitation of the material which provides luminescence. It is necessary to reflect this characteristic of the process in the very definition of luminescence, which can be formulated as follows: "The yield of luminescence in a stationary state of excitation and luminescence is the ratio of luminescent energy liberated by the material for a definite interval of time to the energy of the exciting light absorbed by the material in the same time, maintaining the given state of excitation."

This definition ignores the directness of the process of producing luminescence at the expense of absorbed energy and emphasizes the necessity of maintaining, by means of absorption, a definite state of excitation which provides luminescence of given intensity of the material.*

*In some cases a superposition of long-lived and instantaneous luminescence is possible; e.g., in crystal phosphors when the exciting light has a de-excitation effect, or when there is direct nonionizing excitation of the luminescent centers of the crystal phosphors.[10] Examples of such complicated processes are considered below.

It is not superfluous to emphasize the difference in meaning of the yield obtained for instantaneous and continuous luminescence in still another respect. In the process of fluorescence ($\tau \sim n \times 10^{-9}$ sec) for any available intensity of excitation, a vanishingly small number of molecules is found in the excited state, so that the yield figure refers to the practically unexcited state of the material; for continuous luminescence and strong excitation it is possible to convert a significant part of the luminescing material into the excited state, and as a result the absorption and other properties of the material are changed appreciably.[3-6] Thus the yield for continuous luminescence is a function of the degree of excitation of the material and depends on the intensity of the excitation.[7-9] In view of the indicated properties of the yield, it is necessary to couple its definition with a precise definition of the state of excitation of the material.

(b) Nonstationary luminescence. In the case of nonstationary luminescence the state of the material and, consequently, the yield will vary continuously. Therefore one can in the first place talk about "instantaneous" yield corresponding to a definite, although extremely short-lived state of excitation of the material, and in the second place about the average yield for the entire process or for a definite time interval.

For the "instantaneous" yield of processes of luminescence which are growing, one can give the expression

$$Y_t = \frac{I_{Lt}}{I_{At}}, \quad (1'')$$

where I_{Lt} and I_{At} refer to the instantaneous luminescence and excitation energy at the instant t. It is easy to see that Y_t is smaller than Y', since formula (1'') neglects all the excitation energy which is stored.

For decaying luminescence, formula (1'') gives a value of the yield greater than unity, and in the absence of excitation ($I_{At} = 0$) the yield tends to infinity. Physically this is completely natural, since the luminescence in a given case takes place at the expense of previous excitation; however, such a meaning of yield says little about the characteristics of the process and state of the material. In this case we have for instantaneous yield of the decay

$$Y_{tT} = \frac{I_{Lt}}{I_{Lt} + I_{Tt}}. \quad (1''')$$

I_{Lt} and $I_{Lt} + I_{Tt}$ will mean, respectively, the energy of excitation transformed into radiation at a given instant and the total energy lost by the material in radiative and nonradiative processes.

For continuous luminescence having stationary and nonstationary states (build-up and decay), the expression

$$Y = \frac{\int_0^{\infty} I_L dt}{\int_0^{t_1} I_A dt}. \quad (2)$$

is correct.

Formula (2) is completely general. It takes into account all the energy absorbed by the material in the excitation time from 0 to t_1 and all the radiated energy arising from absorbed energy. Expression (2) completely fits the meaning of the original definition of fluorescent yield, but (2) extends it to continuous processes which require the calculation of decay and build-up of luminescence. If the effect of excitation for the determination of yield according to formula (2) is much longer than the processes of growth and decay, then formula (2) becomes formula (1'). For pulsed excitation, in which a stationary state is absent and all the luminescence is reduced to the nonstationary processes of build-up and decay, formula (2) can give results essentially different from results obtained by formula (1').

Finally, the average yield for a nonstationary state during a definite time interval is described perfectly well by the expression

$$Y_{ns}=\frac{\int_0^{t_1} I_L\,dt}{\int_0^{t_1} I_A\,dt}, \qquad (2')$$

hen the upper and lower integrals denote energies emitted and absorbed by the material in the time interval rom 0 to t_1. The energy contained in the material before me zero and after t_1 is not accounted for by formula 2').

. The yield for electron and ion excitation, excitation by -rays and radioluminescence, chemiluminescence and riboluminescence.

Determination of the yield from these luminescences s especially difficult. The basic difficulty is the determination of the energy expended in excitation (for example, during triboluminescence it is difficult to establish hat one should regard as the excitation energy). As a onsequence, the question of the yield during the indiated forms of excitation requires special analysis and oes beyond the realm of the present article; however, t is necessary to emphasize the reality of the problem. As a concrete example, let us mention cathodoluminesense. In this case, the principal losses of energy on the art of the exciting electron beam do not occur after absorption in the crystal, but during the scattering of the lectrons by its surface; in addition, there are significant osses due to the generation of x-rays by the electron eam. It is difficult to calculate both losses with sufficient precision; therefore, one usually relates the emitted energy to the energy of the electron current directed t the phosphor. The quantity measured by such a method s not yield, but a coefficient of utilization of energy of he exciting electron current and depends strongly on the hickness of the layer and other parameters not connected with the nature of the phosphor.

. The concept of partial yields.

The original definition of yield referred to solutions hich give one form of radiation. However, even in the ase of molecular luminescence, three competing types of luminescenses often occur: fluorescence, delayed fluorescence, and phosphorescence, each varying differently with changes in experimental conditions. It is natural, herefore, to study the partial yields of emission from he indicated processes. Application of the concept of ield to the luminescence of crystal phosphors is still more complicated. A study of the luminescence from rystal phosphors led to the conclusion that there are sually several luminescent centers in them, and each center emits differently. Several processes having different kinetics can proceed simultaneously. Thus, it is possible to effect the direct excitation of activator ions without tearing away electrons, the excitation of luminescent centers with liberation of electrons (which gives rise to recombination processes), and the excitation of the crystal lattice which is transferred to the activators.[10] The last two recombination processes also may be complicated. Calculation shows that, luminescence of the ZnS-Mn phosphor, for example, can arise from more than 20 different processes.[9] It is clear that the integrated luminescent yield of crystal phosphors is of little use for explaining the growth of phosphorescence, and that determination of the yields of the individual forms of luminescence is desirable.

We thus see that the idea of "luminescent yield" has still not been thoroughly analyzed for many forms of excitation. With the extension of the idea of yield to continuous luminescence, its use for nonsteady states is also seen to be desirable. In all cases one can recommend the broad use of the idea of partial yields, and a more complete description of the conditions obtaining during determination of the yield than is usually given at the present time.

THE DURATION OF LUMINESCENCE

1. Duration criteria.

S. I. Vavilov introduced the duration of luminescence in a definition of luminescence which characterizes the meaning of this quantity. However, until the present time it has not been given a precise definition.

For a solution of the problems in which the "duration" of luminescence plays a role, one usually asks the following questions:

1. What is the average duration of the luminescence $\bar{\tau}$ (i.e., the average time of storage in the phosphor of that part of the excitation energy which is converted into luminescence)?

2. What is the average duration of the excited state $\bar{\tau}$?

3. In what interval of time t_1 does the intensity of of luminescence decrease by a definite factor?

4. In what interval of time t_2 does the number of excited centers decrease by a definite factor?

5. In what interval of time t_3 does the total luminosity accumulated in the phosphor decrease by a definite factor?

Questions 2 and 4 arise primarily in the solution of theoretical problems; questions 1, 3, and 5 also can arise during theoretical calculations, but above all are very important in practice.

It is fairly obvious that the nonidentical criteria 1-5, used at the present time for determining the duration of luminescence, must be general lead to different values for the duration. Unfortunately, duration figures determined by different authors according to different criteria are often placed side-by-side in general tables, thus leading to many groundless comparisons.

Let us consider formulas corresponding to the definitions of duration given in items 1, 2, 3, 4, and 5.

$$1)\ \bar{\tau}=\frac{\int_0^{\infty} tI(t)\,dt}{\int_0^{\infty} I(t)\,dt}; \qquad (3)$$

$$2)\ \bar{\tau}=\frac{\int_0^{\infty} tn'(t)\,dt}{\int_0^{\infty} n'(t)\,dt}; \qquad (4)$$

$$3)\ \frac{I(t_1)}{I(0)}=A; \qquad (5)$$

$$4)\ \frac{n(t_2)}{n(0)}=Y; \qquad (6)$$

$$5)\ \frac{\int_{t_3}^{\infty} I(t)\,dt}{\int_0^{\infty} I(t)\,dt}=C. \qquad (7)$$

In formulas (3) to (7), I(t) is the intensity of the luminescence; n(t) is the number of excited centers; A, B, and C are constants.

For the exponential decay of luminescence, $I \propto n$; consequently, $\bar{\bar{\tau}} = \bar{\tau} = \tau$, these quantities being uniquely connected with t_1, t_2, and t_3. The latter equal one another for $A = B = C = a$, i.e., $t_1 = t_2 = t_3 = \theta$.

Furthermore, it follows from (3), (4), and (5) that $\theta = -2.3\tau \log a$.

Because of the simple connection between $\bar{\bar{\tau}}$, $\bar{\tau}$, t_1, t_2, and t_3 for exponential decay, it is customary to take any one of these quantities as characteristic for the duration of luminescence. However, for other decay laws, the relationship between the indicated quantities becomes extremely complicated or poorly defined.

As a simple example, let us consider the decay of luminescence according to the law

$$I = (at + b)^{-2}. \qquad (8)$$

In this case, the average duration of luminescence according to (3) tends toward infinity. Thus the idea of average duration of luminescence is generally inapplicable for such processes.

Formulas (5) and (7) lead to significantly different values t_1 and t_3, which depend strongly on the values of the constants A and C. Thus, if in (8) $b/a = 2$, then for $A = C = 0.01$, $t_1 = 18$ and $t_3 = 198$; for $A = C = 0.001$, $t_1 = 60$ and $t_3 = 1998$.

In the general case it is impossible to determine the form of the function n(t) from the form of the function I(t) and, conversely, since

$$I = -\frac{\alpha}{\alpha + \beta}\frac{dn}{dt}, \qquad (9)$$

where α and β are time-dependent probabilities of radiative and nonradiative deactivation processes. Thus, to determine n it is also necessary to know the forms of the functions α and β, without which it is impossible to find τ and t_2 from the quantity I by means of formulas (4) and (6).

For quenching caused by the migration of excitation energy and by the interaction of the diffusing excited particles, n can often be expressed by a formula of the form

$$n = n_0 f(t)\, e^{-\lambda t}. \qquad (10)$$

In this case it is clear that I is not proportional to n.

Sometimes the change in the number of excited particles with time is regarded as being described by the decay law of the luminescence (see refs. 11 and 12, for example).

For complicated decay laws, indication of the value of one of the quantities $\bar{\bar{\tau}}$, $\bar{\tau}$, t_1, t_2, or t_3 says very little about the value of the others.

2. Partial laws of decay and the difficulty of using the formulas of luminescent decay for interpreting the kinetics of luminescence.

In the thirties, the decay law was considered the most important criterion for establishing the nature of luminescence. Because of the complexity of the connection of I(t) with n(t) it is thus evident that a knowledge of the value of I(t) is insufficient to characterize the change of state of a material; however, the decay law remains as one of the properties of luminescence, and its study has two goals—characterizing the course of the decay itself and clarifying, to a certain degree, the kinetics of the processes taking place inside the material. The solution of these problems, however, meets with considerable difficulty.

For a solution of the first problem, one strives to describe the decay process by empirical interpolation formulas. However, very few processes can be characterized by a formula with only one constant (not counting proportionality factors). Even the simple formula of E. Becquerel has two constants. In a formula with several interacting constants, a direct comparison of different luminescences by means of the values of the constants becomes impossible. The formulas lose their descriptiveness and laborious additional calculations are required to explain the characteristics of the luminescence.

When internal processes in phosphors are explained by means of decay laws, theoretical formulas are used. Substantial difficulties arise in this case also: (1) during the derivation of the formulas simplifying assumptions are generally made, which reduce the possibility of using the formulas for actual phosphors; (2) many parameters which characterize the radiating system enter the formulas, and experimental determination of such parameters represents another important problem for the study of phosphors. At the present time one has to content oneself with "approximate" values of the parameters and, naturally, with a qualitative comparison of theory and experiment.

Considering the question of yield, we noted that often (especially in crystal phosphors) several different processes take place simultaneously. It is evident that in these cases it is necessary to talk about the decay and duration of each of the processes individually. In the case of interacting processes, the decay law of each must take account of the existence of all the others and therefore cannot, in principle, be simple. This conclusion refers first of all to crystal phosphors; however, it still cannot be considered as obvious. In the monograph by Adirovich[12] the idea of an "elementary" decay law, represented by a rather complicated expression obtained by a number of approximations, serves as the guiding principle of the investigation. It is evident that a calculation of the actual conditions of the luminescence of phosphors significantly complicates the formula. Analogous formulas proposed by Fok[13] contain 18 constants of the material. In the case of decay of molecular systems the delay in the establishment of vibrational equilibrium[14] of systems of particles can introduce serious complications.

This analysis has illustrated the complexity of certain characteristics of luminescence and the impossibility of describing these inherently complicated quantities by one numerical value or by one simple decay law. In spectroscopy, many numerical parameters of lines—frequency, intensity, half-width, polarization, and transition probabilities—are used to characterize the spectra of a material. In the field of luminescence we have now arrived at a stage where it is impossible to explain discrete processes and their detailed characteristics. A study of the constants of the material which determine the course of the luminescent processes is the most important problem. Analytical relationships must be established between these quantities. Because of the complexity of the processes of luminescence, these relationships cannot, in principle, be simple and in many cases must be replaced by tables.

EFERENCES

.. S. I. Vavilov, Z. Physik **22**, 266 (1924).
2. S. I. Vavilov, Izd. Akad. Nauk. SSSR, "Collected Works," Vol. 1, p. 80. Moscow, 1954.
3. G. Lewis, D. Lipkin, and T. Magel, J. Am. Chem. Soc. **63**, 3005 (1941).
4. V. L. Levshin and A. G. Laktionov, Doklady Akad. Nauk SSSR **103**, 61 (1955).
5. F. Urbach, H. Hemmerdinger, and D. Pearlman (G. Fonda and F. Seitz, editors), "Preparation and Characteristics of Solid Luminescent Materials," p. 279. Wiley, New York, 1948.
6. L. I. Anikina, Trudy Fiz. Inst. Akad. Nauk SSSR **7**, 5 (1956).
7. V. L. Levshin, Zhur. Eksptl. i Teoret. Fiz. **17**, 675 (1947).
8. M. N. Alentsev, Opt. i Spektr. **1**, 240 (1956).
9. V. L. Levshin and V. F. Tunitskaya, Opt. i Spektr. **9**, 223 (1960), Optics and Spectroscopy **9**, 118 (1960).
10. V. L. Levshin, Izvest. Akad. Nauk SSSR, Ser. Fiz. **9**, 315 (1945).
11. M. D. Galanin, Trudy Fiz. Inst. Akad. Nauk SSSR **12**, 33 (1960).
12. E. I. Adirovich, "Certain Problems of the Theory of Luminescence of Crystals," Gosudarst. Izd. Tekh.-Teoret. Lit. Moscow-Leningrad 1956.
13. M. V. Fok, Opt. i Spektr. **2**, 176 (1957).
14. B. I. Stepanov, Trudy. Inst. Fiz. i Mat., Akad. Nauk Belorus. SSR **1**, 58 (1956).

REABSORPTION IN CRYSTALS OF A FINITE THICKNESS (II)*

V. M. Agranovich and Yu. B. Konobeev (pp. 369-384)

Received 1 August 1960

This paper presents results which are derived from a theory of the reabsorption of light in crystals of finite thickness. Calculated values are listed for the stationary case, making is possible to determine the shape of the luminescence spectrum and the quantum yield for phosphors of arbitrary thickness. Accurate new exact equations have been obtained for the nonstationary case (luminescence decay), from which formulas are derived for the average time of luminescence decay. Various asymptotic cases are studied in detail. The results obtained for nonstationary processes can be used in the theory of radiant energy transfer in planetary atmospheres and in the theory of neutron moderation.

INTRODUCTION

It is known that electronic excitation energy in molecular crystals and molecular media, in general, can migrate by means of two mechanisms, namely, by diffusion of excitons (nonradiative mechanism) and by reabsorption. A phenomenological description of this migration can be obtained by investigating the integrodifferential equation (1) in ref. 1.

As in ref. 2, we will consider the case of a phosphor in which the reflection of luminescent light from the surface of the specimen can be neglected. We will also assume that the diffusion length of excitons is small as compared to the displacement caused by reabsorption. Because of this approximation, we will discard the diffusion term in Eq. (1) of ref. 1. As was shown in ref. 2 luminescence characteristics (such as quantum yield) are determined in the stationary case by values of the functions $\varphi(x,z_0)$ and $\chi(x,z_0)$. The values of the functions φ and χ are listed in Tables 1-3 for q = 0.5, 0.8, 0.9 and for different z_0. More detailed tables are listed in ref. 3 for values of x ranging from 0 to 1 and for the same values of q.

It was shown in ref. 4 that, for large z_0, the functions φ and χ have the following asymptotic form:

$$\varphi(x, z_0) = \varphi(x) - C\frac{x\varphi(x)}{1-kx}e^{-kz_0}, \tag{1.1}$$

$$\chi(x, z_0) = C_1\frac{x}{1-kx}\varphi(x)e^{-kz_0}, \tag{1.2}$$

The functions $\varphi(x,z_0)$ and $\chi(x,z_0)$ introduced in refs. 1, 2 in the q-th approximation correspond to the functions $\varphi(x,z_0)$ and $\chi(x,z_0)$ which appear in the theory of the transport of radiant energy (see refs. 5, 6, 9) where $\varphi(x)$ is a solution of Eq. (5) in ref. 1 and the constants C and C_1 are determined by the system of equations:

$$\left.\begin{aligned} C\int_0^1\frac{\varphi(y)}{(1-ky)^2}y\,dy &= C_1\int_0^1\frac{\varphi(y)}{1-k^2y^2}y\,dy,\\ C_1\int_0^1\frac{\varphi(y)}{(1-ky)^2}y\,dy &= 2k\int_0^1\frac{\varphi(y)}{1-k^2y^2}y\,dy. \end{aligned}\right\} \tag{1.3}$$

Here k is a constant whose dependence on the parameter q is given in ref. 5. The asymptotic expressions for $\varphi(x,z_0)$ and $\chi(x,z_0)$ are of interest for large values of x ($x \gg 1$). This case corresponds to weak absorption of the radiation which excites the luminescence and is realized, for example, by irradiation with γ-quanta or x-rays. It can be shown that in this case

$$(1-q)\varphi(x, z_0) = 1 - \varphi_0(z_0) - e^{-\frac{z_0}{x}}\chi_0(z_0) - \frac{1}{x}\left[\varphi_1(z_0) - \chi_1(z_0)e^{-\frac{z_0}{x}}\right]. \tag{1.4}$$

$$(1-q)\chi(x, z_0) = [1-\varphi_0(z_0)]e^{-\frac{z_0}{x}} - \chi_0(z_0) + \frac{1}{x}\left[\varphi_1(z_0)e^{-\frac{z_0}{x}} - \chi_1(z_0)\right]. \tag{1.5}$$

We have introduced the following designation for momenta of an arbitrary function f(x):

*The paper was presented at the Eighth Conference on Luminescence, Minsk, October 1959.

Table 1 (q = 0.5)

z_0	0.05		0.10		0.15		0.20		0.25		0.50	
x	$\varphi(x)$	$\chi(x)$	$\varphi(x)$	$\chi(x)$	$\varphi(x)$	$\chi(x)$	$\varphi(x)$	$\chi(x)$	$\varphi(x)$	$\chi(x)$	$\varphi(x)$	$\chi(x)$
0.0	1.00	0.00	1.00	0.00	1.00	0.00	1.00	0.00	1.00	0.00	1.00	0.00
0.1	1.04	0.64	1.05	0.41	1.06	0.27	1.06	0.18	1.07	0.12	1.07	0.03
0.2	1.04	0.82	1.06	0.66	1.08	0.54	1.09	0.44	1.10	0.36	1.11	0.14
0.3	1.04	0.89	1.07	0.78	1.08	0.68	1.10	0.60	1.10	0.52	1.13	0.27
0.4	1.04	0.92	1.07	0.84	1.09	0.77	1.10	0.70	1.11	0.63	1.14	0.39
0.5	1.04	0.95	1.07	0.89	1.09	0.83	1.10	0.77	1.12	0.71	1.15	0.49
0.6	1.04	0.96	1.07	0.92	1.09	0.87	1.11	0.82	1.12	0.77	1.16	0.57
0.7	1.04	0.97	1.07	0.94	1.09	0.90	1.11	0.85	1.12	0.81	1.17	0.63
0.8	1.04	0.98	1.07	0.95	1.09	0.92	1.11	0.88	1.13	0.85	1.17	0.68
0.9	1.04	0.99	1.07	0.97	1.09	0.94	1.11	0.91	1.13	0.88	1.18	0.73
1.0	1.04	1.00	1.07	0.98	1.09	0.95	1.11	0.93	1.13	0.90	1.18	0.76
2.0	1.04	1.02	1.07	1.03	1.09	1.02	1.12	1.01	1.14	1.01	1.19	0.96
3.0	1.04	1.03	1.07	1.04	1.09	1.05	1.12	1.05	1.14	1.05	1.19	1.04
4.0	1.04	1.03	1.07	1.05	1.10	1.06	1.12	1.07	1.14	1.08	1.21	1.08
5.0	1.04	1.03	1.07	1.05	1.10	1.06	1.12	1.08	1.14	1.09	1.21	1.11
6.0	1.04	1.04	1.07	1.05	1.10	1.07	1.12	1.09	1.14	1.10	1.21	1.12
7.0	1.04	1.04	1.07	1.06	1.10	1.07	1.12	1.09	1.14	1.10	1.21	1.14
8.0	1.04	1.04	1.07	1.06	1.10	1.08	1.12	1.09	1.14	1.11	1.21	1.15
9.0	1.04	1.04	1.07	1.06	1.10	1.09	1.12	1.10	1.14	1.11	1.21	1.15
10.0	1.04	1.04	1.07	1.06	1.10	1.09	1.12	1.10	1.14	1.12	1.21	1.16
30.0	1.04	1.04	1.07	1.07	1.10	1.09	1.12	1.11	1.14	1.13	1.21	1.19
50.0	1.04	1.04	1.07	1.07	1.10	1.10	1.12	1.12	1.14	1.14	1.21	1.20
00.0	1.04	1.04	1.07	1.07	1.10	1.10	1.12	1.12	1.14	1.14	1.21	1.21
∞	1.04	1.04	1.07	1.07	1.10	1.10	1.12	1.12	1.14	1.14	1.21	1.21

z_0	1.0		1.5		2.0		3.0		4.0		5.0	
x	$\varphi(x)$	$\chi(x)$	$\varphi(x)$	$\chi(x)$	$\varphi(x)$	$\chi(x)$	$\varphi(x)$	$\chi(x)$	$\varphi(x)$	$\chi(x)$	$\varphi(x)$	$\chi(x)$
0.0	1.00	0.00	1.00	0.00	1.00	0.00	1.00	0.00	1.00	0.00	1.00	0.00
0.1	1.07	0.01	1.07	0.00	1.07	0.00	1.07	0.00	1.07	0.00	1.07	0.00
0.2	1.11	0.04	1.11	0.01	1.01	0.00	1.11	0.00	1.11	0.00	1.11	0.00
0.3	1.14	0.09	1.14	0.01	1.14	0.01	1.14	0.00	1.14	0.00	1.14	0.00
0.4	1.16	0.15	1.17	0.02	1.17	0.01	1.17	0.00	1.17	0.00	1.17	0.00
0.5	1.18	0.23	1.19	0.03	1.19	0.02	1.19	0.01	1.19	0.00	1.19	0.00
0.6	1.19	0.30	1.20	0.04	1.20	0.02	1.20	0.01	1.20	0.00	1.20	0.00
0.7	1.20	0.36	1.22	0.06	1.22	0.04	1.22	0.01	1.22	0.01	1.22	0.00
0.8	1.21	0.42	1.23	0.10	1.23	0.06	1.23	0.02	1.23	0.01	1.23	0.00
0.9	1.22	0.48	1.24	0.19	1.24	0.12	1.24	0.04	1.24	0.02	1.24	0.01
1.0	1.23	0.53	1.24	0.48	1.25	0.42	1.25	0.16	1.25	0.06	1.25	0.02
2.0	1.26	0.82	1.30	0.73	1.30	0.58	1.31	0.36	1.31	0.25	1.31	0.14
3.0	1.27	0.96	1.32	0.89	1.33	0.76	1.33	0.56	1.33	0.40	1.34	0.29
4.0	1.28	1.03	1.33	0.99	1.34	0.90	1.35	0.70	1.35	0.55	1.35	0.43
5.0	1.28	1.08	1.34	1.06	1.35	0.97	1.35	0.81	1.36	0.66	1.36	0.55
6.0	1.29	1.12	1.35	1.11	1.35	1.03	1.37	0.89	1.37	0.75	1.37	0.66
7.0	1.29	1.14	1.35	1.14	1.36	1.07	1.37	0.94	1.37	0.82	1.38	0.72
8.0	1.29	1.16	1.35	1.17	1.36	1.11	1.37	0.99	1.38	0.88	1.38	0.78
9.0	1.29	1.17	1.35	1.19	1.37	1.13	1.38	1.03	1.38	0.93	1.38	0.83
10.0	1.29	1.18	1.36	1.21	1.37	1.16	1.38	1.06	1.38	0.96	1.38	0.87
30.0	1.30	1.26	1.37	1.32	1.38	1.30	1.40	1.27	1.40	1.24	1.40	1.20
50.0	1.30	1.28	1.37	1.34	1.39	1.34	1.40	1.33	1.40	1.30	1.41	1.29
100.0	1.30	1.29	1.37	1.36	1.39	1.37	1.40	1.40	1.40	1.36	1.41	1.35
∞	1.30	1.30	1.38	1.38	1.39	1.39	1.41	1.41	1.41	1.41	1.41	1.41

Table 2 (q = 0.8)

z_0	0.05		0.10		0.15		0.20		0.25		0
x	φ	χ	φ	χ	φ	χ	φ	χ	φ	χ	φ
0.0	1.00	0.00	1.00	0.00	1.00	0.00	1.00	0.00	1.00	0.00	1.00
0.1	1.06	0.66	1.09	0.44	1.10	0.30	1.11	0.21	1.12	0.16	1.13
0.2	1.07	0.84	1.10	0.70	1.13	0.59	1.15	0.49	1.16	0.41	1.20
0.3	1.07	0.91	1.11	0.82	1.14	0.74	1.17	0.66	1.19	0.59	1.24
0.4	1.07	0.95	1.12	0.89	1.15	0.83	1.18	0.77	1.20	0.71	1.27
0.5	1.07	0.98	1.12	0.93	1.15	0.88	1.18	0.84	1.21	0.80	1.29
0.6	1.07	0.99	1.12	0.96	1.16	0.93	1.19	0.89	1.22	0.86	1.31
0.7	1.07	1.00	1.12	0.98	1.16	0.96	1.19	0.93	1.22	0.90	1.32
0.8	1.07	1.01	1.12	1.00	1.16	0.98	1.19	0.96	1.22	0.94	1.33
0.9	1.07	1.02	1.12	1.01	1.16	1.00	1.20	0.99	1.23	0.97	1.34
1.0	1.07	1.02	1.12	1.03	1.16	1.02	1.20	1.01	1.23	1.00	1.35
2.0	1.07	1.04	1.12	1.08	1.16	1.09	1.20	1.11	1.24	1.12	1.38
3.0	1.07	1.06	1.13	1.10	1.17	1.12	1.21	1.14	1.24	1.16	1.39
4.0	1.07	1.06	1.13	1.10	1.17	1.13	1.21	1.16	1.25	1.19	1.40
5.0	1.07	1.06	1.13	1.10	1.17	1.14	1.21	1.17	1.25	1.20	1.40
6.0	1.07	1.07	1.13	1.11	1.17	1.14	1.21	1.18	1.25	1.21	1.40
7.0	1.07	1.07	1.13	1.11	1.17	1.15	1.21	1.18	1.25	1.21	1.40
8.0	1.07	1.07	1.13	1.11	1.17	1.15	1.21	1.19	1.25	1.22	1.40
9.0	1.07	1.07	1.13	1.12	1.17	1.15	1.21	1.19	1.25	1.22	1.40
10.0	1.07	1.07	1.13	1.12	1.17	1.15	1.21	1.19	1.25	1.22	1.40
30.0	1.07	1.07	1.13	1.12	1.17	1.16	1.21	1.19	1.25	1.23	1.41
50.0	1.07	1.07	1.13	1.12	1.17	1.16	1.22	1.21	1.25	1.24	1.41
100.0	1.07	1.07	1.13	1.13	1.17	1.17	1.22	1.22	1.25	1.25	1.41
∞	1.07	1.07	1.13	1.13	1.17	1.17	1.22	1.22	1.25	1.25	1.41

z	1.00		2.00		3.00		4.00		5.00
x	φ	χ	φ	χ	φ	χ	φ	χ	φ
0.0	1.00	0.00	1.00	0.00	1.00	0.00	1.00	0.00	1.00
0.1	1.13	0.03	1.14	0.01	1.14	0.01	1.14	0.00	1.14
0.2	1.22	0.08	1.23	0.03	1.23	0.01	1.23	0.01	1.23
0.3	1.28	0.16	1.30	0.05	1.30	0.02	1.30	0.01	1.30
0.4	1.33	0.25	1.35	0.07	1.36	0.04	1.36	0.02	1.36
0.5	1.37	0.35	1.40	0.11	1.41	0.05	1.41	0.03	1.41
0.6	1.40	0.44	1.45	0.15	1.46	0.07	1.46	0.04	1.46
0.7	1.42	0.52	1.49	0.20	1.50	0.10	1.50	0.05	1.50
0.8	1.44	0.60	1.52	0.28	1.54	0.14	1.54	0.07	1.54
0.9	1.46	0.66	1.54	0.38	1.56	0.19	1.57	0.09	1.57
1.0	1.47	0.72	1.56	0.54	1.59	0.26	1.60	0.13	1.60
2.0	1.55	1.08	1.71	0.87	1.77	0.62	1.78	0.42	1.79
3.0	1.58	1.24	1.78	1.13	1.85	0.92	1.88	0.71	1.89
4.0	1.59	1.33	1.82	1.29	1.90	1.12	1.94	0.93	1.95
5.0	1.61	1.39	1.84	1.40	1.94	1.28	1.97	1.09	1.99
6.0	1.61	1.43	1.86	1.48	1.96	1.37	2.00	1.22	2.02
7.0	1.62	1.46	1.87	1.54	1.98	1.46	2.02	1.32	2.04
8.0	1.62	1.48	1.88	1.58	1.99	1.52	2.04	1.40	2.06
9.0	1.62	1.50	1.89	1.62	2.00	1.58	2.05	1.48	2.08
10.0	1.63	1.51	1.89	1.65	2.01	1.62	2.06	1.53	2.09
30.0	1.64	1.61	1.93	1.84	2.06	1.92	2.13	1.93	2.16
50.0	1.64	1.62	1.94	1.89	2.07	1.99	2.14	2.02	2.18
100.0	1.65	1.63	1.94	1.92	2.08	2.04	2.15	2.09	2.19
∞	1.65	1.65	1.95	1.95	2.09	2.09	2.16	2.16	2.20

Table 3 (q = 0.9)

z_0	0.05		0.10		0.15		0.20		0.25		0.50	
x	φ	χ	φ	χ	φ	χ	φ	χ	φ	χ	φ	χ
0.0	1.00	0.00	1.00	0.00	1.00	0.00	1.00	0.00	1.00	0.00	1.00	0.00
0.1	1.07	0.67	1.10	0.45	1.12	0.31	1.13	0.23	1.14	0.17	1.15	0.07
0.2	1.08	0.85	1.12	0.72	1.15	0.60	1.17	0.51	1.19	0.44	1.24	0.22
0.3	1.08	0.92	1.13	0.84	1.16	0.76	1.19	0.68	1.22	0.62	1.29	0.39
0.4	1.08	0.96	1.13	0.91	1.17	0.85	1.21	0.79	1.23	0.74	1.33	0.54
0.5	1.08	0.99	1.13	0.95	1.18	0.91	1.21	0.87	1.24	0.83	1.35	0.65
0.6	1.08	1.00	1.14	0.98	1.18	0.95	1.22	0.92	1.25	0.89	1.37	0.74
0.7	1.08	1.01	1.14	1.00	1.18	0.98	1.22	0.96	1.26	0.94	1.39	0.82
0.8	1.08	1.02	1.14	1.02	1.19	1.00	1.23	0.99	1.26	0.98	1.40	0.88
0.9	1.08	1.03	1.14	1.03	1.19	1.03	1.23	1.02	1.27	1.01	1.41	0.93
1.0	1.08	1.03	1.14	1.04	1.19	1.04	1.23	1.04	1.27	1.03	1.42	0.98
2.0	1.08	1.05	1.14	1.09	1.19	1.10	1.24	1.15	1.28	1.15	1.46	1.28
3.0	1.08	1.06	1.14	1.11	1.19	1.15	1.24	1.18	1.28	1.21	1.47	1.31
4.0	1.08	1.07	1.14	1.12	1.20	1.16	1.24	1.19	1.29	1.23	1.48	1.35
5.0	1.08	1.07	1.14	1.12	1.20	1.17	1.24	1.21	1.29	1.24	1.48	1.38
6.0	1.08	1.08	1.14	1.12	1.20	1.17	1.24	1.22	1.29	1.25	1.48	1.40
7.0	1.08	1.08	1.14	1.13	1.20	1.18	1.24	1.22	1.29	1.26	1.49	1.42
8.0	1.08	1.08	1.14	1.13	1.20	1.18	1.25	1.22	1.29	1.26	1.49	1.42
9.0	1.08	1.08	1.14	1.13	1.20	1.18	1.25	1.23	1.29	1.26	1.49	1.43
10.0	1.08	1.08	1.14	1.13	1.20	1.18	1.25	1.23	1.29	1.27	1.49	1.44
30.0	1.08	1.08	1.14	1.14	1.20	1.19	1.25	1.24	1.29	1.28	1.50	1.48
50.0	1.08	1.08	1.14	1.14	1.20	1.20	1.25	1.25	1.30	1.29	1.50	1.49
00.0	1.08	1.08	1.14	1.14	1.20	1.20	1.25	1.25	1.30	1.30	1.50	1.50
∞	1.08	1.08	1.14	1.14	1.20	1.20	1.25	1.25	1.30	1.30	1.50	1.50

z_0	1.00		1.50		2.00		3.00		4.00		5.00	
x	φ	χ	φ	χ	φ	χ	φ	χ	φ	χ	φ	χ
0.0	1.00	0.00	1.00	0.00	1.00	0.00	1.00	0.00	1.00	0.00	1.00	0.00
0.1	1.16	0.04	1.16	0.03	1.17	0.02	1.17	0.01	1.17	0.01	1.17	0.00
0.2	1.27	0.10	1.28	0.06	1.28	0.05	1.29	0.03	1.29	0.02	1.29	0.01
0.3	1.35	0.20	1.37	0.10	1.38	0.08	1.39	0.05	1.39	0.03	1.39	0.02
0.4	1.41	0.30	1.45	0.16	1.46	0.12	1.47	0.07	1.48	0.04	1.48	0.03
0.5	1.46	0.41	1.52	0.22	1.53	0.17	1.55	0.10	1.55	0.06	1.56	0.04
0.6	1.50	0.51	1.57	0.30	1.59	0.23	1.62	0.14	1.63	0.08	1.63	0.05
0.7	1.53	0.61	1.61	0.39	1.64	0.30	1.67	0.18	1.68	0.11	1.69	0.05
0.8	1.56	0.69	1.65	0.50	1.69	0.39	1.73	0.23	1.74	0.14	1.75	0.08
0.9	1.58	0.76	1.67	0.64	1.72	0.49	1.77	0.29	1.79	0.17	1.80	0.10
1.0	1.60	0.83	1.69	0.81	1.75	0.62	1.82	0.37	2.16	0.22	1.85	0.13
2.0	1.69	1.26	1.77	1.07	1.94	1.32	2.10	0.87	2.32	0.56	2.18	0.45
3.0	1.74	1.40	1.93	1.52	2.07	1.41	2.24	1.22	2.42	1.01	2.36	0.81
4.0	1.76	1.50	1.98	1.63	2.13	1.60	2.32	1.47	2.49	1.29	2.48	1.10
5.0	1.77	1.56	2.01	1.72	2.16	1.71	2.38	1.65	2.59	1.50	2.56	1.34
6.0	1.78	1.60	2.03	1.78	2.19	1.80	2.41	1.78	2.54	1.67	2.62	1.52
7.0	1.79	1.63	2.05	1.82	2.21	1.87	2.44	1.88	2.58	1.80	2.66	1.67
8.0	1.79	1.66	2.06	1.86	2.22	1.92	2.46	1.98	2.61	1.90	2.69	1.79
9.0	1.80	1.67	2.07	1.89	2.24	1.96	2.48	2.03	2.63	1.98	2.72	1.89
10.0	1.81	1.69	2.07	1.91	2.24	2.01	2.50	2.08	2.63	2.05	2.74	1.98
30.0	1.82	1.79	2.12	2.06	2.30	2.21	2.59	2.44	2.77	2.54	2.89	2.59
50.0	1.83	1.80	2.13	2.09	2.32	2.26	2.61	2.52	2.80	2.66	2.92	2.75
100.0	1.83	1.82	2.14	2.12	2.33	2.30	2.63	2.58	2.82	2.75	2.95	2.85
∞	1.83	1.83	2.14	2.14	2.33	2.33	2.64	2.64	2.84	2.84	2.97	2.97

Table 4

	0.05				0.8				0.9			
	φ_0	χ_0	φ_1	χ_1	φ_0	χ_0	φ_1	χ_1	φ_0	χ_0	φ_1	χ_1
15	0.26	0.22	0.13	0.12	0.43	0.36	0.21	0.20	0.43	0.36	0.22	0.20
10	0.27	0.20	0.13	0.11	0.44	0.33	0.22	0.19	0.45	0.34	0.23	0.19
15	0.27	0.18	0.14	0.11	0.46	0.31	0.23	0.18	0.46	0.32	0.24	0.19
10	0.27	0.16	0.14	0.10	0.47	0.29	0.24	0.17	0.48	0.30	0.24	0.18
15	0.28	0.15	0.14	0.09	0.47	0.27	0.24	0.17	0.49	0.28	0.25	0.18
10	0.28	0.11	0.14	0.07	0.50	0.21	0.26	0.14	0.53	0.23	0.27	0.15
	0.29	0.05	0.15	0.04	0.53	0.14	0.28	0.10	0.57	0.16	0.30	0.11
	0.29	0.01	0.15	0.01	0.55	0.06	0.29	0.04	0.59	0.09	0.32	0.06
	0.29	0.00	0.15	0.00	0.55	0.03	0.29	0.02	0.60	0.05	0.33	0.04
	0.29	0.00	0.15	0.00	0.55	0.01	0.29	0.01	0.61	0.03	0.33	0.02
	0.29	0.00	0.15	0.00	0.55	0.01	0.29	0.00	0.61	0.02	0.33	0.01

$$f_m = q/2 \int_0^\infty f(x)\, x^m\, dx.$$

The equation

$$(1-\varphi_0(z_0))^2 - \chi_0^2(z_0) = 1-q, \qquad (1.6)$$

is used to obtain Eqs. (1.4) and (1.5). Equation (1.6) follows from the relation between the moments of functions $\varphi(x,z_0)$ and $\chi(x,z_0)$ (see ref. 6):

$$\varphi_0(z_0) = \frac{q}{2} + \frac{1}{2}(\varphi_0^2(z_0) - \chi_0^2(z_0)). \qquad (1.7)$$

It follows from (1.4) and (1.5) that

$$\chi(\infty, z_0) = \frac{1-\varphi_0(z_0)-\chi_0(z_0)}{1-q} = \frac{1}{1-\varphi_0(z_0)-\chi_0(z_0)}. \qquad (1.8)$$

Values of the momenta $\varphi(z_0)$, $\varphi_1(z_0)$, $\chi(z_0)$, and $\chi_1(z_0)$ calculated with the help of Tables 1-3, are listed in Table 4.

THE NONSTATIONARY CASE. AVERAGE "EXPONENTIAL" DE-EXCITATION TIME

(a) It was shown in a paper by the authors[2] that it is sufficient to know the function

$$\Phi(\eta, \gamma, z_0) = \int_0^{z_0} e^{-\eta z}\, \varphi(z, \gamma, z_0)\, dz. \qquad (2.1)$$

to determine the average "exponential" de-excitation decay time.*

* As shown by Samson,[10] the average "exponential" de-excitation time coincides in the q-th approximation with the true time for a brief excitation.

The function $\varphi(z,\gamma,z_0) = \int_0^\infty C(z,\gamma,z_0,\tau)\,d\tau$, where $C(z,\gamma,z_0,\tau)$ is a solution of Eq. (2.2) from ref. 2, must satisfy the following equation:

$$C(z, \gamma, z_0) = C_0(z, \gamma, z_0) + \frac{q}{2}\int_0^{z_0} \varphi(z_1, \gamma, z_0)\, E_1(|z-z_1|)\, dz_1. \qquad (2.2)$$

The function $\Phi(\eta,\gamma,z_0)$ (there is a misprint in Eq. 26, ref. 2!) has the form

$$\Phi(\eta, \gamma, z_0) = \frac{\varphi\left(\frac{1}{\eta}, z_0\right) M\left(\frac{1}{\gamma}, z_0\right) + \varphi\left(\frac{1}{\gamma}, z_0\right) M\left(\frac{1}{\eta}, z_0\right)}{\eta+\gamma} - \frac{\chi\left(\frac{1}{\eta}, z_0\right) N\left(\frac{1}{\gamma}, z_0\right) - \chi\left(\frac{1}{\gamma}, z_0\right) N\left(\frac{1}{\eta}, z_0\right)}{\eta+\gamma} - R_0(\eta, \gamma, z_0). \qquad (2.3)$$

The average exponential de-excitation decay time in the region of the spectrum where reabsorption is unimportant and equal to $\bar{\tau}_{0,d}^{(\nu)}(\gamma) = \Phi(0,\gamma,z_0)/R_0(0,\gamma,z_0)$ can be presented[2] in the following form:

$$\bar{\tau}_0^{(\nu)}(\gamma) = \bar{\tau}_d^{(\nu)}(\gamma) = \bar{\tau}(\gamma) = \frac{M\left(\frac{1}{\gamma}, z_0\right) - N\left(\frac{1}{\gamma}, z_0\right)}{\varphi\left(\frac{1}{\gamma}, z_0\right) - \chi\left(\frac{1}{\gamma}, z_0\right)} + \frac{M(\infty, z_0)}{\varphi(\infty, z_0)} - 1. \qquad (2.4)$$

The functions $M(x,z_0) \equiv \varphi(0, 1/x, z_0)$ and $N(x,z_0) \equiv \varphi(z_0, 1/x, z_0)$, where $x = 1/\gamma$, satisfy a system of equations which have the following form in the q-th approximation:

$$M(x, z_0) = 1 + \frac{q}{2} x \int_0^1 \frac{\varphi(y, z_0) M(x, z_0) + \varphi(x, z_0) M(y, z_0)}{x+y}\, dy - \frac{q}{2} x \int_0^1 \frac{\chi(x, z_0) N(y, z_0) + \chi(y, z_0) N(x, z_0)}{x+y}\, dy, \qquad (2.5)$$

$$N(x, z_0) = e^{-\frac{z_0}{x}} + \frac{q}{2} x \int_0^1 \frac{M(y, z_0)\chi(x, z_0) - M(x, z_0)\chi(y, z_0)}{x-y}\, dy + \frac{q}{2} x \int_0^1 \frac{\varphi(y, z_0) N(x, z_0) - \varphi(x, z_0) N(y, z_0)}{y-x}\, dy. \qquad (2.6)$$

If $q \leq 0.4$ $M(x,z_0) = 2\varphi(x,z_0) - 1$, $N(x,z_0) = 2\chi(x,z_0) - e^{-z_0/x}$. The values of the functions $M(x,z_0)$ and $N(x,z_0)$ are listed in tables 5-7 for q = 0.5, 0.8, 0.9 and for different z_0.

(b) For the calculation of the average "exponential" de-excitation time in thick crystals ($z_0 \gg 1$) asymptotic expressions for the functions $M(x,z_0)$ and $N(x,z_0)$ can be obtained from Eq. (2.4). These expressions make it possible to calculate these functions with the help of functions which are already known. A derivation of new equations for the functions $M(x,z_0)$ and $N(x,z_0)$ is given below; asymptotic expressions for these functions at large values of z_0, derived from these new equations, will be obtained further on.

With this goal in mind, let us differentiate the right and left sides of Eq. (3.1) with respect to z_0. We obtain

$$\frac{\partial\Phi(\eta, \gamma, z_0)}{\partial z_0} = e^{-z_0\eta}\varphi(z_0, \gamma, z_0) + \frac{q}{2}\int_0^{z_0} e^{-z\eta}\frac{\partial\varphi(z, \gamma, z_0)}{\partial z_0}\, dz. \qquad (2.7)$$

Let us also differentiate the right and left sides of Eqs. (2.2) and (9) from ref. 2 with respect to z_0 (in the q-th approximation). It can be easily seen that

$$\frac{\partial C_0(z, \gamma, z_0)}{\partial z_0} = \frac{q}{2} C_0(z_0, \gamma, z_0)\int_1^\infty \frac{C_0(z_0-z, z_0)}{\xi}\, d\xi, \qquad (2.8)$$

$$\frac{\partial\varphi(z, \gamma, z_0)}{\partial z_0} = \frac{q}{2} C_0(z_0, \gamma, z_0)\int_1^m \frac{\varphi(Z_0-Z, \xi, Z_0)}{\xi}\, d\xi + \frac{q}{2}\varphi(z_0, \gamma, z_0)\int_1^\infty \frac{C_0(z_0-z, \xi, z_0)}{\xi}\, d\xi. \qquad (2.9)$$

Substituting (2.9) in (2.7) and using Eq. (9) from ref. 2 and (2.2), and assuming that $z = 0$ and $z = z_0$, we find that

$$\frac{\partial\Phi(\eta, \gamma, z_0)}{\partial z_0} = \chi\left(\frac{1}{\gamma}, z_0\right) N\left(\frac{1}{\eta}, z_0\right) + \chi\left(\frac{1}{\eta}, z_0\right) N\left(\frac{1}{\gamma}, z_0\right) - \chi\left(\frac{1}{\gamma}, z_0\right)\chi\left(\frac{1}{\eta}, z_0\right). \qquad (2.10)$$

It follows from (2.3) and (2.10) that

$$(\eta+\gamma)\Phi + \frac{\partial\Phi}{\partial z_0} = M\left(\frac{1}{\eta}, z_0\right)\varphi\left(\frac{1}{\gamma}, z_0\right) + M\left(\frac{1}{\gamma}, z_0\right)\varphi\left(\frac{1}{\eta}, z_0\right) - \varphi\left(\frac{1}{\gamma}, z_0\right)\varphi\left(\frac{1}{\eta}, z_0\right). \qquad (2.11)$$

Table 5 (q = 0.5)

z_0	0.05		0.10		0.15		0.20		0.25		0.50	
x	$M(x)$	$N(x)$	$M(x)$	$N(x)$	$M(x)$	$N(x)$	$M(x)$	$N(x)$	$M(x)$	$N(x)$	$M(x)$	$N(x)$
0.0	1.00	0.00	1.00	0.00	1.00	0.00	1.00	0.00	1.00	0.00	1.00	0.00
0.1	1.08	0.67	1.11	0.46	1.12	0.32	1.14	0.23	1.15	0.17	1.16	0.06
0.2	1.08	0.86	1.13	0.74	1.16	0.58	1.18	0.50	1.20	0.42	1.24	0.22
0.3	1.08	0.93	1.14	0.84	1.18	0.77	1.20	0.69	1.22	0.62	1.29	0.38
0.4	1.09	0.97	1.14	0.91	1.18	0.86	1.22	0.80	1.25	0.75	1.32	0.52
0.5	1.09	0.99	1.14	0.96	1.19	0.92	1.22	0.88	1.26	0.84	1.35	0.63
0.6	1.09	1.01	1.14	1.00	1.19	0.96	1.23	0.93	1.27	0.89	1.37	0.73
0.7	1.09	1.02	1.15	1.03	1.19	0.99	1.23	0.97	1.28	0.94	1.38	0.80
0.8	1.09	1.03	1.15	1.04	1.20	1.02	1.24	1.00	1.28	0.99	1.39	0.87
0.9	1.09	1.03	1.15	1.04	1.20	1.04	1.24	1.03	1.29	1.02	1.40	0.92
1.0	1.09	1.04	1.15	1.04	1.20	1.05	1.24	1.05	1.29	1.04	1.41	0.95

z_0	1.0		1.5		2.0		3.0		4.0		5.0	
x	$M(x)$	$N(x)$	$M(x)$	$N(x)$	$M(x)$	$N(x)$	$M(x)$	$N(x)$	$M(x)$	$N(x)$	$M(x)$	$N(x)$
0.0	1.00	0.00	1.00	0.00	1.00	0.00	1.00	0.00	1.00	0.00	1.00	0.00
0.1	1.16	0.03	1.16	0.01	1.16	0.01	1.16	0.00	1.16	0.00	1.16	0.00
0.2	1.25	0.08	1.26	0.03	1.26	0.02	1.26	0.01	1.26	0.00	1.26	0.00
0.3	1.33	0.16	1.33	0.07	1.34	0.04	1.34	0.01	1.34	0.00	1.34	0.00
0.4	1.38	0.25	1.39	0.12	1.40	0.06	1.40	0.02	1.40	0.01	1.40	0.00
0.5	1.42	0.35	1.44	0.19	1.45	0.11	1.45	0.04	1.45	0.02	1.45	0.00
0.6	1.45	0.45	1.49	0.27	1.49	0.15	1.49	0.06	1.49	0.02	1.49	0.01
0.7	1.48	0.54	1.52	0.38	1.53	0.23	1.53	0.08	1.53	0.03	1.53	0.01
0.8	1.50	0.61	1.55	0.55	1.56	0.34	1.56	0.13	1.56	0.04	1.56	0.01
0.9	1.52	0.69	1.58	0.59	1.60	0.49	1.60	0.19	1.60	0.08	1.60	0.03
1.0	1.54	0.74	1.59	0.70	1.62	0.66	1.62	0.27	1.62	0.10	1.62	0.04

Similar calculations for the function $\Phi(-\eta,\gamma,z_0) \equiv e^{-z_0\eta}\ \Phi_1(\eta,\gamma,z_0)$ give:

$$-\eta\Phi_1+\frac{\partial\Phi_1}{\partial z_0}=\chi\left(\frac{1}{\gamma},\ z_0\right)M\left(\frac{1}{\eta},\ z_0\right)+$$
$$+\varphi\left(\frac{1}{\eta},\ z_0\right)N\left(\frac{1}{\gamma},\ z_0\right)-\chi\left(\frac{1}{\gamma},\ z_0\right)\varphi\left(\frac{1}{\eta},\ z_0\right). \qquad (2.12)$$

Having determined the function $\Phi(-\eta,\gamma,z_0)$ from (2.3) with the help of the equation (see ref. 2):

$$\varphi(0,\ -\gamma,\ z_0)=e^{\gamma z_0}\varphi(z_0,\ \gamma,\ z_0),$$
$$\varphi(z_0,\ -\gamma,\ z_0)=e^{\gamma z_0}\varphi(0,\ \gamma,\ z_0), \qquad (2.13)$$

we obtain

$$\gamma\Phi_1+\frac{\partial\Phi_1}{\partial z_0}=\chi\left(\frac{1}{\eta},\ z_0\right)M\left(\frac{1}{\gamma},\ z_0\right)+\varphi\left(\frac{1}{\gamma},\ z_0\right)N\left(\frac{1}{\eta},\ z_0\right)-$$
$$-\varphi\left(\frac{1}{\gamma},\ z_0\right)\chi\left(\frac{1}{\eta},\ z_0\right). \qquad (2.14)$$

Table 6 (q = 0.8)

z_0	0.05		0.10		0.15		0.20		0.25		0.50	
x	M	N	M	N	M	N	M	N	M	N	M	N
0.0	1.00	0.00	1.00	0.00	1.00	0.00	1.00	0.00	1.00	0.00	1.00	0.00
0.1	1.13	0.72	1.18	0.52	1.22	0.39	1.25	0.30	1.26	0.25	1.30	0.14
0.2	1.14	0.90	1.21	0.81	1.28	0.68	1.34	0.60	1.36	0.54	1.48	0.38
0.3	1.14	0.98	1.24	0.94	1.31	0.88	1.38	0.84	1.43	0.79	1.60	0.59
0.4	1.14	1.02	1.25	1.01	1.33	0.98	1.40	0.96	1.46	0.94	1.68	0.80
0.5	1.15	1.05	1.25	1.06	1.34	1.04	1.41	1.05	1.48	1.03	1.74	0.97
0.6	1.15	1.06	1.25	1.09	1.35	1.10	1.42	1.11	1.50	1.11	1.78	1.10
0.7	1.15	1.08	1.25	1.12	1.36	1.14	1.43	1.16	1.51	1.17	1.80	1.22
0.8	1.15	1.08	1.26	1.13	1.37	1.18	1.43	1.22	1.52	1.21	1.82	1.32
0.9	1.15	1.09	1.26	1.15	1.37	1.20	1.45	1.23	1.53	1.26	1.83	1.39
1.0	1.15	1.09	1.26	1.16	1.38	1.21	1.45	1.25	1.53	1.29	1.84	1.45

z_0	1.0		2.0		3.0		4.0		5.0	
x	M	N	M	N	M	N	M	N	M	N
0.0	1.00	0.00	1.00	0.00	1.00	0.00	1.00	0.00	1.00	0.00
0.1	1.34	0.09	1.35	0.08	1.36	0.06	1.37	0.04	1.37	0.01
0.2	1.58	0.22	1.65	0.14	1.66	0.08	1.66	0.05	1.66	0.02
0.3	1.75	0.38	1.84	0.24	1.88	0.14	1.88	0.07	1.88	0.03
0.4	1.89	0.55	2.03	0.37	2.08	0.22	2.10	0.12	2.10	0.05
0.5	2.02	0.72	2.21	0.50	2.28	0.31	2.29	0.16	2.30	0.06
0.6	2.11	0.87	2.36	0.64	2.45	0.42	2.48	0.23	2.48	0.08
0.7	2.19	1.03	2.51	0.80	2.62	0.56	2.64	0.33	2.64	0.11
0.8	2.25	1.18	2.64	0.96	2.76	0.73	2.81	0.45	2.81	0.14
0.9	2.31	1.33	2.73	1.17	2.88	0.93	2.94	0.62	2.95	0.18
1.0	2.36	1.45	2.76	1.35	2.95	1.15	3.04	0.80	3.08	0.22

Table 7 (q = 0.9)

z_0	0.05		0.10		0.15		0.20		0.25		0.	
x	M	N	M	N	M	N	M	N	M	N	M	
0.0	1.00	0.00	1.00	0.00	1.00	0.00	1.00	0.00	1.00	0.00	1.00	
0.1	1.15	0.73	1.22	0.54	1.26	0.42	1.29	0.33	1.31	0.28	1.37	
0.2	1.16	0.92	1.25	0.83	1.34	0.76	1.38	0.70	1.44	0.63	1.60	
0.3	1.16	1.00	1.27	0.97	1.36	0.93	1.44	0.91	1.51	0.86	1.75	
0.4	1.17	1.04	1.28	1.05	1.38	1.04	1.47	1.03	1.55	1.02	1.86	
0.5	1.17	1.07	1.29	1.09	1.39	1.11	1.50	1.12	1.58	1.12	1.92	
0.6	1.17	1.08	1.29	1.12	1.40	1.16	1.51	1.18	1.59	1.20	1.98	
0.7	1.17	1.10	1.29	1.15	1.40	1.20	1.51	1.23	1.61	1.27	2.03	
0.8	1.17	1.11	1.30	1.17	1.41	1.22	1.51	1.27	1.62	1.32	2.06	
0.9	1.17	1.11	1.30	1.18	1.41	1.25	1.52	1.31	1.63	1.36	2.09	
1.0	1.17	1.12	1.30	1.20	1.42	1.26	1.52	1.33	1.63	1.41	2.11	

z_0	1.00		1.50		2.00		3.00		4.00		5.	
x	M	N	M	N	M	N	M	N	M	N	M	
0.0	1.00	0.00	1.00	0.00	1.00	0.00	1.00	0.00	1.00	0.00	1.00	
0.1	1.43	0.13	1.46	0.10	1.48	0.08	1.50	0.07	1.51	0.06	1.52	
0.2	1.75	0.30	1.80	0.24	1.84	0.21	1.90	0.17	1.90	0.15	1.97	
0.3	2.02	0.54	2.11	0.45	2.18	0.39	2.28	0.30	2.35	0.25	2.40	
0.4	2.24	0.76	2.44	0.65	2.55	0.57	2.68	0.47	2.76	0.40	2.81	
0.5	2.41	0.99	2.68	0.90	2.85	0.82	3.03	0.67	3.13	0.57	3.19	
0.6	2.55	1.19	2.83	1.10	3.06	1.00	3.34	0.85	3.47	0.74	3.55	
0.7	2.67	1.37	3.12	1.34	3.34	1.25	3.62	1.03	3.80	0.90	3.90	
0.8	2.77	1.52	3.26	1.46	3.60	1.38	3.92	1.22	4.12	1.10	4.24	
0.9	2.85	1.64	3.42	1.62	3.81	1.55	4.20	1.41	4.42	1.28	4.55	
1.0	2.93	1.74	3.56	1.70	4.01	1.65	4.44	1.56	4.66	1.48	4.80	

Using the equations for the functions $\varphi(x,z_0)$ and $\chi(x,z_0)$ obtained in ref. 4,

$$\varphi(x,\ z_0)=1+\frac{q}{2}\int_0^1\frac{dy}{y}\int_0^{z_0}e^{-(z_0-s)\left(\frac{1}{x}+\frac{1}{y}\right)}\varphi(x,\ s)\,\varphi(y,\ s)\,ds, \qquad (2$$

$$\chi(x,\ z_0)=e^{-\frac{z_0}{x}}+\frac{q}{2}\int_0^1\frac{dy}{y}\int_0^{z_0}e^{-\frac{(z_0-s)}{x}}\varphi(x,\ s)\,\chi(y,\ s)\,ds, \qquad (2$$

along with (2.2), and (2.14), we obtain new equations fo the functions $M(x,z_0)$ and $N(x,z_0)$:

$$M(x,\ z_0)=1+\frac{q}{2}\int_0^1\frac{dy}{y}\int_0^{z_0}e^{-(z_0-s)\left(\frac{1}{x}+\frac{1}{y}\right)}$$

$$[\varphi(x,s)\,M(y,s)+\varphi(y,s)\,M(x,s)]\,ds, \qquad (2$$

$$N(x,\ z_0)=e^{-\frac{z_0}{x}}+\frac{q}{2}\int_0^1\frac{dy}{y}\int_0^{z_0}e^{-\frac{z_0-s}{x}}$$

$$[\varphi(x,s)\,N(y,s)+\chi(y,s)\,M(x,s)]\,ds. \qquad (2$$

(c) Asymptotic expressions for the functions $M(x$ and $N(x,z_0)$ at large values of z_0 can be derived from the equations obtained above for these functions. All c culations will be conducted for the case $q<1$.

Let us note in advance that if $z_0=\infty$, that is, if th crystal can be considered as a semi-infinite layer, th $N(x,z_0)=0$ and $M(x,z_0)$ is transformed into a function determined by the equation

$$M(x)=1+\frac{q}{2}\,x\int_0^1\frac{\varphi(y)\,M(x)+\varphi(x)\,M(y)}{x+y}\,dy. \qquad (2$$

With the help of an equation for the function φ_x, Eq. (2.19) is easily reduced to the form

$$\frac{M(x)}{\varphi(x)}=1+\frac{q}{2}\,x\int_0^1\frac{M(y)\,\varphi(x)}{x+y}\,dy. \qquad (2$$

Equation (2.20) was first obtained in ref. 2. The same reference includes a table of values of the funct $M(x)$. Hereinafter we will consider the function $M(x)$ known.

Let us examine the system of equations (2.17) and 8), assuming $z_0 \gg 1$. Let us search for an asymp- expression of the function $M(x,z_0)$ in the form

$$M(x, z_0) = M(x) - m(x) z_0 e^{-2kz_0}, \quad (2.21)$$

re k is the constant mentioned above and determined ef. 5.

Substituting (1.1), (1.2), and (2.21) in (2.17), discard- all terms which are smaller than $z_0 e^{-2kz_0}$ by one or- of magnitude, and using (2.19), we find that

$$m(x) = \frac{q}{2} x \int_0^1 [\varphi(x) m(y) + \varphi(y) m(x)] \frac{dy}{x+y-2kxy}. \quad (2.22)$$

Taking account of the fact that, according to ref. 5, constant k satisfies the equation $q/2 \int_0^1 \varphi y/(1-ky)\, dy = 1$, solution of Eq. (2.22) can be written down as follows:

$$m(x) = D \frac{x}{1-kx} \varphi(x), \quad (2.23)$$

where D is a constant ($0 \leq x \leq 1$).

At large values of z_0, the function $M(x,z_0)$ is thus given by the expression

$$M(x, z_0) = M(x) - D \frac{x\varphi(x)}{1-kx} z_0 e^{-2kz_0}. \quad (2.24)$$

In the same way, Eq. (2.18) gives us the following asymptotic expression for the function $N(x,z_0)$

$$N(x, z_0) = D_1 \frac{x\varphi(x)}{1-kx} z_0 e^{-kz_0}, \quad (2.25)$$

where D_1 is a new constant.

We propose the following method for determining the constants D and D_1. Assuming $x = 1/m$, with $m < 1$, let us represent the system of equations (2.5) and (2.6) in the form

$$M\left(\frac{1}{m}, z_0\right) = \frac{D_M\left(\frac{1}{m}, z_0\right)}{D\left(\frac{1}{m}, z_0\right)}; \quad N\left(\frac{1}{m}, z_0\right) = \frac{D_N\left(\frac{1}{m}, z_0\right)}{D\left(\frac{1}{m}, z_0\right)}. \quad (2.26)$$

$$D_M\left(\frac{1}{m}, z_0\right) = \begin{vmatrix} 1 + \frac{q}{2}\int_0^1 \frac{\varphi\left(\frac{1}{m}, z_0\right) M(y, z_0) - \chi\left(\frac{1}{m}, z_0\right) N(y, z_0)}{1+my} dy, & \frac{q}{2}\int_0^1 \frac{\chi(y, z_0)}{1+my} dy, \\ e^{-z_0 m} + \frac{q}{2}\int_0^1 \frac{\chi\left(\frac{1}{m}, z_0\right) M(y, z_0) - \varphi\left(\frac{1}{m}, z_0\right) N(y, z_0)}{1-my} dy, & 1 - \frac{q}{2}\int_0^1 \frac{\varphi(y, z_0)}{1-my} dy, \end{vmatrix}, \quad (2.27)$$

$$D_N\left(\frac{1}{m}, z_0\right) = \begin{vmatrix} 1 - \frac{q}{2}\int_0^1 \frac{\varphi(y, z_0)}{1+my} dy, & 1 + \frac{q}{2}\int_0^1 \frac{\varphi\left(\frac{1}{m}, z_0\right) M(y, z_0) - \chi\left(\frac{1}{m}, z_0\right) N(y, z_0)}{1+my} dy, \\ \frac{q}{2}\int_0^1 \frac{\chi(y, z_0)}{1-my} dy, & e^{-z_0 m} + \frac{q}{2}\int_0^1 \frac{\chi\left(\frac{1}{m}, z_0\right) M(y, z_0) - \varphi\left(\frac{1}{m}, z_0\right) N(y, z_0)}{1-my} dy. \end{vmatrix}. \quad (2.28)$$

It was shown in ref. 4 that

$$D\left(\frac{1}{m}, z_0\right) = 1 - \frac{q}{2m} \ln \frac{1+m}{1-m}. \quad (2.29)$$

$= k$, then $D(1/k, z_0) = 0$ (see ref. 5).

We thus obtain two expressions from (2.26)

$$D_M\left(\frac{1}{k}, z_0\right) = 0, \quad D_N\left(\frac{1}{k}, z_0\right) = 0.^* \quad (2.30)$$

It can be shown that by taking account of the two re- onships which were used to determine the constants

$$D_\varphi\left(\frac{1}{k}, z_0\right) = 0, \quad D_\chi\left(\frac{1}{k}, z_0\right) = 0, \quad (2.31)$$

nd C_1 (see ref. 4), the two expressions (2.30) are re- ed to one, which can be represented in the form

$$e^{-kz_0} \frac{q}{2}\int_0^1 \frac{M(y, z_0)}{1+ky} dy + \frac{q}{2}\int_0^1 \frac{N(y, z_0)}{1-ky} dy = \frac{\chi\left(\frac{1}{k}, z_0\right)}{\varphi\left(\frac{1}{k}, z_0\right)} \left[\frac{q}{2}\int_0^1 \frac{M(y, z_0)}{1-ky} dy + e^{-kz_0} \frac{q}{2}\int_0^1 \frac{N(y, z_0)}{1+ky} dy\right]. \quad (2.32)$$

Let us examine the ratio

$$\frac{\chi\left(\frac{1}{k}, z_0\right)}{\varphi\left(\frac{1}{k}, z_0\right)} = \frac{D_\chi\left(\frac{1}{k}, z_0\right)}{D_\varphi\left(\frac{1}{k}, m\right)}.$$

Since the expressions (2.31) are valid for $m = k$, let us expand the functions $D_\varphi(1/m, z_0)$ and $D_\chi(1/m, z_0)$ into a series in the difference m-k (for m close to k) and let us restrict ourselves to the first term of the expansion. Taking (1.1), (1.2), and (2.31) into account and separating out the largest terms in the expansion, we will then find that

$$\frac{\chi\left(\frac{1}{k}, z_0\right)}{\varphi\left(\frac{1}{k}, z_0\right)} \simeq z_0 e^{-kz_0} C_1. \quad (2.33)$$

Let us introduce Eqs. (2.24) and (2.25) into Eq. (2.32). Comparing the coefficients of the largest terms on the right and the left sides of the ratio (2.32), which apparently have a z_0-dependence of of the form $z_0 e^{-kz_0}$, and taking (2.33) into account,

$$D_1 = \frac{C_1 \frac{q}{2}\int_0^1 \frac{M(y)\, dy}{1-ky}}{\frac{q}{2}\int_0^1 \frac{\varphi(y)\, y\, dy}{(1-ky)^2}}. \quad (2.34)$$

It can be shown (see Appendix to this paper), that

*See note at the end of the paper.

$$\frac{q}{2}\int_0^1 \frac{M(y)\,dy}{1-ky} = \varphi\left(\frac{1}{k}\right) = \frac{1}{k\cdot q\cdot \int_0^1 \frac{x\varphi(x)\,dx}{1-k^2x^2}}. \qquad (2.35)$$

It therefore follows from (2.34), (2.35), and (1.3), that

$$D_1 = C_1^2\varphi^2\left(\frac{1}{k}\right). \qquad (2.36)$$

We have thus determined the constant D_1. To determine the constant D we will use the equation

$$M_0(z_0) = \frac{q}{2} + M_0(z_0)\varphi_0(z_0) - N_0(z_0)\chi_0(z_0). \qquad (2.37)$$

Let us demonstrate how this equation is obtained. For this purpose we will multiply the right and the left sides of Eq. (2.5) by q/2 and integrate it with respect to x from 0 to 1. We obtain

$$\frac{q}{2}\int_0^1 M(x, z_0)\,dx = \frac{q}{2} + \frac{q^2}{4}\int_0^1\int_0^1 \frac{x\,dx\,dy}{x+y}[M(x,z_0)\varphi(y, z_0) \qquad (2.38)$$

$$+ M(y, z_0)\varphi(x, z_0) - N(x, z_0)\chi(y, z_0) - N(y, z_0)\chi(x, z_0)].$$

Remembering that the equation

$$\int_0^1\int_0^1 \frac{xf(x,y)\,dx\,dy}{x+y} = \int_0^1\int_0^1 \frac{yf(x,y)\,dx\,dy}{x+y} = \frac{1}{2}\int_0^1 dx\int_0^1 dy f(x,y), \qquad (2.39)$$

is valid for any function f(x,y) satisfying the condition f(x,y) = f(y,x), we obtain the desired equation (2.37) from (2.38).

It can be shown in the same way that for infinitely large z_0 the exact equation

$$M_0(\infty) = \frac{q}{2} + M_0(\infty)\varphi_0(\infty). \qquad (2.40)$$

is valid.

Calculating the momenta of the functions in Eq. (2.37) with the help of Eqs. (1.1), (1.2), (2.24), (2.25), and comparing the coefficients of large terms, which have the same dependence on z_0, we find

$$D(1-\varphi_0(\infty)) = C_1D_1\frac{q}{2}\int_0^1 \frac{\varphi(x)\,x\,dx}{1-kx} = C_1D_1\frac{1}{k}(1-\varphi_0(\infty)). \qquad (2.41)$$

Finally, we obtain expressions for the constants D and D_1 in terms of constants C_1 and C

$$D_1 = C_1^2\varphi^2\left(\frac{1}{k}\right),\quad k\cdot D = C_1^2\varphi^2\left(\frac{1}{k}\right). \qquad (2.42)$$

If the asymptotic expressions for functions $\varphi(x,z_0)$, $\chi(x,z_0)$, $M(x,z_0)$, and $N(x,z_0)$ are introduced in formula (2.4), expressions can be obtained for $\bar{\tau}(\gamma)$ in thick crystals. However, we will not give the resulting equations here.

(d) It is of interest to obtain asymptotic expressions for the functions $M(x,z_0)$ and $N(x,z_0)$ for arbitrary z_0 and large x (low absorption coefficients). Let us assume in formulas (2.26), (2.27), and (2.28) that $1/m = x \gg 1$, and let us expand the expressions in them in powers of 1/x and let us restrict ourselves to the first term of the expansion. Then the approximate expressions for functions $M(x,z_0)$ and $N(x,z_0)$ for large x can be represented

$$M(x, z_0) = \varphi(x, z_0)\left[1 + \frac{M_0(1-\varphi_0) + N_0\chi_0}{1-q}\right.$$

$$\left. - \frac{1}{x(1-q)}(M_1(1-\varphi_0) + M_0\varphi_1 + N_0\chi_1 - N_1\chi_0)\right]$$

$$- \chi(x, z_0)\left[\frac{N_0(1-\varphi_0) + M_0\chi_0}{1-q} - \frac{1}{x(1-q)}(M_1(1-\varphi_0)\right.$$

$$\left. + N_0\varphi_1 + M_0\chi_1 - N_1\chi_0)\right], \qquad (2.43)$$

$$N(x, z_0) = \chi(x, z_0)\left[1 + \frac{M_0(1-\varphi_0) + N_0\chi_0}{1-q}\right.$$

$$\left. + \frac{1}{x(1-q)}(M_1(1-\varphi_0) + M_0\varphi_1\right.$$

$$\left. + N_0\chi_1 - N_1\chi_0)\right] - \varphi(x, z_0)\left[\frac{N_0(1-\varphi_0) + M_0\chi_0}{1-q}\right.$$

$$\left. + \frac{1}{x(1-q)}(N_1(1-\varphi_0) + N_0\varphi_1 + M_0\chi_1 - M_1\chi_0)\right], \qquad (2.44)$$

where the functions $\varphi(x,z_0)$ and $\chi(x,z_0)$ are given by and (1.5). For brevity, we omitted the argument z_0 designating the momenta of functions φ, χ, M, and

It follows from (2.43) and (2.44), on account of (2 that

$$M(\infty, z_0) = N(\infty, z_0) = \varphi(\infty, z_0)\left[1 + \frac{q}{2(1-q)}\right.$$

$$\left. - \frac{N_0(z_0)(1-\varphi_0(z_0)) + M_0(z_0)\chi_0(z_0)}{1-q}\right]$$

$$= \varphi(\infty, z_0)[1 + \varphi(\infty, z_0)(M_0(z_0) - N_0(z_0))]. \qquad (2.45)$$

It is interesting to investigate the value

$$\tau(x=\infty) = \lim\frac{M(x, z_0) - N(x, z_0)}{\varphi(x, z_0) - \chi(x, z_0)}$$

$$+ \frac{M(\infty, z_0)}{\varphi(\infty, z_0)} - 1.$$

since for $x \to \infty$, $\lim_{x\to\infty} M(x,z_0) = \lim_{x\to\infty} N(x,z_0)$ and $\lim_{x\to\infty}\varphi = \lim_{x\to\infty}\chi(x,z_0)$.

We can reveal the indeterminacy in expression with the help of expressions (2.43), (2.44), (2.45), (1. and (1.5)

$$\tau(x=\infty) = \frac{1}{1-q} -$$

$$\frac{2\varphi(\infty, z_0)[M_1(z_0) - N_1(z_0) + \varphi(\infty, z_0)\varphi_1(z_0) - \chi_1(z_0)(M_0 - N}{z_0 - 2\varphi(\infty, z_0)(\varphi_1(z_0) - \chi_1(z_0))}$$

For $z_0 \to \infty$, $\bar{\tau}(x=\infty) \to 1/(1-q)$, in agreement the results obtained previously.[7,8]

The average "exponential" de-excitation decay for arbitrary crystal thickness can be calculated wit help of formula (2.47) and Table 8, which listed valu the momenta of functions $M(x,z_0)$ and $N(x,z_0)$. The f mula is inconvenient at small values of z_0, however, since, in order to calculate $\bar{\tau}(x=\infty)$, it is necessary know the values of functions φ, χ, M, N and of their menta with very great accuracy. We will therefore d rive another approximate formula for the calculation $\bar{\tau}(x=\infty)$ for small crystal thicknesses, that is, for small z_0.

Let us first note that it follows from Eqs. (2.1) (2.3), and also from (12) and (15) of ref. 2, that

Table 8

q	0.5				0.8				0.9			
z_0	M_0	N_0	M_1	N_1	M_0	N_0	M_1	N_1	M_0	N_0	M_1	N_1
0.05	0.27	0.23	0.14	0.13	0.45	0.38	0.23	0.21	0.52	0.44	0.26	0.24
0.10	0.28	0.21	0.14	0.12	0.49	0.38	0.25	0.21	0.57	0.43	0.29	0.25
0.15	0.29	0.20	0.15	0.12	0.52	0.36	0.27	0.21	0.61	0.44	0.31	0.26
0.20	0.30	0.19	0.15	0.11	0.55	0.36	0.28	0.22	0.65	0.44	0.33	0.26
0.25	0.31	0.18	0.16	0.11	0.57	0.36	0.30	0.22	0.68	0.44	0.36	0.27
0.5	0.33	0.14	0.17	0.09	0.66	0.35	0.35	0.22	0.82	0.43	0.44	0.28
1.0	0.34	0.09	0.18	0.06	0.76	0.28	0.42	0.19	1.02	0.42	0.58	0.28
2.0	0.35	0.04	0.19	0.03	0.85	0.22	0.48	0.16	1.22	0.36	0.72	0.25
3.0	0.35	0.02	0.19	0.02	0.88	0.16	0.50	0.12	1.31	0.31	0.78	0.22
4.0	0.35	0.00	0.19	0.00	0.89	0.10	0.51	0.06	1.36	0.28	0.82	0.20
5.0	0.35	0.00	0.19	0.00	0.89	0.03	0.51	0.02	1.40	0.26	0.84	0.18

$$\frac{q}{2}\int_0^1 dy \int_0^{z_0} C_0\left(z, \frac{1}{y}, z_0\right) dz$$

$$= \frac{q}{2}\int_0^1 R_0\left(0, \frac{1}{y}\right) dy = \varphi(\infty, z_0)\,(\varphi_1(z_0) - \chi_1(z_0)), \qquad (2.48)$$

$$\frac{q}{2}\int_0^1 dy \int_0^{z_0} \varphi\left(z, \frac{1}{y}, z_0\right) dz = \frac{q}{2}\int_0^1 \Phi\left(0, \frac{1}{y}\right) dy$$

$$= \varphi(\infty, z_0)\,[M_1(z_0) - N_1(z_0)$$

$$+ (M_0(z_0) - N_0(z_0))\,(\varphi_1(z_0) - \chi_1(z_0))\,\varphi(\infty, z_0)]. \qquad (2.49)$$

The left-hand sides of Eqs. (2.48) and (2.49) can be ulated approximately for $z_0 \ll 1$ as follows

$$\frac{q}{2}\int_0^1 dy \int_0^{z_0} C_0\left(z, \frac{1}{y}, z_0\right) dz$$

$$= \frac{q}{2}\int_0^1 dy \cdot z_0 \frac{1}{2}\left(C_0\left(0, \frac{1}{y}, z_0\right) + C_0\left(z_0, \frac{1}{y}, z_0\right)\right)$$

$$= \frac{z_0}{2}\,(\varphi_0(z_0) + \chi_0(z_0)), \qquad (2.50)$$

$$\frac{q}{2}\int_0^1 dy \int_0^{z_0} \varphi\left(z, \frac{1}{y}, z_0\right) dz$$

$$= \frac{q}{2}\int_0^1 dy \cdot z_0 \frac{1}{2}\left(\varphi\left(0, \frac{1}{y}, z_0\right) + \varphi\left(z_0, \frac{1}{y}, z_0\right)\right)$$

$$= \frac{z_0}{2}\,(M_0(z_0) + N_0(z_0)). \qquad (2.51)$$

It follows from expressions (2.48), (2.49), (2.50), and 1) that, for small z_0, the average "exponential" de- tation time of the crystal $\overline{\tau}(x = \infty)$ can be calculated the help of the formula

$$\tau(x = \infty) = \frac{\varphi(\infty, z_0) - M_0(z_0) - N_0(z_0)}{\varphi(\infty, z_0)\,(1 - q)}. \qquad (2.52)$$

It follows from this expression that in the limit case $\to 0$ $\overline{\tau}(x = \infty) \to 1$, since $M_0(z_0) \to q/2$; $N_0(z_0) \to q/2$; $z_0) \to 1$.

ENDIX

Let us demonstrate that

$$\frac{q}{2}\int_0^1 \frac{M(y)\,dy}{1 - ky}\,dy = \varphi\left(\frac{1}{k}\right).$$

For this purpose let us multiply the left and right s of (2.19) by $(q/2)/(1/1 - kx)$ and integrate it with respect to x from 0 to 1. We obtain

$$\frac{q}{2}\int_0^1 \frac{M(x)\,dx}{1 - kx} = -\frac{q}{2}\ln(1 - k)$$

$$+ \frac{q^2}{4}\int_0^1\int_0^1 \frac{dx\,dy\,x}{(x + y)\,(1 - kx)}\,[\varphi(x)\,M(y) + \varphi(y)\,M(x)]. \qquad (*)$$

Let us use the equation

$$\frac{x}{(x + y)\,(1 - kx)} = \frac{1}{(1 - kx)\,(1 + ky)} - \frac{y}{(1 + ky)\,(x + y)}.$$

In order to use this equation to determine the value of k, let us represent (*) in the following form:

$$\frac{q}{2}\int_0^1 \frac{M(y)\,dy}{1 - ky}\left(1 - \frac{q}{2}\int_0^1 \frac{\varphi(y)\,dy}{1 + ky}\right) = -\frac{q}{2k}\ln(1 - k)$$

$$+ \frac{q}{2}\int_0^1 \frac{dy}{1 + ky}\left(M(y) - \frac{q}{2}\,y\int_0^1 \frac{M(y)\,\varphi(x) + M(x)\,\varphi(y)}{y + x}\,dx\right).$$

It can be demonstrated that the equation for k is equivalent to the following equation (see ref. 5):

$$\frac{q}{2k}\ln\frac{1 + k}{1 - k} = 1.$$

Using Eqs. (2.19) and (5) from ref. 1, as well as (2.10), we obtain

$$\frac{q}{2}\int_0^1 \frac{M(y)\,dy}{1 - ky}\,\frac{1}{1 - \frac{q}{2}\int_0^1 \frac{\varphi(y)\,dy}{1 + ky}} = \varphi\left(\frac{1}{k}\right) = \frac{1}{qk\int_0^1 \frac{x\varphi(x)\,dx}{1 - k^2x^2}}.$$

Note to page 000. According to formula (18) of ref. 2, the functions $\varphi(1/m, z_0)$ and $\chi(1/m, z_0)$ can be repre- sented, in a form similar to (2.26):

$$\varphi\left(\frac{1}{m}, z_0\right) = \frac{D_\varphi\left(\frac{1}{m}, z_0\right)}{D\left(\frac{1}{m}, z_0\right)},$$

$$\chi\left(\frac{1}{m}, z_0\right) = \frac{D_\chi\left(\frac{1}{m}, z_0\right)}{D\left(\frac{1}{m}, z_0\right)}.$$

REFERENCES

1. V. M. Agranovich, Izvest. Akad. Nauk SSSR, Ser Fiz. 23, 40 (1959).
2. V. M. Agranovich and Yu. V. Konobeev, Opt. i Spektr. 6, 648 (1959), Optics and Spectroscopy 6, 421 (1959).
3. S. Chandrasekhar and D. Elbert, Astrophys. J. 115, 244 (1952).

4. V. V. Sobolev, Astron. Zhur. **34**, 336 (1957).
5. V. V. Sobolev, "Transfer of Radiant Energy in the Atmospheres of Stars and Planets," Gosudarst Tekh. Izd., Moscow, 1956.
6. S. Chandrasekhar, "Transfer of Radiant Energy," Izd. Inostrannaya Lit., Moscow, Leningrad, 1953.
7. V. M. Agranovich, Opt. i Spektr. **3**, 84, 1957.
8. M. D. Galanin, Trudy Fiz. Inst. Akad. Nauk SSSR 339 (1950).
9. W. A. Ambartsumyan, Doklady Akad. Nauk SSSR 257 (1943).
10. A. M. Samson, Izvest. Akad. Nauk SSSR, Ser. Fi **24**, 496 (1960).

SOME CONCENTRATION EFFECTS IN PLASTIC SCINTILLATORS

L. S. Kukushkin and L. L. Nagornaya (pp. 385-389)

Received 9 August 1960

Qualitative calculations are presented which make it possible to describe concentration effects on a number of the optical characteristics of plastic scintillators. The behavior of the luminescence spectra of plastic scintillators based on polystyrene with different concentrations of luminescing additives is studied. It is shown that the experimental data are in good agreement with the point of view presented.

1. Much literature has been devoted to studies of the optical properties of plastic scintillators (see the surveys[1,2]). In these papers the luminescence spectrum of the entire system of molecules introduced into the host material in the capacity of a luminescing additive is tacitly identified with the luminescence spectrum of isolated molecules of the luminescing additive. However, the structure of these host materials is such that, generally speaking, different molecules of the luminescing additive are found in different external conditions. For this reason the spectra of the different molecules can be somewhat shifted in relation to each other. In addition to this, characteristics such as the luminescence quantum yield and the lifetime of the excited state, which are sensitive to external influences, can also be different for different molecules of the luminescing additive.

Thus if we have a system consisting of N isolated molecules of the luminescing additive in a host medium which is optically inert with respect to these molecules, the expressions for the quantum yield of the luminescence η_0, the lifetime of the excited state τ_0, and the normalized luminescence spectrum p_0 of this system can be written in the form

$$\eta_0 = \sum_{k=1}^{N} c_k \eta_k; \quad \tau_0 = \sum_{k=1}^{N} c_k \tau_k; \quad p_0(\lambda) = \frac{1}{\sum_{k=1}^{N} c_k \eta_k} \cdot \sum_{k=1}^{N} c_k \eta_k p_k(\lambda),$$

where c_k is the excitation probability of a k molecule. Starting with a certain concentration of luminescing additive the electron excitation is no longer connected with a specific molecule of luminescing additive and migrates through the system. The higher the concentration of luminescing additive and the stronger the resonance interaction, the greater the speed of the transfer. (For commonly used concentrations the magnitude of the resonance interaction is proportional to the degree of overlapping of the absorption and luminescence spectra.)

We will examine the case of low concentration of the luminescing additive ($\sim 10^{-3}$ moles/liter), for which the wave function of the system can be written in the form of a product of the wave functions of the individual molecules. As a consequence of this, the path of the excit tion through the system of luminescing additive mole cules can be described in the following way:

$$\left.\begin{aligned} \frac{d\rho_k(t)}{dt} &= \sum_{i=1}^{N} [\alpha_{ik}\rho_i(t) - \alpha_{ki}\rho_k(t)] - \frac{1}{\tau_k}\rho_k(t); \\ \rho_k(0) &= c_k; \quad \sum c_k = 1, \end{aligned}\right\}$$

where $\rho_k(t)$ is the probability that molecule k is excited at the moment t; α_{ik} is the number of transitio in unit time from an i molecule to a k molecule; and τ_k is the lifetime of the excited state of a k molecul isolated from the remaining molecules of luminescin additive.

The individual excitations do not interact with ea other when the ultraviolet radiation source is of conv tional intensity; this justifies the condition that $\Sigma c_k =$

A similar equation has been examined by Förste for a system of molecules which are in entirely ident conditions and consequently have completely corresp ing spectra, quantum yield values, etc., that is, for molecules with $\alpha_{ik} = \alpha_{ki}$ (this occurs in low viscosity solutions).

In our case, generally speaking, $\alpha_{ik} \neq \alpha_{ki}$, which leads to the dependence of a number of the optical ch acteristics of the system on the concentration of the luminescing additive. The nature of these dependenc becomes graphically clear if it is taken into consider that even a very small relative displacement of the s tra of the i and k molecules leads to a substantial d ference in the values of α_{ik} and α_{ki} (moreover, if th molecule spectra are displaced to the long waveleng side in comparison to the i molecule spectra, then α_{ki}).

It is easy to see from (1) that the probability of excitation in a k molecule as a result of fluorescenc or intramolecular deactivation is equal to $(1/\tau_k)\mu_k$, where $\mu_k = \int_0^\infty \rho_k(t)dt$. Consequently the optical charac istics of the system take the form

$$\eta = \sum \frac{1}{\tau_k}\mu_k\eta_k; \quad \tau = \sum \mu_k; \quad p(\lambda)\,\eta = \sum \frac{1}{\tau_k}\mu_k p_k(\lambda)\,\eta_k.$$

For the calculation of $\{\mu_k\}$ we have, from (1),

$$\frac{\mu_k}{\tau_k} - c_k = \sum_i (\alpha_{ik}\mu_i - \alpha_{ki}\mu_k). \quad (2)$$

If it is assumed, for example, that $c_k = 1/N$, then path of the excitation through the system will have a cific trend—the "current" of excitations moving to- d molecules with shifts into the long-wavelength side ne spectra will exceed the "current" moving away n them; that is, the contribution of the "long-wave" ecules to the optical properties of the system will ease when $\alpha_{ik} \neq \alpha_{ki}$ in comparison with the case of a em of isolated molecules with the same distribution tion. This is graphically demonstrated in the ex- le of a system of two molecules. In this case

$$\frac{\mu_2}{\tau_2} = \frac{1}{2} \cdot \frac{1 + \alpha_{12}\tau_1 + \alpha_{21}\tau_2}{1 + 2\alpha_{12}\tau_1}; \quad \frac{\mu_1}{\tau_1} = 1 - \frac{\mu_2}{\tau_2}, \quad (3)$$

is, when $\alpha_{21} > \alpha_{12}$ and $\tau_1 \leq \tau_2$, $\mu_1/\tau_1 > \mu_2/\tau_2$.

If ξ is understood to stand for such an optical char- ristic of the system as η, τ, or $p(\lambda)\eta$, then the vari- n of ξ under a transition from a system of isolated ecules to a system in which transfer of the excitation ugh the molecules of luminescing additive is possible ritten in the form

$$\xi - \xi_0 = \Delta\xi = \sum \xi_k \left(\frac{\mu_k}{\tau_k} - c_k\right)$$

because of (2),

$$\Delta\xi = \sum_k \xi_k \sum_i (\alpha_{ik}\mu_i - \alpha_{ki}\mu_k) = \sum_{k;\, i>k} (\xi_k - \xi_i)(\alpha_{ik}\mu_i - \alpha_{ki}\mu_k). \quad (4)$$

The notation (4) is convenient in the case when the e of ξ_k changes monotonically as a function of the unt of shift of the spectra. This is the situation with pect to the quantum yield value in a significant num- of cases—the shift of the spectra to the long-wave- th side is accompanied by a decrease in the quantum d (moreover, in addition to this the lifetime of the ted state is occasionally reduced).

Let us now change the designations of the molecules uminescing additive in such a way that with $i > k$, would be $\geq \alpha_{ki}$; that is, the greater the index of the ecule the further toward the short-wavelength side spectrum is shifted. Let us consider the limiting es. Let the difference $\alpha_{ik} - \alpha_{ki}$ be small. Thus, if s assumed that $c_k = 1/N$ and $\tau_k = \tau$, then the zeroth roximation for μ_k from (2) yields

$$\mu_k^{(0)} = \frac{\tau}{N}$$

the first approximation of the method of successive roximations leads to the expression

$$\Delta\xi = \frac{\tau}{N} \sum_{k;\, i>k} (\xi_k - \xi_i)(\alpha_{ik} - \alpha_{ki}). \quad (5)$$

Thus, if $\xi_i \geq \xi_k$ for $i > k$, then the value of ξ de- eases with increasing concentration of the luminescing ditive.

In the case when not only the difference $\alpha_{ik} - \alpha_{ki}$ but o the α_{ik} themselves are small, the first approxima- n gives

$$\Delta\xi = \frac{1}{N} \sum_{k;\, i>k} (\xi_k - \xi_i)(\alpha_{ik}\tau_i - \alpha_{ki}\tau_k). \quad (6)$$

It is seen from (6) that the generally occurring case $\tau_i \geq \tau_k$ when $i > k$ enhances the effect. Actually, the shorter the lifetime of the excited state of the k molecule the more quickly it becomes possible for it to acquire a new portion of the excitation.

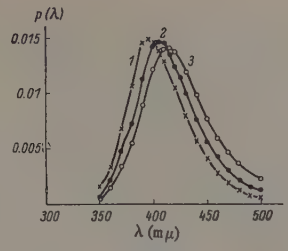

Fig. 1

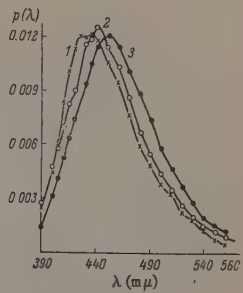

Fig. 2

Fig. 1. Concentration dependence of the luminescence spectra of 2-(4-biphenyl)-5-(9-phenanthryl)-oxadiazole-1,3,4 in polystyrene with monochromatic excitation at λ = 334 mμ. Concentration of luminescing additive (in moles/liter): curve 1—10^{-4}; curve 2—10^{-3}; curve 3—3×10^{-2}.

Fig. 2. Concentration dependence of the luminescence spectra of tetraphenylbutadiene (TPB) in polystyrene with monochromatic excitation at λ = 334 mμ. Concentration of luminescing additive (in moles/liter): curve 1—3×10^{-4}; curve 2—10^{-2}; curve 3—3.5×10^{-2}.

The case of a system in which $\xi_i \geq \xi_k$ and $\tau_i \geq \tau_k$ when $i > k$ also leads to the condition $\Delta\xi \leq 0$. This follows directly from (3) for a system of two molecules. For the general case the proof can be carried out by the method of induction (each time more "long-wavelength" molecules should be added), with the following impositions on the spatial distribution of the molecules of luminescing additive of the usually occurring conditions: (1) the probability of finding a molecule of the additive in any volume of scintillator is proportional to the volume and to the concentration of the luminescing additive; (2) different orientations of the additive molecules in relation to each other are equally probable.

We note that changes in the system $\{c_k\}$, that is, changes in the exciting source or the transmission conditions, can show up to a substantial degree in the character of the concentration effects: thus, for example, an increase in the weight of those c_k which correspond to "short-wavelength" molecules leads to an intensification of both the concentration displacement effect of the luminescence spectra and the concentration quenching effect, while an increase in the weight of the c_k's corresponding to "long-wavelength" molecules can cause these effects to disappear or even change sign.

2. To confirm the considerations presented above we measured the concentration dependence of the luminescence spectra of a number of luminescing additives in polystyrene. These experiments are of interest in themselves, since the location of the luminescence spectra substantially influences the scintillation performance of plastic scintillators. It turns out that for some of them the long-wavelength displacement of the luminescence spectra reaches ~250 A (Figs. 1 and 2) when the concentration is increased within the limits of 10^{-4}-10^{-2} moles/liter, while the absorption spectra remain practically unchanged.

A similar situation is observed for certain oxadiazoles and pyrazolin derivatives.

In agreement with the point of view put forth above, a change in the character of the concentration displacement of the luminescence spectra was found when the excitation source ($\{c_k\}$) was varied. Corresponding results for the case of 1,3-diphenyl-5-(n-biphenylene)-pyrazoline-Δ^2 are shown in Fig. 3. Although the maxima of spectra 1 and 1′ practically coincide, these spectra as a whole are noticeably displaced relative to one another. An additional fact in support of the mechanism described is that the concentration displacement effect on the luminescence spectra is not observed when the kinds of luminescing additives studied are in liquid solvents.

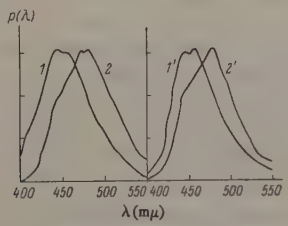

Fig. 3. The dependence of the luminescence spectra of 1,3-diphenyl-5-(n-biphenyline)-pyrazoline-Δ^2 excited by light with a wavelength $\lambda = 313$ mμ (1,2) and $\lambda = 405$ mμ (1′, 2′) on concentration. Concentration (in mole/ℓ): 1,1′—10^{-5}; 2,2′—3×10^{-2}.

Among the causes capable of producing the long-wavelength displacement of the luminescence spectra one should first mention reabsorption and the change in the distribution function of the additive molecules (see above) with change in concentration. The presence of the second cause must be accompanied by a corresponding concentration displacement of the absorption spectra. Thus the fact that the absorption spectra are practically unchanged when the concentration of luminescing additive is changed excludes the second cause.

In order to reduce the effects of reabsorption we took the luminescence spectra "frontally" and the excitation was accomplished with the light of mercury lines lying in the region of high absorption by the luminescing additive. However, the choice of excitation source and the method of obtaining the luminescence spectra did not make it possible to get rid of reabsorption effects entirely. For this reason we performed a calculation (which we will not reproduce here because of its extensiveness, but which is based on a rather general principle of ref. 4) with the aid of which we were able to show that the contribution of reabsorption to the concentration change in the luminescence spectra shown in Figs. 1 and 2 is negligible. In addition, the circumstance that some substances with practically identical degrees of overlapping of absorption and luminescence spectra have a totally different character and value of the concentration change of their luminescence spectra may serve as evidence of the nonreabsorption nature of the displacement of the luminescence spectra for a number of luminescing additives. Such substances are, for example, BNO and TPB: for BNO the displacement of the luminescence spectrum maximum is 150 A when the concentration is changed in the range of 3×10^{-5}–3×10^{-2} moles/liter but TPB with the same value of overlapping of spectra is displaced 250 A.

Finally, we cite one more experimental fact which gives evidence against the reabsorption explanation of concentration change in the luminescence spectra: it was found that the luminescence spectrum, taken "frontally" of a polystyrene block with 10^{-2} moles/liter of TPB and a height of 15 mm, which was excited in the intense absorption range of the luminescing additive coincided to high degree of accuracy with the luminescence spectrum of a thin layer with a 0.035 mm thickness which was obtained from the same block. Quantitative comparison of the computations with the experimental data is beyond the scope of this paper.

In conclusion the authors express their gratitude to V. D. Bezuglyi for his discussion of the results of the work.

REFERENCES

1. I. M. Rozman and S. F. Kilin, Uspekhi Fiz. Nauk. 6[illegible] 459 (1959), Soviet Phys.-Uspekhi 2, 856 (1960).
2. I. M. Rozman, Izvest. Akad. Nauk SSSR, Ser. Fiz. 2[illegible] 36 (1958).
3. T. Förster, Ann. Physik 62, 55 (1948).
4. V. M. Agranovich and Yu. V. Kenoveev, Opt. i Spek[illegible] 6, 648 (1959), Optics and Spectroscopy 6, 421 (1959)

LUMINESCENCE OF p-TERPHENYL IN A MIXTURE OF TOLUENE AND CARBON TETRACHLORIDE

S. F. Kilin, K. A. Kovyrzina, and I. M. Rozman (pp. 390-396)

Received 11 August 1960

The dependence of the yield and duration of the photo- and high-energy luminescence of p-terphenyl in toluene were investigated as a function of the concentration of the quencher—carbon tetrachloride. The constants of quenching were determined, as well as the efficiency of energy transfer, for different methods of excitation. Comparison with the diffusion theory of quenching shows that the values of the constants for the quenching of toluene and for the energy transfer can be obtained only on the assumption of a large radius of the sphere of action ($R \geq 20$ A).

RODUCTION

One of the characteristic features of the high-energy inescence of organic substances is its low energetic d. Even for fast electrons, the specific scintillation ie is only $s_0 = \eta/40$ ev^{-1}, (η is the quantum yield of rescence), which is about one fifth of the maximum sible value.[1] The reason for this phenomenon is not r. In this connection, a comparison of the fluores-ce and of high-energy luminescence of various sys-s is of great interest. In the present paper the nching of the luminescence of a solution of p-terphenyl oluene (concentration 5 gm/liter) by carbon tetra-ride is investigated. In this system, the transfer of itation energy takes place from toluene to p-terphenyl, the quenching of excited molecular states is accom-hed by the dissolved oxygen and the carbon tetrachlo-e. We have investigated the dependence of the yield and duration of the luminescence on the concentration of CCl_4, other conditions being equal.

We shall use the following kinetic scheme* to describe

heme (1) contains the assumption that all S* (or A*) e the same probabilities of quenching or energy trans-, and that these quantities do not change with time.

processes which occur between the excited mole-es of toluene (S) and p-terphenyl (A):

$$\left.\begin{array}{ll} S^* \to S + h\nu_1 & k_e \\ S^* \to S & k_i \\ S^* + Q \to S + Q & k_q \\ S^* + A \to S + A^* & k_t \\ A + h\nu_1 \to A^* & Pk_e\ (P \leqslant 1) \\ A^* \to A + h\nu_2 & k'_e \\ A^* \to A & k'_i \\ A^* + Q \to A + Q & k'_q \end{array}\right\} \quad (1)$$

stands for the CCl_4 molecules; the column on the right es the rate constants of the corresponding reactions. e values of k_q and k'_q are proportional to the concen-tions of CCl_4 ($k_q = K_q C_q$), and k_t is the concentration p-terphenyl. Quenching by oxygen and concentration nching are included in the k_i.

The efficiency of the energy transfer from S* to A given by

$$T = \frac{Pk_e + k_t}{k_e + k_i + k_q + k_t},$$

the quantum yield of toluene without quencher ($k_q = 0$) without the acceptor ($k_t = 0$) is

$$\eta_{10} = \frac{k_e}{k_e + k_i} = k_e \tau_{10},$$

i.e.,

$$T = \frac{P\eta_{10} + \tau_{10} k_t}{1 + \tau_{10}(k_t + k_q)}. \quad (2)$$

For a p-terphenyl concentration of 5 gm/liter, $\tau_{10} k_t \gg 1$ (see below), so that radiation transfer can be completely disregarded ($\eta_{10} \sim 0.01$).[2]

The fluorescent yield by direct excitation of p-terphenyl is

$$\eta_{12} = \frac{k'_e}{k'_e + k'_i + k'_q}$$

and

$$\frac{\tau_{i20}}{\tau_{i2}} = 1 + \tau_{20} K'_q C_q, \quad (3)$$

where η_{20} and τ_{20} are the yield and the duration of fluorescence without quenching, respectively.

The purpose of the measurements was the comparison of the quenching constants K_q and K'_q for excitation by ultraviolet and ionizing radiation, respectively. It is It is easy to determine K'_q for light excitation if the wavelength of the exciting radiation is in a region where the solvent is transparent. Ionizing radiations are absorbed completely by the solvent. The method used to determine the value of K'_q was therefore based on the measurement of the duration of the luminescence. In the present case, the mean duration of the luminescence is made up of the duration of the energy transfer from toluene to paraterphenyl and the lifetime of the excited state of the p-terphenyl molecule,[3] i.e.,

$$\tau_S = \tau_{12} + \tau_2.$$

Since (see previous footnote)

$$\tau_2 = \frac{\tau_{20}}{1 + \tau_{20} K'_q C_q}, \quad (4)$$

the value of K'_q can be determined, if $\tau_{12} \ll \tau_2$.

In the general case, the luminescence of p-terphenyl is made up partly in connection with the direct absorption of the exciting radiation by the molecules of this compound (α_2), and partly due to the energy transfer from toluene. In a steady state, the intensity of luminescence is

$$I = F(\alpha_2 + \alpha_1 T)\eta_2. \quad (5)$$

By measuring the dependence of I on the concentra-

tion of the quencher, the quenching constant K_q can be determined.

The yield of photo- and high energy luminescence of p-terphenyl in xylene with CCl_4-quenching was studied by Galanin and Chizhikova. They showed that when the concentration of p-terphenyl is 5 gm/liter, the quenching of α- and γ-scintillations is the same. Lipsky and Burton[5] give the results of yield measurements of the photo- and γ-luminescence of p-terphenyl in toluene and benzene with bromobenzene quenching. They show that in both solutions, γ-luminescence is quenched somewhat more strongly than photoluminescence.

EXPERIMENTAL PART

Commercial toluene, carbon tetrachloride, and p-terphenyl were subjected to an additional purification. Ten volumes of toluene were shaken with one volume of sulfuric acid, then washed with water, dried, and fractionated. The carbon tetrachloride was purified by Klein's[6] procedure. Terphenyl obtained from the Kharkov Pure Reagent Factory was distilled under high vacuum.

A series of solutions was prepared from these substances. In all cases, the concentration of p-terphenyl was 5 gm/liter. The carbon tetrachloride concentration varied between 0 and 2 moles/liter. All solutions were saturated with air. The experiments were conducted at 25°C.

The intensity of fluorescence was measured by excitation in the absorption band of toluene (λ_1 = 265 mμ) and in the absorption band of p-terphenyl (λ = 297 or 302 mμ). The lines λ_1 and λ_2 were separated from the spectrum of the mercury lamp PRK-8 by means of two monochromators in series. The intensity of the background due to scattered light was lower than the limit of sensitivity of the detecting-recording apparatus (FEU-18 photomultiplier and galvanometer with a sensitivity of 2×10^{-10} amp/mm). The solutions were introduced into a rectangular quartz cell 10 × 10 mm (in the order of increasing concentration of the quencher). The fluorescence was measured in the direction of the exciting light (the luminescence of quartz was taken into consideration; it amounted to 8% of the intensity of the fluorescence of the solution with the highest concentration of the quencher, 0.624 mole/liter). The fluorescent intensity of the solution was reduced to equal fluxes of the exciting photons by means of a quantum counter.

The relative yield of the high energy, radiation-induced luminescence was determined by measuring the average current of the photomultiplier under the same conditions of excitation by β-particles of Pm^{147} or by α-particles of Po^{207}. For this purpose we used a metallic cell, which was rigidly connected with the reagent holder. The top of the cell was covered by fused quartz; its bottom had a window covered by an aluminum film about 4μ thick. Both the height and the diameter of the cell were 18 mm. The measurements were made without optical contact with the photocathode.

For x-ray excitation,[7] the duration of the luminescence was measured with a phase fluorometer. The accelerating potential was 60 kv, the frequency of modulation 20 Mc/s.

RESULTS OBTAINED

Figure 1 shows the curves: intensity ratio of the unquenched (I_0) and quenched (I) solutions vs. concentration, for various excitation conditions. In the case of direct excitation of p-terphenyl, the I_{20}/I_2 values satisfy the Stern-Volmer equation with a quenching constant $\tau_{20}k'_q$ = 15 liters/mole, which is in good agreement with the results of ref. 5 for p-terphenyl in xylene. With excitation in the toluene band (λ_1), the quenching is considerably stronger. The quenching action of CCl_4 in this case is twofold: firstly, since the transfer of excitation energy from toluene to p-terphenyl requires a certain time, there is a partial quenching of the energy donor and, secondly, the energy acceptor is also subjected to quenching; this follows from the results with λ_2 excitation. The successive action of the two quenching processes results in a supra-linear dependence of I_{10}/I_1 on C_q (curve 2). The degree of quenching for excitation with α- or β-particles is even greater (curve 3).

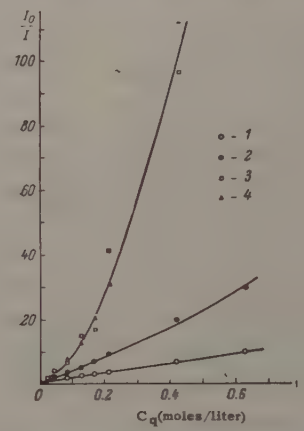

Fig. 1. Dependence of the intensity of luminescence of a p-terphenyl solution in toluene on the concentration of carbon tetrachloride. Exciting radiation: 1—light, 297 or 302 mμ; 2—light, 265 mμ; 3—α-particles; 4—β-particles

Figure 2 gives the results of measurements made with the phase fluorometer.

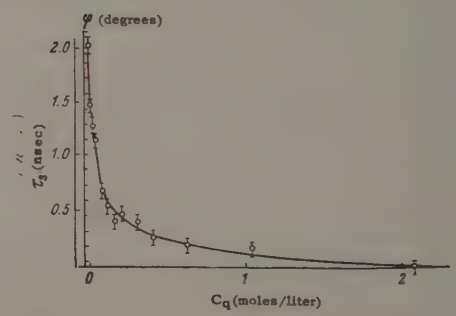

Fig. 2. Dependence of the average duration of scintillations on the concentration of CCl_4.

As is well known, the duration of luminescence is determined in phase methods by measuring the phase difference between the exciting radiation modulated with the frequency ω, and the intensity of luminescence. For the relationship holds

$$\tau^{fl} = \frac{1}{\omega} \operatorname{tg} \varphi_0.$$

If $\omega\tau^{fl} \ll 1$, then τ^{fl} is equal to the average dura- of luminescence, regardless of the decay law.[8]

For x-ray excitation, the apparatus yields the value $_s$, plus a certain constant ψ, i.e., $\varphi = \varphi_s + \psi$. A di- method of determining ψ (or of the "zero" of the ratus) is the utilization of a scintillator whose lumi- ence is so short-lived that the value of φ_s is beyond sensitivity of the instrument. For instance, in ref. e zero was determined with the luminescence of air, ne assumption that $\tau \approx 0.2$ nsec. However, there are cations that $\tau \approx 1$ nsec for air.[10]

It can be seen from Fig. 2 that for large C_q the e shift φ_s in our measurements approaches values h are near the limit of sensitivity of the fluorometer. apolation of φ to zero luminescence yield permits elimination of ψ. It was found that even without the ncher, $\omega\tau^{fl} \ll 1$. Consequently, the value τ^{fl} agrees good approximation with the average value of the tillation duration τ_s. For an unquenched solution, 20 nsec, which agrees with the results of ref. 10. high concentrations of the quencher ($C_q > 0.5$ es/liter)

$$\frac{\tau_s}{I_2} = \text{const},$$

is, the value of K'_q does not depend on the type of tation (Fig. 3).

In order to calculate the quenching constant of ene K_q we shall use the following relationships, ob- ed from Eqs. (5) and (2):

$$\frac{i_0}{i_0 - i} = \frac{(\alpha_{20} + \alpha_{10}T_0)(1 + yC_q)}{(\alpha_{10} - \alpha_1)T_0 + (\alpha_{20} - \alpha_2)(1 + yC_q) + \alpha_{10}T_0yC_q}.$$

re $i = I/I_2$ and $y = (1 - T_0)\tau_{10}K_q$; the index 0 refers he unquenched solution. Since CCl_4 does not absorb t of the wavelength λ_1, its influence on α_2 can be lected ($C_q \leq 0.6$ moles/liter). Consequently, for photo- tation,

$$\frac{i_0}{i_0 - i} = \left(1 + \frac{\alpha_2}{\alpha_1 T_0}\right)(1 + y^{-1}C_q^{-1}).$$

As follows from Fig. 4, the experimental results sfy this equation, and

$$y = (1 - T_0)\tau_{10}K_q = 20 \text{ liters/mole} \qquad (6)$$

It can be assumed for excitation with charged par- es that $\alpha_2 = \alpha_{20}$ and $\alpha_1 = \alpha_0 (1 - 0.18\, C_q)$. In that e we obtain

$$\frac{i_0}{i_0 - i} = \left(1 + \frac{\alpha_2}{\alpha_{10}T_0}\right)\frac{y}{0.18 + y}(1 + y^{-1}C_q^{-1}).$$

From the experimental data of Fig. 4, it follows that

$$y_s = (1 - T_{s0})\tau_{s0}K_{qs} = 35 \text{ liters/mole} \qquad (7)$$

ch is almost twice as large as in the case of photo- tation,*

* quantities related to the high energy induced lumi- cence are identified hereinafter with the symbol s.

he effectiveness of the transfer t_0 is being determined ordingly (5), with the help of the formula

$$T_0 = \frac{\frac{I_{10}}{I_{20}} - \alpha_2}{1 - \alpha_2},$$

ere I_{10} and I_{20} are the intensities of the inescence for excitation with equal photon fluxes λ_1 and λ_2. According to the measurements, the ratio of the molar coefficients of absorption by p-terphenyl and toluene is 170 (for λ_1), and $\alpha_2 = 0.25$. Since

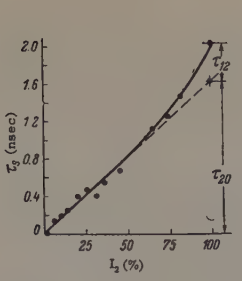

Fig. 3

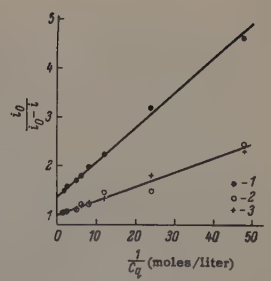

Fig. 4

Fig. 3. Relationship between the average duration of scintillations and the yield of fluorescence of p-terphenyl.

Fig. 4. Influence of CCl_4 on the luminescence of p-terphenyl in toluene. Exciting radiation: 1—light, λ = 265 mμ; 2—α-particles; 3—β-particles.

$$\frac{I_{10}}{I_{20}} = 0.920 \pm 0.010,$$

it follows that

$$T_0 = 0.894 \pm 0.013,$$

which is in good agreement with the data of ref. 11.

The transfer efficiency T_{s0} can be calculated from the duration of luminescence τ_s. From Fig. 3 we obtain $\tau_{12} \approx 0.4$ nsec, and since, according to our data, τ_{s0} = 5.6 nsec,

$$T_{s0} \approx 0.9.$$

A similar result is obtained if values of τ_s from ref. 10 and τ_{20} from our measurements are used. Identical values of T_0 and T_{s0} also follow from the data of Lipsky and Burton[5] who measured the transfer constants for γ- and photoexcitation. Within the errors of measurements (±6%), these quantities are equal.

DISCUSSION OF RESULTS

The value of the quenching constant of p-terphenyl (15 liters/mole) is in good agreement with the diffusion theory of quenching, according to which

$$\tau_{20}K'_q = 4\pi pRD\tau_{20} \approx 7.6 \cdot 10^{21} pRD\tau_{20} \text{ liters/mole}$$

R is the sum of the kinetic radii of the molecules of p-terphenyl and CCl_4, D is their mutual diffusion coefficient, and p is the quenching probability during the molecular encounter. Substituting the numerical values $p \approx 1$, $R \approx 5 \times 10^{-8}$ cm, $D \approx 3 \times 10^{-5}$ cm^2/sec, and τ_{20} = 1.6 nsec (Fig. 3), we obtain

$$\tau_{20}K'_q = 18 \text{ liters/mole}$$

For toluene, quenching and energy transfer have considerably greater probabilities. For photoexcitation,

$$\tau_{10}K_q = 190 \text{ liters/mole and } \tau_{10}K_q = 390 \text{ liters/mole}$$

Since the value τ_{10} is between 5.6 and 7.4 nsec,[10] these large values for the quenching and transfer con-

stants can be obtained only by assuming a large radius for the "sphere of action," namely, $R \geq 20$ A. Similar results have led Lipsky and Burton[5] to the hypothesis of the existence in the solvent of small regions with an ordered structure in which the energy of excitation is present in the form of an exciton.

The dependence of y on the type of excitation [see Eqs. (6) and (7)] may be related to several differences in the energy transfer. To explain the results obtained, it is sufficient to assume that T_{s0} is smaller than T_0 by only 9%. The accuracy of the experimental data is not sufficient to exclude this possibility. It is interesting to note that it follows from the data of ref. 5 that the value of y_s/y decreases somewhat with increasing p-terphenyl concentration. It is possible that the dependence under consideration is connected with the process of quenching itself. For instance, the effect of the quencher is stronger in high energy, radiation-induced luminescence because of a reaction with the ions. If a sufficiently long-lived complex S*Q is formed, then recombination with electrons will not result in the formation of an excited molecule S*, as occurs in the absence of Q. The capture of electrons by molecules of the quencher is also possible. The existence of such reactions must result in an additional decrease of the yield of the high energy, radiation-induced luminescence.

REFERENCES

1. I. M. Rozman, E. A. Andreeshchev, and S. F. Kili Izvest. Akad. Nauk SSSR, Ser. Fiz. 23, 102 (1959)
2. T. P. Belikova and M. D. Galanin, Opt. i Spektr. 1 168 (1956).
3. I. M. Rozman and S. F. Kilin, Uspekhi Fiz. Nauk 459 (1959), Soviet Phys.-Uspekhi 2, 456 (1960).
4. M. D. Galanin and Z. A. Chizhikova, Opt. i Spektr 196 (1958).
5. S. Lipsky and N. Burton, J. Chem. Phys. 31, 1221 (1959).
6. A. K. Klein, J. Assoc. Offic. Agr. Chemists 32, 3 (1949).
7. E. E. Baroni, S. F. Kilin, K. A. Kovyrzina, I. M. Rozman, and V. M. Shoniya, Pribory i Tekh. Eksp No. 3 (1961).
8. L. A. Kuznetsova, B. Ya. Sveshnikov, and V. I. Shirokov, Opt. i Spektr. 2, 578 (1957).
9. H. Knau, Z. Naturforsch. 12a, 881 (1957).
10. R. K. Swank, H. B. Phillips, W. S. Buck, and L. J. Basile, IRE Trans. on Nuclear Sci. NS-5, 183 (19
11. S. G. Cohen and A. Weinreb, Proc. Phys. Soc. B6 593 (1956).

THE YELLOW LUMINESCENCE OF ZINC OXIDE

Ya. M. Zelikin and A. P. Zhukovskii (pp. 397-402)

Received 1 August 1960

The different hypotheses concerning the centers responsible for the yellow luminescence band of ZnO are discussed and subjected to experimental verification. The conclusion reached is that an excess of oxygen and some kind of structural defects are necessary for the development of yellow luminescence.

Zinc oxide is a very interesting subject for the study of the nature of luminescence centers. Zinc oxide is a typical crystal phosphor and is very similar to zinc sulfide, but differs from the latter in that it is not activated by impurity metals. This circumstance is favorable for a study of the luminescence of self-activated phosphors in its purest form.

There are two known luminescence bands in the visible portion of the zinc oxide spectrum—a green one with a maximum near 510 mμ and the yellow with its maximum about 610 mμ. This work is devoted to a study of the nature of the luminescence centers responsible for the yellow band.

PREPARATION OF THE SAMPLES

Metallic zinc was distilled repeatedly in a vacuum and the middle fraction was separated each time. A spectral analysis of the zinc purified in this way (the second fraction of the third distillation), which was conducted at our request at the State Institute of Nickel Industry, gave the following results which are shown in Table 1.

The purified zinc was burned and the zinc oxide powder obtained was baked in air for an hour at a temperature of 1000°C. The basic zinc oxide raw materia which luminesced weakly with a greenish-yellow light at room temperature was prepared by this method.

Table 1

Impurity	Concentration (%)	Impurity	Concentration (%)
Cu	1.7 × 10-5	Al	6 × 10-6
Pb	< 1.2 × 10-6	Mn	< 2 × 10-6
Ni	1 × 10-6	Cd	< 2 × 10-5

The baking of the ZnO powder was carried out in long (30 cm) quartz combustion boat which was divide into 10 identical transverse sections. This was done i order to study the effects of subsequent thermal treat ment on the luminescence properties of the oxide. Th boat was inserted into a quartz tube which was connec to a vacuum system. A tubular furnace with a special nonuniformly wound heating coil was slipped on the ou side of the tube. The temperatures were determined the midpoints of the sections of the boat and are show in Table 2.

Table 2

Section No.	1	2	3	4	5	6	7	8	9
Temperature (°C)	480	555	630	730	815	910	980	1020	980

The luminescence spectra were recorded at liquid
ɔgen temperature utilizing an FEU-14 photomultiplier.
ɔnochromator with a diffraction grating (the disper-
of the instrument was 23 A/mm) served as the dis-
ing instrument. A PRK-4 mercury-quartz lamp with
FS-3 filter was used for the excitation. Corrections
he spectral sensitivity of the photomultiplier tube
e been incorporated into the results of the measure-
ts.

For preparation of samples having green lumines-
e, the original powder was baked in an argon atmos-
re for 40 minutes in the apparatus described above.
luminescence spectra of the powders obtained from
erent sections of the boat are shown in Fig. 1. It is
from the figure that the intensity of the green lumi-
ence band is sharply increased for the sample baked
ae inert medium at a temperature ≃ 800°C, while the
ɔw band intensity is reduced. All the samples obtained
aking at higher temperatures have a bright green
nescence.

In order to obtain samples with a yellow lumines-
e, ZnO powder having a bright green luminescence
subjected to a similar thermal treatment in an oxy-
stream. The spectra of the corresponding samples
shown in Fig. 2. In this case the appearance of yel-
luminescence bands is observed to be associated
the sample baked at a temperature of ≃ 800°C. A
er growth in the yellow luminescence band intensity
a simultaneous decrease in the green intensity are
d in connection with the samples baked at higher
peratures.

NATURE OF THE CENTERS RESPONSIBLE FOR THE GREEN AND YELLOW LUMINESCENCE BANDS OF ZINC OXIDE

It is customary to consider that superstoichiometric
is responsible for the green radiation of ZnO. There
nly differences of opinion relative to whether this
atom[1] or an ion localized at a lattice point[2] or at
terstice.[3] The yellow luminescence band of ZnO has
studied considerably less. Extremely diverse
s of view, some of which are in direct contradiction,
been expressed in the literature regarding the lo-
ation and nature of the centers responsible for the
yellow luminescence. Miller,[4] without looking into
ature of the centers, indicated that the yellow lumi-
ence centers are characteristic of the surface only
not the volume of the crystals. The author drew this
lusion on the basis of his observation of the disap-
ance of the yellow luminescence after lightly etching
ZnO surface.

We carried out similar experiments on our samples.
ZnO samples presubjected to different thermal
tment were etched by weak hydrochloric acid. In all
s a reduction of the yellow band intensity in com-
son to the green was observed. However for the sam-
which had been baked for longer periods of time at
er temperatures a longer etching in the acid was
ired to obtain an appreciable weakening of the yel-
luminescence; moreover, an effect of this kind could
generally be obtained for a sample of ZnO prepared
hermal decomposition of zinc nitrate.* It follows

* prepared the zinc nitrate by the interaction of metal-
inc (second fraction of the third distillation) with
e distilled chemically pure nitric acid.

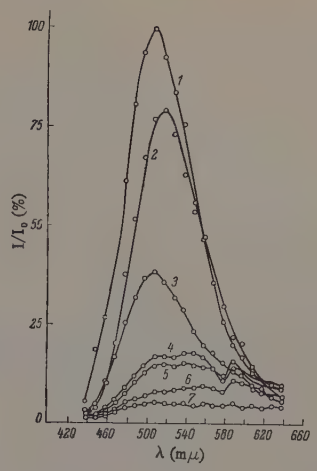

Fig. 1

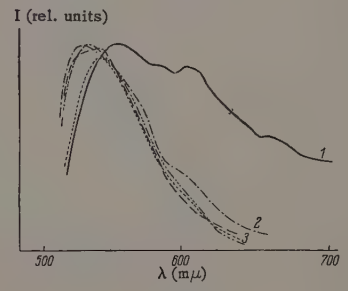

Fig. 2

Fig. 1. The luminescence spectra of samples baked for 40 minutes in an argon atmosphere. Baking temperature (°C): curve 1—980; curve 2—910; curve 3—815; curve 4—480; curve 5—555; curve 6—630; curve 7—730.

Fig. 2. Luminescence spectra of samples baked for 40 minutes in an oxygen stream. Temperature of baking (°C): curve 1—1020; curve 2—815; curve 3—480-730. All the curves are normalized to equal ordinates at their maxima.

from these experiments that the yellow luminescence centers are localized not only near the surface but can be found in the entire volume of the crystal.

Let us now turn to the question of the nature of the centers which are responsible for the yellow luminescence.

The assumption has been made that the yellow luminescence can be attributed to superstoichiometric zinc. Thus Shalimova[1] considers that the yellow luminescence appears in those samples having a high concentration of superstoichiometric zinc. Increasing the concentration of the latter intensifies the perturbing action of the ZnO crystal lattice on the zinc atom energy levels, which in turn leads to removal of the forbiddenness from the $^3P_0$—$^1S_0$ transition. In Shalimova's opinion this transition in the excess zinc atom which finds itself in the ZnO lattice corresponds to the yellow luminescence band. Konovalov[3] attributes the yellow luminescence band to a zinc ion located at a lattice node next to an oxygen vacancy. He considers the intensification of the yellow luminescence which he observed after baking the samples in a

vacuum as one of the confirmations of his explanation. Inasmuch as our experiments in the study of the conditions under which the yellow luminescence occurs contradicted Konovalov's conclusions, we decided, wherever possible, to accurately repeat his experiments with baking in a vacuum. A recheck did not at all corroborate Konovalov's observations. It appears to us that the hypothesis attributing the yellow luminescence band to excess zinc must be rejected if only for the reason that the yellow luminescence intensity is decreased after baking in an inert medium and is increased after the same thermal treatment in an oxidizing atmosphere (Figs. 1 and 2).

The hypothesis has been expressed that additions of impurity metals are responsible for the ZnO luminescence. Schmidt[5] considered an impurity of cadmium in the ZnO as the responsible agent. Randall[6] attributed the origin of the activation to manganese but this hypothesis was conclusively disproved by the work of Osiko.[7]

In order to clarify whether impurities are responsible for the yellow luminescence of ZnO we investigated the effect on the luminescence of the addition of the following metals: Fe, Cu, Ni, Pb, Cd, Sb, Sn, Mg, Be, Al, Ga, and In. In doing so we used the method of diffusion of the impurities into the phosphor from the solid phase. To do this a piece of the metal was pressed into each of the sections of the boat containing ZnO which had a green luminescence and was then heated for 40 minutes in an oxygen stream. For powders heated above certain specific temperatures changes in the luminescence were noted for each metal in those parts of the sample immediately adjoining the metal. Some of the metals we investigated (Fe, Cu, Ni) quenched the ZnO luminescence.* In the cases of Cd and Mg a distinct intensification of the yellow band was observed; moreover, an aureole of bright yellow luminescence had already developed after baking at 650°C. An intensification of the yellow luminescence also occurred under the action of the trivalent metals, Al, Ga, and In. In this case the aureole of yellow luminescence developed around the metal only at a temperature ≃900°C. The fact that the luminescence spectra of the samples subjected to the action of the different metals were the same and identical to the luminescence spectrum of an uncontaminated sample of zinc oxide shows that it is impossible to connect the yellow luminescence band with the specific action of any particular metal. It must be assumed that it is characteristic of the sample of pure zinc oxide itself. A sample of very pure zinc oxide was prepared to check this assumption. ZnO powder was obtained by burning the purest zinc in an oxygen stream. The zinc was purified by means of five distillations in a vacuum, the middle fraction being selected each time. The results of a spectral analysis of this sample are shown in Table 3.

*The quenching action of these and some other metals was observed by Konovalov.[3]

Table 3

Impurity	Concentration (%)	Remarks
Cu	2.5×10^{-6}	The analysis was performed at the State Institute of the Nickel Industry.
Pb	$< 1.2 \times 10^{-6}$	
Ni	$< 1 \times 10^{-6}$	
Al	3×10^{-6}	
Mn	$< 2 \times 10^{-6}$	
Cd	$< 2 \times 10^{-5}$	

After being baked in an oxygen stream, the ZnO powder obtained from the extra pure zinc displayed a bright yellow luminescence. It was decided to subject a sam ple of this kind of zinc oxide to additional purificatio from cadmium (an impurity that is carried along wit the zinc and is difficult to separate from it). Since th difference in the vapor tensions of CdO and ZnO is ve large at high temperatures, distilling off the CdO fro the zinc oxide is an extremely effective purification technique. Hence we utilized this method. The ZnO powder was baked in an argon atmosphere at 1100°C. During the baking, a thin layer of ZnO sublimate enriched with cadmium collected on the walls of the qua tube. After cooling, the ZnO powder had a bright gre luminescence. Following a baking in oxygen the colo the luminescence became yellow once more. Many re titions of this purification method did not lead to ever the most insignificant reduction in the intensity of th yellow luminescence of the sample under considerati

Our observations in aggregate make it possible t draw the conclusion that the yellow luminescence is n associated with the activating action of any metal but is inherent in the purest zinc oxide.

In several references in the literature[7-9] it has b maintained that excess oxygen is responsible for the low luminescence of ZnO. Our experiments indicate yellow luminescence centers are not created in zinc oxide as a result of baking in the absence of oxygen, with or without impurities, and in a temperature rang of treatment from 500 to 1200°C; that is, the presenc of oxygen is essential for their formation. However, also follows from our experiments that even in the p ence of oxygen it is necessary to bake at a temperatu no less than 700°C for yellow luminescence centers t form. Even heating for 20 hours at 600°C does not g a corresponding effect, whereas a 40 minute baking a a temperature of about 800°C leads to the appearanc yellow luminescence (Fig. 2). This make it possible draw the conclusion that the presence of a specific d fect structure in the ZnO is apparently essential for appearance of the centers.

The formation of structural defects can occur in nection with an over-all increase in the number of di locations in the lattice after high temperature baking can also be a consequence of a polymorphic transfor tion. It has been stated in the literature[1,10] that the y low band is associated with a high temperature modi tion of zinc oxide. There is a large amount of indire evidence that significant changes in the ZnO lattice t place in the interval 700-800°C. Ewles[11] detected an abrupt change in the density and internal conductivity ZnO at a temperature of 700°C, which he connected the transformation of the ZnO to another modificatio The abrupt change in conductivity near a temperatur 700°C has also been noted in a number of other pape The emergence of the yellow luminescence that we o served (Fig. 2) begins in exactly this temperature in val.

All these facts made the hypothesis of a connect of the yellow luminescence with a high temperature fication of ZnO sufficiently plausible. However, info tion about the presence of two modifications in ZnO contradictory. Some of the sources—refs. 14 and 15 indicated the presence of two modifications, and othe refs. 16 and 18—only one. An x-ray study of ZnO sa ples baked up to 1300°C did not reveal changes in th type of structure.[19,20] In spite of this, it seems to us one should not consider the question of the presence a second modification in zinc oxide as being solved the x-ray studies in the references indicated were c

ed on cooled samples. Although the lattice as a e transforms to a stable modification at room tem- ture, it is not ruled out that defects which are lumi- ence centers stabilize a small region of the high erature modification around themselves. These oregions can create the conditions in the phosphor he appearance of the yellow luminescence band, but ot be detected by the x-ray method because of their ll concentration.

In order to solve the question of the presence of a temperature modification in ZnO we obtained Debye ler patterns of ZnO at room temperature and at C. No new lines indicating the emergence of another cture were detected in the Debye powder pattern cor- onding to a temperature of 900°C. This allows one sume that the changes which took place in the ZnO ce in the 700-800°C region were not connected with ymorphic transformation. It is probable that a ening of the lattice occurs in this temperature in- al accompanied by an abrupt increase in the degree dislocation, the temperature of the loosening (T_1) approximately 0.5 $T_{melt.}$ (in °K). In the case of $T_1 \simeq 850$°C. The green and yellow luminescence s emerge in ZnO immediately after it is baked close is temperature (Fig. 1 and Fig. 2).

The results of our experiments described below are stent with the concept that the presence of struc- defects is necessary for the appearance of yellow nescence in ZnO. Drops of acids (HNO_3, H_2SO_4, HCl, thers)* were applied to ZnO powder having green

bly distilled, chemically pure acids were used.

nescence. The portions of the powder moistened by cid developed a bright yellow luminescence after g in air.* Apparently the corresponding salt was

y in the case of oxygen-containing acids does baking inert atmosphere lead to the emergence of yellow nescence.

ed by interaction with the acid, and as a result of rocesses of dissociation and oxidation was trans- ed to the zinc oxide with loosened defective struc-

The intensifying effect, described above, of certain ls (Cd, Mg, Al, Ga, In) on the yellow luminescence nO can also be understood from this point of view. fact that the different metals give rise to lumines- e that is the same with regard to spectrum and is ical to the luminescence of the pure oxide makes it ible to surmise that the role of these metals was to to the formation of a specific type of defects which also develop in pure zinc oxide under known condi-

Thermal de-excitation data (Fig. 3) on ZnO samples d in a stream of oxygen at different temperatures ated that for the same samples that develop yellow nescence there also appears a new peak in the ther- de-excitation curve (compare Fig. 2 and Fig. 3). In ral the samples with yellow luminescence have in- ntly higher de-excitation light sum values. These rvations also give evidence in favor of the argument samples with yellow luminescence have more in- ic structural defects.

It is evident that a number of the hypotheses enumer- above on the nature of ZnO yellow luminescence cen-

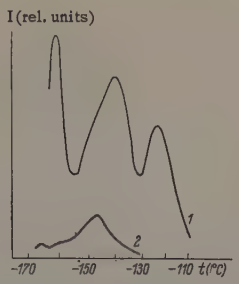

Fig. 3. Thermal de-excitation curves of samples baked for 40 minutes in a stream of oxygen. Baking temperature (°C): curve 1—815; curve 2—730.

ters should be rejected and the point of view should be maintained that an excess of oxygen and some kind of structural defects are essential for development of yellow luminescence. It is possible that defects enter into the composition of the luminescence center but it is not ruled out that their role amounts to providing the possibility for oxygen to diffuse in the crystal.

REFERENCES

1. K. V. Shalimova, Doctoral dissertation, Institute of Physics, Academy of Sciences of the USSR, Moscow, 1952.
2. N. Riehl and H. Ortmann, Z. Elektrochem. **60**, 149 (1956).
3. G. A. Konovalov, Trudy Siberia Fiz.-Tekh. Inst. **32**, 34 (1953).
4. R. N. Miller, "Semiconducting Materials." Izd. Inostrannaya Lit., Moscow, 1954.
5. G. C. Schmidt, Ann. Physik **13**, 622 (1904).
6. I. T. Randall, Trans. Faraday Soc. **35**, 2 (1939).
7. V. V. Osiko, Opt. i Spektr. **7**, 770 (1959), Optics and Spectroscopy **7**, 454 (1959).
8. F. A. Kröger and H. I. Vink, J. Chem. Phys. **22**, 250 (1954).
9. L. N. Shekhter, I. A. Myasnikov, and S. Ya. Pshezhetskii, Proc. Fifth Conf. on Luminescence, Tartu, 1957, p. 125.
10. I. Tafel, Ann. Physik **14**, 206 (1904).
11. I. Ewles, Phil. Mag. **45**, 957 (1923).
12. F. I. Vergunas, Trudy Siberia Fiz.-Tekh. Inst. **24**, 184 (1947).
13. W. Iander and W. Stamm, Z. anorg. u. allgem. Chem. **199**, 165 (1931).
14. A. F. Wells, "Structural Inorganic Chemistry." Clarenden Press, Oxford, 1945.
15. G. B. Bokii, "Introduction to Crystal Chemistry." Izd. Moskov. Gosudarst. Univ., 1954.
16. B. F. Ormont, N. A. Goryunova, I. N. Ageeva, and N. N. Fedorova, Izvest. Akad. Nauk SSSR, Ser. Fiz. **21**, 133 (1957).
17. "Strukturberichte." Leipzig, 1941.
18. R. W. G. Wyckoff, "The Structure of Crystals." Chemical Catalog Co., New York, 1935.
19. A. B. Shekhter and Yu. M. Moshkovskii, Doklady Akad. Nauk SSSR **72**, 339 (1950).
20. P. A. Ivannikov, A. V. Frost, and M. I. Shapiro, Doklady Akad. Nauk SSSR **1**, 124 (1933).

INTERFERENCE OF LUMINESCENT EMISSION FROM AN EVAPORATED PHOSPHOR

N. A. Vlasenko, V. K. Miloslavskii, and I. N. Shklyarevskii (pp. 403-409)

Received 18 October 1960

The interference of luminescent emission from a thin layer of evaporated ZnS:Mn phosphor excited by monochromatic ultraviolet radiation is investigated. An explanation is given of the experimentally observed peculiarities of this effect which distinguish it from the usual interference arising in the same nonexcited evaporated phosphor illuminated by an external source of light. The interference pattern of the luminescent emission is calculated on the assumption that there exists no coherence between the elementary radiators.

Luminescent sources have been used in interference experiments[1,2] to prove that the individual particles of the substance emit coherent light with an opening angle practically equal to 180°. As far as we know, no one has yet considered the interference of luminescent emission in the case when the radiators themselves fill a resonant cavity with a thickness of the order of a few wavelengths. Yet due to the special position of the light sources, such an interference is far from trivial.

In this paper we describe the results of an investigation of this type of interference.

EXPERIMENTAL INVESTIGATIONS

The interference of luminescence light was observed on thin wedge-shaped layers of the evaporated ZnS:Mn phosphor prepared by a method described earlier.[3] Such layers are highly transparent and homogeneous. When the evaporated phosphor is excited by light at $\lambda = 365$ mμ, it gives rise to a characteristic luminescence which is nonuniform in intensity and color. Both the intensity and the color depend on layer thickness. When the latter is increased, the color at the luminescence maxima varies within the wavelength limits of 520-650 mμ, which correspond to the boundaries of the emission band of the ZnS:Mn phosphor with a maximum at 590 mμ.

The interference picture arising at the front side of the sample is similar in all details (apart from a certain difference in intensity) to the interference picture observed on the side of the base. It differs sharply, however, from the usual interference picture observed for the same though unexcited phosphor traversed by light of the same spectral composition (luminescence of an identical evaporated phosphor). This difference consists in the following: (1) The visibility of the interference being investigated is much higher than the visiliby of the usual interference. (2) Within the range of low orders of interference in the alternation of color with increasing layer thickness occurs in an unusual fashion in the case considered: light green coloring is followed by yellow, red, and then again yellow. For higher interference orders (up to the 8-10th), this sequence of colors is maintained, though their relative intensities and hues are changed somewhat. Thus for the yellow portion of the spectrum two maxima and two minima are observed within one interference order. Let us note that we could not find any polarization effects when we observed these interference lines through a Nicol prism.

The lines of equal chromatic order obtained on the luminescent sample excited by monochromatic ultraviolet radiation are also unusual in appearance. In photographing the lines of equal chromatic order we used simplified arrangement described in detail in ref. 5, distinct from the arrangement used by Tolanskii.[4] T luminescent wedge-shaped sample was pressed clos the slit of an ISP-28 spectrograph with the edge of th wedge perpendicular to the slit. The sample was illu nated by a parallel beam (incident at a small angle) the exciting light with $\lambda = 365$ mμ obtained by means a filter from the radiation of a PRK-2 mercury lamp

Figure 1a shows the interference pattern thus o tained for one of the samples, while for the sake of c parison we show in Fig. 1b the interference pattern the same sample illuminated by white light. Since th reflection coefficients of the sample surfaces are re tively low, the interference lines are washed out. A parison of these interference patterns shows that, in first case, in addition to the inclined system of lines which coincides in position and number of lines with system shown in Fig. 1b, a second system of weaker horizontal lines is clearly noticeable. There are twi as many horizontal as inclined lines per unit length the wedge. The inclined lines are not continuous but sist of several segments which have the appearance having been torn at the minima by the horizontal sys of lines. They are broadened in the portions where t intersect with the horizontal lines, then gradually na and weaken in the center of the intervals between th horizontal lines. They give the impression that each the inclined lines consists of several steps displace relative to each other.

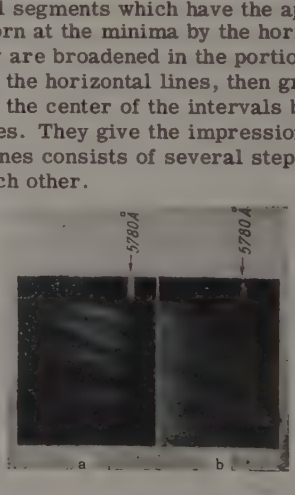

Fig. 1

A comparison of the intensities of neighboring ima and minima of both interference pictures at a fi wavelength shows that the visibility of lines of equal chromatic order (just as of lines of equal width) is higher in the first case than in the second.

When the same evaporated phosphor is excited electron beam or by nonmonochromatic ultraviolet ation (iron arc and Wood's filter), the interference

continuous, and the system of horizontal lines is ab-
t. This shows that the unusual appearance of the in-
ference pattern which we described is connected with
monochromaticity of the exciting light. Interference
nonochromatic exciting light can results in an in-
nogeneous intensity distribution of the exciting radia-
n inside the layer. This creates an inhomogeneity in
luminescence light.

Figure 2 is evidence of the effect of the interference
ultraviolet radiation on the intensity distribution of the
inescence. Figure 2a shows a photograph of lines of
al width in reflected light (λ = 365 mμ), while Fig. 2b
ws a photograph of the interference picture of the
inescent emission from the same sample. There are
nterference maxima between the light vertical refer-
e lines in Fig. 2a. In Fig. 2b there are between the
ne reference lines (shown here dark) 4 principal
xima and between them 4 weaker maxima. This is
interference picture described at the beginning of the
cle.

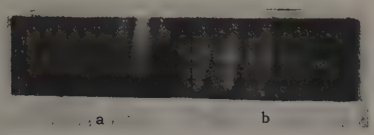

Fig. 2

The external appearance of the interference picture
ends very strongly on the angle α at which the exciting
t falls on the sample. (See Fig. 3.) The change in the
rference picture may be connected with a displace-
nt of the interference lines of the exciting light.

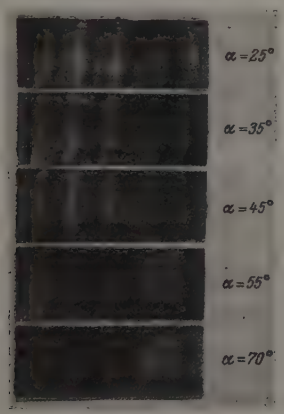

Fig. 3

A similar dependence may be observed if the angle
ncidence of the exciting light on the sample is kept
d while the angle of observation is varied. If inter-
ence is observed from the side of the base while the
t side of the sample is silvered, there is a marked
rpening of the interference lines.

EORETICAL CALCULATION

Let us perform a theoretical calculation to explain
complex nature of the observed interference phe-
enon. Even when the phosphor is excited uniformly,
interference formulas for luminescent emission
uld differ from the usual ones due to the special lo-
on of the light sources.

Let us consider a plane parallel phosphor area of thickness t bounded by two transparent media I and II. (See Fig. 4.) Let us denote by r_1 and r_2, respectively, the amplitudes of the reflection coefficients at these boundaries. Consider in particular one of the elementary radiators O located at a distance x from medium I. We shall consider only the rays which are perpendicular to the phosphor boundary.* Assuming that the elementary

*Since the index of refraction μ of zinc sulfide is large, in the case of a small exit pupil, rays incident on the boundary with angles differing from $\varphi = 0$ will not reach the eye of the observer.

radiator (classical dipole) emits coherent light with an opening angle[1,2] of 180°, we obtain the system of rays which is shown schematically in Fig. 4. Let us assume finally that the light emitted by different elementary radiators is mutually incoherent.

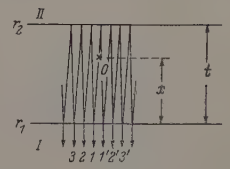

Fig. 4

It is easily seen that the total amplitude of radiation entering medium I is

$$A_x = a_0\sqrt{1-r_1^2}\left(e^{i\delta x} + r_2 e^{i(\delta-\delta x)}\right)\sum_{n=1}^{\infty}(r_1r_2)^{n-1}e^{i(n-1)\delta}, \qquad (1)$$

where a_0 is the amplitude of the light emitted by an elementary radiator,

$$\delta = \frac{4\pi\mu t}{\lambda} \text{ and } \delta_x = \frac{2\pi\mu x}{\lambda}.$$

The intensity of this radiation is determined by the usual formula

$$I_x = A_x A_x^* = \frac{a_0^2(1-r_1^2)\left[1+r_2^2+2r_2\cos(\delta-2\delta_x)\right]}{1-2r_1r_2\cos\delta+(r_1r_2)^2}. \qquad (2)$$

To find the total intensity of the light emitted from a given point of the phosphor, we must sum the intensities of all the elementary radiators located on a segment of length t. Since the number of luminescence centers is large, the summation may be replaced by an integration

$$I = Ns\int_0^t I_x dx = \frac{At(1-r_1^2)}{1-2r_1r_2\cos\delta+(r_1r_2)^2}\left[1+r_2^2+2r_2\frac{\sin\delta}{\delta}\right], \qquad (3)$$

where N is the density of elementary radiators, s is the beam cross section, and $A = Ns\overline{a_0^2}$. Equation (3) expresses the luminescence light as a function of the emitted wavelength and of the thickness of the phosphor assuming that it is excited uniformly. The total intensity is proportional to phosphor thickness and also differs from the usual case by the factor in the square brackets.

Since the intensity of luminescence light at a given point O in the phosphor is proportional to the energy density of the exciting light, which in our case is a function of phosphor thickness, we must take that circumstance into account. Let the exciting light fall normally on the sample from the side of medium II and then, after reflection from boundary I, experience multiple reflections. Two systems of waves going in opposite directions will pass through the point O. Their total amplitude at the point O will be

$$A'_x = \alpha_0 \sqrt{1-\rho_2^2}\left[e^{i\left(\frac{\Delta}{2}-\Delta x\right)}e^{-\frac{K}{2}(t-x)} + \rho_1 e^{i\left(\frac{\Delta}{2}+\Delta_x\right)}e^{-\frac{K}{2}(t+x)}\right]\times$$

$$\times\sum_{n=1}^{\infty}(\rho_1\rho_2)^{n-1}e^{i(n-1)\delta}e^{-(n-1)Kt}, \qquad (4)$$

where α_0 is the amplitude of the exciting light, ρ_1 and ρ_2 are the amplitude coefficients of reflection, $\Delta = 4\pi\mu_0 t/\lambda_0$, $\Delta_x = 2\pi\mu_0 x/\lambda_0$, μ_0 is the index of refraction of zinc sulfide for $\lambda_0 = 365$ mμ, and K is the energy coefficient of absorption by the evaporated ZnS:Mn phosphor for the same wavelength. Due to the smallness of the index of absorption $\mu\chi = K\lambda/4\pi$, we ignore the phase shifts at the boundaries.

From Eq. (4) we obtain as the energy density W_x of the exciting light at the point O

$$W_x = B\frac{(1-\rho_2^2)\left(e^{-K(t-x)}+\rho_1^2e^{-K(t+x)}+2\rho_1e^{-Kt}\cos 2\Delta_x\right)}{1-2\rho_1\rho_2e^{-Kt}\cos\Delta+(\rho_1\rho_2)^2e^{-2Kt}}, \qquad (5)$$

where B is a constant.

The intensity of luminescence of an elementary radiator is proportional to the product of Eqs. (2) and (5). To find the total intensity this product must be integrated from 0 to t. Ignoring the terms that contribute little to the radiation intensity, we obtain the following expression

$$I = C(\lambda)\frac{(1-r_1^2)(1+r_2^2)(1-\rho_2^2)\left[1-(1-\rho_1^2)e^{-Kt}-\rho_1^2e^{-2Kt}\right]}{K\left[1-2r_1r_2\cos\delta+(r_1r_2)^2\right]\left[1-2\rho_1\rho_2e^{-Kt}\cos\Delta+(\rho_1\rho_2)^2e^{-2Kt}\right]}, \qquad (6)$$

where $C(\lambda)$ is a coefficient of proportionality which depends on the shape of the emission bands.

Equation (6) represents the intensity of luminescence as a function of the wavelength and the thickness of the evaporated phosphor which was excited nonuniformly due to interference of the exciting light.

DISCUSSION OF RESULTS

We deduce from our investigations and calculations that the interference picture of the luminescent emission is a complex combination of two interference phenomena.

We can construct the experimental dependence of the intensity on phosphor thickness by the following procedure: We microphotometer the interference diagram of Fig. 1a for some fixed wavelength and translate the darkening in terms of intensity. The result is represented in Fig. 5, curve 1, and consists of a series of maxima and minima of different height and depth, respectively. An analogous dependence for the same wavelength of the luminescent light may be constructed using ratio (6) (Fig. 5, curve 2). This comparison was carried out for $\lambda = 590$ mμ. In the calculation we used the following numerical values for the quantities appearing in Eq. (6): $\mu = 2.32$, $\mu_0 = 2.65$, $r_1 = 0.4$, $r_2 = 0.21$; $\rho_1 = 0.45$, $\rho_2 = 0.26$, and $K = 5\times10^3$ cm^{-1}. To eliminate $C(\lambda)$ from Eq. (6), the calculated curve was made to coincide with the experimental one at the point $t = 445$ mμ.

The agreement between the theoretical and experimental curves must be considered good if we take into account the fact that in the actual evaporated phosphor the distribution of luminescence centers along the sample is not completely uniform.

A similar picture of intensity distribution may be observed if Fizeau bands are photographed through a sufficiently narrow-band filter. The true picture (Fig. 2b) is close to that described, since the latter is calculated for the wavelength of the maximum of the phosphor

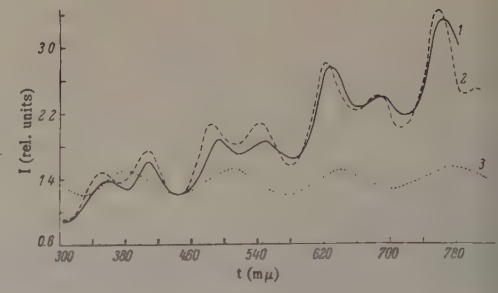

Fig. 5

emission band.

Curve 3 of Fig. 5 was obtained by microphotom of the interference diagram of Fig. 1b for $\lambda = 590$ m A comparison of curves 1 and 3 gives a clear under of their different degree of visibility.

The complex nature of the interference pattern Fig. 1a is also easily explained. Here the horizonta lines are the lines of equal thickness of the exciting "developed" by the luminescent light. Their horizo direction shows that all wavelengths of the band emi by the phosphor are present at the point in the phos obtained by the intersection of an equal thickness li the exciting light with the spectrograph slit. Due to uniform excitation and intensity distribution in the p phor emission band, the inclined lines of equal chro order are distorted and have the appearance of brok lines.

Using Eq. (6) we can construct a "topographic" ture of the observed interference. The results of th culation performed without taking into account the i tensity distribution with wavelength of the phosphor sion band are shown in Fig. 6a, using the coordinate and λ. The solid curves represent here lines of equ intensity while the straight horizontal lines are line maximum phosphor excitation whose position is det mined by the interference condition $2\mu_0 t = k\lambda_0$. The clined straight line is the line of the maximum of th band of equal chromatic order which would have occ under uniform phosphor excitation. It satisfies the dition $2\mu t = m\lambda$.

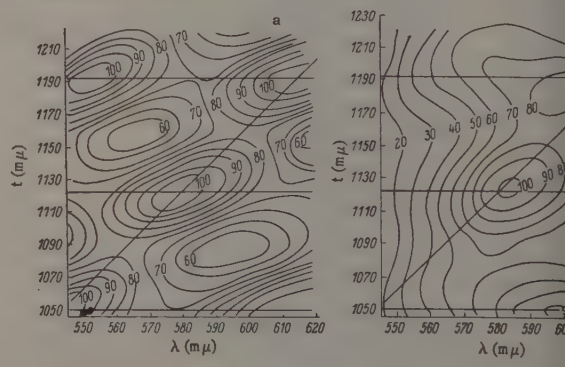

Fig. 6

The interference maxima appear at the interse points of two systems of lines corresponding to both ima. Thus the highest intensity areas appear as spo arranged in checkerboard fashion, which gives to th terference lines the appearance of stepwise curves.

In an actual case the picture described is disto by the spectral distribution of intensity in the phos

ssion band. Figure 6b shows the interference pic- obtained taking into account the emission spectrum e ZnS:Mn phosphor. Here the intensity maxima are laced relative to the points of intersection of the systems mentioned above.

Thus the appearance of the interference picture in 1a is fully explained by nonuniform phosphor excita- and by the intensity distribution in its emission band. As stated above, Eq. (3) differs from the usual Airy nula by the factor contained in the square brackets. variable term $2r_2 \sin\delta/\delta$ of this factor contributes e at large phosphor thicknesses. It is important, ever, at small thicknesses, since it is the reason the intensity distribution in the first interference r will differ from that, say, in the tenth. Unfortu- ly, however, we have been unable to carry out an rimental verification, due to the low luminescence nsity of a thin phosphor layer.

Let us consider the problem of coherence of the nescent emission. In deriving Eqs. (1)-(6) we as- ed that the light emitted by different elementary ators was incoherent even though the spacing be- n them is small compared with the wavelength while ifetime of excited Mn ions is of the order of 10^{-3} If we assumed that due to resonance interaction he sources located on the segment t emitted coherent , we would have to integrate Eq. (1) first and then ider the intensity. As a result the final formula d be of a different form. However, the ratio (6) es well with experiment. Hence the light emitted by ifferent radiators cannot be considered coherent.

At the same time we may not assert that individual ps of radiators situated close together cannot emit coherent light. If this takes place, Eq. (1) should be ascribed not to an individual radiator but to such a group of radiators which will not change the appearance of the formulas derived. Unfortunately it does not appear possible to carry out an experimental verification of this assertion. We succeeded in showing experimentally that light emitted by different phosphor areas is not coherent. The interference pattern in the Rayleigh arrangement disappeared as soon as the luminescent phosphor was placed behind the double slit.

The special conditions in which are found the elementary radiators enclosed in a resonating cavity were pointed out to us several years ago in private conversation by academician K. D. Sinel'nikov of the Academy of Sciences of the Uzbek SSR. The authors take this opportunity to express their deep appreciation to K. D. Sinel'nikov for the discussion and for his interest in this work.

REFERENCES

1. P. Selenyi, Ann. Physik 35, 444 (1911).
2. S. I. Vavilov, "Collected Works," vol. 1, p. 368. Izd. Akad. Nauk SSSR, Moscow, 1954.
3. N. A. Vlasenko, Proc. Seventh Conf. on Luminescence, Tartu, 1959, p. 365.
4. S. Tolanskii, Uspekhi Fiz. Nauk 30, 103 (1946).
5. I. N. Shklyarevskii, V. K. Miloslavskii, O. S. Pakhomova, and A. N. Ryazanov, Uchenye Zapiski Khar'kovsk. Univ., Trudy Fiz. Otdel. 6, 147 (1955).
6. V. L. Levshin, "Photoluminescence of Liquid and Solid Substances." Gosudarst. Izd. Tekh.-Teoret. Lit., Moscow-Leningrad, 1951.

TUDY OF THE EMISSIVE POWER OF CERTAIN HIGH-MELTING COMPOUNDS IN THE INFRARED REGION

G. V. Samsonov and V. V. Pen'kovskii (pp. 410-414)

Received 30 September 1960

It is shown that, in the region from 4 to 14 μ, the intensity of the radiation from a Globar and from silicon carbide-molybdenum silicide and silicon carbide-silicon nitride-molybdenum silicide composites is the same. The position of the maxima in the emission spectrum of silicon carbide does not change on addition of molybdenum silicide (3-14 mole %), but the addition of 6 mole % silicon nitride to silicon carbide leads to a shift of the maxima toward shorter wavelengths.

Compounds with a high melting point, in particular ous silicides, find diverse industrial application.[1] At ame time, the physical properties of compounds of class, regardless of the considerable quantity of rele- works, have been far from fully studied. One of the t studied properties is the emissive power in the in- ed region of the spectrum. Only high-melting oxides[2-4] silicon carbide[5,6] have been fully investigated in this ect. However, emission spectra of the latter have obtained only in the relatively low-temperature re- (700-1100°C), while data on the emission of silicon ide (or various composites based on it) at higher eratures are of great interest in both the practical the theoretical respect.

In the present work, a study is made of the emissive power of high-melting composites based on silicon carbide at higher temperatures (up to and including 1500°C).

For our study, we chose silicon carbide-molybdenum silicide and silicon carbide-silicon nitride-molybdenum silicide composites, which, as we have established, are stable against oxidation on heating to 1400-1500°C in air.

Mixtures were prepared in the following ratios from silicon carbide and molybdenum silicide: 85% SiC-15% $MoSi_2$, 80% SiC-20% $MoSi_2$, 60% SiC-40% $MoSi_2$. For the preparation of the ternary composites, silicon carbide, molybdenum silicide, and silicon were mixed, the quantity of the latter corresponding to the calculated quantity of Si_3N according to the reaction

$$3Si + 2N_2 = Si_3N_4.$$

All the starting materials were used in powder form. The diameter of the particles of silicon and molybdenum silicide amounted to less than 53 μ, of silicon carbide to less than 10 μ. After mixing, the preparation of the rod-shaped samples (diameter 5-6 and length 80-100 mm) was carried out in the following way. To 100 gm of mixture was added 52 gm of a 35% alcoholic solution of bakelite (in the case of mixtures containing silicon, 25 gm of a 45% solution was required). The resulting mass was ground to a damp condition, charged into a special mole,[7] and extruded through an opening with a diameter of 5-6 mm under a pressure of 1-2 metric tons/cm². The raw blanks were dried 8-12 hr in air, then 2-3 hr in a drying cabinet at 150° C, and were sintered in a furnace, after preliminary treatment in it for 30-40 min at 500°C to remove the decomposition products of the bakelite.

The sintering of the silicon carbide-molybdenum silicide composites was carried out in a hydrogen atmosphere; to obtain the silicon carbide-silicon nitride-molybdenum silicide composites, the raw blanks were sintered in a nitrogen atmosphere. The free silicon was thereby converted to Si_3N_4. The sintering schedules and the composition of all the composites are presented in Table 1. The porosity of the samples after sintering amounted to 30-35%. It was established by chemical analysis that the silicon carbide-molybdenum silicide composites after sintering have a composition very close to the composition as blended. In addition, they contain up to 7 wt % free carbon. The silicon nitride content of the ternary combinations is considerably lower than the calculated figure, apparently because of marked carbide formation at 1600°C (this is confirmed by the relatively low content of free carbon, or its absence, in these samples).

Table 1. Sintering Schedules and Composition of High-Melting Composites Based on Silicon Carbide

Composite	Temperature (°C)	Time (min)	Composition (%)			
			SiC	Si_3N_4	C_{free}	$MoSi_2$
85% SiC—15% $MoSi_2$	2180	15	83.0	—	2.08	14.73
80% SiC—20% $MoSi_2$	2160	15	74.0	—	7.20	18.74
60% SiC—40% $MoSi_2$	2100	15	57.0	—	2.45	40.56
SiC — Si_3N_4—$MoSi_2$(A)	1600	90	63.0	12.25	1.50	22.70
SiC — Si_3N_4—$MoSi_2$(B)	1600	90	71.0	12.55	0	16.95

After sintering, terminals were mounted on the ends of the samples. For this purpose, tubes with an external diameter of 10 mm and an internal diameter of 7 mm were pressed from molybdenum silicide (according to the method described in ref. 7) and cut into pieces 10-15 mm in length. The sintered rod was inserted into the cut section and molybdenum silicide powder was loaded in, after which the section was sealed up at both ends with a mixture of molybdenum silicide and bakelite lacquer. After drying at 150°C, the samples were sintered in a hydrogen atmosphere at 1600° for 20 min in a furnace provided with a tubular graphite heater.

The finished samples were subjected to testing for stability against oxidation at high temperatures. The heating was accomplished by a 220 volt ac circuit through an autotransformer; the temperature was checked by an optical pyrometer, type OPPIR-09. The electrical resistance of the sample at first increases on heating (probably on account of the burning out of the free carbon), but it becomes stable after being held at 1400°C for 3 hr. The operating conditions of all the composites investigated are presented in Table 2.

Table 2. Heating Conditions of Emitters Made from Composites Based on Silicon Carbide

Composite	Temperature (°C)			
	1400		1500	
	Current (amp)	Voltage	Current (amp)	Voltage
85% SiC + 15% $MoSi_2$	4.0—4.1	110—112	4.5	120
80% SiC + 20% $MoSi_2$	4.0	120—122	4.2	133—135
SiC + Si_3N_4 + $MoSi_2$(A)	7.1	78—80	7.3	85—86
SiC + Si_3N_4 + $MoSi_2$(B)	3.85	120—122	4.5	130—232

Samples made from a silicon carbide-molybdenum silicide composite withstand heating to 1500°C for 8 h (we did not conduct more prolonged tests). At a temperature of 1400°C, the same samples did not break down in the course of 25 hr, and this period does not appear to be the limit. Silicon carbide-silicon nitride-molybdenum silicide composites withstood heating to 1500°C for 6 hr without breakdown (again we did not conduct more prolonged tests), but when the temperature is raised above 1600-1650°C the sample cracks. The temperature distribution along the length of the samples was very uniform in all cases. It was necessary to cool the sample terminals with water.

The emission spectra of the silicon carbide-molybdenum silicide composites were obtained by means of an infrared automatic recording spectrometer, type VIKS, constructed in the Institute of Physics, USSR Academy of Sciences. The spectra were studied over the range 4-15 μ (with a rock-salt prism), the spectrometer slit being opened automatically. The recording time for each emission spectrum amounted to 17 min.

In Fig. 1 are presented the emission spectra of a Globar* and of composites containing respectively 15 and 40 wt % (4.5 and 15 atom %) of $MoSi_2$ at 1300° and 1500°. Since the radiation of the samples was not compared with black-body radiation, the ordinates in Fig. 1 represent radiation intensity expressed in arbitrary units. The ordinate values correspond to their height in mm measured with a precision of 1 mm on the recorded spectrogram for each of the samples.

*Ready-made Globars on hand in the laboratories of the Institute of Physics, USSR Academy of Sciences, and of Rostov University were used for the emission measurements.

The emission spectra of the ternary silicon carbide-silicon nitride-molybdenum silicide composites were obtained on a type IKS-6 spectrometer. As in the preceding case, the working wavelength interval lay within the limits 4-15 μ, and the spectrometer slit was again opened automatically. In order to exclude the scattered light fraction from the total intensity, a fraction which is very significant at short wavelengths, two readings were taken for each division of the drum—one with a lithium fluoride filter (which transmits only the scattered light) and one without it. The signal intensity was determined from the scale displacement of the spot of a mirror galvanometer measured with a precision of 1 mm.

In Fig. 2 are presented the emission spectra of a Globar and of the two silicon carbide-silicon nitride-molybdenum silicide composites at temperatures of 1300°, 1400°, and 1500°C. The radiation intensity is expressed in arbitrary units corresponding to the spot displacement values (in mm).

From comparison of the emission spectra of the Globar and the silicon carbide-molybdenum silicide composites, and also of the Globar and the ternary silicon carbide-silicon nitride-molybdenum silicide com

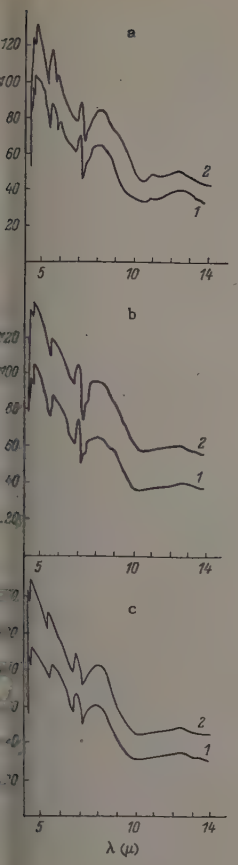

Fig. 1

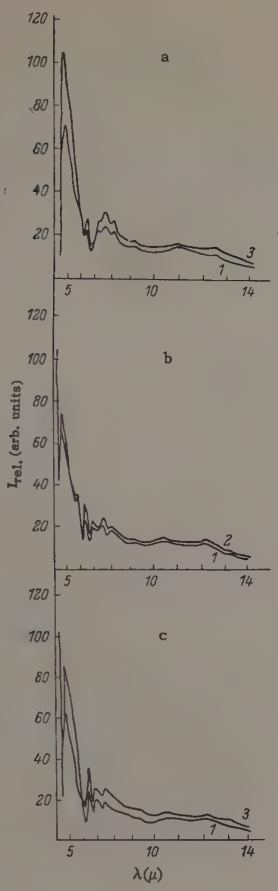

Fig. 2

Fig. 1. Emission spectra of a Globar and of SiC-$MoSi_2$ composites at temperatures of 1300°C (curves 1) and 1500°C (curves 2). Source: a—Globar; b—85% SiC-15% $MoSi_2$; c—60% SiC-40% $MoSi_2$.

Fig. 2. Emission spectra of a Globar and of SiC-Si_3N_4 composites at temperatures of 1300°C (curves 1), 1400°C (curves 2), and 1500°C (curves 3). Source: a—Globar; b—SiC-Si_3N_4-$MoSi_2$ (A); c—SiC-Si_3N_4-$MoSi_2$ (B).

tes, it follows that the radiation intensity is prac-lly the same in all cases. The maxima on the emis-. curves of the Globar correspond to the absorption ima of silicon carbide.[8] We note that the maximum = 4.5 μ is not a characteristic maximum of silicon oide, but is produced by the presence of the added stances, since the energy corresponding to it corre-nds to the 1s state of the impurity level.[9] The indis-tness of the maximum at λ = 12.6 μ, which corre-nds to the fundamental vibration frequency of the Si—C d, is explained by the considerable inexactness in the surement of radiation intensity in this region.

The positions of the maxima on the emission curves ne Globar and the silicon carbide-molybdenum silicide positions coincide completely at all temperatures. s the addition of molybdenum silicide in a quantity up 5 atom % does not show any influence on the emission ilicon carbide in the infrared region. This may be ex-ned by the fact that molybdenum silicide is a metal-like compounds, in which the ionic bond character is extremely small. Therefore, the characteristic radiation of molybdenum silicide in the infrared region is very slight (it is found principally in the visible region of the spectrum).

A more peculiar picture is observed in the case of the ternary silicon carbide-silicon nitride-molybdenum silicide composite. As can be seen from Table 3, the emission maxima in this case are somewhat shifted in comparison with the Globar spectrum. Since the effect of the added molybdenum silicide may be neglected in this region, this shift can be brought about only by the presence of silicon nitride. This consideration is confirmed by the fact that the same values of the shift are observed for both compositions (A and B), in which the silicon nitride content is the same (Table 1).

Table 3. Position of the Maxima in the Emission Spectra of Silicon Carbide and the Ternary Silicon Carbide-Silicon Nitride-Molybdenum Silicide Composite

Temperature (°C)	Material	Wavelength (μ)						
1300	SiC	6.45	7.1	7.6	8.0	9.15	10.8	12.5
	SiC—Si_3N_4—$MoSi_2$ (A)	6.45	6.9	7.5	7.9	9.3	10.5	12.1
	SiC—Si_3N_4—$MoSi_2$ (B)	6.45	6.9	7.5	—	9.3	10.5	12.2
1400	SiC	6.45	7.1	7.6	8.0	9.15	10.8	12.6
	SiC—Si_3N_4—$MoSi_2$ (A)	6.45	6.9	7.5	7.9	9.3	10.5	12.1
	SiC—Si_3N_4—$MoSi_2$ (B)	6.45	6.9	7.5	—	9.3	10.6	12.2
1450	SiC	6.45	7.2	7.6	8.0	9.15	10.8	12.6
	SiC—Si_3N_4—$MoSi_2$ (B)	6.45	6.9	7.5	—	9.3	10.5	12.2
1500	SiC	6.45	7.1	7.6	8.0	9.15	10.8	12.6
	SiC—Si_3N_4—$MoSi_2$ (B)	6.45	6.9	7.5	—	9.3	10.5	12.1

On addition of silicon nitride, all the maxima in the silicon carbide emission spectrum are displaced toward shorter wavelengths. The maximum at λ = 9.15 μ, which shifts toward longer wavelengths, and the one at λ = 6.45 μ, whose position does not change, constitute exceptions. The former maximum, which has also been observed by other authors,[6] apparently relates not to silicon carbide, but to the SiO_2 impurity which inevitably forms on prolonged heating to high temperatures on account of the oxidation of SiC and Si_3N_4. The displacement of the maxima in the spectrum of the silicon carbide-silicon nitride composite may be explained in the following way. Silicon nitride is a compound in which the ionic bond character is significantly larger than it is in silicon carbide (the width of the forbidden band amounts to 3.91 ev for silidon nitride[10]). Therefore, at minor additions of silicon nitride (up to 6 mole %), additional asymmetry in the electron density distribution arises on account of the greater electron concentration around the carbon and nitrogen atoms. The vibrations of the interatomic Si—C bond, which originate through a dynamic change in the electron density distribution, prove therefore to be difficult in comparison with pure silicon carbide (more energy is required to establish them in consequence of which the vibration frequency must also increase). As one goes from the fundamental frequency (λ = 12.60 μ) to higher frequencies, this effect grows weaker in view of the additional dispersion of the electrons, and at some frequency it becomes equal to zero. It can be seen from Table 3 that such a reduction in the shift is actually observed—at λ = 6.45 μ, shifts of the maxima no longer take place.

The authors express their recognition to A. F. Mal'nev and A. F. Yatsenko for their help with the experiments and for providing equipment.

REFERENCES

1. G. V. Samsonov, "Silicides and Their Use in Practice." Izd. Akad. Nauk Ukrain. SSR, Kiev, 1959.
2. J. Lecomte, "Le Rayonnement Infrarouge." Gauthier-Villars, Paris, 1948. Gosudarst. Izd. Fiz.-Mat. Lit., Moscow, 1958.
3. R. A. Friedel and A. G. Sharky, Rev. Sci. Instr. **18**, 928 (1947).
4. J. Ritzow, Ann. Physik **19**, 769 (1933).
5. S. Silverman, J. Opt. Soc. Am. **38**, 989 (1948).
6. J. E. Stewart and J. C. Richmond, Science **124**, 94 (1956); J. Res. Natl. Bur. Standards **59**, 605 (1957).
7. G. V. Samsonov and P. S. Kislyi, Dopovidi Akad. Nauk Ukr.R.S.R. No. 1, 46 (1959).
8. W. J. Spitzer, D. Kleinman, and D. Walsh, Phys. Rev. **113**, 127 (1959).
9. M. Namba, J. Phys. Soc. Japan **14**, 228 (1959).
10. G. V. Samsonov and G. G. Tsebulya, Ukrain, Fiz. Zhur. **5**, 618 (1960).

HAVE YOU SENT IN YOUR SUBSCRIPTION FOR NEXT YEAR? – SEE ORDER CARD IN THIS ISSUE.

Filler Material – Not in Russian original.

ON THE MECHANISM OF THE WEAKENING OF THE CN BANDS (VIOLET SYSTEM) IN AN ARC

V. S. Rossikhin and I. L. Tsikora (pp. 415-417)

Received 13 October 1960

It has been established in a number of experimental ks[1] that, on the addition of alkaline-earth elements to rc or spark gap between carbon electrodes (dis- ge in air), the intensity of the CN bands is weakened factor of 1.5-2, sometimes even more. The weaken- f the CN bands may be considered as a consequence e influence of the "third" elements introduced into rc discharge. Therefore, the weakening may be as- ted: (1) with a change in the effective ionization po- al of the gas, which leads to a change in the tempera- of the arc column, and consequently to a change in ntensity of the bands of the CN radical; (2) with ical and chemical quenching, brought about by col- ns of the CN molecules with the particles (mole- , atoms) introduced into the arc gap; (3) with a ge in the character of the entry of atomic or molec- carbon into the arc gap (the nitrogen concentration sumed constant).

The formation of a CN radical between carbon elec- s in an arc burning in air may come about as the t of the following processes:

$$C\,[^3P] + N\,[^4S_{3/2}] \rightarrow CN\,[X^2\Sigma^+] + 8.13 \text{ ev}, \quad (1)$$

$$C_2\,[^3\Pi_u] + N_2\,[X^1\Sigma_g^+] \rightarrow 2CN\,[X^2\Sigma^+] + 0.24^1 \text{ ev}, \quad (2)$$

$$^1\Sigma] + N_2[X^1\Sigma_g^+] \rightarrow CN\,[X^2\Sigma^+] + NO\,[X^2\Pi] - 4.6 \text{ ev}. \quad (3)$$

dissociation energy of the C_2 molecule is taken n ref. 2.

The last reaction appears improbable in view of its endothermicity.

During the burning of an arc between carbon elec- es, carbon vaporizes in the form of atoms and mole- s. According to Wieneke's data,[3] the partial pressure omic carbon at an arc temperature from 4000 to °K is larger by several orders of magnitude than partial pressure of C_2. One may therefore assume , in the column of an alternating-current arc with on electrodes, burning at atmospheric pressure, formation of the CN radical comes about basically ugh the combination of carbon atoms with the nitro- of the air.

If we start with such a mechanism of CN formation, the third hypothesis which we have stated above can- serve as the cause of the CN band weakening, since equilibrium concentration of atomic carbon in the perature interval studied by us (4800-5700°K) re- ns almost constant.[3] Our investigations have shown the volatility of the electrodes when an arc burns water and aqueous salt solutions also remains un- ged. We have therefore investigated experimentally the possibility of CN band weakening on account of first two causes.

In order to elucidate the mechanism of the weakening of the bands of the CN radical, we have measured the temperature of the arc between pure carbon electrodes when distilled water, and also aqueous solutions of $MgCl_2$, KI, KBr, KCl, and KOH, were introduced into the arc gap; we have also measured the ratio of the intensity of the CN band (3883 A) when distilled water was introduced into the arc ($I_{CN(H_2O)}$) to the intensity of the same band ($I_{CN(\quad)}$) when the above-mentioned aqueous solutions were introduced.

The temperature measurement was performed by the method of unresolved CN bands, as worked out by Spier and Smit-Miessen.[3]

Solutions containing 0.21% metal were introduced into the discharge gap of a fulgurator in the form of a cup, in the center of which was set a carbon electrode. The surface of the electrode was fixed 1 mm above the surface of the solution. A carbon rod, sharpened into a truncated cone with a plane 2 mm in diameter, served as upper electrode. A DG-1 alternating-current arc generator served to excite the spectrum; the current was held constant at 3.5 amp in all the investigations. Spectrograms were taken by means of an ISP-28 spectrograph on iso-orthochromatic plates with a sensitivity of 32 standard units. The exposure for each solution was chosen in such a way that the blackening lay within the normal region. The conversion from measured blackening to intensity was accomplished by the construction of a characteristic curve for each plate.

As in quantitative spectral analysis, a diffuse image of the arc gap was projected on the spectrograph slit during the intensity and temperature measurements. Consequently, we obtained a spectral image of the arc which was averaged over its volume.

In Table 1 are presented the results of the temperature measurements according to the data of one of the plates. In Table 2 are presented the results of measurements of the intensity ratio $I_{CN(H_2O)}/I_{CN(\quad)}$ under the same conditions, and also the values calculated by us for the ratio N'_m/N''_m according to the formula

$$\lg \frac{N'_m}{N''_m} = \lg \frac{N'_0}{N''_0} + \frac{E}{k}\left(\frac{1}{T_2} - \frac{1}{T_1}\right),$$

where N'_0 and N''_0 are the equilibrium numbers of CN molecules in the normal state at those particular temperatures. In the third column of Table 2 are presented the values of the ratio $N'_{m(H_2O)}/N''_{m(\quad)}$, as calculated by us according to this formula. (N'_m is the number of excited CN molecules at the temperature T_1 corresponding to the introduction of distilled water, and N''_m is the number of excited CN molecules at T_2, corresponding to the introduction of one of the solutions into the arc.) We took the values of the total concentration of CN mole-

Table 1

Substance	T (°K)	Substance	T (°K)
H_2O	5690 5660 5780	KBr	5520 5600 5560 5500
Average . .	5710	Average . .	5545
$MgCl_2$	5680 5560 5680 5560	KCl	5080 5040 5080 5140
Average . .	5620	Average . .	5085
KJ	5540 5420 5520 5560	KOH	4740 4900 4780 4760
Average . .	5535	Average . .	4795

Table 2

Substance	$\frac{I_{CN(H_2O)}}{I_{CN\ (solution)}}$	$\frac{N'_m}{N''_m}$
$MgCl_2$	1.74, 1.86, 1.73	1.09
KJ	3.08, 3.23, 3.38	1.10
KBr	2.51, 2.39, 2.57	1.05
KCl	2.23, 2.08, 2.13	1.38
KOH	4.26, 4.06, 4.16	1.85

cules at different temperatures from the work of Leskov and Vasil'eva.[6]

Comparing the values calculated by us for the ratio N'_m/N''_m with the experimentally obtained intensity ratio $I_{CN(H_2O)}/I_{CN(\quad)}$, one can easily see that there is a considerable disagreement between them, which is especially large when a KOH solution is introduced into the arc. This difference seems to indicate that the weakening of the CN bands is not of a purely thermal character. It is apparently associated also with the elementary processes going on in the arc plasma. The following may be such processes:

$$CN\,[B^2\Sigma^+] + K\,[^2S_{1/2}] + A \longrightarrow CN\,[X^2\Sigma] + K\,[^2P_{1/2,\,3/2}] + A,$$

$$CN\,[B^2\Sigma^+] + OH\,[^2\Pi] \longrightarrow CO\,[X^1\Sigma] + NH\,[X^3\Sigma^-].$$

REFERENCES

1. V. D. Pisarev and T. A. Ivanova, Trans. Tenth Co on Spectroscopy, vol. 2, p. 254. Izd. L'vovsk. Uni L'vov, 1958.
2. W. A. Chupka and M. G. Ingram, Mem. Soc. Roy. Liège 15, 373 (1955).
3. R. Z. Wieneke, Z. Physik 146, 39 (1956).
4. M. M. Smit-Miessen and J. L. Spier, Physica 9, 1 (1942).
5. M. M. Smit-Miessen and J. L. Spier, Physica 9, 4 (1942).
6. A. V. Leskov and L. P. Vasil'eva, Izvest. Akad. N SSSR, Ser. Fiz. 22, 696 (1958).

SINGLE SLIT, THREE-BEAM INTERFEROMETRY

V. G. Khomazyuk (pp. 417-419)

Received 3 November 1960

It is well-known that by means of two-beam interferometry the path differences of beams of light may by determined with an accuracy of up to 0.02 λ.[1,2] When Fabry-Perot etalons are used the accuracy is increased to 0.001 λ; however, because of the limited availability of the etalons they are not widely applied. For this reason the method of three-beam interferometry,[3-5] which yields an accuracy of 1/200-1/300 λ, at first proved to be promising and of much interest.[5] However, since until now its realization was based on either the use of the not readily available Michelson interferometer or on the Rozhdestvenskii interferometer,[6] so far this method also has not come into widespread use (we know of only one practical work[7]).

We did not encounter in the literature the practical application of three slits alone (without interferometers) placed in the same plane at equal distances apart (the width of each of the outside slits being half the width of the central slit), although this theoretical problem has been examined several times.[3,7]

It appears to us that a considerable simplification of the practical application of three beam interferometry can be achieved through the use of the method of "single slit, three-beam interferometry" described below which is based on the application of only one slit in place of three, without the use of interferometers of any kind.

The essence of the proposed method is as follow

By means of a lens an image of a light source is formed on a slit located at the focus of a second achr matic lens. A plane parallel glass or quartz plate of 0.5 mm thickness is placed behind the second lens in path of the parallel beam of light (the thickness of the plate and its refractive index should be known with hi interferometric accuracy).

The apparatus for the measurement of Fresnel diffraction described by Obreimov[1] looked just like t Consequently, if we project the diffraction pattern on the entrance slit of the spectrograph (the slits are m ally perpendicular to one another, the edge of the pla is parallel to the orientation of the auxiliary slit), we will obtain at the exit the well-known chain of interfe ence bands.

If now one adds to the previous etalon plate, whi for instance, was placed below the optic axis of the a paratus, a second identical plate at a distance of 3-5 above it, one obtains in the focal plane of the spectro graph the interference pattern shown in Fig. A (spec graph ISP-22). If we then place a lens in the path of

llel beam of light which passed through the plates he gap ("slit") between them, and focus the auxi- slit onto the spectrograph slit, we will obtain the interference pattern shown in Fig. B.

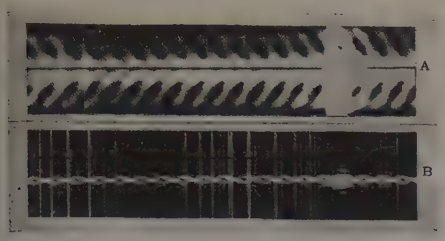

The theoretical representation of the interference rn of Fig. B can be obtained by starting from the ession obtained by Obreimov[1] for the case of a sin- talon plate:

$$= \cos^2 \pi n + 2 \sin^2 \pi n \, [c^2(u) + s^2(u)] + \sin 2\pi n \, [s(u) - c(u)] \quad (1)$$

corresponding equation for the second plate which nall derive from expression (1).

In expression (1) the following nomenclature was : I_1 is the intensity of the light,

$$u = x \sqrt{\frac{2}{z\lambda}}, \quad (2)$$

e x is the distance from the edge of the plate (con- ed positive in the direction towards its interior), z e distance from the plate to the screen (slit of the trograph), and c(u) and s(u) are the Fresnel inte-

$$c(u) = \int_0^u \cos \frac{\pi x^2}{2} \, dx; \quad s(u) = \int_0^u \sin \frac{\pi x^2}{2} \, dx, \quad (3)$$

h, as is well-known, are odd functions

$$c(-u) = -c(u); \quad s(-u) = -s(u). \quad (4)$$

It is evident that the expression for the distribution e intensity I_2 in the interference pattern caused by econd plate can be obtained from expression (1) if everse the sign of the quantity x, which is equivalent anging the sign of the quantity u in Eq. (2).

Using expression (4) we obtain from Eq. (1) the ex- sion we are seeking

$$= \cos^2 \pi n + 2 \sin^2 \pi n \, [c^2(u) + s^2(u)] - \sin 2\pi n \, [s(u) - c(u)]. \quad (5)$$

Since in the case of the two plates coherent beams are focused onto the slit of the spectrograph yielding two interference patterns simultaneously, a new interference pattern will appear in which the intensity distribution I is equal to the sum of the intensities I_1 and I_2:

$$I = I_1 + I_2 = 2 \{ \cos^2 \pi n + 2 \sin^2 \pi n \, [c^2(u) + s^2(u)] \}. \quad (6)$$

If we assume that the parallel beams of light, having a path difference n equal to zero or a whole number of wavelengths, are focused by the lens (without diffraction) to form an image of the auxiliary slit onto the slit of the spectrograph, then the first component of Eq. (6) will in this case determine the character of the interference pattern (the second will be zero). When $n = (2k + 1)\lambda/2$ the interference and diffraction patterns will be given by the second term (the first term will be equal to zero). In this case two principal maxima and a series of secondary maxima and minima will be observed on the interferogram (Fig. B; see also ref. 1).

In the form described above, the method of "single slit, three-beam interferometry" may be applied to the determination of path differences of beams with an accuracy of 1/200-1/300 λ in cases which were previously proposed for solution by the method of three slit, three-beam interferometry,[3,5,7] as well as to the determination of refractive indexes of solids, liquids, and gases (with an accuracy of about 0.02 λ).

Moreover, one can use a single etalon plate placed in the center of the parallel beam of light in such a way that the outer rays will pass above and below the plate. It is evident that in this case the appearance of the interference pattern will be the same as in the case when two etalon plates are used.

REFERENCES

1. I. V. Obreimov, "On the Application of Fresnel Diffraction to Physical Measurements." Izd. Akad. Nauk SSSR, Moscow, Leningrad, 1945.
2. V. G. Khomazyuk, Vestnik Moskov. Univ., Ser. Mat., Mekhan., Astron., Fiz. i Khim. No. 4, 171 (1958).
3. F. Zernike, J. Opt. Soc. Am. **40**, 326 (1950).
4. M. Bottema and F. Zernike, J. Opt. Soc. Am. **41**, 870 (1951).
5. V. O. Yur'ev, Uspekhi Fiz. Nauk **47**, 146 (1952).
6. G. P. Startsev, Doklady Akad. Nauk SSSR **95**, 1181 (1954).
7. C. Rénet and J. Viénot, Rev. opt. **32**, 27 (1953).

LUMINESCENCE OF IONIC FORMS OF URANIN IN LIQUID AND SOLID SOLUTIONS

V. S. Adamov and L. T. Kantardzhyan (pp. 419-422)

Received 28 November 1960

In investigating any of the luminescence parameters of organic molecules it is very important to know whether the luminescence is determined by the molecule itself or by its ionic forms. Careful study, taking into account the possible ionic forms of the investigated molecule, allows a correct interpretation of the results of an experimental investigation of such parameters as the law of decay, the emission and absorption spectra, the yield, the polarization, etc. The simultaneous presence of several luminescence centers (as different luminescent ionic forms) can by itself be one of the reasons for an experimentally observed complex law of luminescence decay, for a varying degree of polarization of the luminescence in different spectral regions and for some other observed effects. From this point of view a clarification of the possibility of coexistence in the investigated object of various ionic forms of the molecule is of definite interest.

Absorption and luminescence spectra of fluorescein and uranin solutions were studied as a function of pH in refs. 1-4. Zanker and Peter[5] determined from absorption spectra the regions of existence (the pK values) of the cation and of the singly and doubly charged anions of fluorescein. It was shown in ref. 6 that three ionic forms are also apparent in the luminescence spectra of uranin solutions, and singly and doubly charged anions were associated with definite spectral bands. An effort is made in the present paper to explain which ionic forms may be responsible for the luminescence of uranin activated hard sugar-candies and borate beads.

The uranin concentrations in liquid and solid solutions were 10^{-5} gm/ml and 10^{-5} gm/gm, respectively. Reabsorption was practically excluded by a suitable choice of thicknesses of the investigated samples. Luminescence spectra were obtained on a photoelectric apparatus.[1] pH values of liquid solutions were determined using a pH meter with a glass electrode.

Before starting to investigate possible ionic forms of uranin in hard media, we found it expedient to try to discover in the luminescence spectra of liquid uranin solutions a spectral band characteristical of the cation, as was done in ref. 6 with regard to singly and doubly charged anions. A well substantiated association of all three ionic forms of uranin with definite bands in the luminescence spectrum of liquid solutions would allow us in future to use a comparison of the luminescence spectra of liquid and solid solutions of uranin as a means of judging the ionic concentrations in the latter. To establish such an association we undertook a study of the luminescence spectra of acid solutions of uranin in sulfuric, hydrochloric, and nitric acids. The investigation revealed that changes in the spectra as a function of the pH of the solutions are precisely the same for the three indicated acids and that the appearance of the spectra is determined by the degree of acidity of the solution and not by the nature of the acid. The latter has an influence only on the absolute value of the intensity of luminescence.

Luminescence spectra of liquid solutions of uranin are represented in Fig. 1, and they show clearly the three characteristic bands. The spectra of alkaline uranin lutions at pH values >8 are represented by almost s metrical curves with a single sharply defined band having a maximum at 515 mμ (Fig. 1, curves 1 and 2 When the pH is decreased from about 8 to about 4 th spectra undergo a continuous change—a new broad b with a maximum in the region of 540-550 mμ appear along with the band at 515 mμ, the intensities in the ima of both bands becoming almost equal for pH valu around 4 (Fig. 1, curves 3, 4). A third band with a m imum in the region 470-480 mμ appears in the spect at pH values around 2, and if the pH is decreased fur this band increases considerably with a simultaneou decrease in the intensity of the 515 and 540-550 mμ In the limiting case of a very acid solution this band so strongly developed that the spectrum is represent by a rather large band slowly falling on the long wav length side (Fig. 1, curves 5 and 6).

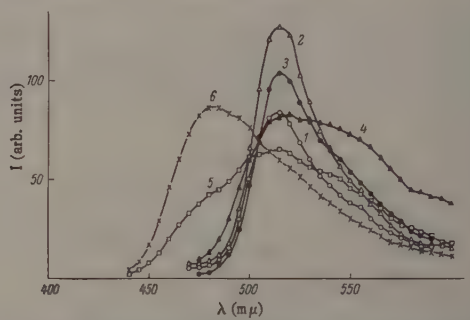

Fig. 1. Luminescence spectra of liquid solutions of uranin at various pH values. Curve 1—0.0001 N KOH (pH = 9.0); curve 2—1 N KOH (pH = 14.0); curve 3—0.000001 N HCl (pH = 7.1); curve 4—0.0001 N HCl (pH = 4.1); curve 5—2 N H_2SO (pH < 2); curve 6—4 N HNO_3.

The presence of three characteristic bands in t luminescence spectra of uranin solutions and the ob served changes in the bands as a function of the pH solutions can be well explained by the existence of 3 ionic forms belonging to the uranin molecule, provi the band with the maximum at 470-480 mμ is associ with the cation and the bands at 540-550 and 515 mμ associated with singly and doubly charged anions, re spectively.*

*A band with a maximum at 530 mμ was associated ref. 6 with a singly charged anion. Our investigatio indicated that the appearance of this band is not cha teristic of the singly charged anion and was evident caused by the presence of dioxane in the solution.

Luminescence spectra of uranin in hard sugar- dies show a strong dependence on the pH of the orig liquid solution. Changes observed in them are analo to changes in the luminescence spectra of liquid ura solutions.

Spectra of hard sugar-candies prepared from alkaline
in solutions are similar to the spectra of the original
tions. (Fig. 2, curves 3 and 4). The luminescence in-
ity increases with increased alkalinity of the solution
oduced into the sugar. It proved however to be impos-
e to pursue the effect of increasing intensity to the
iting case of a very strong alkali, inasmuch as we did
succeed in preparing hard sugar-candies from such
tions. A comparison of the luminescence spectra of
d sugar-candies prepared from alkaline uranin solu-
s with the spectra of Fig. 1 points to a doubly charged
n as a predominant ionic form in such hard sugar-
dies. Luminescence spectra of hard sugar-candies are
racterized in the interval of intermediate pH values
he solutions by the appearance and noticeable develop-
t of a band with a maximum at 540-550 mμ (Fig. 2,
ves 1 and 2), and, upon further increase in acidity to
values around 2, by the appearance and development
band with a maximum at 470-480 mμ (Fig. 2, curves
d 6), which can be explained by the presence in the
d sugar-candies of a singly charged anion and a ca-
as well as a doubly charged anion.

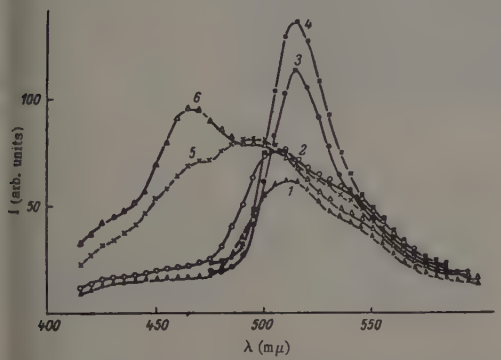

Fig. 2. Luminescence spectra of hard sugar-candies prepared from liquid solutions of uranin having different pH values. Curve 1—0.000001 N H_2SO (pH = 6.8); curve 2—0.0001 N H_2SO (pH = 4.0); curve 3—0.0001 N KOH (pH = 9.0); curve 4—0.001 N KOH (pH = 10.7); curve 5—0.0005 N H_2SO (pH = 3.2); curve 6—0.001 N H_2SO (pH = 2.9).

The observed changes in the spectra of hard sugar-
es as a function of the pH of the original liquid so-
ns are caused by the possibility that three ionic
s of uranin may exist in the candies, the continuous
se of these changes being caused by the simultaneous
ence of the three forms in a definite ratio which de-
s on the pH.

Luminescence spectra of borate beads prepared from
in solutions with various values of pH are shown in
3. These spectra are almost completely insensitive
e pH of the original solutions and have an appearance
similar to that of the spectrum of a very acid liquid
ion of uranin. Such similarity first serves as a con-
firmation of an assumption by Pringsheim[3] that the cation is the prevailing ionic form in a borate bead and, secondly, it can serve as a characteristic of the degree of acidity of a borate bead as a medium with an acidity corresponding to pH < 2.

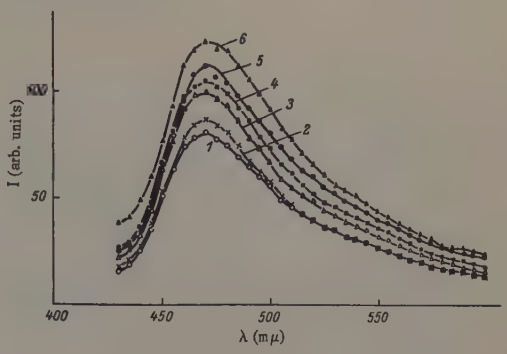

Fig. 3. Luminescence spectra of borate beads prepared from liquid solutions of uranin having different pH values. Curve 1—0.3 N KOH (pH = 13.8); curve 2—H_2O; curve 3—0.0001 N H_2SO (pH = 4.0); curve 4—0.001 N H_2SO (pH = 2.9); curve 5—2 N H_2SO (pH < 2); curve 6—5 N H_2SO .

The results of the present work indicate an essential difference between the luminescent particles formed by introduction of uranin from solution into a borate bead and the particles formed in a hard sugar-candy. The luminescence in a borate bead is caused essentially by uranin cations, while in a hard sugar-candy any of the three ionic forms or a combination of them can be responsible for luminescence. This circumstance should always be kept in mind for molecules which dissociate to ions, when their luminescence is studied in hard media.

The authors express their gratitude to M. A. Avetisyan for assistance with the paper.

REFERENCES

1. B. Batscha, Chem. Ber. 59, 311 (1926).
2. V. L. Levshin, "Photoluminescence of Liquid and Solid Substances." Gosudarst. Izd. Tekh-Teoret. Lit., Moscow, Leningrad, 1951.
3. P. Pringsheim, "Fluorescence and Phosphorescence." Izd. Inostrannaya Lit., Moscow, 1951. Interscience, New York, 1949.
4. L. T. Kantardzhyan, Izvest. Akad. Nauk SSSR, Ser. Fiz. 23, 131 (1959).
5. V. Zanker and W. Peter, Chem. Ber. 1, 572 (1958).
6. E. V. Grigoryan, L. T. Kantardzhyan, and S. S. Chirkinyan, Izvest. Akad. Nauk SSSR, Ser. Fiz. 24, 771 (1960).
7. L. T. Kantardzhyan, Opt. i Spektr. 2, 378 (1957).

ELECTRO-X-RAY LUMINESCENCE OF KBr CRYSTALS

A. S. Andrianov and M. L. Kats (pp. 422-423)

Received 15 March 1961

It is well known that alkali halide compounds have been very successfully used as subjects for solving the most fundamental problems of crystal-phosphor luminescence. It is therefore of great interest to use this class of substances in investigations of electroluminescence.

Vorob'ev and Kuchin[1] studied the possibility of luminescence of alkali halides for field intensities which were close to the breakdown value. However, no one has as yet observed electroluminescence in alkali halide phosphors under normal experimental conditions. We therefore have undertaken an investigation of the electro-x-ray luminescence which we had observed in these phosphors, that is, of the luminescence which appears under the simultaneous action of x-rays and an electric field.

The experiments were performed on solid condensers prepared in the following way. A layer of powdered alkali halide mixed with melamine-formaldehyde and alkyd resin was deposited onto a glass blank covered with a transparent conducting coating of tin dioxide. After this layer of powder suspended in a dielectric had dried and polymerized, it was covered by a layer of aluminum deposited by vacuum evaporation; this layer of aluminum served as a second electrode. A condenser made in this way was then inserted in the x-ray beam produced by a URS-70 half-wave generator fitted with a BSV-Cu tube. The x-rays were incident on the aluminum covered face of the condenser and the visible radiation was measured or observed through the transparent substrate with the help of an FEU-19 photomultiplier and an oscilloscope or a microammeter.

We investigated condensers with dielectric layers that contained pure potassium bromide. Such condensers did not exhibit any electroluminescence when subjected to the electric field alone even if the intensity of the field was increased up to breakdown values. When such condensers were irradiated by x-rays, the luminescence could be observed even in the absence of a field. Brightness waves of the x-ray luminescence, recorded in an oscilloscope, are shown in Fig. 1a. Figure 1b shows the condenser brightness waves for a sample subjected to x-rays and an electric field simultaneously (1200 volts, 50 cps, layer thickness 0.2 mm).

A comparison of Figs. 1a and 1b shows clearly that when an electric field is applied to the condenser the shape of the brightness wave remains practically unchanged, but the intensity of the luminescence increases considerably (in what follows, we shall refer to the simultaneous action of x-rays and an electric field as electro-x-ray luminescence). Furthermore, the intensity amplification factor ρ increases as the applied voltage increases (Fig. 2).

The amplification of the x-ray luminescence of the KBr crystals under the action of the electric field can be attributed either to the excitation of impurities which are accidentally included in minute concentrations in even the purest crystals or else to the excitation of the host crystal itself. In the first of these cases, the effect of direct ionization of activating impurities by the field is

Fig. 1

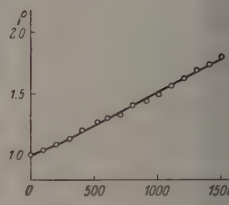

Fig. 2

Fig. 1. Brightness waves of x-ray luminescence (a) and electro-x-ray luminescence (b) in KBr crystals. The upper curves are standard sinusoidal signals.
Fig. 2. Dependence of the luminescence-intensity amplification factor ρ on the applied voltage V.

completely excluded, because all the activators in al halide crystal phosphors whose luminescence spectr entirely within the visible part of the spectrum have deep-lying, ground-state levels. The absence of any electroluminescence in the experimental samples wh they were subjected to an electric field without simu taneous irradiation of the condenser with x-rays tes to the correctness of this assertion.

In this case, a more acceptable explanation appe to be that the activator centers are excited by inelas collisions with electrons which have been scattered the conduction band by the x-rays and accelerated to optical energies by the electric field. However, if th is the correct mechanism for the effect, the amplifi tion should increase as the activator is added to the tal and as the concentration of activator is increase to the highest values for which concentration quench is not significant). In order to test this hypothesis, studied the electro-x-ray luminescence of KBr-Sn p phor which has a bright photoluminescence in the sp region where the FEU-19 has its highest sensitivity which is distinguished by a relatively low value of th citation potential of the activator centers. However, amplification effect was not significantly greater tha had been for the pure KBr crystals.

If it is assumed that the electro-x-ray luminesc is determined by the properties of the pure crystal, this luminescence could be caused either by recomb tion of free electrons with localized holes or, inver by recombination of free holes with localized electr

nally, by band to band transitions with the formation citons whose annihilation results in radiation emis- In all these cases, the amplification effect which rs under the action of the field can be attributed to elocalization of electrons or holes from trap levels e field.

REFERENCE

1. A. A. Vorob'ev and V. D. Kuchin, Izvest. Tomsk. Politekh. Inst. 91, 385 (1956).

RESULTS OF SPECTROCHEMICAL ANALYSIS WITH A COMBINATION ELECTRIC DISCHARGE AS A LIGHT SOURCE

G. D. Cristescu and M. Giurgea* (pp. 424-426)

*S. I. Parkhon University, Bucharest

Received 30 March 1961

he investigations presented in this paper were con- d with a spectral source which was introduced by f the writers[1] and which consisted of a superposi- f a direct current and of a high frequency jet. The atus used in this work is depicted in Fig. 1. The f the electrical scheme on the left is a high fre- y oscillator of the usual type, with a frequency eable between 3×10^7 and 6×10^7 cps, the part on ght is a tuned resonance circuit connected with the ator and containing a capacitor with plates CC′ and uctance B. Between the plates of the capacitor is a sharp metallic point V which serves as a lower ode. The upper plate of the capacitor C has the of a ring, which permits the introduction into the between the plates of an auxiliary electrode S, is connected through a choke coil with one of the of a dc source (minimum voltage 1000 volts). The pole of the source is connected with the mid-point induction coil B through another choke coil and a tat, thus being connected with the electrode V.

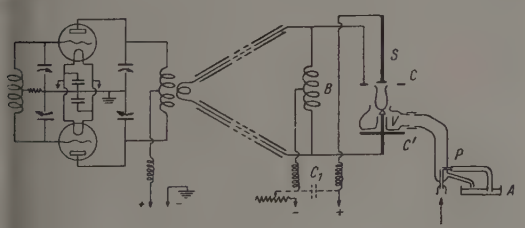

Fig. 1

ERAL REMARKS ON THE EMISSION OF THE OURCE

As has been shown in ref. 1, the combination dis- e makes it possible to obtain the desired energy of ation which corresponds to the temperatures of the requency jet-electric arc system. Thus, by changing urrent of the constant component of the electric dis- e within the limits 0.1-1 amp, lines appear in the sion spectrum of the source that are characteristic metal of which the electrode V is composed, in rder of increasing excitation energy. For instance, nes 4248.96, 4507.5, and 4509.39 A, the excitation energies of which are 7.99, 8.32, and 7.99 ev, respectively, can be obtained from a copper point.

The presence of condenser C_1 with a capacitance of several microfarads (indicated by dashed lines in Fig. 1) permits the obtaining of pulsed currents of great strength, which cause new lines, corresponding to higher excitation energies, to appear in the spectrum. Furthermore, by a gradual increase of the intensity of the constant component of the discharge one can achieve an increase and then a decrease of the intensity of certain lines with low excitation energies. In the above-mentioned region of the intensity of the constant component, for a frequency of 4×10^7 cps and a discharge length of 35 mm, this phenomenon was observed for the sodium doublet with $V_{exc.}$ = 2.10 ev, and for the calcium line λ = 4226.73 A ($V_{exc.}$ = 2.93 ev).

With an increase in the strength of the dc component of the discharge, the appearance of the latter also changes. For instance, if there is a small amount of sodium in the discharge, it can easily be noticed that with an increase in the intensity of the dc component, the yellow part of the discharge moves toward the colder regions of the latter, that is, toward the outer layer. Under certain conditions of the discharge, band spectra may be obtained, whereas under other conditions, spectral lines are prevailing. For instance, either bands of the oxides of the metals Al, Cu, Pb, Mg, etc., or lines of these metals may become stronger. Thus the source can be used also for the production of certain band spectra.

RESULTS OF THE SPECTROCHEMICAL ANALYSIS

In order to use the source for analytical purposes it was necessary to stabilize its emission, and also to cause the substance to be analyzed to be introduced into the discharge in a uniform manner. The first condition (in addition to the constancy of the dc supply)* requires

*Under these conditions the work was conducted without the capacitor C_1.

the use of a nonoxidizing fixing electrode V with a high melting point. For this reason a platinum point was used for the lower, negative electrode, in the form of a small cylinder 8 mm in diameter and 3 mm high, which ended with a conical needle. This electrode did not noticeably change during the course of the work. The nature of the

upper, positive electrode S is of much lesser importance, so that both nickel and copper could be used successfully.

With an increase of the constant current in the discharge (after it has reached a certain value), the discharge becomes unstable, and the intensity of the dc component fluctuates within certain limits. After this region is passed, the discharge again becomes stable. For the quantitative analysis we used currents smaller than those at which the discharge became unstable. Under these conditions measurements made by means of photograph photometry showed a sufficient stability of the emission of the source.

To satisfy the second condition, we introduced the substance into the discharge as an atomized solution.[2] The atomizer P depicted in Fig. 1 can work either in a closed system or as an external atomizer, depending on the position of the vessel A containing the solution to be analyzed. The atomizer is connected with a glass vessel which has the form depicted in the figure, and which is placed on the lower plate of the capacitor C′ of the resonance circuit.

The spectra were obtained by illuminating the slit of a Fuess spectrograph (which had a length of the visible part of the spectrum of 6 cm) through a system with double projection which separated the radiation emitted by the middle portion of the source; this portion comprised about one third of the length of the discharge.

The purpose of the present work was to find the lowest detectable concentration and the precision in determination of concentration of some single-component solutions. Aqueous solutions of $Pb(NO_3)_2$ and $NH\,VO_3$ were used for this purpose. The elements Pb and V were chosen because of the importance of detection of traces of Pb in occupational poisoning, and of traces of V in some petroleum products. At the same time, these elements have stable lines in the visible part of the spectrum which have energies of excitation convenient for us.

In the case of lead, the identification was made with the spectral line $\lambda = 4057.82$ A; the smallest detectable concentration was 5×10^{-8} gm atom/cm^3. For the identification of vanadium a group of lines was used with the wavelengths 4379.2, 4384.7, 4389.9, 4395.2, 4406.6, and 4408.5 A. The limiting sensitivity for this element was 5×10^{-7} gm atom/cm^3. Since in the region of the lines selected for the identification of vanadium there are band spectra of the N_2 molecule in the spectrum of the source, and they produce a background preventing the observation of lines from the element under investigation when its concentration is low, we used argon for atomizing. Under these conditions, vanadium could be detected in concentrations of 10^{-8} gm atom/cm^3.

For comparison, under the same experimental conditions the lower limits of detectable concentrations of lead and vanadium were determined by using only the high frequency spark. The values of 2×10^{-7} gm atom/cm^3 for lead, and 1.7×10^{-7} gm atom/cm^3 for vanadium were found. In order to establish the accuracy of concentration determinations with the described source, we used aqueous solutions of ammonium vanadate with concentrations of 7×10^{-8}-5×10^{-7} gm atom/cm^3.

The adopted working conditions were as follows: the length of the high-frequency jet was 70 mm, the distance between the electrodes V and S was 35 mm, the frequency of the oscillating circuit was 4×10^7 cps, the current of the dc component was 250 ma, atomizing by argon a excess pressure of 80 torr. In order to establish st thermal conditions, the apparatus was run under no conditions for about three minutes before any expos were taken. The stability of the emission by the sou under the described working conditions permitted th construction of a concentration calibration curve wi the use of an internal standard.

The intensity of spectral lines was determined means of calibration curves constructed with a neut step-filter. Figure 2 depicts a calibration curve (lo arithm of intensity in arbitrary units as a function c logarithm of concentration) for the spectral line $\lambda =$ 4379.2 A. The points on the curve are averages of t measurements. The examination of the data shows t spectral analysis of vanadium in the concentration r in question and under the working conditions used, c be made with an error of about 3% which is due mai to the errors of photographic photometry.

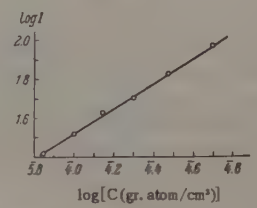

CONCLUSIONS

It follows from the foregoing that the spectral s described is suitable for various spectroscopic app tions: production of band spectra, obtaining of vari excitation conditions in the case of line spectra, qu tive and quantitative spectrochemical analysis. For qualitative analysis of some elements (for instance, as those investigated in the present work), the sour provides a sensitivity which exceeds that of an anal in a flame or in a high-frequency jet.[3] This can be plained by the fact that conditions which correspond temperatures higher than those in the last mentione sources are created for emission. On the other han source provides a stability of emission comparable that of the flame and of the ordinary high-frequency and exceeding the stability of emission by an electr or spark. It should be also mentioned that the sour permits the analysis of a substance in a solution, w is an important advantage in the practice of spectro chemical analysis.

REFERENCES

1. G. D. Cristescu, Studii si Cercetări de Fisică 1 (1959); Ann. Physik 6, 153 (1960).
2. E. Badarau, M. Giurgea, G. Giurgea, and A. Tru Proc. Sixth Intern. Conf. on Spectroscopy, Lond 1957, p. 441.
3. H. Lundegardh, Die quantitative Spectralanalyse Elemente II, Jena, 1934.

ON THE ELECTROLUMINESCENCE EXCITATION PROCESS IN ZINC SULFIDE

A. N. Georgobiani (pp. 426-428)

Received 14 April 1961

n the current literature, the electroluminescence tion process is viewed in the following way: the eeded to induce direct excitation by tunneling of ons through the potential barrier (Zener effect) is arge, and before this mechanism can begin to play in the process, avalanche breakdown takes place. reakdown voltage for ZnS is about 10^6 volts/cm as substantial tunneling of electrons from the e to the conduction band will occur only for a field order of 10^7 volts/cm, according to calculations hed by a number of workers.[1-3]

owever, the assertions of these authors are valid the field is concentrated over a rather large re- since in order for an avalanche to develop it is al- necessary that an electron gather enough energy so e probability of ionizing the crystal lattice, or a escence center, by the electron will be larger than obability that the electron will escape from the re- which the field is concentrated. The dimensions stallites in polycrystalline zinc sulfide are ~10^{-3} such material fundamental excitation is concen- in a region of the crystal which is at least an order nitude smaller than its over-all dimension.

ref. 5, the impact ionization coefficient α, i.e., obability that an electron will produce ionization in sing 1 cm of path in zinc sulfide, was calculated. thor of that paper applied the theory of impact tion developed for germanium and silicon to ZnS; umed that as far as the theory is concerned, the al difference between zinc sulfide and the ele- ry semiconductors is the difference in their widths forbidden energy gap, since the free path length l electrons in ZnS is of the same order of magnitude germanium and silicon (~120 A).[6,7] In ZnS, $l \approx 50$ to [2,5] The calculation presented in ref. 5 showed that [-4] when the field is ~10^6 volts/cm. In other words, field is equal to 10^6 volts and is concentrated in a of the order of 10^{-4} cm and one electron is in- into this region, then before it leaves the region ctron will produce approximately one ionization. t be pointed out that the magnitude of the field cal- d in this way is lower than what it should be because ulfide differs from germanium and silicon in that it rtially ionic bonding.

et us consider now how large the field would have to this same region of the crystal in order to account e experimentally observed light emission if it is as- d that the excitation is directly induced by the field r effect). According to our measurements, the ap- ion of 800 volts across an electroluminescent con- r* about 5×10^{-3} thick resulted in the emission of

method of fabrication and the composition of the oluminescent condenser were the same as in ref. 8.

3×10^{13} to 4×10^{13} quanta/cm^2 sec. The frequency applied voltage was 500 cps, i.e., about 3.5×10^{10} /cm^2 were emitted during each pulse. The crystal- ad dimensions of about 10^{-3} cm; therefore, the ion from a single layer of such crystals would amount to about 0.7×10^{10} quanta/cm^2. The electroluminescence energy yield is approximately equal to 4%.[9] If it is assumed that all the energy losses associated with electroluminescence can be attributed to nonradiative recombination, then we obtain an upper limit on the number of ionization events. It is easy to show that about 1.75×10^{11} ionizations/cm^2 take place in a single crystal layer. In a layer of 10^{-4} cm thickness, there are about 10^{18} valence band electrons/cm^2. Consequently, a fraction of about 1.75×10^{-7} of all the valence electrons participate in the excitation of the crystal. The equation for the probability of ionization by the field (Zener effect) has the following form:

$$W = \frac{eEd}{2\pi\hbar} \exp\left\{-\frac{\pi}{4e\hbar E}\sqrt{2m^*}\Delta^{3/2}\right\}.$$

where E is the magnitude of the electric field; e and m* are the charge and effective mass of the electron; Δ is the width of the forbidden gap; d is the period of the crystal lattice; $\hbar$ is Planck's constant. If values of d = 2.35 A[10] and $m^* = 0.25\ m_e$,[3] where m_e is the electron mass, are substituted into this equation, it is found that the required number of ionization events can be produced by the electric field if it has a magnitude of $E \approx 3 \times 10^6$ volts/cm in the region where it is concentrated.

The current state of breakdown theory is such that it is sufficiently accurate for describing relations qualitatively, whereas quantitative calculations based thereon lead to values which are only good to an order of magnitude. Therefore, the difference between the field needed for electroluminescence excitation by electron impact and that needed for direct excitation by the electric field (by tunneling of electrons through the potential barrier) should be considered insignificant in our case.

Thus, the assertions made by some authors[1-3] to the effect that the excitation of electroluminescence in zinc sulfide cannot be attributed to direct excitation by the electric field are clearly ungrounded. Generally speaking, in concrete cases, both impact ionization and direct field-induced ionization can occur in varying degrees. For example, if the excitation region of the crystal is too small to develop an avalanche, but the field in this region is still quite high, then field-induced excitation (Zener effect) occurs. On the other hand if conditions are favorable for an avalanche to develop (both the field and the region in which it is distributed are large enough), then impact ionization will predominate over field-induced ionization.

Furthermore, it was shown in ref. 11 that both the voltage dependence and the temperature dependence of average brightness indicate that the process which determines the average brightness is a tunneling transition. In the same paper, it was suggested that the tunneling transition which determines the dependence of brightness on voltage was penetration of electrons from the surface phase of the electroluminophor into the ZnS crystal and, further, that these electrons participated in impact ionization of the crystal lattice and the luminescence centers. The calculation presented in this paper

shows that this tunneling transition can also be connected with direct field-induced ionization of the crystal lattice and of the luminescence centers. At this time, it is not possible to prefer one model over the other.

REFERENCES

1. G. Destriau and H. F. Ivey, Proc. Inst. Radio Engrs. 43, 1911 (1955).
2. P. Zalm, Philips Research Repts. 11, 353, 417 (1956).
3. W. W. Piper and F. E. Williams, Solid State Physics 6, 95 (1958).
4. W. Lehmann, J. Electrochem. Soc. 107, 657 (196
5. G. Newmark, Phys. Rev. 116, 1425 (1959).
6. A. G. Chynoweth, Phys. Rev. 109, 1537 (1958).
7. S. L. Miller, Phys. Rev. 105, 1246 (1957).
8. A. N. Georgobiani and M. V. Fok, Opt. i Spektr. 775 (1960), Optics and Spectroscopy 9, 407 (1960
9. W. Lehmann, J. Electrochem. Soc. 106, 585 (195
10. B. V. Nekrasov, "Course in General Chemistry." Goskhimizdat, Moscow, 1952.
11. A. N. Georgobiani and M. V. Fok, Opt. i Spektr. 188 (1961), Optics and Spectroscopy 10, 95 (1961

HYDROGEN BONDING OF KETONES WITH CHLOROFORM AS REVEALED IN THE BA OF THE CARBONYL GROUP STRETCHING VIBRATION

G. S. Denisov (pp. 428-431)

Received 24 April 1961

The existence of the $Cl_3CH...O=C$ hydrogen bond has been unequivocally demonstrated,[1-3] but its effects on the νCO band have not been thoroughly studied. On the one hand, Gordy's viewpoint[4] is widespread: the shift of the νCO band of acetone toward lower frequencies on going from the pure liquid to a $CHCl_3$ solution is ascribed to the formation of a $CH...O=C$ bond. On the other hand, in studying the effect of the dielectric properties of the medium on the frequency and intensity of the νCO band, chloroform is used along with other solvents which do not form a hydrogen bond with the carbonyl group.[5]

In this work we have investigated acetone, which possesses the minimum electron-donating capacity in the saturated ketone series, pivalone (2,2,4,4-tetramethyl-3-pentanone) and camphor, whose electron-donating capacity is close to the maximum, and dipropyl ketone, which possesses an intermediate value of the electron-donating capacity.[6] The spectra of solutions of these ketones in $CHCl_3$, hexane, and mixtures of the two in varying proportions have been obtained. The concentration of the ketone amounted to 0.1-0.3 mole/liter, and the cell thickness was 74 μ. The work was conducted on an IKS-6 instrument with NaCl prisms, furnished with an OAP-1 detector (the calculated spectral slit width was 3.0 cm^{-1}).

In connection with the fact that the appearance of a finite displacement of the absorption bands[2,7] serves as one of the spectroscopic criteria of the presence of a hydrogen bond—i.e., the appearance of structure in the band when this displacement is not large—the question of the shape of the νCO band of ketones in the absence of a hydrogen bond arises. It has been found by a number of authors that the νCO band in the Raman[8] and infrared absorption spectra[9] of many ketones (liquid, solid, and in solution) consists of several (up to five) components. Josien and collaborators[10] analyzed some results obtained by the authors of refs. 9 and drew the conclusion that these results were clearly erroneous. In the single case of cyclopentanone, the doublet character of the νCO band does not provoke doubts and is convincingly explained by the effect of Fermi resonance.[11]

Our data show that, in the absence of a hydrogen bond, the νCO band of the ketones which we have stu is simple. Some of the spectra obtained are present in the figure. It is easy to see that, in the spectra of lutions in $CHCl_3$ and in a mixed solvent containing C the νCO band of all the ketones investigated (except acetone)* is complex and consists of three compone

*As has previously been noted,[16] the weak band at 17 cm^{-1} in the spectrum of a colution of acetone in hex is not associated with the νCO vibration.

the relative intensity of which depends on the compo tion of the solvent. An increase in the fraction of ch form produces a weakening of the high-frequency co ponent and the gradual appearance and increase in i sity of the two low-frequency components.

The observed structure of the νCO band may be plained by the existence of two types of complexes— and 1:2—between ketone molecules and chloroform molecules. The high-frequency band corresponds to sorption by unassociated ketone molecules, the cent component belongs to the equimolar complex, and th low-frequency band belongs to the complex of a keto molecule with two chloroform molecules. The possi bility of forming a 1:2 complex is associated with th presence of two free electron pairs in the oxygen at of the carbonyl group. Actually, cases are known of participation of a carbonyl group in two intermolecu hydrogen bonds (the mixed crystal $(NH_2)_2CO \cdot H_2O_2$[12]) intermolecular and one intramolecular bond (salicyl acid dimer[13]), and two intramolecular bonds (1,8-di- hydroxyanthraquinone and 2,2′-dihydroxybenzopheno A triplet structure was recently found in the νCO ba of diphenyldiethylurea in solvents containing $CHCl_3$ $CHBr_3$; this was also explained by the existence of c plexes of the 1:1 and 1:2 compositions.[15]

Analysis of the results obtained permits us to d the following conclusions.

1. The magnitude of the splitting increases wit increase in the electron-donating capacity of the ke The relative shift, $[(\nu_0 - \nu)/\nu_0] \times 10^3$ (ν_0 is the frequ of the νCO band in hexane solution), increases in th

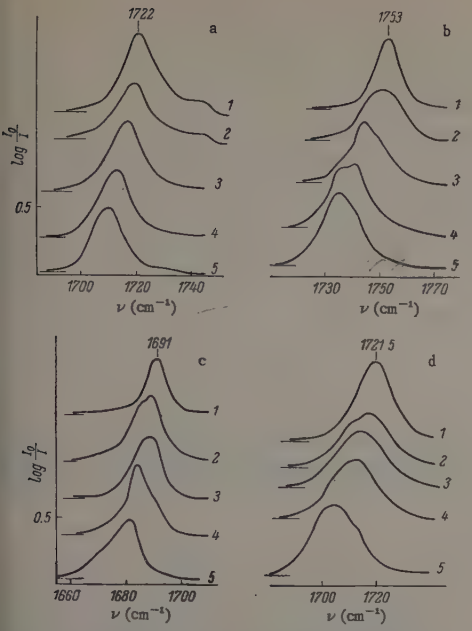

The νCO band in the absorption spectra of the solutions of ketones in hexane-chloroform mixtures. Substance: a—acetone; b—camphor; c—pivalone; d—dipropyl ketone. Chloroform content of the mixture moles/liter): a: curve 1—0, curve 2—1.5, curve 3—4.1, curve 4—9.2, curve 5—12.5; b: curve 1—0, curve 2—0.48, curve 3—1.5, curve 4—6.2, curve 5—12.5; c: curve 1—0, curve 2—0.57, curve 3—1.2, curve 4—3.0, curve 5—12.5; d: curve 1—0, curve 2—0.78, curve 3—1.6, curve 4—3.0, curve 5—12.5. (Ketone concentration = 0.03 mole/liter, d = 490 μ.)

ng way in the sequence dipropyl ketone, camphor, one: 5.2, 5.7, 5.9 for the 1:1 complex and 9.0, 10.3, for the 1:2 complex. A dependence of the same sort previously established for the bond of type OH...O=C.[6]

2. The distance between the bands of the monomer he 1:1 complex is greater than that between the bands e 1:1 and 1:2 complexes; i.e., the attachment of the chloroform molecule to the ketone molecule pro- s a band shift which is greater than the further shift ght about by the attachment of a second molecule nd 8 cm^{-1} for camphor and pivalone, 9 and 6.5 cm^{-1} dipropyl ketone). This apparently testifies to the ter stability of the bond in the 1:1 complex than of bond in the 1:2 complex.

3. In contradistinction to the strong bond of type .O=C,[6] the steric requirements in the case of piva- manifest themselves in a reduction (as compared mphor) in the equilibrium constant for hydrogen formation, as may be judged from the relative in- ty of the bands in the triplet, but not in a reduction e magnitude of the shift. This indicates that the HC equilibrium distance is determined by the inter- ns within this group, while the screening of the onyl group by methyl radicals does not find expres- in any noticeable way through the value of the equi- um distance.

We must deal separately with the case of acetone, which displays special behavior: we did not succeed in observing structure in the νCO band at any concentration of $CHCl_3$, while its halfwidth diminishes from 16 (solutions in hexane) to 14.5 cm^{-1} (solution in $CHCl_3$). If we consider, by analogy with the other ketones, that complexes of the 1:1 and 1:2 compositions really exist, and if we assume that the observed contour is the envelope of three closely-spaced bands which are not resolved because of their considerable width, then on this basis the transition from a solution in hexane (simple band) to a solution containing chloroform (complex band) would have to lead to an increase in the halfwidth, which conflicts with experiment. We note for comparison that in dipropyl ketone the halfwidth increases from 16 to 23.5 cm^{-1}, and in diisopropyl ketone (according to the data of ref. 16) from 10 to 19.5 cm^{-1}.

But if we consider that formation of the equimolar complex is the fundamental equilibrium in the acetone-chloroform system (such a conclusion has been drawn, for example, from a study of the melting-point diagrams[17] and heats of mixing[18]), and if we ascribe to the formation of just this complex the shift of the νCO band toward lower frequencies (12 cm^{-1}) on going from a hexane solution to a chloroform solution, then such a result conflicts with the regularity established for the other ketones. For acetone, we should expect a shift less than the 9 cm^{-1} found for dipropyl ketone, and this means that these arguments are also inadmissible.

Comparison of the νCO frequencies of acetone dissolved in $CHCl_3$ and $CHBr_3$ (according to the data of ref. 16, these are 1711.5 and 1708 cm^{-1} respectively) shows that the band shift is greater in $CHBr_3$, although hydrogen bonding with bromoform, by reason of the lesser proton-donating capacity of the latter, should lead to a smaller shift of the νCO band as compared with chloroform. Summing up, one may consequently assert that, in these solvents, the hydrogen bond is not the fundamental cause of the shift of the νCO band of acetone toward lower frequencies. The cause may be intermolecular interaction of another type or the dielectric effect of the solvent as a medium.

The author thanks V. M. Chulanovskii for his interest in the work and for discussion of the results.

REFERENCES

1. C. M. Huggins and G. C. Pimentel, J. Chem. Phys. 23, 896 (1955).
2. V. M. Chulanovskii and M. P. Burgova, Opt. i Spektr. 2, 330 (1957).
3. C. M. Huggins, G. C. Pimentel, and J. N. Shoolery, J. Chem. Phys. 23, 1244 (1955).
4. W. Gordy, J. Am. Chem. Soc. 60, 605 (1938).
5. E. Hirota, Bull. Chem. Soc. Japan 27, 295 (1954).
6. G. S. Denisov, Doklady Akad. Nauk SSSR 134, 1131 (1960).
7. O. Redlich, Chem. Rev. 44, 1 (1949).
8. E. Gray and M. Bottreau, Compt. rend. acad. sci. 240, 2134 (1955);
E. Gray, Cahiers Phys. 10, 71 (1956);
C. Mangin and M. Bottreau, Compt. rend. acad. sci. 242, 2637 (1956).
9. E. Gray and C. Mangin, J. phys. radium 15, 9 (1954);
E. Gray and M. Bottreau, J. phys. radium 15, 200 (1954); Compt. rend. acad. sci. 240, 2134 (1955);

J. Depireux, Bull. Soc. chim. Belg. 66, 218 (1957); F. Taboury, Cahiers phys. 10, 24 (1956).
10. C. Castinel, G. Chiurdoglu, M. L. Josien, J. Lascombe, and E. Vanlanduyt, Bull. soc. chim. France 807 (1958).
11. C. L. Angell, P. J. Krueger, R. Lanzon, L. C. Leitch, K. Noak, R. J. D. Smith, and R. N. Jones, Spectrochim. Acta Vol. 15, 926 (1959).
12. "New Investigations in Crystallography and Crystal Chemistry. Collection III. Crystal Structures," p. 34. Izd. Akad. Nauk SSSR, Moscow, 1951.
13. L. Pauling, "The Nature of the Chemical Bond and the Structure of Molecules and Crystals," p. 300. Izd. Inostrannoi Lit., Moscow, 1947. 3rd ed., Co Univ. Press, 1960.
14. U. Liddell, Ann. N.Y. Acad. Sci. 69, 70 (1957).
15. J. Lascombe, Thesis. Bordeaux, 1960.
16. N. S. Bayliss, A. R. H. Cole, and L. H. Little, Austral. J. Chem. 8, 26 (1955).
17. G. I. Korinek and W. G. Schneider, Can. J. Chem 35, 1157 (1957); A. N. Campbell and E. M. Kartzmark, Can. J. C 38, 652 (1959).
18. J. R. Lacher, J. J. McKinley, and J. D. Park, J. Am. Chem. Soc. 70, 2598 (1948).

THE REDISTRIBUTION OF ELECTRONS AMONG THE LOCALIZED LEVELS OF SILV HALIDE PHOSPHORS AND THE STIMULATING ACTION OF THE EXCITING LIGHT

V. M. Belous (pp. 431-433)

Received 26 January 1961

Different methods[1-4] can be used to study the distribution of electrons among capture levels in crystalline phosphors under conditions of steady state luminescence as well as after the exciting radiation is cut off. In phosphors exhibiting a luminescence flash under the action of "red" light, the solution of the indicated problem is usually connected with a study of the flash properties of the phosphor.[5-12]

It has already been established[13] that the action of infrared light can cause a blue luminescence flash in silver chloride. It has now been found that a whole series of mixed silver halide phosphors also exhibits flash properties under irradiation by light of long wavelength.*

*The flash properties of mixed silver halide phosphors will be discussed in detail elsewhere.

The halogen compounds of silver are very suitable subjects in this connection for a study of the distribution of electrons among capture levels by the method of infrared "probing."

In this paper we present results of a study, using this method, of the variation in the number of electrons on capture levels as a function of the duration of the dark interval between the cutoff of steady state excitation and the turning on of infrared. The study of luminescence was carried out at liquid nitrogen temperatures on AgCl single crystals grown by the method of Kiropoulos* and

*The author wishes to express his appreciation to S. I. Golub for kindly furnishing the samples.

Bridgman,* on fused AgCl layers, and on AgCl single

*This AgCl crystal was obtained from the Institute of Crystallography of the Academy of Sciences of the USSR. The author thanks G. Ya. Seregina for its preparation.

crystals with a AgI impurity (AgCl + 0.1 mole % AgI, AgCl + 1 mole % AgI) also grown by the Kiropoulos method. The flash properties of the blue band (λ_{max} = 480 mμ) were studied for all AgCl samples and for AgCl + 0.1 mole % AgI, while the green band flash was studied for the AgCl + 1 mole % AgI single crystal which luminesces in the green (λ_{max} = 520 mμ). The luminescence was recorded by a FEU-19M photomultiplier with a SZS-18 filter. The voltage from the pho multiplier was applied at the input of a ENO-1 oscil graph. An incandescent lamp (1000 watts, 110 volts) used at the infrared source (KS-19 filter). Lumines was excited by the mercury 313 and 365 mμ lines is by a quartz monochromator. A more detailed descr of the experimental arrangement is given in ref. 13.

The following sequence was used in the experin The samples were excited for 15 sec, after which th ultraviolet light was turned off. The infrared radiat was turned on after a definite interval, and the flash recorded. Then the sample was again excited for 15 and the flash was measured this time after another interval. Special experiments showed that the infra intensity used was fully adequate for a complete lib tion of the light sum stored on the flash levels.

A study of the curves giving the magnitude (I) o flash as a function of the duration (t) of the dark int has shown that for all the enumerated samples thes curves have a peak for excitation by both the 313 m 365 mμ lines. For a given substance, the position o peak on the time scale depends on the intensity E of ultraviolet light used to excite luminescence.

Figure 1 shows as an example the results for a single crystal grown by the Kiropoulos method. Gra A shows the dependence of I on E. The arrows with numbers mark the intensities of the ultraviolet ligh to excite luminescence. The time dependence of the flash magnitudes corresponding to the indicated int sity values are shown in graphs B. The nature of th curve showing the functional dependence of I on E i quite analogous to that found earlier for fused layer The following results may be noted: If phosphor lu cence is excited by ultraviolet radiation with an int for which the quantity I falls with increasing E, the position of the maximun on the I(t) curves is sharpl placed to higher t values as compared with the pos of the same maximum in the case when luminescen excited by ultraviolet with an intensity correspondi the range where I increases with increasing E. (See 1, graph B, curves 1-4.) (The larger is E, the larg displacement.)

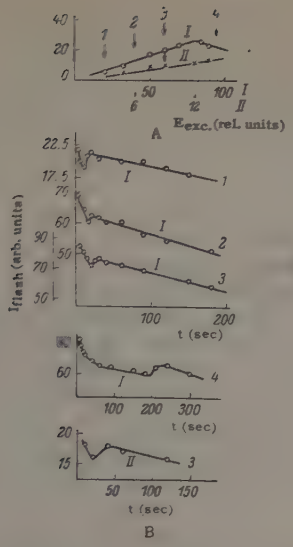

Fig. 1. Magnitude of the flash as a function of the intensity of the exciting light (A) and the duration of the dark interval (B). $\lambda_{exc.}$ (in mμ): curves I—365; curves II—313. AgCl single crystal grown by the Kiropoulos method.

The experimental material obtained confirms beyond the considerable role of the stimulating action of the ng light in the luminescence of the halogen compounds ver. This role manifests itself not only in the limita- f the number of electrons stored on capture levels 1, graph A, curve I) but shows up also in the process ctrons leaving the flash levels even after the stimu- light has been turned off. The presence of a maxi- on the I(t) curves indicates that in the dark electrons distributed among localized levels. Most probably, crease in the number of electrons on the flash is due to their "leakage" from the shallower . Following an analogy between properties of the n and ZnS:Ni phosphor studied by Tolstoi and co- rs,[14,15] we also assume that the AgHal phosphors wo systems of localized levels for electrons. But in ast to the case of ZnS:Mn and ZnS:Ni, in the case of l, the infrared "probes" the deepest levels, the in- d flash levels. In this case the shallower levels are supplying" levels.[14] We should note that in ZnS:Cu: osphors Vinokurov and Fok[16] have recently dis- ed the presence of a maximum in the curves repre- ng the flash magnitude as a function of the duration dark interval after the exciting light is extinguished. When luminescence is excited by ultraviolet light of derable intensity, the initial regions of the I(t) s represent hyperbolas (Fig. 1B, curve 4) charac- ng the process of electron departure from the in- d flash levels in the absence of electron redistribu- among levels. Evidently in this case when the stimu- effect of the exciting light becomes considerable, rocess of the additional filling of the infrared flash s by electrons is displaced by a considerable time val t as compared with the onset of the analogous ss of electron redistribution among levels when escence is excited by ultraviolet light of low inten- (See Fig. 1b, curves 1-3). Thus if we reduce to the scale and to equal intensity the I(t) curves obtained in the two cases (when luminescence is excited by ultraviolet with an intensity corresponding to the rising branch of the I(E) curve and an intensity corresponding to the decreasing branch, respectively), then the difference between the two curves at the values of the initial instants t (the ΔI(t) curve) may characterize the process of electron "leakage" from shallow traps to deep ones. In Fig. 2 curve 1 represents the function I(t) when the intensity of the exciting ultraviolet light is equal to 40 relative units (Fig. 1A, curve I), while curve 2 represents the case when the intensity of the ultraviolet is equal to 95 relative units. Since, in the region where the stimulating action of the exciting light manifests itself, there is no longer a proportionality between the light sum stored on the deep levels and the intensity of the exciting light, we have to do the following to reduce to equal intensity the flash values of curve 2: We must divide I not by 95 relative units but by that intensity value on the rising branch of the I(E) curve for which the same light sum is stored as in the case of excitation by ultraviolet light with an intensity of 95 relative units. In our case we must divide the values of I on curve 2 by 70 relative units. The curve ΔI(t) thus obtained (Fig. 2, curve 3) is characterized by a relatively fast rise and slow fall. This time dependence is quite analogous to those obtained for the same process of electron redistribution among levels by Tolstoi and co-workers for the ZnS:Mn and ZnS:Ni phosphors.[14,15]

In conclusion we should like to draw attention to the fact that the presence of a complex system of capture levels and the redistribution of electrons among these levels is apparently a phenomenon common to many classes of crystalline phosphors.[14-18] In this connection a series of additional problems must be considered in the light of the relaxation theories of these phosphors. The experimental material obtained for AgHal gives reason to believe that the hyperbolic dependence of the luminescence decay curve obtained for these phosphors[19,20] represents not an elementary but an integral decay law.

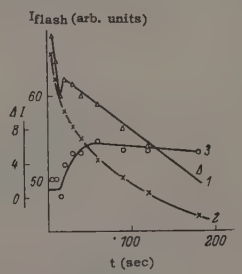

Fig. 2. Flash magnitude as a function of the duration of the dark interval. Curves 1 and 2—excitation by ultraviolet light of different intensities; curve 3—difference between the ordinates of curves 1 and 2 (ΔI). AgCl single crystal grown by the Kiropoulos method.

The author wishes to express his appreciation to T. Ya. Sere for taking continuous interest in this work.

REFERENCES

1. V. V. Antonov-Romanovskii, Izvest. Akad. Nauk SSSR, Ser. Fiz. 10, 477 (1946).
2. Ch. B. Lushchik, Trudy Inst. Fiz. i Astron., Akad. Nauk Eston. SSR, No. 3, 3 (1955); ibid. No. 4, 42 (1956).

3. M. L. Kats, "Luminescence and Electron-Hole Processes in Photochemically Colored Crystals of Alkali Halide Compounds." Izd. Saratovsk. Univ., 1960.
4. C. Bull, D. E. Mason, J. Opt. Soc. Am. 41, 718 (1951).
5. V. L. Levshin, V. V. Antonov-Romanovskii, Z. L. Morgenshtern, and Z. A. Trapeznikova, Zhur. Eksptl. i Teoret. Fiz. 17, 949 (1947).
6. V. L. Levshin, Izvest. Akad. Nauk SSSR, Ser. Fiz. 12, 217 (1948).
7. I. A. Parfianovich, Zhur. Eksptl. i Teoret. Fiz. 21, 314 (1951); Izvest. Akad. Nauk SSSR, Ser. Fiz. 15, 669 (1951).
8. C. E. Mandeville and H. O. Albrecht, Phys. Rev. 97, 347 (1955).
9. S. A. Popok and F. D. Klement, Zhur. Eksptl. i Teoret. Fiz. 17, 915 (1947).
10. K. S. K. Rebane, Trudy Inst. Fiz. i Astron., Akad. Nauk Eston. SSR No. 4, 81 (1956); ibid. No. 8, 105 (1958).
11. P. A. Khellenurme, Trudy Inst. Fiz. i Astron., A Nauk Eston. SSR No. 6, 132 (1957).
12. L. A. Vinokurov, Opt. i Spektr. 1, 901 (1956).
13. V. M. Belous and N. G. D'yachenko, Opt. i Spekt 10, 649 (1961), Optics and Spectroscopy 10, 341
14. N. A. Tolstoi, N. N. Tkachuk, M. Ya. Tsenter, Z Mansurova, and A. V. Burlakov, Opt. i Spektr. 1 719 (1956).
15. N. A. Tolstoi, A. M. Tkachuk, and N. N. Tkachul Opt. i Spektr. 2, 759 (1957).
16. L. A. Vinokurov and M. V. Fok, Opt. i Spektr. 1 225 (1961), Optics and Spectroscopy 10, 112 (196
17. Ch. B. Lushchik, F. N. Zaitov, V. Ya. Kark, L. Teiss, and I. V. Yaek, "Proc. Fifth Conf. on Lu nescence (Crystalline Phosphors), Tartu, 1955.
18. I. A. Parfianovich, Opt. i Spektr. 2, 392 (1957),
19. S. I. Golub, Sbornik Fiz.-Mat. Fak. Odessk. Uni 59 (1951); ibid. 5, 27 (1954).
20. V. Arkhangel'skaya and P. P. Feofilov, Doklady Nauk SSSR 91, 1055 (1953).

BOOK REVIEW

DIE TERPENE. SAMMLUNG DER SPEKTREN UND PHYSIKALISCHEN KONSTANTEN TEIL I. SESQUITERPENE

By J. Pliva, M. Horak, V. Herout, and F. Šorm. Akademie-Verlag, Berlin, 1960

(pp. 434-435)

The publication of an atlas of the infrared spectra of sesquiterpenoid compounds, which has been undertaken by a group of Czechoslovak scholars, is an important event for those who are interested in the study of the ethereal oils and in the elucidation of the structure of their components.

The study of the terpenes attained a brilliant development in the first half of the 20th century. The structure of the more complex compounds—the sesquiterpenes and polyterpenes in general—was elucidated to only a small extent. The appearance of new methods of investigation—chromatography and spectroscopy—had a beneficial influence on the development of our ideas in this complicated field of natural products. Chromatography made possible the separation of a mixture of substances into individual compounds. Spectroscopy (in particular infrared spectroscopy) made the study of these an easier task. The role of infrared spectroscopy has proved even more significant. According to the proposition of Šorm, Pliva, and Herout, the spectroscopic characteristics of the hydrogenated sesquiterpenes are made the basis of a classification of sesquiterpenoid compounds. By comparing the hydrocarbons separated from ethereal oils, after being subjected to hydrogenation, with known hydrogenated sesquiterpenes, the investigator directly solves the question of the type of sesquiterpene to which the hydrocarbon under study pertains. The subsequent work of the investigator is thus made easier to a significant degree. In the case of the occurrence of compounds with various functional groups (alcohols, aldehydes, ketones, etc.) in the ethereal oils, one should go over from the functional compounds to the hydrocarbons.

Infrared spectra simplify to a considerable deg recognition of compounds separated from ethereal identifying them with compounds which are already and have been described.

The infrared spectra presented in the atlas of t Czech scholars were taken by means of a single-be Perkin-Elmer infrared spectrometer (model 12B). prism material—rock salt—limits the range of the surements to 650-2000 cm^{-1}. Liquid substances we measured almost exclusively without the use of a s Solid substances were measured, in the case of a lo melting point, in the fused state; in the opposite cas they were measured in the usual solvents (CCl_4 and

In the tables, aside from the data characterizin infrared spectra, the reader will find information o structure of the compounds, their physical properti and their origin; references to the relevant literatu are also given. One must wish for the authors, who carried out a great work, a successful conclusion t labor.

It would be very desirable to broaden the range measurements, no longer being limited to only 650- cm^{-1}. The frequencies of the CH, CH_3, =CH, and O stretching vibrations lie far outside the 650-2000 c limits. Furthermore, in the ethereal oils we also e counter acetylenic compounds (frequency region 21 3300 cm^{-1}).

G. V. Pigul

Spectroscopic methods are widely applied to th lution of various structural and analytical problems

e methods attain particular significance in the study tural materials of complicated composition and struc- when the use of purely chemical methods is associ- with a considerable expenditure of labor and does not ys lead to the goal. In view of this, the collection of on the spectra of natural products and their deriva- is a very timely task. However, in order to accom- it, one must have sufficiently pure substances, the ration of which from natural materials, or alterna- y their synthesis, is a very complex problem by itself. no wonder, therefore, that there are relatively few tral data of this sort, and moreover that they are, as le, scattered over an extensive literature. What has said applies in full measure to the terpenes also. publication of the atlas under review is therefore to onsidered as a significant event in spectroscopic ature.

The value of this atlas is determined first of all by act that it is based on numerous and detailed investi- ons of natural terpene-containing products, carried by the Czech scholars. As a result of these investiga- , which have significantly enriched terpene chem- , a unique collection of individual terpenoid hydro- ons and related compounds has been created.

The present atlas, which is apparently the first part broadly conceived publication, contains the spectra out 200 sesquiterpenes and their derivatives. There 28 spectral charts in the atlas, 210 × 295 mm, made heavy white paper. On the front of the charts are ented certain important constants of the samples in- gated (refractive index, specific gravity, specific tion, melting and boiling points), the empirical and ctural formulas of the substance (if the latter is n), a short description of the method of obtaining it, so on. In certain cases information is also presented e ultraviolet absorption spectrum of the substance— positions of the absorption maxima and the extinction ficients corresponding to them. The main position on chart is occupied by the infrared absorption curve of substance in the 650-2000 cm^{-1} region, measured by ns of a single-beam Perkin-Elmer spectrometer, model 12B or 12C, with an NaCl prism. A frequency scale (linear) and a wavelength scale are laid off along the horizontal axis, the percent transmission along the vertical axis. The authors do not make use of the back of the charts. All the spectral charts are numbered in a definite order according to a classification based on the entire carbon skeleton of the compound. Some compounds in the catalog are shown on two or more charts (up to five); on these charts are presented the constants and spectra of samples obtained by different methods. A small brochure is attached to the catalog, containing explanations of the charts, general information on the methods for obtaining the substances and measuring their spectra, and also a short sketch of the field of their application. The set includes a special cover of transparent plastic which may be used for copying the absorption curves.

Unfortunately, data on the original measurements of the absorption band frequencies, a knowledge of which is necessary in solving certain problems, are lacking from the charts. They may be determined from the absorption curves, but with low accuracy, all the more so since these curves are not the originals but copies. The absence of data on the absorption in the region of the CH bond stretching vibrations is also not entirely justified. In a number of cases, a knowledge of the absorption curve in this region may be of great help.

In spite of the defects noted, this valuable publication will undoubtedly find wide use, not only in carrying out investigations in the field of terpene chemistry, but also in solving more general questions of molecular structural analysis. One can therefore only express a wish for the quickest possible appearance of the remaining parts of this outstanding work.

The atlas under review is published in the GDR (East Germany) with the assistance of the Commission on Spectroscopy of the German Academy of Sciences. The production aspect of the publication deserves a high rating.

V. Aleksanyan

NEWS

THE 15th ROZHDESTVENSKII LECTURE

(p. 436)

Two papers were read on the occasion of the 15th ndestvenskii lecture on May 18, 1961.

The Rozhdestvenskii lecturer, N. P. Penkin, who is loping Rozhdestvenskii's classical work on anomalous ersion, reported new research on anomalous dis- ion in metal vapors. In the first part of the lecture iscussed results obtained in studies of atomic exci- n and ionization processes in a low pressure gas harge plasma, showing that a plasma in a high tem- ture furnace (the King type) is isothermal. The lec- included interesting new results on the establish- t of statistical equilibrium in the discharge and the zation processes in collisions of the second type.

In the second part of the lecture, Penkin explained w method of determining oscillator strengths, devel- by his colleagues and himself, based on a simul- ous measurement of dispersion ("hooks") and total rption. He gave the results of systematic measurements of absolute and relative oscillator strengths for spectra of atoms of groups I, II, and III of the periodic table, and also of atoms with a completed 3d-shell. The experimental data were compared with quantum-mechanical calculations of the f-numbers. The report showed that D. S. Rozhdestvenskii's "hook" method may still be successfully used in the solution of many problems of modern physics.

In his paper, "A New Branch of Infrared Technology-Thermal Vision," M. M. Miroshnikov considered the method of operation and the field of application of different infrared devices which form an image of objects at low temperatures. The lecturer considered the energy relationships leading to the choice of diameter and numerical aperture of the optical system. He also noted the features of the signal amplifier and reproducer in infrared image systems and considered the construction and characteristics of some instruments.

PERSONALIA

THE 60th BIRTHDAY OF BORIS YAKOVLEVICH SVESHNIKOV

(p. 437)

In August, 1961, Professor Boris Yakovlevich Sveshnikov, Doctor of Physical-Mathematical Sciences and prominent specialist on the luminescence of organic compounds, celebrated his 60th birthday and his 30th active year in the field of science.

B. Ya. Sveshnikov's scientific career began in S. I. Vavilov's laboratories, first in Moscow and later in Leningrad. As early as 1934, when he was a graduate student, he developed the modern theory of diffusion decay of fluorescence in solutions and demonstrated its complete agreement with experiment. This theory is also applied to the kinetics of bimolecular reactions in solutions. Some consequences of the theory were verified experimentally only recently, following advances in fluorimetric technique; the study of chemiluminescence was closely linked to this series of investigations. Systematic quantitative study of the kinetics of chemiluminescence enabled B. Ya. Sveshnikov to obtain much important data on the mechanism of this complex phenomenon.

During the war, B. Ya. Sveshnikov devoted all his strength and knowledge to strengthening the defenses of our country. After the war he applied himself vigorously to basic problems in the luminescence of organic molecules, and most of his papers in these years refer to phosphorescence of organic compounds. B. Ya. Sveshnikov studied all the basic features of this very important phenomenon and considered the kinetics of phosphorescence in detail. His dostoral dissertation (1951) is still the only monograph treating the majority of topics in the luminescence of organic luminors.

The study of radiationless transfer of electron excitation energy in concentrated dye solutions occupied a large place in Sveshnikov's work. Quantitative data on concentration depolarization and concentration decay for dyes in solution were published in 1940 in a joint paper with P. P. Feofilov, and were the basis for most of the work in this field.

B. Ya. Sveshnikov has always paid great attentio training young scientists. Several dissertations have prepared under his direction.

At present, with his collaborators, he is working tively on basic problems in the field of the luminesce of organic compounds.

The editorial staff of the journal Optika i Spektr skopiya congratulate B. Ya. Sveshnikov on his 60th b and wish him good health and further scientific succe

S. E. FRISH, HONORED WORKER IN SCIENCE AND TECHNOLOGY OF THE RSFSR

(p. 438)

In a decree of June 15, 1961, the Presidium of the Supreme Soviet of the RSFSR conferred the title of Honored Worker in Science and Technology of the RSFSR on Sergei Eduardovich Frish, the prominent specialist in atomic and gas discharge spectroscopy and spectral analysis, Corresponding Member of the Academy of Sciences of the USSR, and editor in chief of the journal Optika i Spektroskopiya.

On behalf of all Soviet scientists in the field of o and spectroscopy, the editorial staff of the journal O i Spektroskopiya warmly congratulates Sergei Eduar ovich on receiving his high award and wishes him he and further success in his work.

LETTERS TO THE EDITOR

ON THE ARTICLE—THE ABSORPTION SPECTRUM OF LIQUID AND SOLID OXYGEN UNDER PRESSURE (12,600-3000 A), by V. Dianov-Klovkov

Opt. i Spektr. 7, 621 (1959), Optics and Spectroscopy 7, 377 (1959)

(p. 439)

Repetitions of the measurements have shown that alues of ε_m for the last point (ρ = 1.61 gm/cm^3) in 2 are too low, and the curves $\varepsilon_m = f(\rho)$ do not show s region the leveling off which was associated with $\rightarrow \beta$ transition. This transition actually takes place ~ 1.9 gm/cm^3 (T = 78°K) and is accompanied again by turbidity of the layer. Thus, the statements made in the article concerning the nature of the $\gamma \rightarrow \beta$ transition are not valid.

V. Dianov-Klokov

ERRATA

(p. 439)

In Table 1 of my paper "The Nature of the Elementary llators of the Uranium Ion" [Opt. i Spektr. 8, 824]), Optics and Spectroscopy 8, 433 (1960)] an error made, arising apparently from not taking account of act that in excitation of luminescence in LiF-U crys- by radiation at λ = 365 meters, both σ_e and π_e oscil- s take part in the absorption simultaneously. Thus ualitative comparison of the experimental data with 1 is ambiguous and quantitative estimates of the in- ty of the components are necessary. Table 1 (p. translation page 434) should be as follows:

λ (A)	Type of radiator	λ (A)	Type of radiator
4828	π_e	5012	π_e
4884	π_e	5017	π_m
4920	π_e	5024	π_m
4941	π_e	5051	π_m?
4948	π_m	5057	π_e?
4993	π_m	5067	π_m
5002	π_m	5136	π_e?

The chief conclusion of this paper—that luminescence of hexavalent uranium must be considered a superposition of forced electric and magnetic dipole radiation—remains valid.

I wish to thank A. A. Kaplyanskii for drawing my attention to the lack of agreement between part of the data presented in my paper and data that he obtained in piezospectroscopic studies of the same specimens.

P. Feofilov

(p. 439)

In our paper entitled "The Vibrational Spectra of ates. II" [Opt. i Spektr. 10, 79 (1961), Optics and troscopy 10, 37 (1961)], we made an error in re- ing to the interpretation of the spectrum of the ion eO]$^{2-}$; these data were taken from the paper by G. tavitska and Ya. I. Ryskin [Opt. i Spektr. 10, 343 1), Optics and Spectroscopy 10, 172 (1961)]. Also, in Table 2 of our paper, the assignment of the valence vibrations as_{YXY}' and as_{YXY} (of the chain $[X_2Y_6]_\infty$ with structure Na_2SiO_3) to the symmetry types B_2 and A_2 should be reversed.

A. I. Lazarev and T. F. Tenisheva

A New Publication

APPLIED OPTICS

to be published by The Optical Society of America

Editor: JOHN N. HOWARD, *Geophysics Research Directorate, Bedford, Mass.*

APPLIED OPTICS will publish in the areas of applied optics and closely related scientific and technic fields, e.g. physical, electron, ion, ultraviolet and space optics, lens design and optical formulas, plasm solid state and crystal optics. **APPLIED OPTICS** will be issued bimonthly from January 1962 an will feature

.....A leader review paper on one of the major aspects of optics or its applications, e.g., new infrare detectors, new optical materials, applications of physical optics in manufacturing process contro This review will be about 10,000 words long and will set the **feature** subject of each issue.

.....Contributed technical papers—3000/5000 words each—about ten per issue—in **any area** applied optics.

Shop and technical notes — Book reviews — Letters to the Editor
Reports of Meetings — Personalia — Meetings Calendar
Optical Activities in
Government — The Universities — Industry

** Each issue will feature one area of applied optics, which feature will be the responsibility of a Subject Editor.

1962	JANUARY	— OPTICAL PUMPING AND MASERS	BRUCE H. BILLINGS
	MARCH	— SPACE OPTICS	LLOYD G. MUNDIE
	MAY	— FOREIGN OPTICS	DAVID Z. ROBINSON
	JULY	— OPTICAL ENGINEERING	RODERIC M. SCOTT
	SEPTEMBER	— INFRARED	JOHN N. HOWARD
	NOVEMBER	— INFORMATION THEORY	F. DOW SMITH
1963	JANUARY	— ASTRONOMY	JAMES G. BAKER
	MARCH	— INSTRUMENTATION	W. L. HYDE
	MAY	— INTERFEROMETRY	R. A. WOODSON

APPLIED OPTICS will be the one publication devoted solely to applied optics in its broadest sense an designed to meet the interests of scientists, engineers, technologists, technicians—in a word, opticists- working in optics or its applications, in fields borderline to optics and employing optical technique

Special prepublication rates for founder subscribers

All orders for a three year period, placed prior to publication, will be entered at the following special rate:

O.S.A. members—3 yr. sub. $15.00 **Non-members—3 yr. sub. $25.00**

Yearly subscription rates will be

O.S.A. members—$6.00 **Other AIP Societies members—$8.00** **Non-members—$10.00**

Subscriptions and inquiries should be sent to

Optical Society of America

1155 Sixteenth Street, N.W., Washington 6, D.C.

** Part of each issue.

(FILLER MATERIAL - NOT IN RUSSIAN ORIGINAL)

OOK REVIEW

ie Terpene. Sammlung der Spektren und physikalischen Konstanten. Teil I. Sesquiterpene. By J. Pliva, M. Horak, V. Herout, and F. Šorm . . . . . G. V. Pigulevskii . . . . . V. Aleksanyan 236 (434)

he 15th Rozhdestvenskii Lecture 237 (436)

he 69th Birthday of Boris Yakovlevich Sveshnikov 238 (437)

. E. Frish, Honored Worker in Science and Technology of the RSFSR 238 (438)

n the Article—The Absorption Spectrum of Liquid and Solid Oxygen Under Pressure (12,600-3000 A), by V. Dianov-Klokov . . . . . V. Dianov-Klokov 239 (439)

rratum . . . . . P. Feofilov 239 (439)

rrata . . . . . A. I. Lazarev and T. F. Tenisheva 239 (439)

EDITOR'S NOTE

Comments on the scientific content of the translated Russian articles published in OPTICS AND SPECTROSCOPY are invited. They should be addressed as a Letter to the Editor of the Journal of the Optical Society of America and forwarded to the Editor of that journal, Dr. D. B. Judd, National Bureau of Standards, Washington 25, D. C.

UNIVERSITY OF ILLINOIS 3
LIBRARY
UNDERGRADUATE DIV
NAVY PIER GRAND AVE
CHICAGO 11 ILL

VOL. XI, NO. 3 OPTICS AND SPECTROSCOPY SEPTEMBER 196

CONTENTS

(Numbers in parentheses are original Russian page numbers.
These Russian page numbers are also quoted at the head of each paper.)

The Extended Fok Method in a Multiconfiguration Approximation for the Helium Atom . . . . . K. K. Eringis, P. Sh. Fridberg, and V. K. Shugurov 161 (297
The Excitation of Atoms and Ions by Electron Impact. I. Calculation Ignoring Exchange . . . . . L. A. Vainshtein 163 (301
A Direct Method of Measuring the Mean Lifetime of Excited Ionic Levels . . . . . Yu. M. Kagan and Ya. P. Koritskii 166 (308
Time Resolved Emission Spectra of a Spark Discharge in Inert Gases in the Region 5000-10,000 A . . . . . M. P. Vanyukov, V. R. Muratov, and I. A. Mukhitdinova 169 (312
Restricted Motions in Transition Metal Complexes . . . . . I. B. Bersuker 172 (319
Infrared Spectra of Phthalocyanines. II. Interaction of Sublimed Layers of Phthalocyanines With Gaseous CH_3COOH, HCl, and HBr . . . . . A. N. Sidorov and A. N. Terenin 175 (325
Effect of Temperature on the Absorption of Monosubstituted Benzenes in the Region of the C—H Stretching Vibrations . . . . . M. P. Lisitsa and I. N. Khalimonova 179 (332
Second-Order Raman Spectra in Some Liquids . . . . . Ya. S. Bobovich 184 (342
Determination of Macroradical Conformations by Their Electron Paramagnetic Resonance (EPR) Spectra . . . . . I. S. Milevskaya and M. V. Vol'kenshtein 188 (349
Light Scattering in Crystalline Polymers. II. Investigation of the Temperature Dependence of the Index of Refraction of the Crystalline and Amorphous Phases of Polychloroprene and the Determination of the Degree of Crystallization . . . . . O. N. Trapeznikova, G. E. Novikova, and S. V. Minakova 190 (353
On the Influence of Crystal Structure on the Vibrational Spectrum of the Hydrogen Bond . . . . . A. I. Stekhanov and Z. A. Gabrichidze 193 (359
Notes on the Concepts of "Yield," "Mean Lifetime," and "Decay Law" and Their use in Luminescence . . . . . V. L. Levshin 195 (362
Reabsorption in Crystals of a Finite Thickness. II . . . . . V. M. Agranovich and Yu. B. Konobeev 199 (369
Some Concentration Effects in Plastic Scintillators . . . . . L. S. Kukushkin and L. L. Nagornaya 206 (385
Luminescence of p-Terphenyl in a Mixture of Toluene and Carbon Tetrachloride . . . . . S. F. Kilin, K. A. Kovyrzina, and I. M. Rozman 209 (390
The Yellow Luminescence of Zinc Oxide . . . . . Ya. M. Zelikin and A. P. Zhukovskii 212 (397
Interference of Luminescent Emission From an Evaporated Phosphor . . . . . N. A. Vlasenko, V. K. Miloslavskii, and I. N. Shklyarevskii 216 (403
Study of the Emissive Power of Certain High-Melting Compounds in the Infrared Region . . . . . G. V. Samsonov and V. V. Pen'kovskii 219 (410

SHORT COMMUNICATIONS

On the Mechanism of the Weakening of the CN Bands (Violet System) in an Arc . . . . . V. S. Rossikhin and I. L. Tsikora 223 (415
Single Slit, Three-Beam Interferometry . . . . . V. G. Khomazyuk 224 (417
Luminescence of Ionic Forms of Uranin in Liquid and Solid Solutions . . . . . V. S. Adamov and L. T. Kantardzhyan 226 (419
Electro-X-Ray Luminescence of KBr Crystals . . . . . A. S. Andrianov and M. L. Kats 228 (422
Results of Spectrochemical Analysis With a Combination Electric Discharge as a Light Source . . . . . G. D. Cristescu and M. Giurgea 229 (424
On the Electroluminescence Excitation Process in Zinc Sulfide . . . . . A. N. Georgobiani 231 (426
Hydrogen Bonding of Ketones with Chloroform as Revealed in the Band of the Carbonyl Group Stretching Vibration . . . . . G. S. Denisov 232 (428
The Redistribution of Electrons Among the Localized Levels of Silver Halide Phosphors and the Stimulating Action of the Exciting Light . . . . . V. M. Belous 234 (431